ABSTRACT

DEPARTMENT OF CHEMISTRY

JAVIER SANTOS-PEREZ B.S. PONTIFICAL CATHOLIC UNIVERSITY OF PUERTO RICO, 1994

SYNTHESIS AND CHARACTERIZATION OF A NEW CLASS OF THIOPHENE - CONTAINING IMIDAZOLES AS FLUORESCENT AND NONLINEAR OPTICAL MATERIALS

Advisor: Professor Xiu Ren Bu

Dissertation dated December 2004

Photoresponsive molecules have a broad range of potential applications, for example in optical, energy, and biomedical technologies. Fluorophores and second order nonlinear optical (NLO) chromophores are photoresponsive molecules used as signaling materials and frequency doublers or electro-optical modulators, respectively.

The research presented here describes the synthesis, characterization, and potential applications of a group of highly fluorescent molecules and NLO chromophores containing benzene, imidazole and thiophene rings. Methyl, methoxy, and dimethylamino groups were used as electron donor groups while formyl and nitro groups were used as electron acceptors.

The fluorescence properties of a series of dyes containing donor groups and a formyl group attached to a thiophenyl ring were investigated. X-ray structural determination revealed a steric crowding, which causes a molecular twist in the ground state. The fluorescence quantum yield for these fluorophores was found in the range of 0.004-1.0. It was determined that these fluorescent molecules emit light from a non-polar locally excited (LE) state and a polar intramolecular charge transfer (ICT) excited state. The dye containing the dimethylamino group was characterized by dual fluorescence in moderate polar solvents. The excited state dipole moments and excited state lifetimes were found to increase as the strength of the donor group increases. A linear correlation was obtained for the Stokes shift versus the solvent polarity parameter $E_T(30)$ and the Hammett's constant σ^+. Solvatochromic studies revealed a solvent polarity dependence on fluorescence properties.

Macromolecules containing selected fluorophores were synthesized. The fluorescence quantum yield of the macro-systems was found to be lower than the respective monomer. A series of NLO chromophores having donor groups (i.e., methyl, methoxy, and dimethylamino) and nitro as acceptor were synthesized. They were studied in terms of the nonlinear optical coefficient $\exists\mu$ and thermal stability. The chromophores containing a thiophenyl stilbene conjugation showed superior NLO properties and moderate thermal stability in comparison with their respective analogs. The synthesis of macromolecules containing selected chromophores is also reported.

Finally, preliminary synthesis and characterization of other potentially photo-responsive compounds are presented.

SYNTHESIS AND CHARACTERIZATION OF A NEW CLASS OF THIOPHENE CONTAINING IMIDAZOLES AS FLUORESCENT AND NONLINEAR OPTICAL MATERIALS

A DISSERTATION

SUBMITTED TO THE FACULTY OF CLARK ATLANTA UNIVERSITY

IN PARTIAL FULFILLMENT OF THE REQUIREMENTS FOR

THE DEGREE OF DOCTOR OF PHILOSOPHY IN CHEMISTRY

BY

JAVIER SANTOS-PEREZ

DEPARTMENT OF CHEMISTRY

ATLANTA, GEORGIA

DECEMBER 2004

ACKNOWLEDGMENTS

I would like to express my gratitude to the committee members. Thanks go to High Performance Polymers and Composites (HiPPAC) Center at Clark Atlanta University, National Aeronautic and Space Administration (NASA), and Biomedical Research Support (MBRS) for the financial support. Special thanks go to Dr. Eric A. Mintz, Dr. Kofi Bota, Dr. Michael A. Meador, Dr. Mark Mitchell, and Dr. Gabriel García. Finally, I would like to dedicate this work to my mother, María A. Pérez; my father, Walter Santos; my sister, Angélica M. Santos; and my loving wife, Marisabel Lebrón.

TABLE OF CONTENTS

LIST OF FIGURES

Figure

LIST OF TABLES

Table

LIST OF ABBREVIATIONS

Å	angstroms (10^{-10} m)
β	molecular hyperpolarizability
CT	charge transfer
δ	chemical shift in NMR
D	Debye (dipole moment unit)
d	doublet (spectra)
deg, °	degree (X-ray crystal)
Δf	solvent polarity function
DSC	differential scanning calorimetry
ε	molar absorptivity
E_{abs}	energy of the absorption maximum
EFISH	electric field second harmonic generation
E_{fl}	energy of the fluorescence transition
Eq.	equation
equiv	equivalents
ESIPT	excited state intramolecular proton transfer
esu	electrostatic unit

Φ_{fl}	fluorescence quantum yield, fluorescence efficiency
GC-MS	gas chromatography-mass spectrometry
hv	light
ICT	intramolecular charge transfer
J	coupling constant (NMR)
k_{nr}	rate constant for non-radiative process
k_r	rate constant for radiative process
λ	wavelength
$\lambda_{cut\text{-}off}$	wavelength of electronic transparency
LE	locally excited state
λ_{em}	maximum emission wavelength
λ_{exc}	maximum excitation wavelength
λ_{max}, λ_{abs}	maximum absorption wavelength
M	molarity (concentration)
m	multiplet (spectra)
mp	melting point
$\mu\beta$	nonlinear optical coefficient
μ_e	excited state dipole moment
μ_g	ground state dipole moment
ν	frequency
n	refractive index

N	normality (concentration)
NLO	nonlinear optical
nm	nanometers
ns	nanoseconds
ppb	parts per billion
ppm	parts per million
r^2	linear correlation, goodness of fit
rt	room temperature
σ^+	Hammett constant
s	singlet (spectra)
S_o	ground state
S_1	first excited state
S_2	second excited state
τ, τ_{fl}	excited state lifetime
t	triplet (spectra)
T_5	5% decomposition temperature
T_d	decomposition temperature
TGA	thermogravimetric analysis
TICT	twisted intramolecular charge transfer
TLC	thin layer chromatography
T_m	melting point (extracted from DSC)
TMS	tetramethylsilane (NMR)

CHAPTER I

INTRODUCTION

Section 1 Fluorescent Organic Molecules and Their Properties

1.1 *Overview of Fluorescent Organic Molecules*

Interest in fluorescent organic molecules has increased dramatically as their potential applications in areas such as analytical and environmental chemistry, and materials science have been realized.[1] The key role of these photo-responsive molecules is found in their signaling of recognition events such as switches.[2] In addition, some of these molecules are able to absorb two photons, which is of interest for optical memory storage and imaging of biological structures.[3]

Significant attention has been given to the sensing and switching ability of organic fluorescent compounds. Among the advantages of organic fluorescent molecules are their high sensitivity for analyte detection,[4] "on-off" switch ability,[5] easy response detection,[6] feasibility to enhance sensibility,[7] and potential for incorporation of functional groups for molecular recognition.[1b,4b] These potential applications are directly related to the fluorescence efficiency and flexibility of the structural design of the fluorophores (species that possess the ability to fluoresce). The knowledge and understanding of the photophysical properties of these molecules have aided in the design of fluorophores for specific applications. One unique application is the monitoring of Ca^{2+} concentration

inside living cells during muscle contraction utilizing a chelating agent equipped with a fluorophore.[1f]

The photophysical response of fluorescent molecules depends upon the environment to which they are subjected. Therefore, since most fluorescence data is obtained in solution, the effect of solvent properties on the photophysical response of fluorophores has been extensively investigated.[8] Such events can be readily measured as a perturbation in absorbance, emission and/or excitation spectra, or excited state lifetime. The understanding of the photophysical properties of fluorophores is essential to develop their applications.

In the following sections the origin of fluorescence, photophysical properties, design of fluorescent sensors, applications, and recent findings will be discussed.

1.2 *Nature of Molecular Fluorescence*

To produce fluorescence a molecule must absorb energy from some source such as radiant or chemical energy and be raised to a higher energy level (excited state).[9] Shown in Figure 1 is a general energy diagram that describes the electronic processes of most aromatic molecules with an S_o ground state. After a molecule absorbs energy, it leads initially to the first excited single state (S_1). In cases where the molecule is excited to a higher excited singlet states (S_2, S_3, ...) the energy is believed to decay rapidly in about 10^{-12} s to the S_1 state. When the molecule releases the energy from the S_1 state to its ground state (S_o) much of the absorbed energy may be emitted as fluorescence (light) in 10^{-8} s or less. Molecules can also undergo a number of non-radiative processes, which

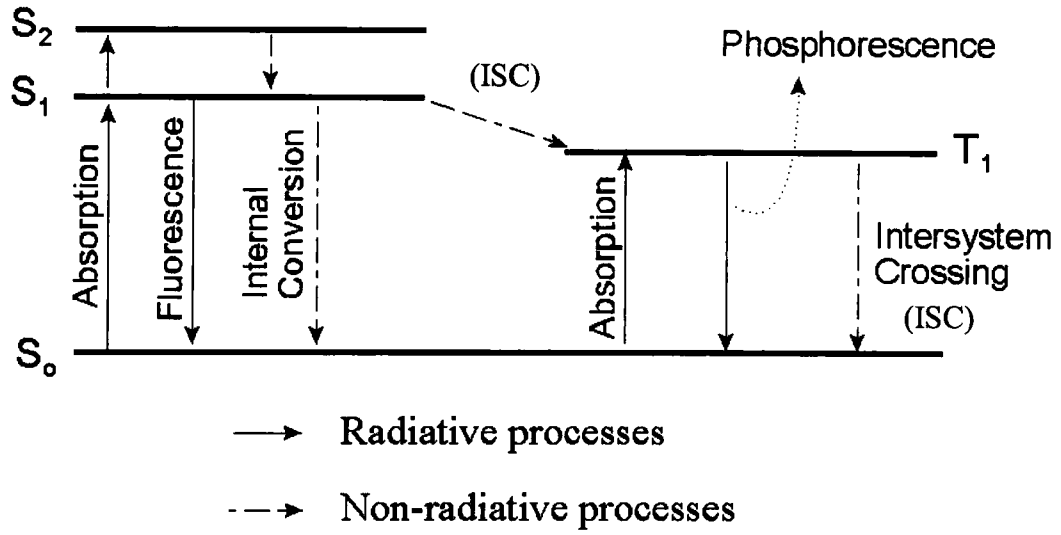

Figure 1. *Jablonski diagram for photophysical processes.*

may lower their fluorescence efficiency. For example some compounds may go through an energy change from the S_1 state to the triplet state (T) resulting in phosphorescence. The phosphorescence duration may vary from nanoseconds to hours after the initial energy absorption takes place.

Although many organic compounds and elements are fluorescent, not all of them possess the striking feature of visual fluorescence. In many cases aromatic compounds having alternate single and double bonds in an unbroken sequence are expected to possess visible fluorescence in organic solvents.[9] For example, fluorescein has an unbroken sequence of π bonds and exhibits a strong visible fluorescence contrary to phenolphthalein where the conjugate system is broken as shown below. On the other hand, aliphatic compounds do not exhibit fluorescence.[9]

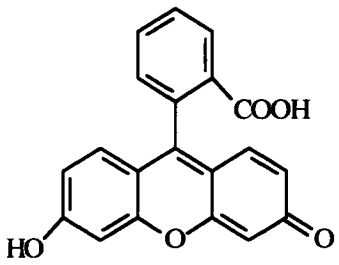

Fluorescein
Exhibit visible fluorescence

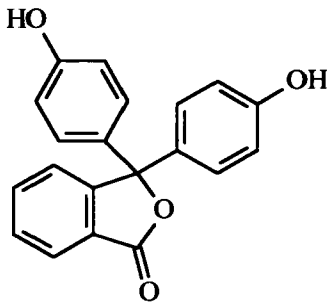

Phenolphthalein
Does not exhibit visible fluorescence

1.3 *Photophysical Properties of Fluorescent Organic Molecules*

Fluorescent molecules are generally characterized by three types of electronic spectra:[10] a) absorption, a process in which a chemical species in a transparent medium selectively decreases the intensity of certain frequencies of electromagnetic radiation. b) excitation, which is the relative efficiency of different wavelengths of exciting radiation to cause fluorescence, and c) emission, which is the relative intensity of radiation emitted at various wavelengths. These spectra provide considerable information about the electronic structure of the fluorophore. For example, the energy dissipated during the lifetime of the excited state before returning to the ground state. The latter is a physical constant known as Stokes shift[4b,11] which can be calculated from equation 1. The Stokes shift is expressed in cm^{-1} where λ_{exc} and λ_{em} are the corrected maximum wavelengths (in nanometers) for excitation and emission, respectively. It is worth mentioning that the absorption maxima can be used in place of λ_{exc}.[11]

$$\text{Stokes shift} = \left(\frac{1}{\lambda_{exc}} - \frac{1}{\lambda_{em}} \right) \times 10^7 \qquad \text{Eq. 1}$$

The quantum yield of fluorescence or fluorescence efficiency (Φ_{fl}) is a characteristic property that describes the ratio of the total energy emitted per quantum (photons) of energy absorbed (Eq. 2). The higher the value of Φ_{fl}, the greater the fluorescence efficiency of a given compound. Quantum fluorescence efficiency can be obtained as absolute or relative values. The absolute Φ_{fl} is the luminescence intensity integrated over the entire spectrum which is independent of the power of the excitation source.

$$\Phi_{fl} = \frac{\text{number of photons emitted}}{\text{number of photons absorbed}} \qquad \text{Eq. 2}$$

Because of the complexity in determining the absolute Φ_{fl}, alternative methods have been developed. These alternative methods involve a comparison of the luminescence maxima of the compound under investigation and a reference compound for which the absolute Φ_{fl} is known. In this work, the relative fluorescence efficiency will be refereed to as Φ_{fl}. Different equations have been formulated for the determination of Φ_{fl}. The most widely used expressions are given in equations 3 and 4. Equation 3 is applied when the compound under investigation (1) and the reference compound (2) are in the same solvent, where Φ is the fluorescence efficiency, E is the area under the corrected emission spectrum curve, A is the absorbance and P is the relative photon yield of

the radiation source at the excitation wavelength. When the compound of interest is in a different solvent than the reference compound, equation 4 is normally used, where n is the refractive index of the respective solvents and E and A have the same definitions as in equation 3.

$$\frac{\Phi_1}{\Phi_2} = \frac{E_1}{E_2} \cdot \frac{A_2}{A_1} \cdot \frac{P_2}{P_1} \qquad \text{Eq. 3}$$

$$\frac{\Phi_1}{\Phi_2} = \frac{E_1}{E_2} \cdot \frac{A_2}{A_1} \left(\frac{n_1}{n_2} \right)^2 \qquad \text{Eq. 4}$$

The lifetime of the excited state (τ) is another important characteristic of luminescent materials. The lifetime indicates how long it takes the excited electrons to return, on average, to the ground state or in other words, how long the state (e.g. S_1, S_2, ...) has been populated. The excited state lifetimes for fluorescent compounds are in the range of 10^{-9} to 10^{-7} s, while for phosphorescent compounds they are 10^{-4} to 10^{-2} s.

The rate constant for radiative (k_r) and non-radiative (k_{nr}) processes can be approximated by equations 5 and 6, respectively, if the fluorescence decay curves are monoexponential.[12o] The Φ_{fl} is the fluorescence efficiency and τ_{fl} is the excited state lifetime.[4b] The rate constant k_r involves all possible radiative processes and k_{nr} is the sum of all other modes of de-excitation (relaxation) such as internal conversion,

intersystem crossing, and geometry twist in the excited state.[4b] Usually, these rate constants are solvent and temperature dependent.[4d]

$$k_r = \frac{\Phi_{fl}}{\tau_{fl}} \qquad \text{Eq. 5}$$

$$k_{nr} = \frac{1 - \Phi_{fl}}{\tau_{fl}} \qquad \text{Eq. 6}$$

The fluorescence properties of a compound can be perturbed in a number of ways, for example: a) Φ_{fl} tends to decrease at high concentration of the fluorophore; this is called self-quenching, b) in some cases Φ_{fl} changes as a function of temperature,[1d] c) Φ_{fl} is very sensitive to the molecular subtituents. They affect the intramolecular charge transfer (ICT),[12b,d] d) the presence of an analyte which interacts with the fluorophore,[13] e) Φ_{fl} values may also vary with excitation wavelengths (e.g., the Φ_{fl} of quinine is 0.48 at an excitation of 313 nm and 0.54 at 365 nm in 1N H_2SO_4),[14] and f) solvent effects.[1e,8b,15] Intermolecular interactions between the solvent and fluorophore often produce effects on the electronic properties of the flourescent molecules. For example, the Φ_{fl} of 4-dimethylaminobenzonitrile has been widely investigated because of its twisted intramolecular charge transfer effect which is solvent dependent. An increase in Φ_{fl} for dimethylaminobenzonitrile was found upon lowering the solvent polarity.

1.4 *Twisted Intramolecular Charge Transfer Phenomena*

The twisted intramolecular charge transfer (TICT) phenomenon is usually observed in fluorescent molecules with large motions between donor and acceptor groups.[12] It is a geometrical torsion in the excited state that affects the intramolecular charge transfer. Molecules that undergo the TICT phenomena are known as TICT compounds. The majority of TICT compounds reported in the literature contain amino groups.[12e] A well known TICT compound is 4-dimethylaminobenzonitrile;[12f,g] other examples are dapoxyl sulfonic acid[1c] (*Molecular Probes, Inc.*) and 2,3,5,6-tetraarylbenzo[1,2-b;5,4-b']difuran[16] (*NASA Glenn Research Center, Polymers Branch*).

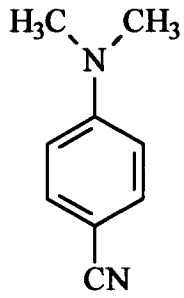

4-dimethylaminobenzonitrile

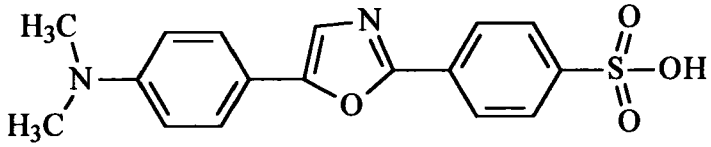

Dapoxyl sulfonic acid

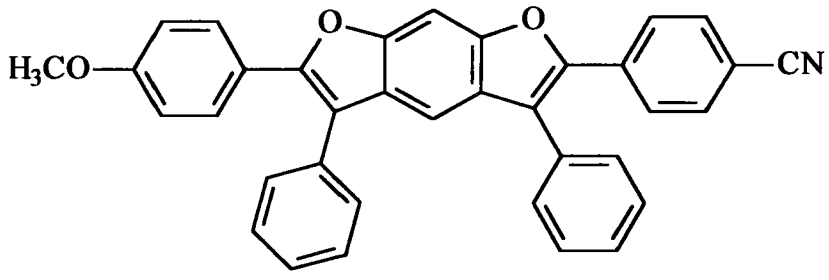

2,3,5,6-tetraarylbenzo[1,2-b;5,4-b']difuran

Most TICT compounds exhibit dual fluorescence in moderately polar solvents like acetonitrile. The dual fluorescence occurs from two different excited states, one being a nonpolar locally excited (LE) state and the other a strongly polar excited state (called TICT state).[12n,o]

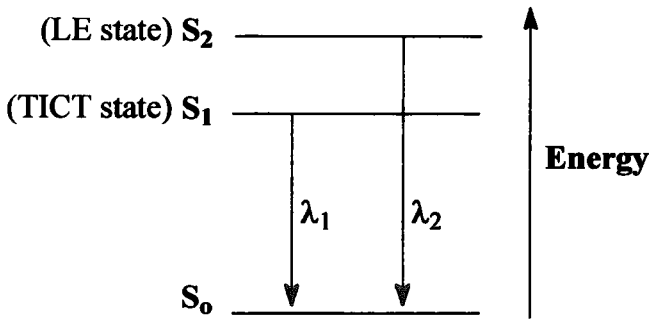

The above excited states diagram represents the dual fluorescence of a typical TICT compound where the TICT state emits at wavelength of λ_1 and the locally excited (LE) state emits at λ_2. Note that this does not include any excited state, structural or solvent effect relaxation. In the emission spectra, the band at shorter wavelength represents the fluorescence from the LE state while the longer wavelength band (called TICT emission) corresponds to the TICT state. The latter is due to intramolecular electron transfer accompanied by a structural change in the excited state resulting from molecular twisting. The degrees of electron transfer and structural change are controlled by local polarity in addition to the size and free volume of the rotating moiety. The emergence of a TICT emission band in polar solvents suggests that the TICT state has a large dipole moment, which interacts more strongly with the polar solvent. The energy gap between the TICT state (S_2) and the ground state (S_o)

decreases with an increase in solvent polarity indicating stabilization.[12] The TICT state is very sensitive to microscopic polarity environments, which makes TICT molecules excellent probes for examining microscopic molecular environments.[12h-k] Although a structureless emission band at the red side of the fluorescence emission of the LE state can be attributed to the TICT phenomena in polar solvents, dual fluorescence in nonpolar solvents does not necessarily support a TICT process.[12m] In some cases the contribution of TICT is enough to observe dual fluorescence in both protic polar and aprotic polar solvents when a molecule contains both donor and acceptor groups.

However, TICT compounds that exhibit fluorescence from a single excited state are also known. These TICT compounds exhibit fluorescence from the polar charge transfer excited state (TICT state) only. This can occur if there is no energy barrier separating the precursor and product species, which can induce an extremely rapidly excited-state relaxation resulting in emission from the TICT state only.[12o] The latter has been observed in conformationally restricted and ground state twisted systems such as 2,3,5,6-tetraarylbenzo[1,2-b;5,4-b']difuran (see page 8),[16] 6-cyanobenzoquinuclidine, and 2,6,N,N-tetramethyl-4-aminobenzonitrile.[12p,q]

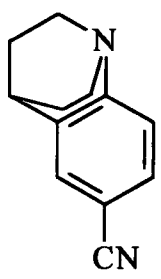

6-cyanobenzoquinuclidine

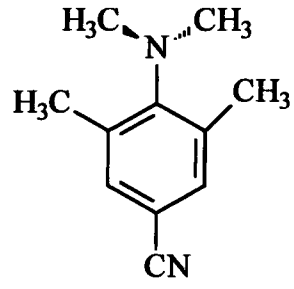

2,6,N,N-tetramethyl-4-aminobenzonitrile

Although the TICT hypothesis has been well investigated[12r] and accepted to explain the behavior of some intramolecular charge transfer excited states, other mechanisms have been proposed, for example, a planar intramolecular charge transfer (PICT) process,[12s] a wagged ICT model,[12t] and a rehybridization ICT.[12w]

In some cases the dual fluorescence has been attributed to the formation of excimer or exciplex. An excimer (or excited dimer) is a complex between two identical molecules, one in an electronically excited state and the other in the ground state. An exciplex (or excited complex) is a complex between an electronically excited molecule and a ground state molecule of a different kind, either solvent molecules or another component in the solution.[12i]

1.5 *Solvent Effects on Fluorescent Molecules: Polarity Parameters*

Solvents may drastically affect the chemical and physical properties of molecules through specific and non-specific interactions.[17] The role of the solvent in determining the photophysics of dye molecules can be divided into dynamic solvent effects (non-specific interactions or collisional) and static solvent effects (specific interactions). Dynamic solvent effects are the result of collisions between the solvent molecules and dye molecules. Static solvent effects occur when the dye molecules and solvent molecules form a complex. These effects are especially important in excited state relaxation processes involving photoinduced torsional rotation about chemical bonds.[17d,e] It is well known that the polarity of a solvent greatly influences the energies of the electronic states as well as the photophysical properties in

aromatic systems.[17f] Thus, the solvent effects for molecules have been of intense investigation. A series of empirical parameters for the polarity of solvents has been developed. These empirical parameters are useful in the understanding of photophysical properties. For example, the dipole moment of a molecule in the ground (μ_g) or excited (μ_{exc}) state could be determined by Mataga and Lippert theory:[17g-i] $\nu_{abs}-\nu_{em} = (2/hca^3)(\mu_{exc}-\mu_g)^2 F(\varepsilon,n)$, where $F(\varepsilon,n)$ is an empirical polarity parameter (see Result and Discussion, Section 4.2, Eq. 9).

Solvents are classified into three main categories: Protic, dipolar aprotic, and non-polar aprotic.[17j] Protic is used to describe solvents which possess a proton-donating functional group, which includes alcohols, amines, and carboxylic acids. These groups have both a large dipole moment and capacity for hydrogen bonding. Dipolar aprotic solvents possess a large dipole moment and donor properties but no acidic protons. Examples include dimethyl sulphoxide, nitriles, and ketones. Non-polar aprotic solvents are liquids with only slight dipole moments, no acidic protons or donor-acceptor properties. Typical examples are hydrocarbons, halocarbons, and ethers. However, within these categories a wide range of solvent behavior is found, which makes it difficult to quantify since invariably mixture of different intermolecular forces must be considered. Table 1 lists a series of empirical polarity parameters[17a,b] and refractive index[18] (n, at 20 °C) for selected solvents.

Table 1. *Polarity Parameters and Refractive Index for Selected Solvents*

Solvent	E_T	π^*	SPP	n
H_2O	1.00	1.09	0.962	1.33299
methanol	0.762	0.60	0.857	1.3288
ethanol	0.654	0.54	0.853	1.361
1-butanol	0.602	0.47	0.837	1.3993
2-propanol	0.546	0.48	0.848	1.3776
cyclohexanol	0.500	---	---	1.4641
CH_3CN	0.460	0.75	0.895	1.3444
t-butanol	0.389	0.41	0.829	1.3878
acetone	0.355	0.71	0.881	1.3588
$ClCH_2CH_2Cl$	0.327	0.807	0.890	1.4448
CH_2Cl_2	0.309	0.82	0.876	1.4242
$CHCl_3$	0.259	0.760	0.786	1.4459
EtOAc	0.228	0.545	0.795	1.3723
1,4-dioxane	0.164	0.553	---	1.4224
toluene	0.099	0.535	0.655	1.4961

The $\mathbf{E_T}$ (also known as Dimroth-Reichardt's $E_T(30)$ scale) scale is based on the solvatochromic shift of the maximum of the first absorption band of 2,6-diphenyl-4-(2,4,6-triphenyl-1-pyridiniumyl)phenoxide. Normalized values range from 0.000 for tetramethyl silane to 1.000 for water.[8a] The π^* (Kamlet-Abboud-Taft π^* scale) is a scale established from the average solvatochromic behavior of a number of indicator solutes.[8a,17c] The **SSP** is a solvent polarity/polarizability scale based on the solvatochroism of the probe 2-(N,N-dimethylamino)-7-nitrofluorene and its homomorph

2-fluoro-7-nitrofluorene. This scale spans values between 1 for DMSO and 0 for the gas phase.[8a]

1.6 *Design of Fluorescent Molecular Sensors*

The current state of knowledge acquired in sensor chemistry is sufficient to understand, and even predict, the response of fluorescent molecular sensors as well as permitting custom-design for specific applications.[12c] The general structure of a molecular fluorescent sensor for specific analytes consists of "fluorophore-spacer-receptor" molecules as shown below:

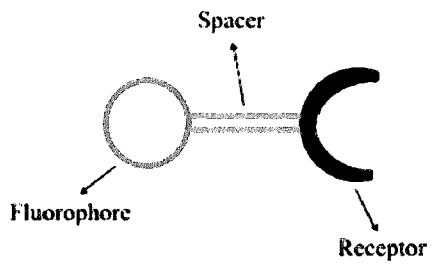

The fluorophore is the specie that produces the photophysical response when an analyte interacts with the receptor site. When the fluorophore is able to communicate a change in its environment sensing has occurred. Usually, the response can be detected by a change in absorption, emission, fluorescence efficiency, excited state lifetime, and/or Stokes shift of the fluorophore.

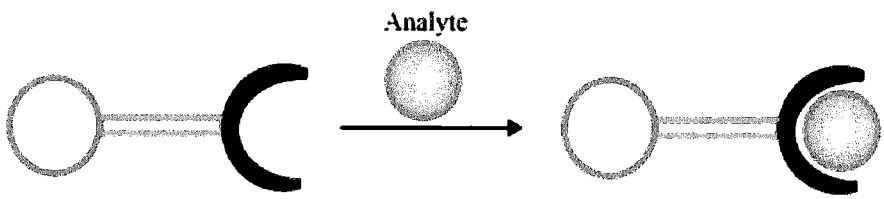

1.7 *Recent Advances in Fluorescent Molecular Sensors*

1.7A *Fluorescent Molecular Thermometer*

Luigi Fabbrizzi and co-workers reported in 1999 a fluorescent molecular thermometer based on a tetraaza macrocycle Ni(II) complex covalently linked through a $-CH_2-$ spacer to a naphthalene fluorophore as shown below.[1d]

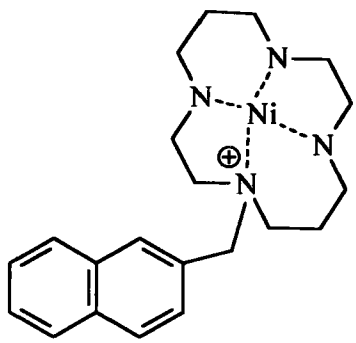

Although other luminescent systems in which the emission varies with temperature have been reported, the above system is distinguished by the use of a metal complex for this purpose. The emission intensity of this Ni(II) complex increases steadily with increasing temperature in the range of 27 to 65 °C. This system could open the way for the design of molecular probes for temperature imaging in biological fluids. Another advantage of this system is its structure since the fluorophore can be replaced at will to impart solubility in water or to provide emission at a desired wavelength range.

1.7B *Fluorescent Sensors for the Detection of Ions*

Different approaches have been applied for the detection of trace ions in solution. Kipp and co-workers recently reported a new system for the sensing of divalent metal ions based on tetra(bipyridilphenyl)porphyrin shown below:[19]

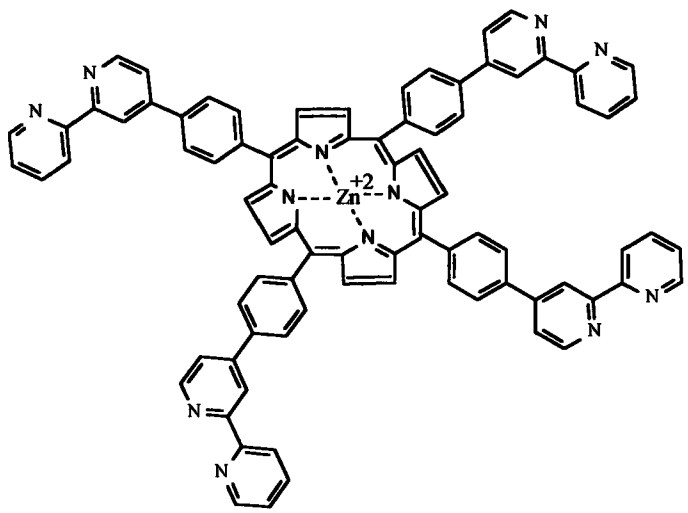

The luminescence of this system was found to be unperturbed by Na(I), Ca(II), Cr(II), Mn(II), Zn(II), Cd(II) and Pb(II) at concentrations of 0.1 to 10^{-3} M. However, measurable quenching was observed for Fe(II), Co(II), Ni(II), and Cu(II) in the range of 10^{-3} to 10^{-4} M. It was found that these metals were capable of quenching the porphyrin fluorescence by an electron transfer mechanism. On the other hand if the porphyrin above does not contain zinc the quenching is observed for all metal ions investigated. Thus, the introduction of Zn(II) into the porphyrin system is essential for the ion selectivity observed.

The in situ measurement of K^+ in biological systems is of great interest, however, its selective detection is difficult because of the competition with Na^+ which generally is present in a much larger concentration. Crown ethers are one of the best molecular systems available to distinguish alkali ions. Although many substrates have been reported to be sensitive for K^+ and Na^+ only modest selectivity was found until recently. The bis-crown-distyryl benzene shown below forms intermolecular sandwich complex with K^+, but not with Na^+, resulting in a dramatic increase in emission intensity, thus providing excellent selectivity for K^+ over Na^+.[13]

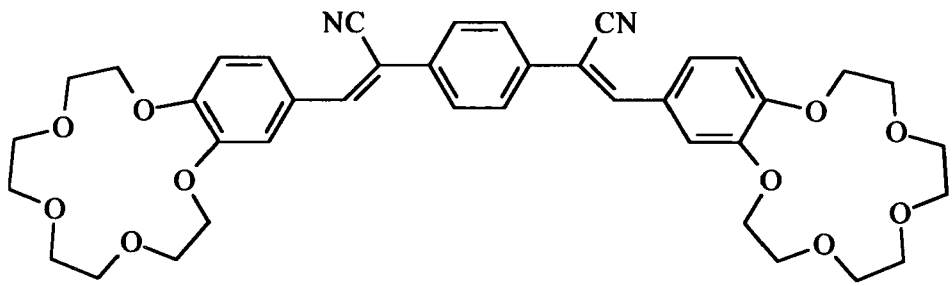

For the above system, a large fluorescence enhancement with K^+ is attributed to the formation of the Z-E isomer. Having two crown ethers was demonstrated to be essential for such selectivity. Similar systems with only a single crown ether exhibit no change in the luminescence intensity upon the addition of Na^+ or K^+.

A system that could be used for the photodynamic transport of metal ions across an organic membrane has been designed by Winkler and co-workers.[4a,c] The metal ion binding of these fluorophores are photo-reversible or chemically reversible. The emission intensity of the fluorophores, shown below, dramatically increases in the presence of Mg(II), Zn(II) or Hg(II). However, only a moderate increase in emission intensity was observed for other metal ions such as Li(I), K(I), Ca(II), Ba(II), Cd(II), and Al(III), while no significant change in emission was observed for Fe(III), Co(II), Ni(II), and Cu(II).

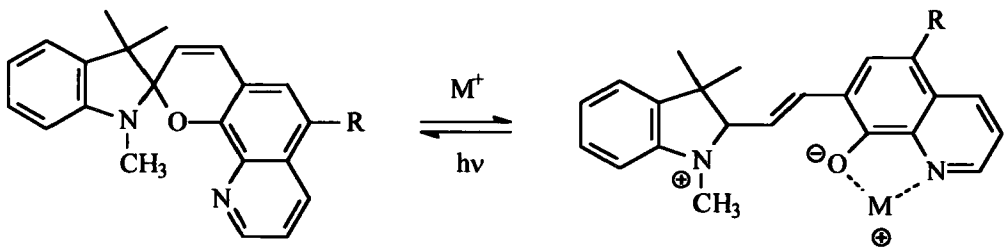

The above spiropyran derivatives where R=H or NO_2 were found to be highly fluorescent and possess a part per billion (ppb) sensitivity for Mg(II), Zn(II), and Hg(II). In addition, the fluorophore containing R = NO_2 liberates the metal ions with the regeneration of the metal-free spiropyran system when the metal chelate is irradiated with visible light for 30 seconds to 5 minutes. Although the same behavior was not observed when R = H, the metal-free spiropyran can be regenerated chemically with the addition of 1 equivalent of nitrilotriacetic acid ($N[CH_2CO_2H]_3$). These spiropyran systems were reported to be capable of detecting Zn(II) at 30 ppb in benzene when R = NO_2 and at 6.5 ppb in ethanol when R = H.

Another approach for the design of selective metal ion chemosensors with potential biological applications has been reported by Torrado and co-workers.[1b] The fluorescent polypeptide, shown below, is water soluble. Systems with a shorter link (lower n) from the peptidyl backbone to the fluorophore resulted in more efficient fluorescence quenching, producing a greater fluorescence change for Cu(II) relative to Ni(II), Fe(II), Co(II), and Zn(II). Combinatorial methods could be utilized to screen molecules of this type for the development of specific ion probes.

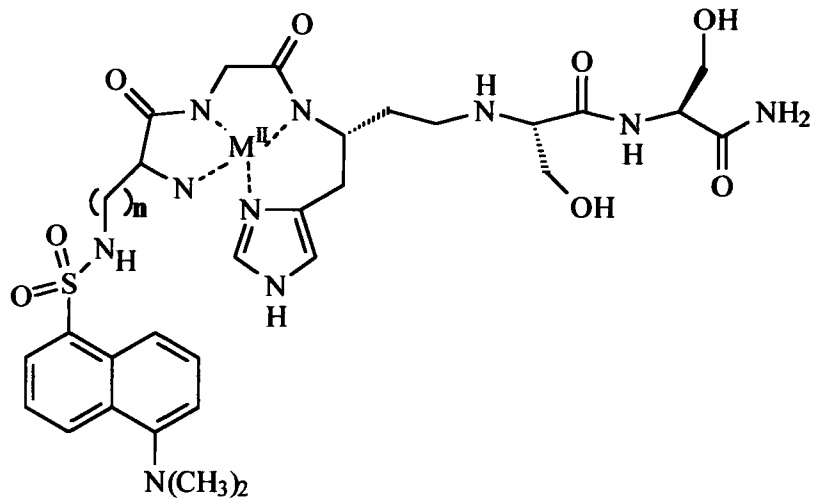

1.8 *Methods for Enhancing Fluorescence Sensitivity*

1.8A *Energy Migration in Conjugated Polymers*

Molecule-based fluorescence sensors in the form of fluorophore-spacer-receptor may possess limited sensitivity. However, if the fluorophore can be funtionalized and attached to a conjugated polymer its sensitivity can be amplified to satisfy the demands of traces detection applications. The ability of conjugated polymers to improve sensitivity is the result of their highly delocalized π-electron system. The most common mechanisms are based on ion-induced conductivity fluctuations resulting from electrostatic effects or by perturbing the conjugation of the polymer.[21] Other mechanisms rely upon the efficient energy transfer properties of the conjugated polymers to produce amplified fluorescence response for the detection of traces of analytes. Such efficient energy migration indicates that the conjugated polymers behave like a "molecular wire".[22]

A binding event to a fluorophore-receptor unit that is interconnected by a conjugated polymer creates an excitation within the system which can migrate through the entire polymer backbone (molecular wire) quenching all fluorescent units (excitons). A complete quenching can be obtained if the energy transfer is faster than the fluorescence lifetime. On the other hand, single molecular fluorophore-receptor units are quenched individually resulting in a weak signal response relative to those attached to a conjugated polymer backbone as illustrated in the following diagram.

Quenching of Fluorescent Units Interconnected by Conjugated Polymers[22b]

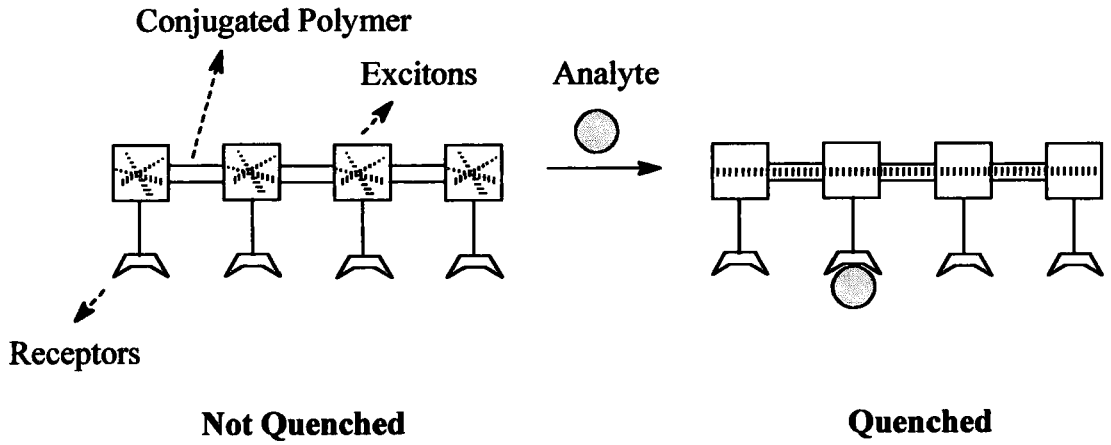

Quenching of Single Molecular Fluorescent Units

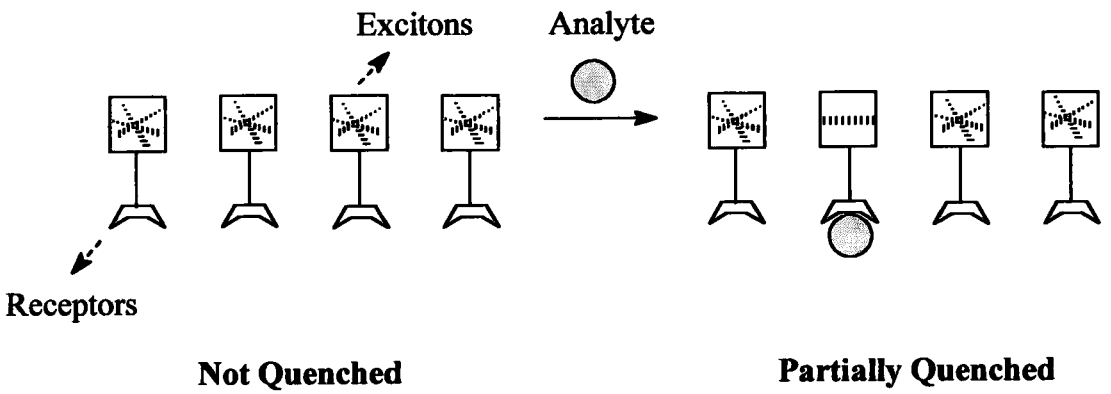

A good example of fluorescence quenching enhancement in a polymer system is shown below. In this approach a squaraine π-conjugated polymer was used as "molecular wire". This system is highly sensitive to alkali metals ions such as Li^+, K^+, and Na^+ at micromolar concentrations. On the other hand, a single unit of squaraine exhibited only a marginal change in its emission intensity under identical experimental conditions.[7b]

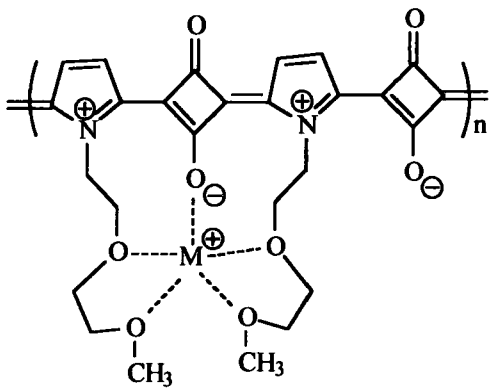

Versus

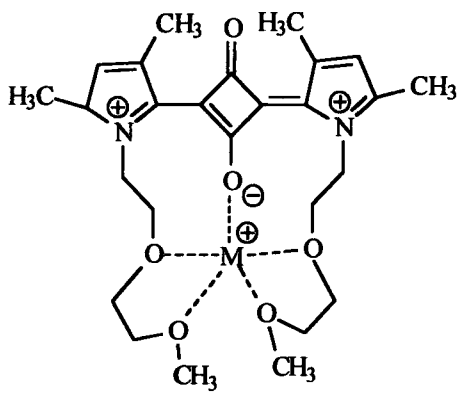

High sensitivity for alkali metal ions

Low sensitivity for alkali metal ions

The conjugated polymer shown below has been found to display a 65-fold enhancement in sensitivity relative to its monomer.[21,22]

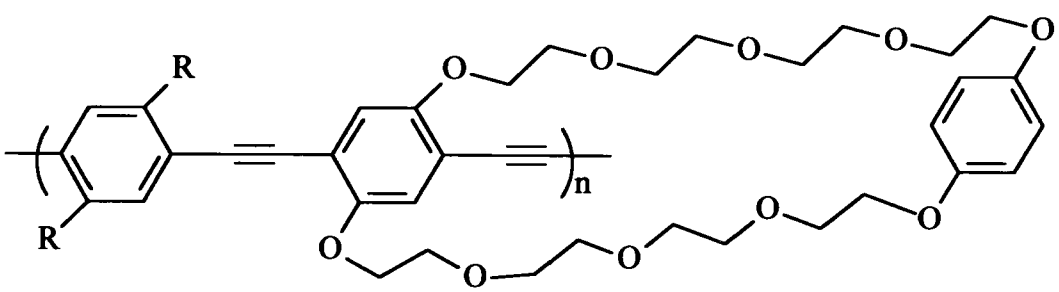

1.8B *Number of Receptor Sites*

Enhancement of fluorescence response caused by a recognition event can be also obtained by increasing the number of receptor sites linked to the fluorophore. A system containing one and two crown ethers as receptor sites have been compared recently by W-S Xia and co-workers.[13] For the fluorophore with two crown ether receptors a large increase in emission is observed after the addition of Na^+ or K^+. However, the same fluorophore containing only one receptor site resulted in no change in luminescence intensity upon addition of Na^+ or K^+.

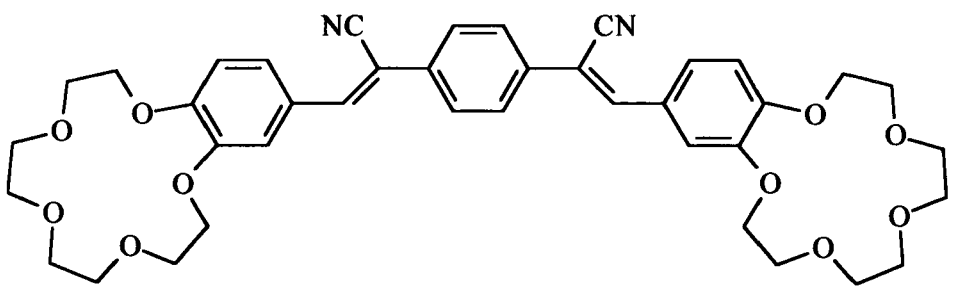

With two receptor sites: Emission increases in the presence of Na^+ or K^+

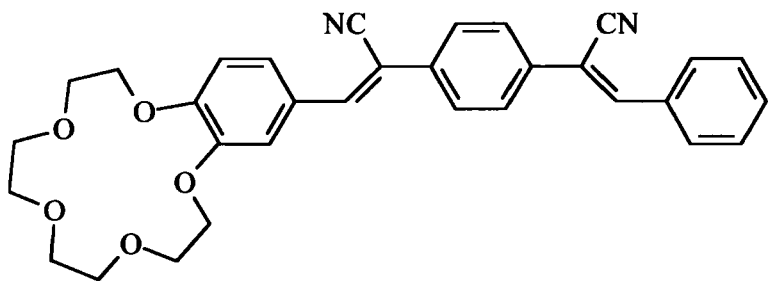

With one receptor site: No change in emission intensity is observed in the presence of Na^+ or K^+

References

1. a) J. S. Marvin, H. W. Helinga, *J. Am. Chem. Soc.*, **1998**, *120*, 7-11. b) A. Torrado, G. K. Walkup, Barbara Imperiali, *J. Am. Chem. Soc.*, **1998**, *120*, 609-610. c) Z. Diwu, C. Zhang, D. H. Klaubert, R. P. Haugland, *Journal of Photochemistry and Photobiology A: Chemistry*, **2000**, *131*, 95-100. d) M. Engeser, L. Fabbrizzi, M. Licchelli, D. Sacchi, *Chem. Commun*, **1999**, 1191. e) Y. Fang, G. Ning, D. Hu, J. Lu, *Journal of Photochemistry and Photobiology A: Chemistry*, **2000**, *135*, 141-145. f) R. Y. Tsien, *Biochemistry*, **1980**, *19*, 2396.

2. L. Fabbrizzi and A. Poggi, *Chemical Society Reviews*, **1995**, 197.

3. a) A. diaspro, M. Robello, *J. Photochem. Photobiol. B, Biol.*, **2000**, *55*, 1-8. b) K. D. belfield, D. J. Hagan, E. W. Van Stryland, K. J. Schafer, R. A. Negres, *Organic Letters*, **1999**, *1*, 10,. c) A. S. Dvornikov, I. Cokgor, P. M. Rentzepis, *IEEE Non Linear Optics: Materials, Fundamentals and Applications*, **1998**, 257.

4. a) J. D. Winkler, C. M. Bowen, V. Michelet, *J. Am. Chem. Soc.*, **1998**, *120*, 3237-3242. b) S. Fery-Forgues, M-T Le Bris, J-P Guette, B. Valeur, *J. Phys. Chem.*, **1988**, *92*, 6233-6237. c) J. Winkler, K. Deshayes, B. Shao, *J. Am. Chem. Soc.*, **1989**, *111*, 769-770. d) C. C-Gude, W. Rettig, R. Lapouyade, *J. Phys. Chem. A*, **1997**, *101*, 9673-9677.

5. a) S. I. Jun, J. W. Lee, S. Sakamoto, K. Yamaguchi, K. Kim, *Tetrahedron Letters*, **2000**, *41*, 471-475. b) A. P. de Silva, S. A. de Silva, *J. Chem. Soc., Chem. Commun.*, **1986**, 1709.

6. M. J. Marsella, P. J. Carrol, T. M. Swager, *J. Am. Chem. Soc.*, **1995**, *117*, 9832-9841.

7. a) Q. Zhou, T. M. Saeger, *J. Am. Chem. Soc.*, **1995**, *117*, 7017-7018. b) C. R. Chenthamarakshan, A. Ajayaghosh, *Tetrahedron Letters*, **1998**, *39*, 1795-1798.

8. a) J. Catalan, *J. Org. Chem.* **1997**, *62*, 8231-8234. b) G. P. Zanini, H. A. Montejano, C. M. Previtali, *Journal of Photochemistry and Photobiology A: Chemistry*, **2000**, 132, 161-166.

9. Charles E. White and Robert J. Argauer, Fluorescence Analysis: A Practical Approach, Marcel Decker, INC. (New York), **1970**.

10. a) Ref. 9. b) B. M. Krasovistskii and B. M. Bolotin, Organic Luminescent Materials, VCH, (Federal Republic of Germany), **1988**. c) A. P. de Silva, H. Q. N. Gunaratne, T. Gunnlaugsson, A. J. M. Huxley, C. P. McCoy, J. T. Rademacher, T. E. Rice, *Chem. Rev.*, **1997**, *97*, 1515-1566.

11. I. Grabchev, *Journal of Photochemistry and Photobiology A: Chemistry*, **2000**, *135*, 41-44.

12. a) N. I. Makarova, V. A. Kharlanov, M. I. Knyazhanskii, E. P. Olekhnvich, *Russian Journal of Organic Chemistry*, **1999**, *35*, 5, 766-773. b) S-L Wang, T-I Ho, *Journal of Photochemistry and Photobiology A: Chemistry*, **2000**, *135*, 119-126. c) R. A. Bissell, A. P. de Silva, H. Q. N. Gunaratne, P. L. M. Lynch, G. E. H. Maguire, C. P. McCoy, K. R. A. S. Sandanayake, *Topic in Current Chemistry*, **1993**, *168*, 223-265. d) K. G. Casey, E. L. Quitevis, *SPIE-Fluorescence Detection II*, **1988**, *910*, 144. e) W. Rettig, *Topic in Current Chemistry*, **1994**, *169*, 253-299. f) E. Lippet, W. Luder, H. Boos (A. Mangini, Ed.), Advances in Molecular Spectroscopy, Pergamon Press, Oxford, **1962**, p. 443. g) B. J. Hrnjez, P. T. Yardi, M. A. Fox, K. P. Johnston, *J. Am. Chem. Soc.*, **1989**, *111*, 1915-1916. h) Y. Matsushita, T. Hikida, *Chemical Physics Letters*, **1998**, *290*, 349-354. i) N. Mataga, H. Yao, T. Okada, W. Rettig, *J. Phys. Chem.*, **1989**, *93*, 3383. j) O. Kajimoto, M. Futakami, T. Kobayashi, K. Yamasaki, *J. Phys. Chem.*, **1988**, *92*, 1347. k) Y-P Sun M. A. Fox, K. P. Jhonston, *J. Am. Chem. Soc.*, **1992**, *114*, 1187. l) Th. Förster, K. Z. Karper, *Phys. Chem.* (Munich), **1954**, *1*, 275. m) N. Nakashima, N. Mataga, *Bull. Chem. Soc. Jpn.*, **1973**, *46*, 3016. n) Z. R. Grabowski, J. Dobkowski, *Pure & Appl. Chem.*, vol. 55, No. 2, pp. 245-252, **1983**. o) C. C-Gude, W. Rettig, *J. Phys. Chem. A*, **1998**, *102*, 7754-7760. p) W. Rettig, *Angew. Chem. Int. Ed. Engl.*, **1986**, *25*, 971-988. q) E. Lippert, W. Rettig, V. B. Koutecky, F. Heisel, J. A. Miehé, *Advances in Chemical Physics*, **1987**, *68*,1. r) Ref. 11 in A. Morimoto, L.Biczók, T. Yatsuhashi, T. Shimada, S. Baba, H. Tachibana, D. A. Tryk, H. Inoue, *J. Phys. Chem. A*, **2002**, *106*, 10089. s) Ref. 8 in A. Morimoto, et al, *J. Phys. Chem. A*, **2002**, 106, 10089. t) Ref. 6a in A. Morimoto, et al, *J. Phys. Chem. A*, **2002**, *106*, 10089. w) Ref. 6b in A. Morimoto, et al, *J. Phys. Chem. A*, **2002**, *106*, 10089.

13. W-S- Xia, R. H. Schmehl, C-J Li, *J. Am. Chem. Soc.*, **1999**, *121*, 5599-5600.

14. W. R. Dawson, M. W. Winsor, *The Journal of Physical Chemistry*, **1968**, *72*, 9.

15. a) T. Werner, K. Fähnrich, C. Huber, O. S. Wolfbeis, *Photochemistry and*

Photobiology, **1999**, *70*(4), 585-589. b) P. R. Bangal, S. Chakravorti, *Journal of Photochemistry and Photobiology A: Chemistry*, **1998**, *116*, 47-56.

16. Michael A. Meador, NASA Glenn Research Center, Cleveland, OH. Unpublished work.

17. a) Reichardt, Solvent and Solvent Effects in Organic Chemistry, **1988**. b) Ref. 8a. c) M. J. Kamlet, J. L. Abboud, R. W. Taft, *J. Am. Chem. Soc.*, **1977**, *99*, 6027-6037. d) G. R. Fleming, Chemical Applications of Ultrafast Spectroscopy, Oxford University Press, New York, **1986**, 179-195. e) G. R. Fleming, S. H. Courtney, M. W. Balk, *J. Chem Phys.*, **1985**, *83*, 215. f) C. Ley, F. Morlet Savary, J. P. Fouassier, P. Jacques, *Journal of Photochemistry and Photobiology A: Chemistry*, **2000**, *137*, 87-92. g) N. Mataga, *Bull. Chem. Soc. Jpn.*, **1956**, *29*, 465. h) E. Lippert, *Naturforsch.*, **1955**, *109*, 541. i) M. A. El-Kemary, *Journal of Photochemistry and Photobiology A: Chemistry*, **2000**, *137*, 9-14. j) Neil Isaacs, Physical Organic Chemistry, 2nd Ed., John Wiley & Sons, Inc., New York, **1995**, p. 194.

18. Arnold J. Gordon, Richard A. Ford; The Chemist's Companion: A Handbook of Practical Data, Techniques, and References; Wiley-VCH: New York, **1973**.

19. R. A. Kipp, Y. Li, J. A. Simon, R. H. Schmehl, *Journal of Photochemistry and Photobiology A: Chemistry*, **1999**, *121*, 27-36.

20. a) A. Kraft, A. C. Grimsdale, A. B. Holmes, *Angew. Chem. Int. ed.*, **1998**, *37*, 402-428. b) B. Wang, M. R. Wasielewski, *J. Am. Chem. Soc.*, **1997**, *119*, 12-21.

21. a) Q. Zhou, T. M. Swager, *J. Am. Chem. Soc.*, **1995**, *117*, 7017. b) T. M. Swager, C. J. Gil, M. S. Wrighton, *J. Phys. Chem.*, **1995**, *99*, 4886.

22. A) Q. Zhou, T. M. Swager, *J. Am. Chem. Soc.*, **1995**, *117*, 12593. b) Biwang Jiang, Ph.D. Dissertation (**1998**), State University of New York.

Section 2 Second Order Nonlinear Optical Chromophores

2.1 *Overview of Nonlinear Optical Materials*

The interest in nonlinear optical (NLO) materials is based on their superiority over existing materials in areas such as information science and technology.[1] This photonic technology is expected to improve the performance of electronic devices since photons do not suffer from electro-magnetic interference (EMI) as electronic components do. Thus, NLO devices could be built more compactly than electronic ones.[2]

There are inorganic and organic materials with NLO properties. Inorganic crystals, such as $LiNbO_3$ have been used in NLO devices for many years, however, they have several disadvantages such as poor thermal stability, process difficulties, and expensive to manufacture.[3] In addition, it is very difficult to modify these materials in order to fine-tune their optical properties.[4] On the other hand, the NLO properties of organic molecules can be readily fine-tuned via systematic structural and functional group modifications.[5] Others advantages of organic NLO materials are (1) inexpensive to produce, (2) good thermal stability, (3) readily integrated with electronic semiconductor and fiber-optic transmission lines,[6] and (4) lower dielectric constant than inorganic ones, resulting in high sensitivity and better performance.[1]

Device materials must satisfy several requirements, including large electrooptic (EO) coefficients (r_{33}), high thermal stability, poling induced EO activity, and good processability among others.[7] In fact, realization of any individual property is not difficult, however, simultaneous optimization of all these properties is not an easy task.[8] Optimization of one property often causes the attenuation of another.[9]

Organic NLO materials can be separated in two main groups, bulk and molecular materials. In the bulk materials the optical nonlinearity is determined by the electronic characteristics of the bulk medium and its NLO response is related to individual bond polarity. On the other hand, molecular materials are those in which molecular units interact through weak van der Waals interactions. Most organic crystals and polymers belong to the latter category of materials.[10]

2.2 *Structural Requirements for Organic 2nd Order NLO Chromophores*

The ability of molecules to possess second order NLO properties rests on the molecular structure in which electrons can be efficiently transferred to create a net dipole moment.[11] Therefore, most chromophores contain electron donor (D) and acceptor (A) groups separated by a conjugated bridge (π) to increase the dipole moment.

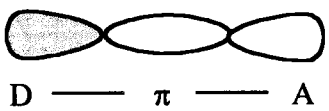

Other requirements for a practical NLO chromophore include chemical stability, thermal stability, solubility, and miscibility with the host polymeric matrix. When the chromophore is exposed to light, charge transfer is generated resulting in a photophysical response as shown below.

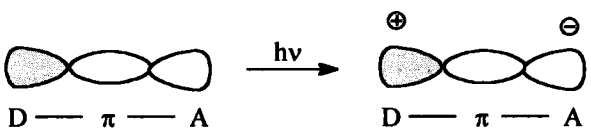

Other materials that exhibit NLO properties are porphyrins[12] and some polymers[13].

The effectiveness of the intramolecular charge transfer to create a net dipole moment in order to generate second order NLO properties is accounted by the first hyperpolarizability (β) value.[14] Therefore, higher β chromophores are expected to have better second order NLO properties.

2.3 *Method to Determine the Molecular Hyperpolarizability* (β)

A common technique to determine the β value is called electric field-induced second-harmonic (EFISH) generation. In this technique a strong dc electric field is applied to a liquid or solution causing a bias on the average orientation of the molecules due to the interaction of the field with the permanent dipoles of the molecules.[1] The β value can be determine by equation 7.

$$\sqrt{I(2\omega)} \propto \gamma^{\circ} = \langle\gamma\rangle + \frac{\mu\beta}{5kT} \qquad \text{Eq. 7}$$

where $I(2\omega)$ is the relative intensity of the frequency double wavelength, $\langle\gamma\rangle$ is the average value of the second hyperpolarizability in different orientations, μ is the dipole moment of the chromophore, k is the propagation constant, and T is the temperature.[11c]

In the literature the molecular nonlinearity is often expressed as $\mu\beta$ instead of β. Usually, these values are given in electrostatic units (esu).

2.4 *Structural Requirements to Increase the Hyperpolarizability* (β)

Extensive research has shown that the molecular second-order hyperpolarizability (β) can be enhanced significantly by increasing donor and/or acceptor strengths and/or by increasing the conjugated pathway between them.[15]

One elegant investigation involving the effect on β value[15] by increasing the strength of donor substituent groups is shown below.

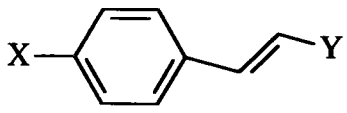

X	Y	β x10^{-30} (esu) *
H	NO_2	8
OCH_3	NO_2	17
OH	NO_2	18
$N(CH_3)_2$	NO_2	50

* in $CHCl_3$

In the above cited research a nitro group was used as the electron acceptor group while the strength of the donor substituent was increased. Note that with increasing strength of the donor group the β value increases. The β value is very low when X = H, suggesting that the molecule possesses only a low dipole moment. Introduction of a methoxy or hydroxy group resulted in a moderate increase of the β value. However, there is not a significant difference between the results from a methoxy and hydroxy group. A dimethylamino group (a strong donor group) dramatically increases the β value, suggesting a large molecular dipole moment in

comparison with the others studied.

The first order Hyperpolarizability, β, can be improved by increasing the conjugation pathway between the electron donor and acceptor groups. This statement was verified by Cheng and co-workers[15] as shown below.

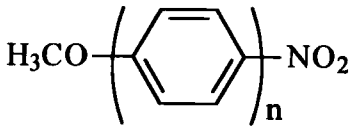

n	β x10^{-30} (esu) *
1	5.1
2	9.2
3	11

* in p-dioxane

Although improvement has been observed by increasing the conjugation length, in some cases increasing the conjugation and changing the substituent groups may compromise the thermal stability of the chromophore. Thus, care is needed in selecting the substituent groups and the structure of the conjugated pathway as well as its length. Research has been conducted to optimize these structural parameters. For example, Rao and co-workers demonstrated that the thiophene group can act as a conjugation pathway, improving the NLO properties relative to a benzene ring. They also found a significant increase in the nonlinear optical coefficient (μβ) value using dicyanovinyl group versus nitro group as an electron acceptor.[11a,18]

The effect of benzene and thiophene rings on the μβ value can be observed below. The introduction of a thiophene ring for a benzene significantly increases the μβ value.

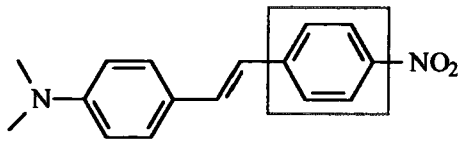

λ_{max} = 424 nm
μβ = 580 x10^{-48}esu

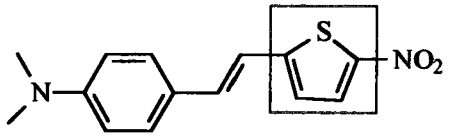

λ_{max} = 478 nm
μβ = 600 x10^{-48}esu

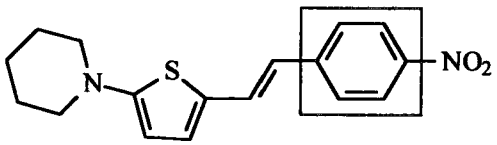

λ_{max} = 460 nm
μβ = 660 x10^{-48}esu

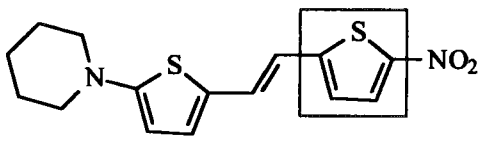

λ_{max} = 516 nm
μβ = 1040 x10^{-48}esu

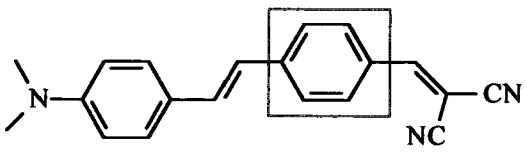

λ_{max} = 468 nm
μβ = 1100 x10^{-48}esu

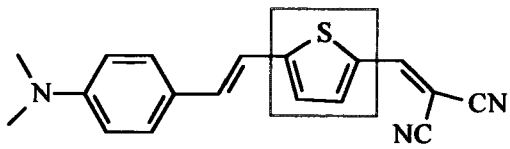

λ_{max} = 513 nm
μβ = 1300 x10^{-48}esu

As mentioned before, analogous chromophores containing dicyanovinyl group (a strong electron withdrawing group) exhibit a higher μβ value than the compounds having nitro group (a relatively weaker electron-withdrawing group).

The orientation of the electron donor and acceptor groups is also an important issue. The latter is because the NLO properties depend on intramolecular charge transfer. A general idea can be obtained from the data shown below.[16]

Structure	β x10^{-30} (esu)
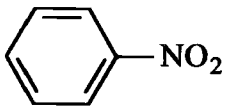	2.2
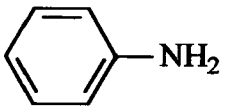	1.1
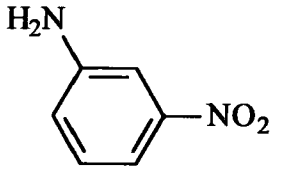	6
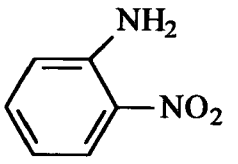	10.2
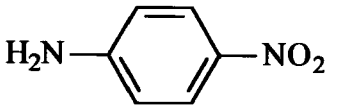	34.5

As shown in the above table, the para and ortho position make possible an effective optical response contrary to the meta position.[16] The efficiency of the intramolecular charge transfer (ICT) depends on the charge transfer resonance within a molecule. The contribution of charge transfer (CT) resonance to the first hyperpolarizability (β) is determinated by a ground state and a low energy charge transfer excited state.[1a,21]

Electron donor (D) and acceptor (A) groups at either para or ortho position allow a direct contribution from the donor to the acceptor as shown below.

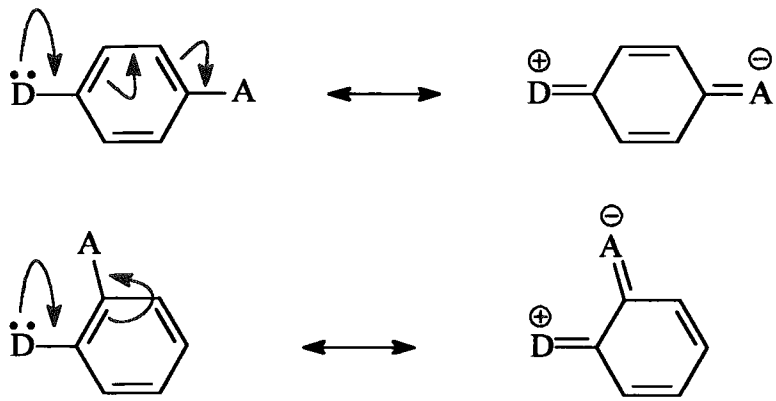

Ground state *CT excited state*

When the donor and acceptor groups are in the meta position the intramolecular charge transfer resonance is forbidden.[17] This explains the low β value obtained for m-nitroaniline.

Another aspect of the structural conformation that may also affect the intramolecular charge transfer is a molecular twist, for example:

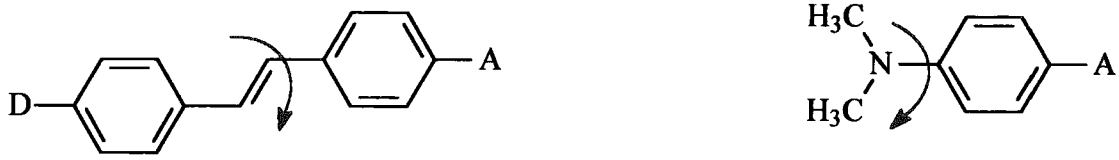

A molecular twist can affect negatively the β value because it can decrease the effectiveness of the intramolecular charge transfer.

2.5 *Selected Recent Publications*

2.5A *Highly Efficient and Thermally Stable Chromophores*

Thiophene has been found to improve NLO properties and thermal stability in conjugated donor-acceptor systems. Cai and co-workers prepared and characterized a series of thienyl-tricyanovinyl-based chromophores with excellent NLO properties and good thermal stability.[18] The molecular nonlinearity ($\mu\beta$) value was found to increase with the incorporation of an additional thienyl moiety, however, this led to a slight decrease in thermal stability (T_d, decomposition temperature) as shown below.

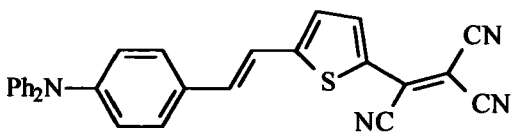

$\mu\beta = 3510 \times 10^{-48}$esu
$T_d = 315\ ^{\circ}C$

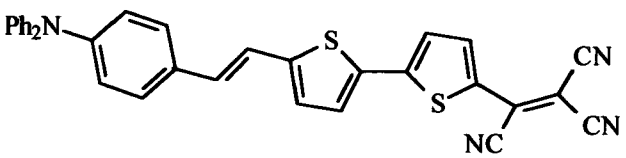

$\mu\beta = 3940 \times 10^{-48}$esu
$T_d = 308\ ^{\circ}C$

A significant improvement in $\mu\beta$ value was obtained with dialkyl amino as electron donor group. However, the T_d decreased greatly. These observations are shown below.

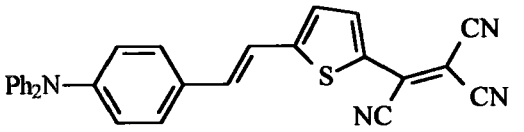

$\mu\beta = 3510 \times 10^{-48}$esu
$T_d = 315\ ^{\circ}C$

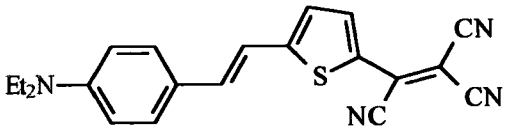

$\mu\beta = 6700 \times 10^{-48}$esu
$T_d = 240\ ^{\circ}C$

2.5B *Polyimide-Based NLO Materials*

Polymeric materials with second order nonlinear optical properties have been extensively studied. For practical applications, these NLO polymeric materials must be soluble in organic solvents and retain their optical quality and thermal stability during and after device fabrication. Although this is challenging, many materials meeting these requirements have been developed; among them, NLO functionalized aromatic polyimides have shown great promise.[19]

An approach to enhance solubility of polyimides is the incorporation of both fluorinated and alicyclic groups. The presence of alicyclic and fluorinated units enhances the solubility of polyimides while maintaining moderate thermal stability (200-300 °C) depending upon which chromophores are attached. Examples of polyimides with and without fluorinated units are shown below.[20]

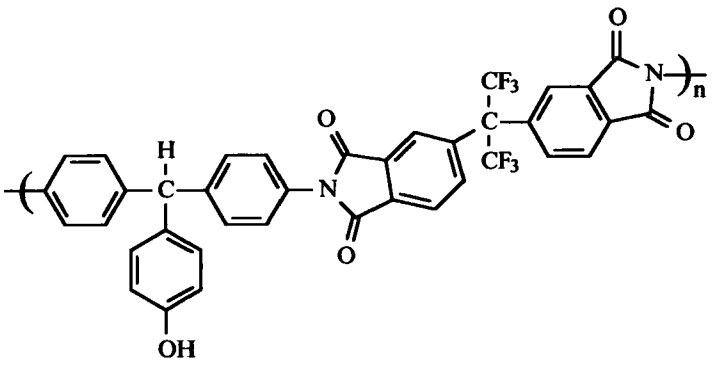

Polyimide with fluorinated units

Very soluble

T_d = 289°C

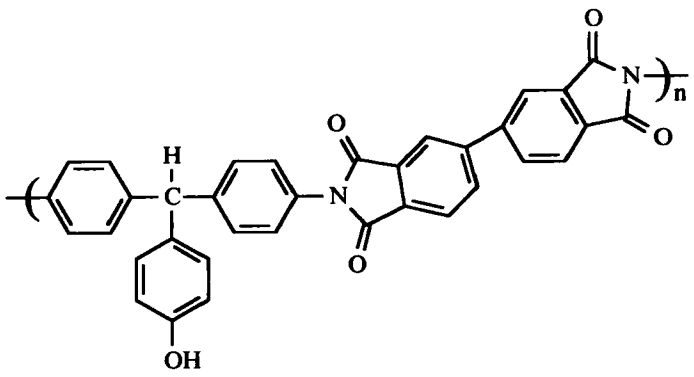

Polyimide without fluorinated units

Mostly insoluble

T_d = 190°C

References

1. a) P. N. Prasad, D. J. Williams, Introduction to Nonlinear Optical Effect in Molecules and Polymers, Wiley-Interscience, New York, **1991**. b) P. N. Prasad, *International Journal of Nonlinear Optical Physics*, **1994**, *3*, (4), 531-541, .

2. P. N. Prasad, B. A. Reinhardt, *Chemistry of Materials*, **1990**, *2*, 660-669.

3. a) S. Allen, *New Scientist*, **1989**, *7*, 59-63,. b) Z. L. Liau, S C. Palmateer, S. H. Groves, J. N. Walpole, L. J. Missagia, *Applied Physics Letters*, **1992**, *60*, (1), 6-8, .

4. O. R. Evans W. Lin, *Chem. Mater.*, **2001**, *13*, 3009-3017.

5. a) W. E. Moerner, S. M. Silence, *Chem. Rev.*, **1994**, *94*, 127-155. b) S. R. Mader, J. E. Sohn, G. D. Stucky, *Materials for Nonlinear Optics: Chemical Perspective*; ACS Symposium series 455, Washington, D. C., **1991**. c) P. N. Prasad, B. A. Reinhardt, *Chemistry of Materials*, **1990**, *2*, 660-669.

6. R. Dagani, *Chem. & Eng. News*, March 4, 22, **1996**.

7. L. R. Dalton, W. H. Steier, B. H. Robinson, C. Zhang, A. Ren, S. Garner, A. Chen, T. Londergan, L. Irwin, B. Carlson, L. Fifield, G. Phelan, K. Kincaid, J. Amend, A. Jen, *J. Mater. Chem.*, **1999**, *9*, 1905-1921.

8. a) A. Harper, S. S. H. Mao, Y. Ra, C. Zhang, J. Zhu, L. R. Dalton, *Chem. Mater.*, **1999**, *11*, 2886-2891. b) C. Zhang, Ph. D. Thesis, University of Southern California, Los Angeles/USA, **1999**. c) S. S. H. Mao, Y. Ra, L. Guo, C. Zhang, L. R. Dalton, A. Chen, S. Garner, W. H. Steier, *Chem. Mater.*, **1998**, *10*, 146-155. d) C. Zhang, A. S. Ren, F. Wang, J. Zhu, L. R. Dalton, *Chem. Mater.*, **1999**, *11*, 1966-1968.

9. C. Zhang, C. Wang, L. R. Dalton, H. Zhang, W. H. Steier, *Macromolecules*, **2001**, *34*, 253-261.

10. K. D. Singer, *Nonlinear Optical Properties of Organic Materials IV*; SPIE Proc., 1460, **1991**.

11. a) V. P. Rao, A. K. Jen, K. Y. Wong, K. Drost, R. M. Mininni, *Nonlinear Optical Properties of Organic Materials V*, SPIE, 1775, 32, **1992**. b) C. T. Shu, W. J. Tsai, A. K-Y Jen, *Tetrahedron Letters*, 37, 39, 7055, **1996**. c) Lawrence L. Brott, Ph.D. Dissertation, University of Cincinnati, Department of Materials Science and Engineering, **1997**. d) ref. 14

12. K. S. Suslick, C. T. Chen, G. R. Meredith, L. T. Cheng, *J. Am. Chem. Soc.*, **1992**, 114, 6928.

13. a) J. K. Gillie, A. P. Haag, K. A. Hazard, M. N. Inbasekaran, P. R. Ashley, T. A. Tumolillo Jr., *Organic Thin Films for Photonic Applications*, 6, **1993**. b) D.R. Robello, P. T. Dao, J. S. Schildkraut, M. Scozzagfava, E. J. Urankar, C. S. Willand, *Chem. Mater.*, **1995**, 7, 284-291. c) M. Ahlheim, A. Fort, Z. Y. Hu, S. R. Marder, J. W. Perry, C. Ruser, M. Staehelin, B. Zysset, *Science*, **1996**, *271*, 335.

14. a) M.B-Desce, V. Alain, L. Midrier, R. Wortmann, S. Lebus, C. Glania, P. Kramer, A. Fort, J. Muller, M. Barzoukas, *Journal of Photochemistry and Photobiology A: Chemistry*, **1997**, *105*, 115-121. b) D. J. Williams, *Angew. Chem. Int. Ed. Engl.*, **1984**, *23*, 690-703.

15. L-T Cheng, W. Tam, S. T. Marder, A. E. Stiegman, G. Rikken, C.W. Spangler, *J. Phys. Chem.*, **1991**, 95, 10643-10652.

16. J. L. Oudar, D. S. Chemla, *The Journal of Chemical Physics*, **1977**, *66*, (6), 2664-2668.

17. Jerry March, Advanced Organic Chemistry, 4th Ed., John Wiley & Sons, New York, pp. 507-511.

18. C. Cai, L. Liakatas, M-S Wong, M. Bosh, C. Bosshard, P. Gunter, S. Concilio, N. Tirelli, U. W. Suter, *Organic Letters*, **1999**, 1, 11, 1847-1849.

19. Chen T-A, Jen A. K-Y, Cai Y., *Macromolecules*, **1996**, 29, 535-539.

20. E-H Kim, I. K. Moon, H. K. Kim, M-H Lee, S-G Han, M. H. Li, K-Y Choi, *Polymer*, **1999**, 40,, 6157-6167.

21. J. L. Ounda, D. S. Chemla, *J. Chem. Phys.*, **1977**, 66, 2664.

Section 3 Organic Molecules Containing Imidazole Derivatives

3.1 *Imidazole-based Molecules: Research and Applications*

Molecules containing imidazole ring(s) have found numerous applications in biological, materials, and optical technologies. Summaries some of these applications are provided below. Molecules containing imidazole derivatives are of great interest because of their antitumor and antibacterial activities,[1] inhibition of acyl-CoA:cholesterol acyltransferase,[2] inhibition of poliovirus,[3] fluorescence properties,[4] complexation ability,[5] molecular reception based on the molecular tweezer concept,[6] two photons absorbing properties,[7] and RNA-protein recognition,[8] among others. Some recent investigations of imidazole derivatives are: anion binding by biimidazoles,[9] solid-state polymeric dye as new laser media,[10] self assembly with copper(II),[11] copper(I)-azoimidazoles complexes,[12] synthesis of benzimidazoles,[13] P,N-chelating ligand for asymmetric catalysis,[5] dyes for artificial light-harvesting,[14] coordination behavior of bis(benziimidazol)pyridine,[15] synthesis of benzimidazoyl thiophenes,[16] contribution of multiple charge transfer chromophore to poled polymer film,[17] intramolecular photoinduced electron transfer for cations,[18] excited state intramolecular proton transfer and metal ion complexation,[19] chiral molecular assemblies through interfacial coordination,[20] trinuclear nickel(II) core,[21] disk-like blue electroluminescent materials,[22] preparation of benziimidazole-imide copolymers,[23] two-photon induced blue fluorescent emission,[24] synthesis and characterization of Zn(II), Cd(II), Hg(II) complexes,[25] spectroscopy and structure of phenyl imidazoles,[26] and selective imidazole recognition.[27]

3.2 *Applications and Investigations of Fluorescent Imidazole Dyes*

Imidazole derivatives that undergo excited-state intramolecular proton transfer (ESIPT) have been subject to numerous investigations. Molecules with ESIPT behavior have potential for applications in laser dyes,[28] photostabilizers,[29] optical memory devices,[30] solar energy concentrators,[31] electroluminescent materials with high photochemical stability,[32] high energy radiation detectors,[33] and fluorescent probes.[34] A good example is 2-(2'-hydroxyphenyl)benzimidazole[35] (shown below) which involves tautomeric forms in the emission of light-ESIPT. This imidazole dye shows high Stokes shift, good thermal stability, and photophysical stability.

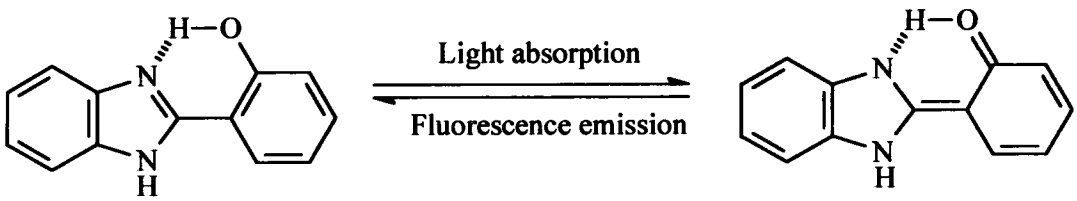

Other analogous molecules that have been investigated are:[36]

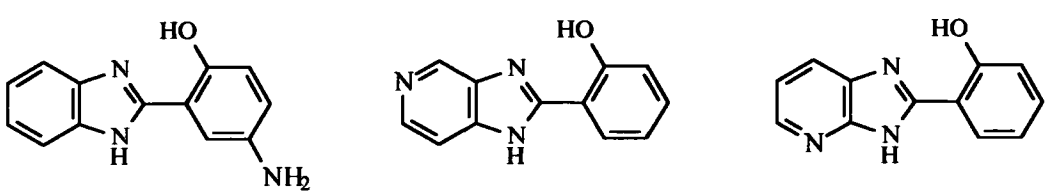

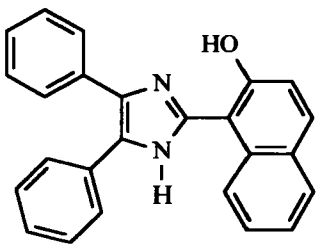

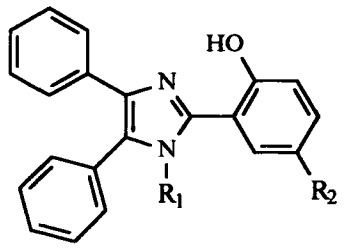

$R_1 = R_2 = H$
$R_1 = H, R_2 = Br$
$R_1 = C_4H_9, R_2 = H$

Imidazole-based fluorophores have also found biological applications. For example, alkyl-linked benzimidazole **I** has improved the anti-pneumocystis carinii pneumonia, the most common cases of mortality in AIDS patients,[37] activity in comparison with non-imidazole molecules.[38]

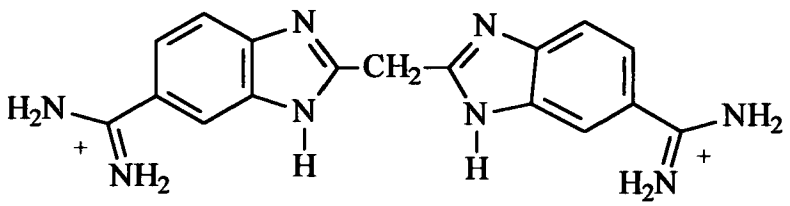

I

Tetrasubstituted imidazole **II** has shown good oral bioavailability in rats and rhesus monkeys, and demonstrates significant improvement in measures of disease progression in a rat adjuvant-induced arthritis model.[39]

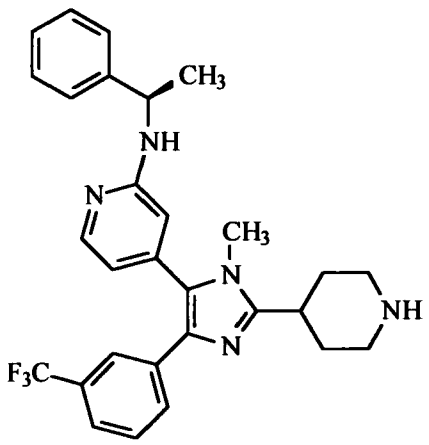

II

Anion binding is another characteristic of imidazoles dyes. One example is the bisimidazole diamides of the form **III** which has shown to serve as multiple H-bond donors and as anion-sensitive fluorophores.[40]

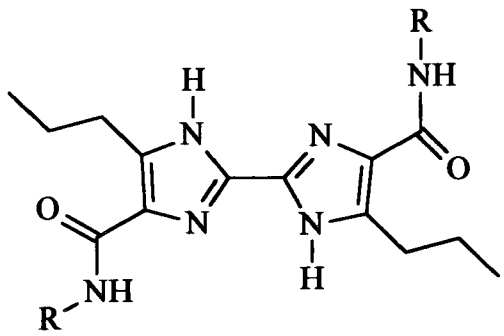

III

It has been reported that 4,5-diphenylimidazole (**IV**) exhibits anomalous fluorescence behavior, most notably, in acidic and basic solutions.[41] The fluorescence behavior of **IV** has been compared with similar molecules such as **V** and **VI**. It was found that the fluorescence quantum yield (Φ) of **IV** is 0.68 and 0.14 for **V** in 0.1 N NaOH. On the other hand, **VI** has a Φ of 0.19 and 0.22 in ethanol and

cyclohexane, respectively.[42]

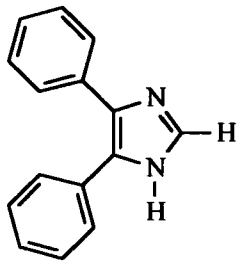

IV

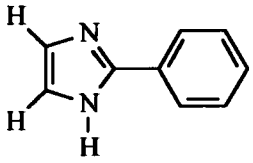

V

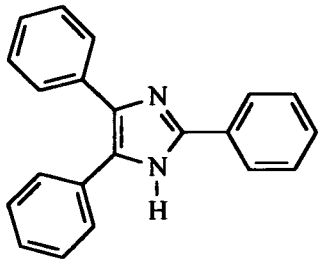

VI

3.3 *Imidazole-based Molecules for Materials Science Applications*

It has been reported that 2-substituted benzimidazole **VII**[43] and **VIII**[20] can easily coordinate with Ag(I) to form a coordination polymer film. Under the coordination inducement, those benzimidazole derivatives **VII** with a very short alkyl chain (R) or even no alkyl substitute can form a stable monolayer through the coordination with Ag(I). In the case of **VIII**, the coordination with Ag(I) resulted in an ultrathin film that became chiral although the ligand itself is achiral. It has been suggested that the chirality was developed due to the formation of a helical coordination polymer through the interfacial coordination.

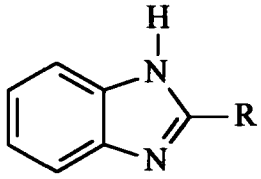

VII

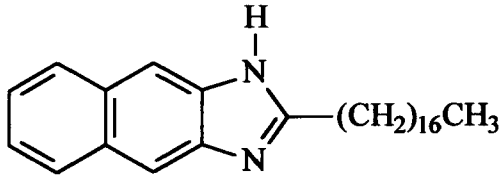

VIII

Benzimidazole derivatives **IX** have shown biological activity in coated formulations. They suppress the secretion of acid in the stomach, which makes them very useful for the treatment of gastric or duodenal ulcers.[44]

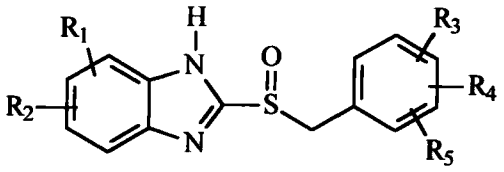

IX

Polyimidazoles of the form **X** and **XI** have been found to be useful as adhesives, coatings, films, membranes, moldings, and composite matrices. They are thermally stable with glass transition temperatures (T_g) ranging from 203 °C to 318 °C. Themogravimetric analysis has shown no weight loss occurring below 300 °C in air or nitrogen with a five percent weight loss occurring at about 400 °C in air and at 495 °C in nitrogen.[45]

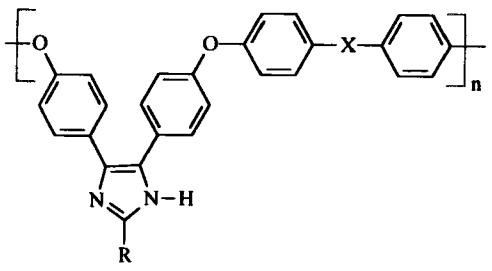

X

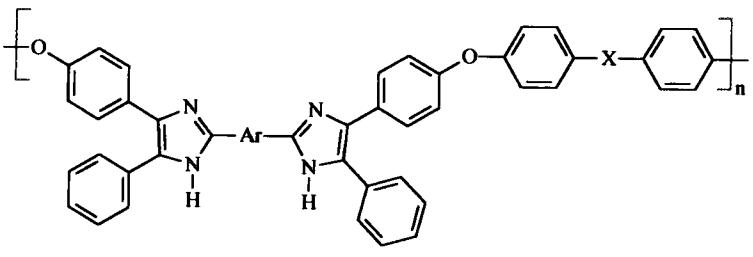

XI

Thin films of thermoplastic poly(arylene ether imidazole) of the form **XII** have been found to be suitable for use as surface modifiers for neat resin epoxy or neat resin bismaleimide panels, as well as for graphite/epoxy or graphite/bismaleimide composite panels.[46]

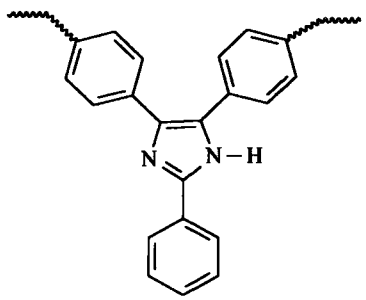

XII

Donor-acceptor imidazole derivatives with the general formula **XIII** and **XIV** have been found to possess nonlinear optical properties, good thermal stability, and solubility.[47]

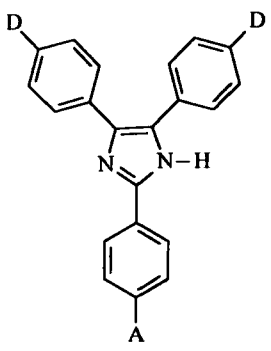

XIII

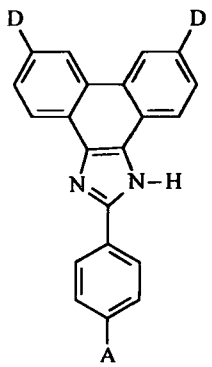

XIV

Polymer **XV** has glass transition temperature of 217 °C and good nonlinear optical response that is stable at temperatures up to 125 °C.[48]

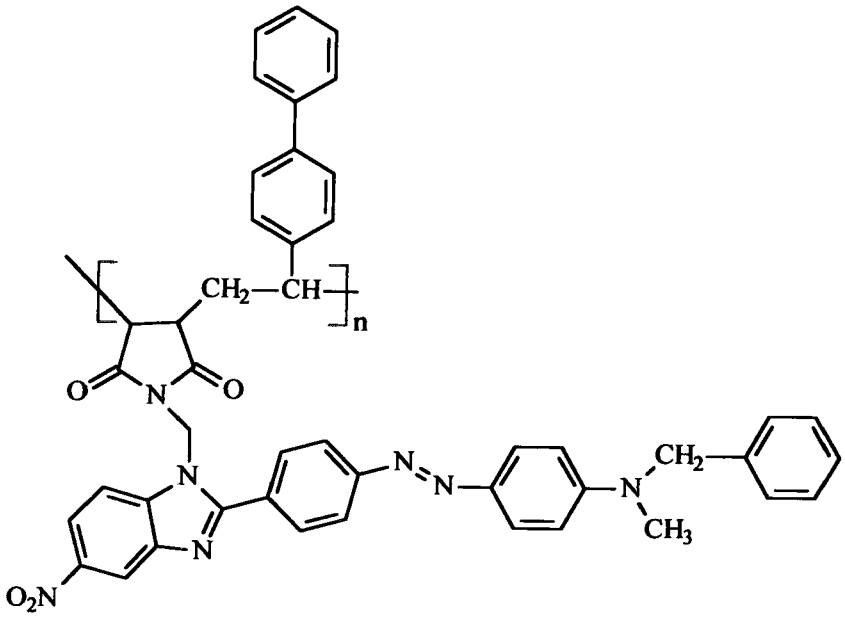

XV

References

1. J. R. Lewis, *Nat. Prod. Rep.*, **1992**, *9*, 81 and 323.

2. T. P. Maduskuie Jr., R. G. Wilde, J. T. Billheimer, D. A. Cromley, S. Gemain, P. J. Gillies, C. A. Higley, A. L. Johnson, P. Pennev, E. J. Shimshick, R. R. Wexler, *J. Med. Chem.*, **1995**, *38*, 1067.

3. Frantz Victor, Thomas J. Brown, Kristina Campanale, Beverly A. Heinz, Lisa A. Shipley, Kenneth S. Su, Joseph Tang, Lori M. Vance, and Wayne A. Spitzer, *J. Med. Chem.*, **1997**, *40*, 1511.

4. F. C. Krebs, H. Spanggaard, *J. Org. Chem.*, **2002**, *67*, 7185.

5. Axel Figge, Hans J. Altenbach, David J. Brauer and Patrick Tielmann, *Tetrahedron: Asymmetry*, **2002**, *13*, 137.

6. F. C. Krebs, M. Jorgensen, *J. Org. Chem.*, **2001**, *66*, 6169.

7. Kannan, R.; He, G. S.; Yuan, L.; Xu, F.; Prasad, P. N.; Dombroskie, A. G.; Reinhardt, B. A.; Baur, J. W.; Vaia, R. A.; Tan, L.-S., *Chem. Mater.*, **2001**, *13*, 1896.

8. T. Hermann, E. Westhol, *Chemistry & Biology*, **1999**, *6*, R335.

9. C. P. Causey, W. E. Allen, *J. Org. Chem.*, **2002**, *67*, 5963.

10. Sunita Singh, V. R. Kanetkar, G. Sridhar, V. Muthuswamy and K. Raja, *Journal of Luminescence*, **2003**, *101*, 285.

11. Liu, H.-K.; Sun, W.-Y.; Tang, W.-X.; Yamamoto, T.; Ueyama, N., *Inorg. Chem.*, **1999**, *38*, 6313.

12. Joydev Dinda, Umasankar Ray, Golam Mostafa, Tian-Huey Lu, Anwar Usman, Ibrahim Abdul Razak, Suchada Chantrapromma, Hoong-Kun Fun and Chittaranjan Sinha, *Polyhedron*, **2003**, *22*, 247.

13. M. R. Kamal, et al., *Heterocycles*, **1999**, *50*, 819

14. A. Pawlik, A. Ouart, S. Kirstein, H-W Abraham, S. Daehne, *Eur. J. Org. Chem.*, **2003**, 3065.

15. A. E. Ceniceros-Gomez, et al., *Heteroatom Chemistry*, **2000**, *11*, 392.

16. K. Starcevic, D. W. Boykin, G. Karminski-Zamola, *Heteroatom Chemistry*, **2003**, *14*, 218.

17. Li, S.; Yang, Z.; Wang, P.; Kang, H.; Wu, W.; Ye, C.; Yang, M.; Yang, X., *Macromolecules*, **2002**, *35*, 4314.

18. G. Jones II, J. A. C. Jimenez, *Tetrahedron Letters*, **1999**, *40*, 8551.

19. M. M. Henary, C. J. Fahrni, *J. Phys. Chem. A*, **2002**, *16*, 5210.

20. J. Yuan, M. Liu, *J. Am. Chem. Soc.*, **2003**, *125*, 5051.

21. H. Adams, S. Clunas, *Inorganic Chemistry Communications*, **2002**, *5*, 211.

22. Y. T. Tao, et al., *J. Mater. Chem.*, **2001**, *11*, 768.

23. M. Berrada, F. Carriere, *J. Mater. Chem.*, **2002**, *12*, 3551.

24. Z-L Huang, H. Lei, *J. Mater. Chem.* **2003**, *13*, 708.

25. R. López-Garzón, et al., *Inorganica Chimica Acta*, **1997**, *258*, 33.

26. M. R. Hockridge, et al., *Chemical Physics Letters*, **1999**, *302*, 538.

27. D. Paul, J. A. Wytko, *Inorg. Chem.* **2002**, *41*, 3699.

28. R. Sastre, A. Costela, *Adv. Mater.*, **1995**, *7*, 198.

29. J. Catalan, F. Fabero, M. S. Guijarro, R. M. Clarumunt, M. D. Santa Maria, *J. Am. Chem Soc.*, **2000**, *112*, 747.

30. X. Chang, G. Tang, G. Zang, Y. Liu, W. Chen, *J. Opt. Soc. Am.*, B 15, **1998**, 854.

31. F. Volmer, W. Rettig, *J. Photochem. Photobiol. A: Chem.*, **1996**, *95*, 143.

32. R.M. Tarkka, X. Zhang, S. A. Jenekhe, *J. Am. Chem Soc.*, **1996**, *100*, 14514.

33. P. T. Chou, M. L. Martinej, *Radiat. Phys. Chem.*, **1993**, *41*, 373.

34. S. K. Das, S. K. Dogra, *J. Chem. Soc., Faraday Trans.*, **1998**, *94*, 139.

35. P. Chou, D. McMorrow, T. J. Aartsma, M. Kasha, *J. Phys. Chem.*, **1984**, *88*, 4596.

36. a) M. G. Holler, L. F. Campo, A. Brandelli, V. Stefani, *J. Photochem. Photobiol. A: Chem.*, **2002**, *149*, 217. b) F. E. L. S. Kol'tsova, A. N. Petrukhin, A. A. Titov, A. I. Shiyonok, N. L. Zaichenko, V. S. Marevtsev, O. M. Sarkisov, *J. Photochem. Photobiol. A: Chem.*, **2003**, *156*, 15. c) M. M. Balamurali, S. K. Dogra, *J. Photochem. Photobiol. A: Chem.*, **2002**, *154*, 81.

37. G. W. Niedt, R. A. Schinella, *Arch. Pathol. Lab. Med.*, **1985**, *109*, 727.

38. a) R. R. Tidwell, S. K. Jones, N. A. Naiman, I. C. Berger, W. R. Brake, C. C. Dykstra, J. E. Hall, *Antimicrob. Agents Chemother.*, **1993**, *37*, 1713. b) R. L. Lombardy, F. A. Tanious, K. Ramachandran, R. R. Tidwell, W. D. Wilson, *J. Med. Chem.*, **1996**, *39*, 1452.

39. Liverton, N. J.; Butcher, J. W.; Claiborne, C. F.; Claremon, D. A.; Libby, B. E.; Nguyen, K. T.; Pitzenberger, S. M.; Selnick, H. G.; Smith, G. R.; Tebben, A.; Vacca, J. P.; Varga, S. L.; Agarwal, L.; Dancheck, K.; Forsyth, A. J.; Fletcher, D. S.; Frantz, B.; Hanlon, W. A.; Harper, C. F.; Hofsess, S. J.; Kostura, M.; Lin, J.; Luell, S.; O'Neill, E. A.; Orevillo, C. J.; Pang, M.; Parsons, J.; Rolando, A.; Sahly, Y.; Visco, D. M.; O'Keefe, S. J., *J. Med. Chem.*, **1999**, *42*, 2180.

40. a) S. Fortin, A. L. Beauchamp, *Inorg. Chem.* **2000**, *39*, 4886. b) C. P. Causey, W. E. Allen, *J. Org. Chem.*, **2002**, *67*, 5963.

41. a) J. Hennessy, A. C. Testa, *J. Phys. Chem.*, **1972**, *76*, 3362. b) P. Takach, A. C. Testa, *J. Photochem.*, **1986**, *34*, 349.

42. A. C. Testa, *Journal of Luminescence*, **1991**, *50*, 243.

43. H. F. Gong, M. H. Liu, *Langmuir*, **2001**, *17*, 6228.

44. European Patent Application (#99307611.6), Hanmi Pharm. Co., **1999**.

45. USA Patent (#5,116,934), National Aeronautics and Space Administration, **1992**.

46. USA Patent (#5,496,639), National Aeronautics and Space Administration, **1996**.

47. a) C. R. Moylan, R. D. Miller, R. J. Twieg, K. M. Betterton, V. Y. Lee, T. J. Matray, C. Nguyen, *Chem. Mater.*, **1993**, *5*, 1499. b) Donald M. Burland, Robert D. Miller, Cecilia A. Walsh, *Chemical Reviews*, **1994**, *94*, 31.

48. T. Verbiest, C. Samyn, et al., *Macromol. Rapid Commun.*, **1998**, *19*, 349.

CHAPTER II

RESULTS AND DISCUSSION

Section 4 Syntheses and Photophysical Properties of Imidazole Dyes

4.1 *Synthesis of Highly Fluorescent Thienyl-Imidazole Aldehydes*

4,4'-Disubstituted benzils **2** (R = H, CH_3, OCH_3) were prepared by the oxidation of the corresponding 4,4'-disubstituted benzoin.[1] Thienyl imidazoles **3** were synthesized in 70-87% yield by the condensation of 2-thiophene carboxaldehyde (**1**) and the corresponding benzil (**2**) as shown in Scheme 1. The reaction mixture was refluxed for 6 h or until the starting material **2** had disappeared as monitored by TLC.

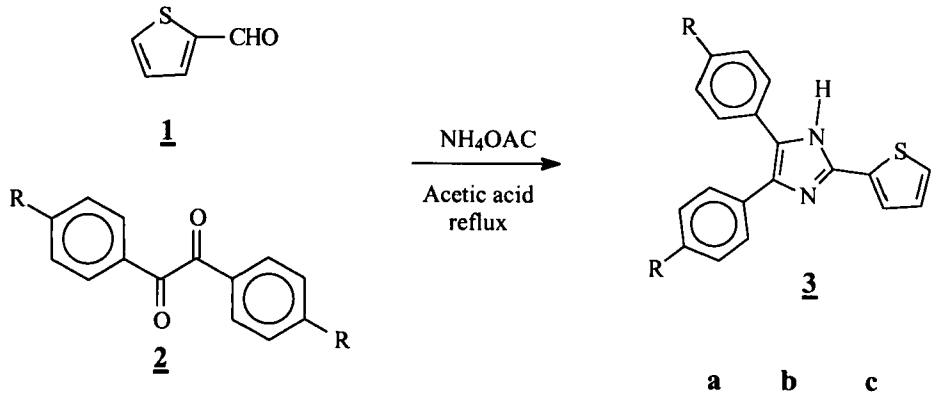

	a	b	c	d
R=	H,	CH_3,	OCH_3,	$N(CH_3)_2$
Yield=	87%,	75%,	82%,	70%

Scheme 1. *Synthesis of thienyl imidazole compounds.*

Longer reaction time up to 15 h did not improve the reaction yield. It was found that compounds 3 exhibit a [1,3]-sigmatropic rearrangement[2] in the imidazole ring (Scheme 2). This hydrogen shift is too fast to observe isomers on the ^{1}H NMR time scale, giving only the average spectrum (Figure 2).

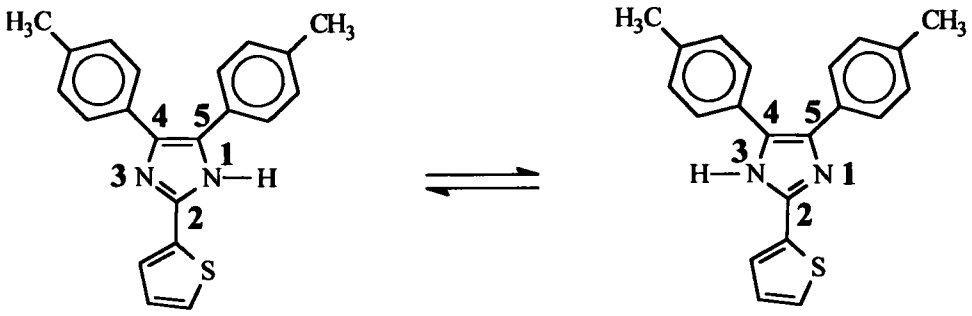

Scheme 2. *[1,3]-Sigmatropic rearrangement on the imidazole ring of* **3b**.

Thienyl imidazoles 3 were methylated to protect the active proton on the imidazole ring (Scheme 3) from potential side reactions in the next step, the formylation reaction. The desired product was obtained when 1.0 to 1.5 equivalents of iodomethane was used. However, a salt of **4** was formed with an excess greater than 1.5 equivalents. The reaction was carried out in DMA at 40-50 °C and potassium carbonate was used as base. The reaction yield was in the range of 65-90%. Once the 1-position of the imidazole ring is methylated the possibility of a proton shift is eliminated. As result the ^{1}H NMR spectra showed two non-equivalent phenyl rings as well as two non-equivalent methyl and methoxy groups for **4b** and **4c**, respectively (Figure 2).

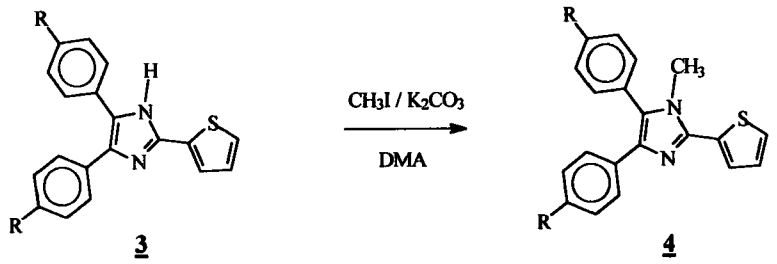

	a	b	c	d
R=	H,	CH_3,	OCH_3,	$N(CH_3)_2$
Yield=	65%,	90%,	86%,	78%

Scheme 3. *Methylation at the 1-position of the imidazole ring.*

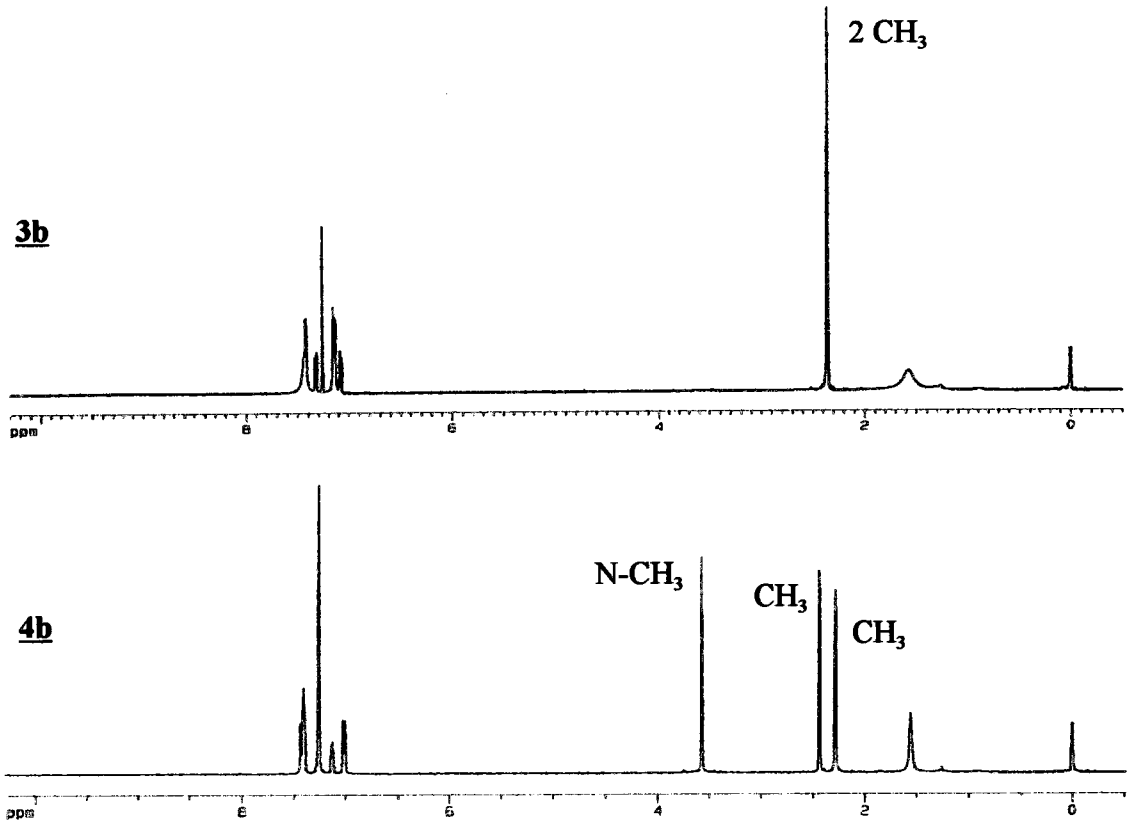

Figure 2. *Comparison of* ^{1}H NMR *spectra of* **3b** *and* **4b** *in* $CDCl_3$*/TMS.*

The [1,3]-sigmatropic rearrangement or tautomeric equilibrium on the imidazole ring has been investigated. Studies of benzimidazole derivatives have shown that the tautomeric equilibrium (Scheme 4) plays an important role in their coordinating behavior.[3] On the other hand, isomers of a benzimidazole derivative have been detected by GC-MS as one compound (Scheme 5). Upon methylation (Scheme 6) the isomers were detected as two different compounds since the hydrogen shift cannot occur.[4]

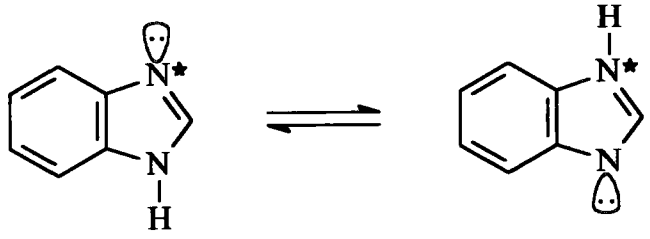

Scheme 4. *Benzimidazole tautomeric equilibrium.*

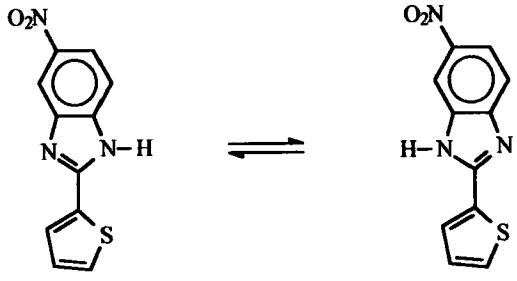

Scheme 5. *Benzimidazole isomers detected by GC-MS as one compound.*

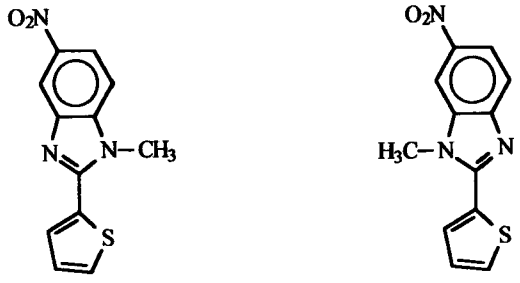

Scheme 6. *Benzimidazole isomers detected by GC-MS.*

Thienyl imidazoles **4** were treated with n-BuLi at -63 °C and then DMF to afford adehydes **5** (Scheme 7). This formylation reaction was very sensitive to moisture and for that reason, glassware, solvent, and reagents had to be strictly anhydrous. Aldehydes **5a-c** were obtained as yellow solids while **5d** was red. A bright visual green fluorescence was observed when these yellow solids were dissolved in organic solvents, such as ethyl acetate, acetone, dichloromethane, or toluene. However, this striking feature was not observed for **5d**.

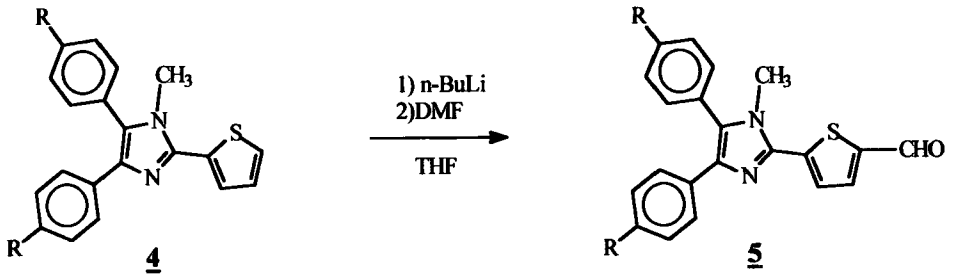

Scheme 7. *Synthesis of highly fluorescent thienyl imidazole aldehydes.*

Crystals of **5b** and **5c** were obtained from methanol and their crystal structures were determined by single crystal X-ray diffraction. The structures and summary of data collection parameters are given in Figures 3 and 4, and Tables 2 and 3, respectively. Table 4 shows a comparison of selected bond lengths for **5b**, **5c**, and average lengths.[5] It is noted that the bond lengths C(7)-C(10) and C(8)-C(17), for both **5b** and **5c**, which connect the donor substituted phenyls with the imidazole ring

are slightly different. This subtle difference may be related to the dihedral angle effect. For example, the aldehyde **5c** has a bond length for C(7)-C(10) of 1.482(18) Å and its related dihedral angle N(1)-C(7)-C(10)-C(11) is 89.43(18) deg. The bond length C(8)-C(17) is 1.474(19) Å while the related dihedral angle is 16.8(2) deg. Note that the dihedral angle N(1)-C(7)-C(10)-C(11) (which has the larger dihedral angle, 89.43(18) deg.) is related to bond C(7)-C(10), which has the longest length, 1.482(18) Å. This observation may suggest that the bond C(7)-C(10) has more carbon-carbon single bond character than C(8)-C(17). This result may be expected since a large dihedral angle could negatively affect the conjugation required for good intramolecular charge transfer, resulting in a longer bond length in comparison with that of a more conjugated system.

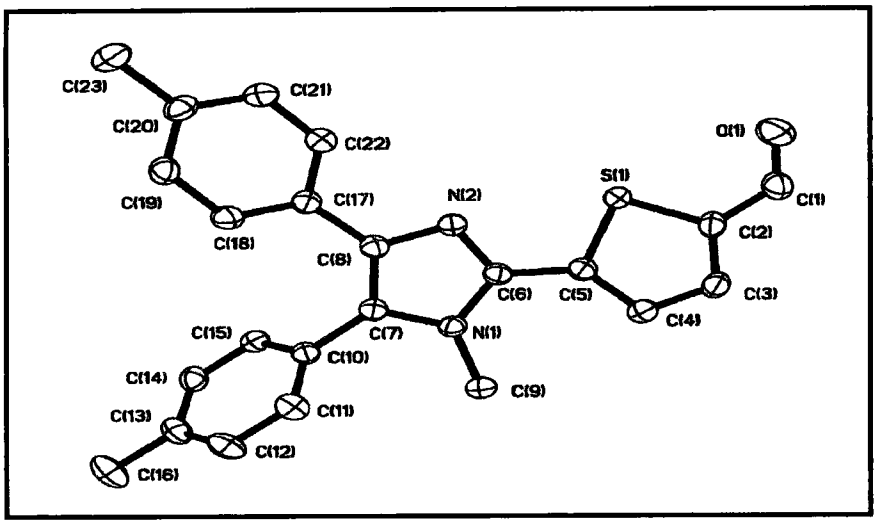

Figure 3. *X-ray structure of fluorophore* **5b**.

Table 2. *Selected Crystal Data Collection Parameters for* **5b**

Temperature:	293(2) K	Data collection:	1.29 - 26.25 deg.
Wavelength:	0.71073 Å	R. collected/unique:	10596 / 3834
Crystal system:	monoclinic, P2(1)/c	Refin. method:	Full matrix l-s F^2
Molecules per unit:	4	Data/rest./param.:	3834 / 0 /260
Calculated density:	1.297 mg/m^3	Goodness fit on F^2:	1.038
Crystal size (mm):	0.833x0.323x0.119	Final R indices:	R1 = 0.0392

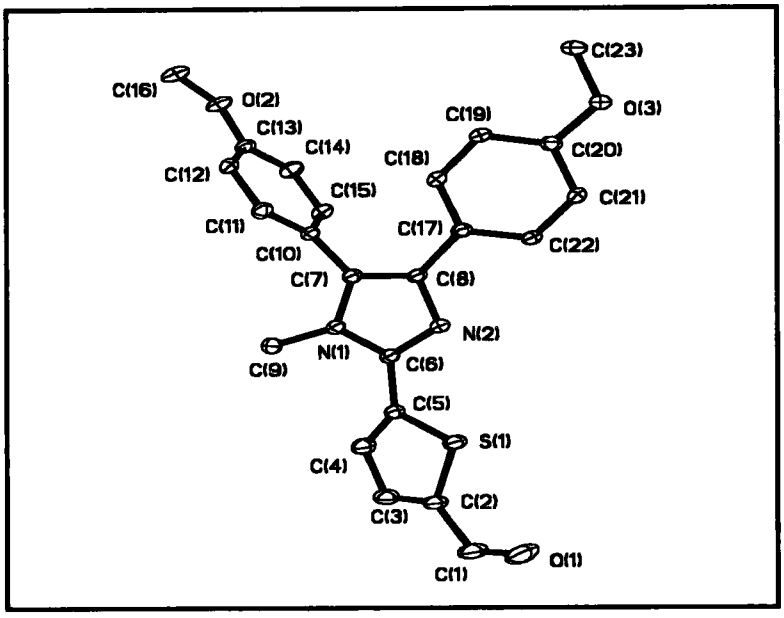

Figure 4. *X-ray structure of fluorophore* **5c**.

Table 3. *Selected Crystal Data Collection Parameters for* **5c**

Temperature:	173(2) K	Th. Data collection:	1.49 - 28.31 deg.
Wavelength:	0.71073 Å	R. collected/unique:	9948 / 4519
Crystal system:	triclinic, P-1	Refin. method:	Full matrix l-s F^2
Molecules per unit:	2	Data/rest./param.:	4519 / 0 / 280
Calculated density:	1.362 mg/m^3	Goodness fit on F^2:	1.018
Crystal size (mm):	0.510x0.170x0.102	Final R indices:	R1 = 0.0360

Table 4. *Selected Bond Lengths* (Å) *for* **5b** *and* **5c**

	5b	**5c**	**Average Length**[5]	**Bond Type**[5]
C(7)-C(10)	1.475(2)	1.482(18)	1.48	C-C, sp^2-sp^2
C(8)-C(17)	1.473(2)	1.474(19)	1.48	C-C, sp^2-sp^2
C(7)-C(8)	1.381(2)	1.382(19)	1.32	C=C, sp^2-sp^2
N(1)-C(7)	1.386(2)	1.381(17)	1.38	C-N, sp^2-N
N(2)-C(8)	1.378(2)	1.374(17)	1.38	C-N, sp^2-N
N(1)-C(6)	1.371(2)	1.368(17)	1.38	C-N, sp^2-N
N(2)-C(6)	1.324(2)	1.325(18)	1.28	C=N, sp^2-N
C(5)-C(6)	1.455(2)	1.453(19)	1.48	C-C, sp^2-sp^2
S(1)-C(5)	1.729(17)	1.723(14)	1.75	C-S, sp^2-S
S(1)-C(2)	1.729(17)	1.723(15)	1.75	C-S, sp^2-S
C(1)-C(2)	1.451(2)	1.445(2)	1.48	C-C, sp^2-sp^2
N(1)-C(9)	1.459(2)	1.464(18)	1.47	C-N, sp^3-N
O(1)-C(1)	1.213(2)	1.214(2)	1.21	C=O, sp^2-O

Table 5. *Selected Angles* (deg.) *for* **5b** *and* **5c**

	5b	**5c**
C(8)-C(7)-C(10)	131.34(15)	130.12(13)
C(7)-C(8)-C(17)	130.48(15)	129.39(13)
N(2)-C(6)-C(5)	121.65(15)	122.00(12)
C(6)-C(5)-S(1)	115.80(12)	116.60(10)
C(1)-C(2)-S(1)	122.37(14)	120.62(13)
C(7)-N(1)-C(9)	126.26(14)	125.10(12)

The solid state structure of **5b** and **5c** reveals that the phenyl and thiophene rings are both twisted out of the plane of the imidazole ring (Table 6). The X-ray analysis of **5b** indicates that one of the phenyl rings is rotated out of the plane of the imidazole plane by 58.9° and the other by 21.3°. On the other hand, it shows that in **5c** one of the phenyl rings is twisted by 89.43° and the other by 16.8°, relative to the imidazole ring. The thiophene ring in **5b** forms a dihedral angle of 10.0°, relative to the imidazole ring, versus 22.81° for the same angle in **5c**. It is notable that **5c**, which possesses the stronger donor group (OCH_3), undergoes more twist at C(8)-C(7)-C(10)-C(15) and S(1)-C(5)-C(6)-N(2) than does **5b**. The latter is consistent with reported observations, where increasing the strength of the donor and/or acceptor groups favor the formation of a twisted ground state.[6] In addition, the aldehyde group in both **5b** (3.4°) and **5c** (2.6°) is nearly coplanar with the thiophene ring (Table 6). In both cases the sulfur atom from the thiophene moiety and the oxygen atom of the aldehyde are syn to each other. Considering the fact that both sulfur and oxygen atoms have lone pairs of electrons, they are expected to be on opposite sides since they would repel each other. However, this behavior in the solid state may be due to crystal packing energies. Although it was not possible to grow crystals of **5a** and **5d**, similar behavior is expected since they have the same basic structure. Thus, X-ray structural analysis has revealed that the aldehydes **5** have a twisted ground state geometry, which in the excited state may induce a twisted intramolecular charge transfer (TICT) effect. The dihedral angles of **5b** along with those of published dyes[7] are shown in

Figure 5. The twist of the phenyl rings in these systems can be attributed to steric crowding.

Table 6. *Selected Dihedral Angles (deg.) for* **5b** *and* **5c**

	5b	**5c**
N(1)-C(7)-C(10)-C(11)	58.9(2)	89.43(18)
C(7)-C(8)-C(17)-C(18)	21.3(3)	16.8(2)
S(1)-C(5)-C(6)-N(2)	10.0(2)	22.81(19)
O(1)-C(1)-C(2)-S(1)	3.4(3)	2.6(2)

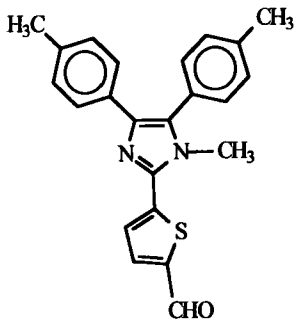

5b

58.9° and 21.3°

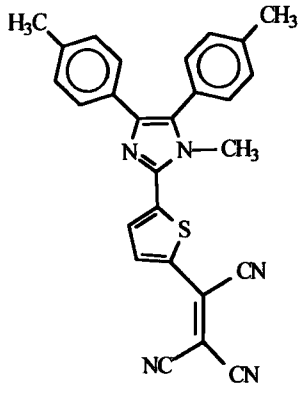

59.34° and 12.40°

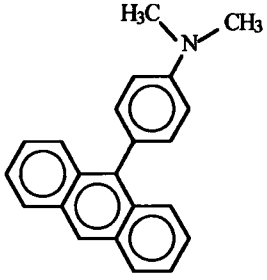

9DPhen

64.2°

Figure 5. *Dihedral angles (deg.) for the donor substituted phenyl rings.*

4.2 *Photophysical Properties of Substituted Fluorescent Dyes*

Absorption spectra of **5** indicate that these compounds undergo some form of intramolecular charge transfer. Typical absorption spectra of substituted **5** consist of two bands (Figure 6), one corresponding to a π,π^* transition (at high energy) and the other to an n,π^* transition (at low energy). The position of the absorption bands for these compounds were found to depend on both substituent groups and solvent polarity. The absorption maxima of aldehydes **5** shift to lower energy (red shift) as the strength of the donor substituent increases ($H < CH_3 < OCH_3 < N(CH_3)_2$). Note that only one absorption band is observed in ethanol and acetone. This observation suggests that there is already an interaction between the respective solvent and the molecule in the ground state.[8] In toluene, **5a** shows only one band at 384 nm while others (**5b**, **5c**, and **5d**) exhibit two bands, one near 300 nm (in the range of 286-311 nm) and the other around 400 nm (in the range of 390-431 nm). In ethanol, the absorption maximum is at 375 nm for **5a**, 382 nm for **5b**, 389 nm for **5c**, and 418 nm for **5d**. The total red shift of the absorption maxima from **5a** to **5d** in ethanol is 43 nm. The total red shift of the band at low energy in other solvents is: 44 nm in acetonitrile, 48 nm in acetone, 45 nm in chloroform, 43 nm in ethyl acetate, 46 nm in 1,4-dioxane, and 47 nm in toluene. A general trend of red shifts was observed in all the solvents investigated.

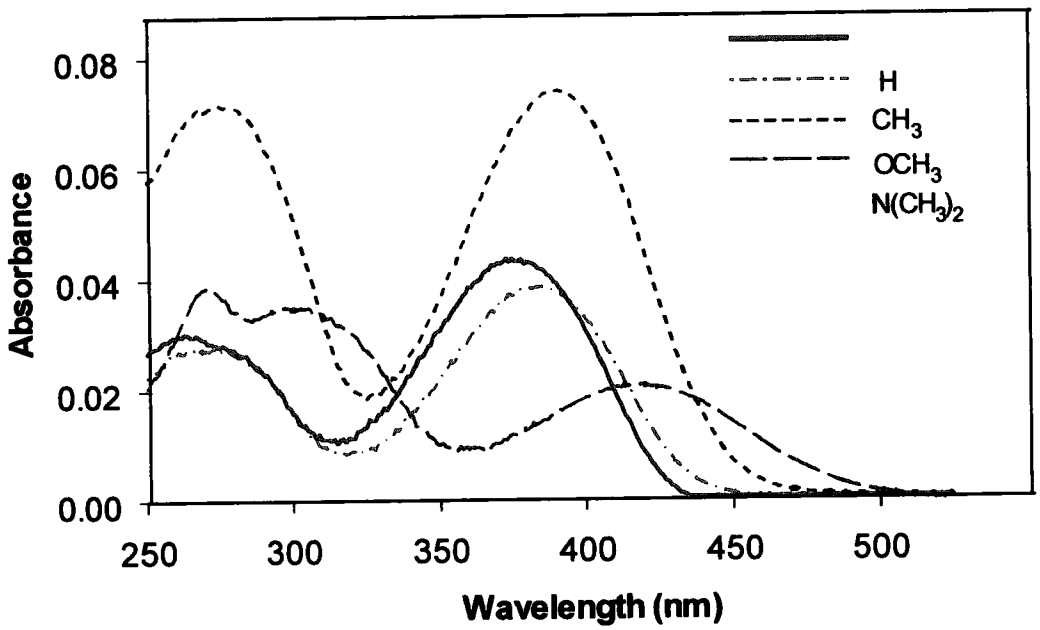

Figure 6. *UV-Vis absorption bands for fluorophores* **5** *in acetonitrile.*

The electronic transparency or wavelength cut-off ($\lambda_{cut\text{-}off}$) of **5** is listed in Table 7. The latter is the wavelength where the molecule in question no longer absorbs light. The $\lambda_{cut\text{-}off}$ on Table 7 was determined where absorption values measured 0.000. This property was also found to be substituent and solvent dependant, in the range of 450-537 nm. In most cases, the $\lambda_{cut\text{-}off}$ decreased in less polar solvents. However, no consistent relationship between substituent and $\lambda_{cut\text{-}off}$ was observed.

Table 7. *Electronic Absorption and Cut-off Properties of Fluorophores* **5**

Fluorophore	Solvent	λ_{max} (nm)	$\lambda_{cut\text{-}off}$ (nm)
5a	Ethanol	375	450
5b	Ethanol	382	464
5c	Ethanol	389	529
5d	Ethanol	418	513
5a	Acetonitrile	263, 375	434
5b	Acetonitrile	267, 385	458
5c	Acetonitrile	278, 391	510
5d	Acetonitrile	306, 419	508
5a	Acetone	376	450
5b	Acetone	384	506
5c	Acetone	391	480
5d	Acetone	424	535
5a	Chloroform	268, 387	447
5b	Chloroform	269, 390	469
5c	Chloroform	278, 400	473
5d	Chloroform	304, 432	547
5a	Ethyl acetate	268, 374	450
5b	Ethyl acetate	270, 382	449
5c	Ethyl acetate	279, 393	476
5d	Ethyl acetate	305, 417	504
5a	1,4-dioxane	260, 381	429
5b	1,4-dioxane	277, 386	459
5c	1,4-dioxane	279, 395	458
5d	1,4-dioxane	304, 427	512

Table 7. (Continued)

5a	Toluene	384	438
5b	Toluene	286, 390	447
5c	Toluene	290, 402	464
5d	Toluene	311, 431	537

The bathochromic shift of the absorption bands of substituted **5** is influenced by the donor strength of substituent groups. Absorption energy decreases with increasing the electron donor strength of the substituent: $N(CH_3)_2 > OCH_3 > CH_3 > H$. Since, the energy of the charge transfer state is influenced by the donor strength of the substituents, it should be possible to describe the energy of the charge transfer absorption band using a linear free energy relationship with the Hammett constant, σ^+.[9] A plot of the energy of the absorption maxima (E_{abs}) versus σ^+ is shown in Figure 7. This plot reveals an excellent linear relationship which indicates that the red shifts observed for the absorption bands are caused in fact by the electronic effect of the substituent groups. The E_{abs} was calculated by using Equation 8, where c is the speed of light (2.9979 $x10^{17}$ nm/s), h is the Planck's constant (1.5837 $x10^{-37}$ Kcal s or 6.626076 $x10^{-34}$ J s), N_A is the Avogadro's number (6.022137 $x10^{23}$ /mol), and λ is the wavelength of the absorption maxima. Equation 8 can be simplified to equation 9.

$$E = \frac{c\ h\ N_A}{\lambda} \qquad \text{Eq. 8}$$

$$E = \frac{28{,}592\ \text{Kcal nm / mol}}{\lambda} \qquad \text{Eq. 9}$$

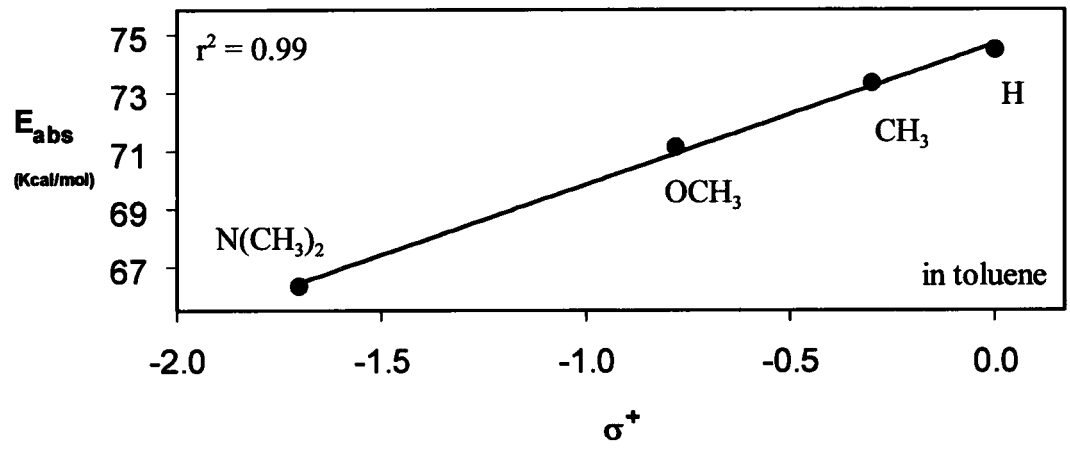

Figure 7. *Energy of absorption maxima of* **5** *as a function of Hammett constant.*

Fluorescence data recorded at room temperature in different solvents are listed in Table 8. It was found that excitation (λ_{exc}), and emission (λ_{em}) maxima and the fluorescence quantum yield (Φ_{fl}) of **5** are all solvent dependent. In this work, solvents with high $E_T(30)$ values will be referred to as polar solvents and those with low $E_T(30)$ values as non-polar solvents (see Table 1). In general, the fluorescence quantum yields of **5** are moderate to high, except **5d**. The highest Φ_{fl} obtained is from **5c**, which has a fluorescence quantum yield of 1.0 in toluene (relative to quinine sulfate) at an excitation wavelength of 365 nm and at room temperature. In polar solvents, the Φ_{fl} for these compounds tends to decrease. For example, the Φ_{fl} of **5a** decreases in solvents going from chloroform (Φ_{fl} = 0.80), acetone (Φ_{fl} = 0.70), acetonitrile (Φ_{fl} = 0.68), to ethanol (Φ_{fl} = 0.09). However, the Φ_{fl} increases from toluene (Φ_{fl} = 0.58) to 1,4-dioxane (Φ_{fl} = 0.72). The low Φ_{fl} in ethanol may be explained by the formation of a hydrogen bond between the fluorophore and the

solvent, resulting in a significant Φ_{fl} quenching. The hydrogen bonding may occur between the ethanol and a nitrogen atom in the imidazole ring. The latter has been also suggested for imidazole derivatives in the literature.[10] Also, fluorescence quenching caused by hydrogen bonding has been reported.[11]

The Φ_{fl} was also found to be substituent dependent. A close examination of the fluorescence quantum yield of **5a** to **5d** in acetone reveals that Φ_{fl} decreases dramatically with increasing electron donor strength ($N(CH_3)_2 > OCH_3 > CH_3 > H$). The same trend is also found in acetonitrile and chloroform. In ethyl acetate, 1,4-dioxane and toluene, the Φ_{fl} shows a different but interesting behavior. First, there is no clear trend in ethyl acetate. Secondly, the Φ_{fl} of **5a** to **5c** actually increases in 1,4-dioxane following the trend: **5a** (Φ_{fl} = 0.72), **5b** (Φ_{fl} = 0.77), to **5c** (Φ_{fl} = 0.82), then suddenly drops with **5d** (Φ_{fl} = 0.16). This trend was also observed in toluene. The significantly lower Φ_{fl} value for **5d** may be attributed to the well known Twisted Intramolecular Charge Transfer (TICT) phenomenon caused by the dimethylamino group.[12] For TICT systems, non-radiative decay processes are often the preferred deactivation pathway. Also, it is well known that non-radiative decay in TICT systems often outweighs the fluorescence. In these systems the radiative and non-radiative rates depend on the twist angles of the donor and acceptor substituents within the molecule.[13]

The λ_{em} and λ_{exc} maxima of **5** in various solvents are shown in Table 8 and their spectra in Figures 8-11. All emission spectra were recorded at an excitation wavelength of 365 nm. Excitation spectra of **5** were measured using the respective

emission maxima of each compound. The emission and excitation spectra were obtained from $1.5x10^{-6}$ M samples, which gave an intensity of absorption maxima in the range of 0.04-0.07.

The emission band of compounds **5a**, **5b**, and **5c** is red-shifted (bathochromic shift) in going from a non-polar solvent to a more polar one (Table 8, Figures 8 to 10). However, for **5d** the red shift is observed from toluene to ethyl acetate and a blue shift (hypsochromic shift) in the more polar solvents (Table 8, Figure 11).

The blue shift of the emission maxima of **5d** in $CHCl_3$, acetone, CH_3CN, and EtOH can be explained by the hydrogen bond donor (HBD) interaction effect. When HBD interactions are present the electronic state energy is lowered by the electrostatic interaction of a positively polarized hydrogen atom of the solvent molecules with a lone pair of electrons on a basic atom of the solute in the ground state or the excited state. During the excitation process, if the electron density migrates away from the basic atom, formation of the hydrogen bond opposes this migration. As a result, a blue shift is observed with an increase of the HBD capacity of the solvent.[35]

It has been reported that $CHCl_3$ and CH_3CN usually act as a non-hydrogen bonding (NHB) solvent, but have shown weak HBD properties with strong acceptor solutes. Ethanol is an amphiprotic hydrogen bond acceptor-donor (HBA-D) and acetone is a hydrogen bond acceptor (HBA) solvent.[18] Based on these classifications, the HBD interaction can occur in $CHCl_3$, CH_3CN and EtOH. But why a blue shift is observed in acetone if this cannot act as a HBD solvent? Maybe the interaction

between the acetone molecules and **5d** in the ground state and/or excited state is so strong that it makes the solvent behave with HBD properties. Although this statement requires more investigation to be confirmed, there is no question about the blue shift in acetone. In fact, the blue shift in acetone is greater than in $CHCl_3$ (Figure 11).

Note that for **5d** the basic atom is the nitrogen from the dimethylamino group, which possesses a lone pair of electrons. As discussed in the introduction section, a dimethylamino group tends to twist in the excited state forming a positive charge on the nitrogen atom. The latter is an indication that the electron density on the nitrogen atom migrates away from it. Therefore, the formation of a hydrogen bond (between the nitrogen on the dimethylamino group and the solvent) will opposes this migration. As a consequence a blue shift in the emission band is observed.

Table 8. *Fluorescent Data of Dyes* **5**

Dye	Solvent	λ_{exc}* (nm)	λ_{em}* (nm)	S. s.** (cm^{-1})	Φ_{fl}
5a	Ethanol	375	529	7763.1	0.094 ± 0.009
5b	Ethanol	377	538	7937.8	0.040 ± 0.001
5c	Ethanol	395	577	7985.4	0.0063 ± 0.0001
5d	Ethanol	324	489	10414	0.0042 ± 0.0001
5a	Acetonitrile	291, 378	500	6455	0.68 ± 0.03
5b	Acetonitrile	291, 381	516	6866.9	0.51 ± 0.02
5c	Acetonitrile	295, 397	550	7007.1	0.15 ± 0.01
5d	Acetonitrile	319	480	10515	0.019 ± 0.001
5a	Acetone	379	489	5935.3	0.70 ± 0.03
5b	Acetone	382	501	6217.9	0.67 ± 0.03
5c	Acetone	396	529	6348.9	0.46 ± 0.02
5d	Acetone	338	466	8126.6	0.018 ± 0.002
5a	Chloroform	291, 383	490	5701.5	0.80 ± 0.04
5b	Chloroform	291, 397	502	5268.6	0.77 ± 0.03
5c	Chloroform	298, 397	532	5771.4	0.56 ± 0.02
5d	Chloroform	337	589	7592.1	0.095 ± 0.001
5a	Ethyl acetate	293, 377	465	5019.8	0.58 ± 0.03
5b	Ethyl acetate	293, 382	474	5081.0	0.73 ± 0.03
5c	Ethyl acetate	296, 397	499	5148.8	0.69 ± 0.03
5d	Ethyl acetate	309, 419	445, 621	7763.3	0.041 ± 0.001
5a	1,4-dioxane	291, 380	460	4576.7	0.72 ± 0.03
5b	1,4-dioxane	295, 388	472	4586.8	0.77 ± 0.03
5c	1,4-dioxane	298, 398	492	4800.4	0.82 ± 0.03
5d	1,4-dioxane	321, 419	442, 587	6830.6	0.16 ± 0.02

Table 8. (Continued)

5a	Toluene	300, 383	455	4131.6	0.58 ± 0.03
5b	Toluene	301, 397	465	3683.5	0.65 ± 0.03
5c	Toluene	305, 397	480	4355.6	1.0 ± 0.04
5d	Toluene	322, 428	440, 558	5443.3	0.34 ± 0.04

*From corrected spectra. **Stokes shift

There is also a solvent effect on the excitation spectra, but it does not involve a shift of the band. The excitation maxima of **5** are relatively insensitive to the solvent polarity as shown in Figure 8 to 11, but sensitive to substituent groups in most cases (Table 8). In non-polar solvents such as toulene, 1,4-dioxane and more polar solvents such as ethyl acetate and chloroform the excitation spectra of **5a-d** are represented by two bands, where the higher energy band is much larger in intensity. Notably, in acetone and ethanol the excitation spectra comprise only one band. This behavior suggests an interaction in the ground state between solute **5** and the solvent. The same behavior was observed in the absorption spectra (Table 7). Another observation is that the intensity of the two excitation bands in toluene, 1,4-dioxane, ethyl acetate and chloroform for **5d** is about the same (Figure 11).

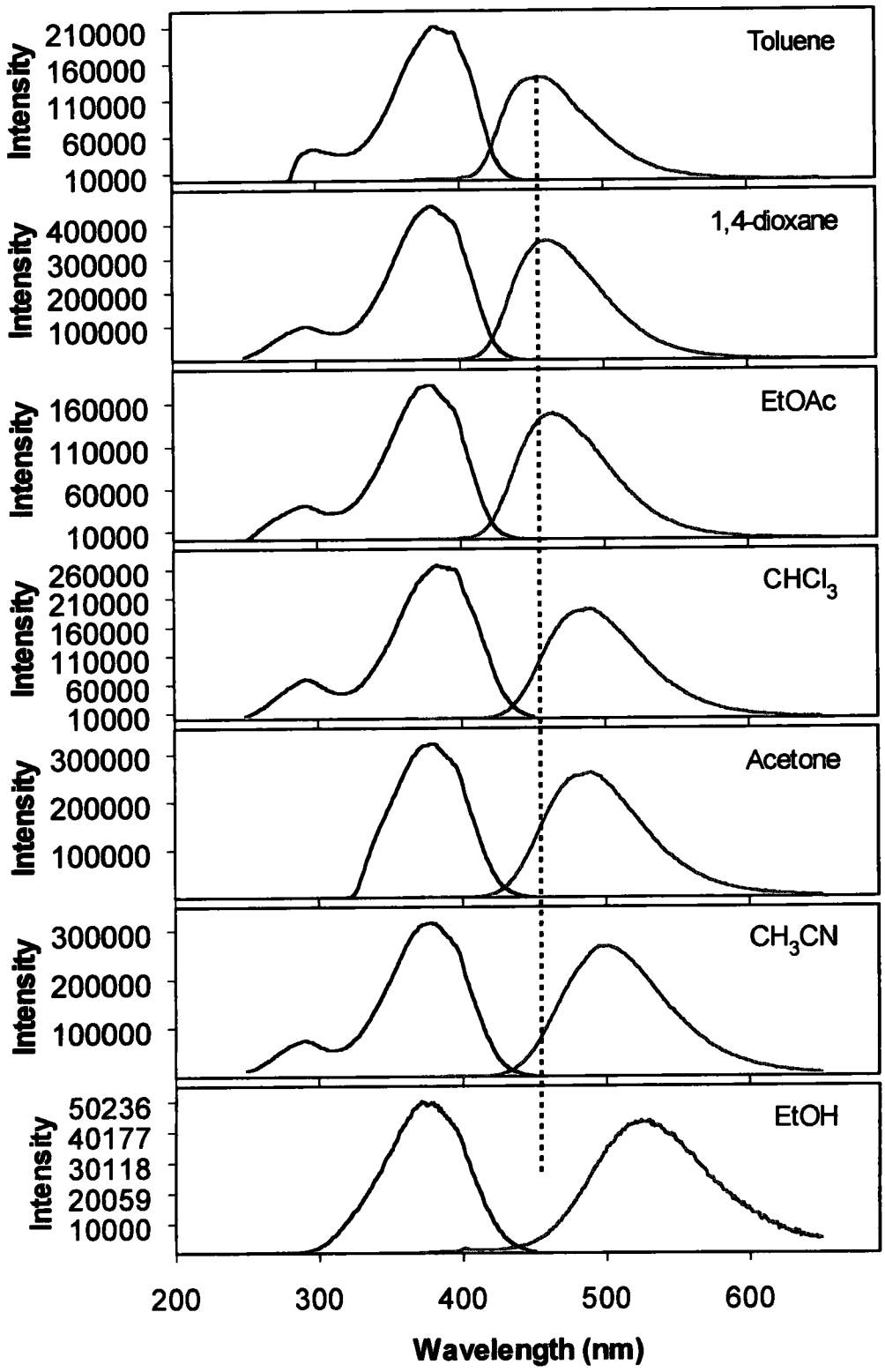

Figure 8. *Excitation (left band) and emission (right band) spectra of* **5a**.

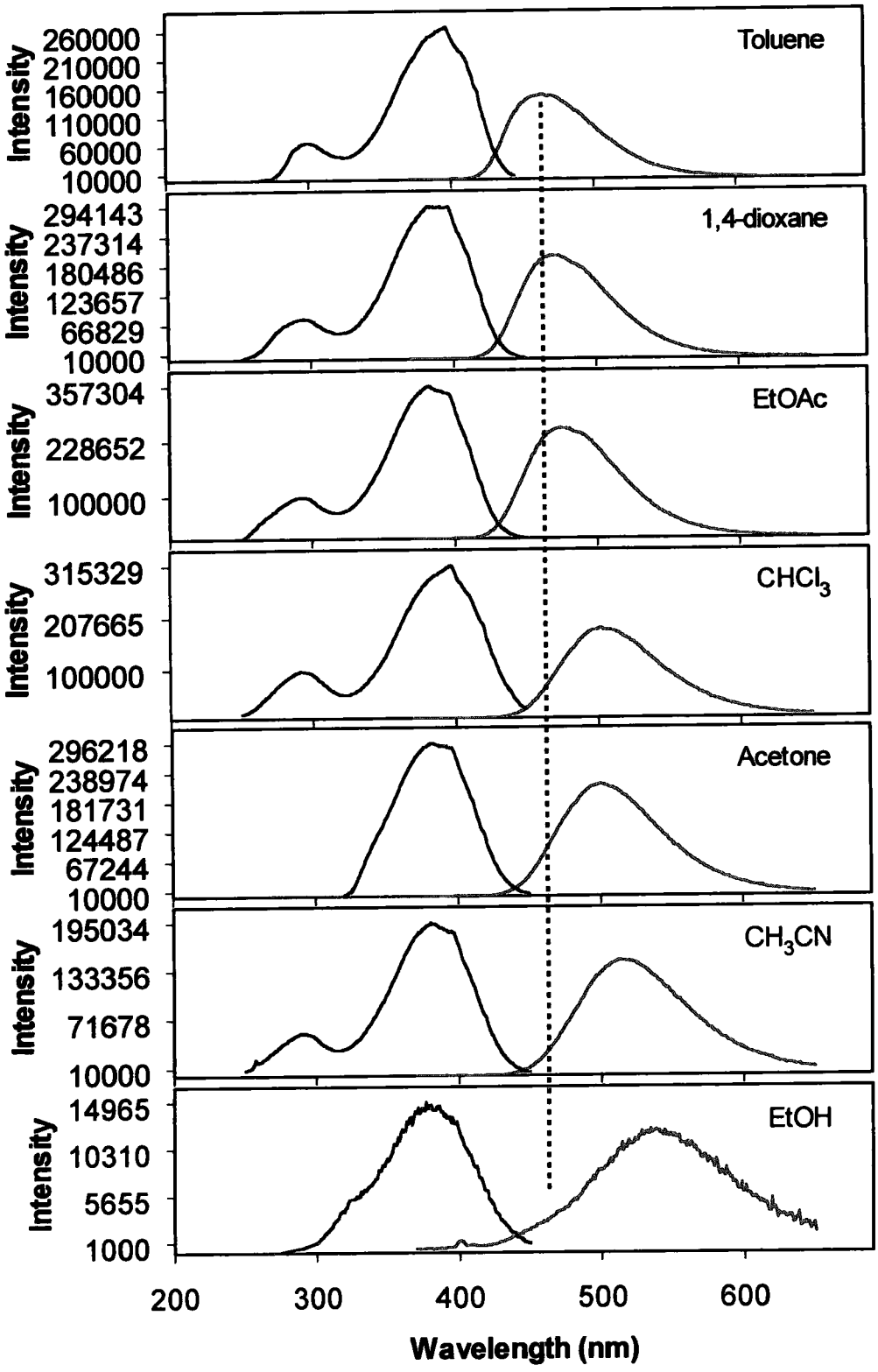

Figure 9. *Excitation (left band) and emission (right band) spectra of* **5b**.

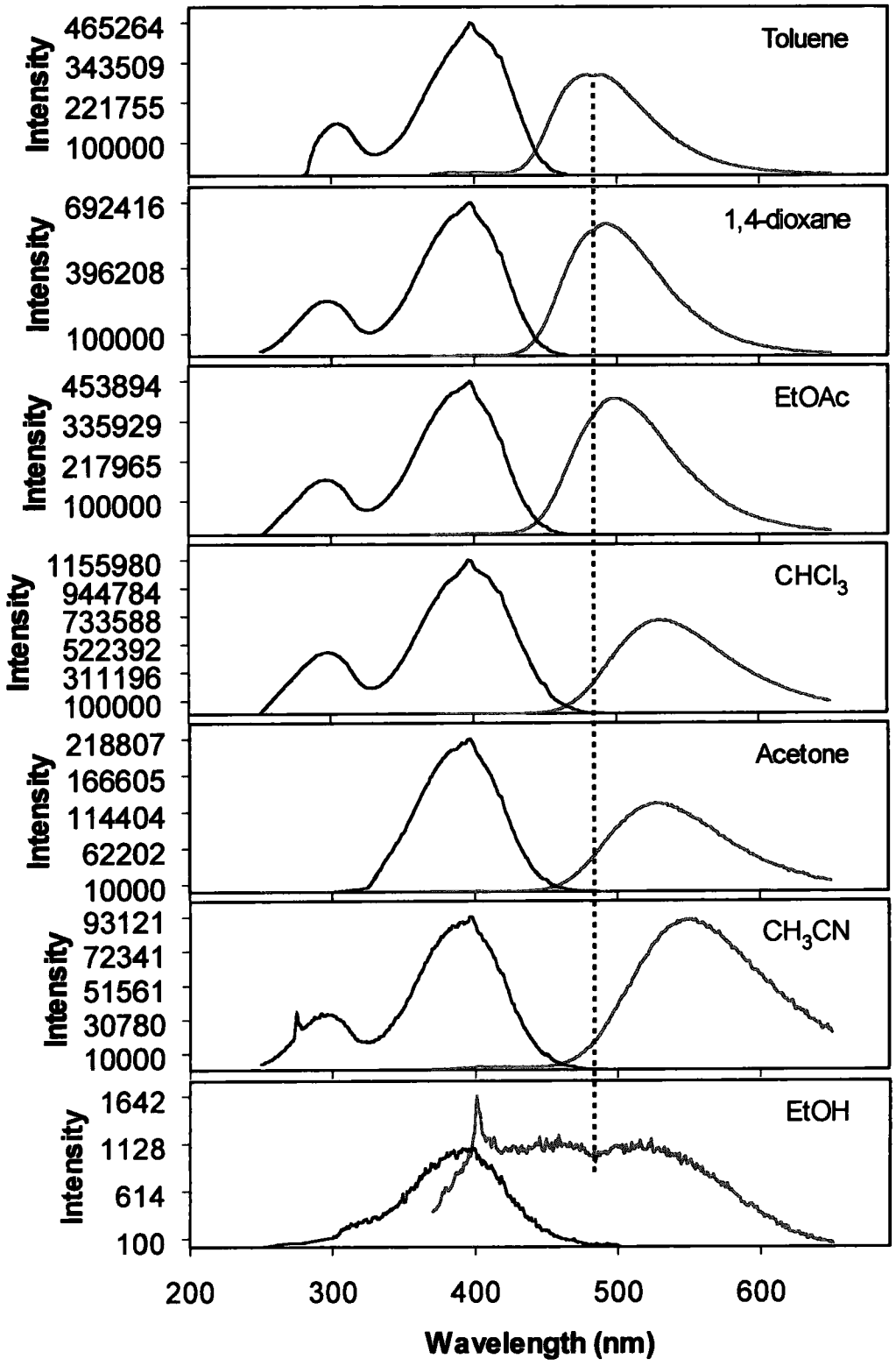

Figure 10. *Excitation (left band) and emission (right band) spectra of* **5c**.

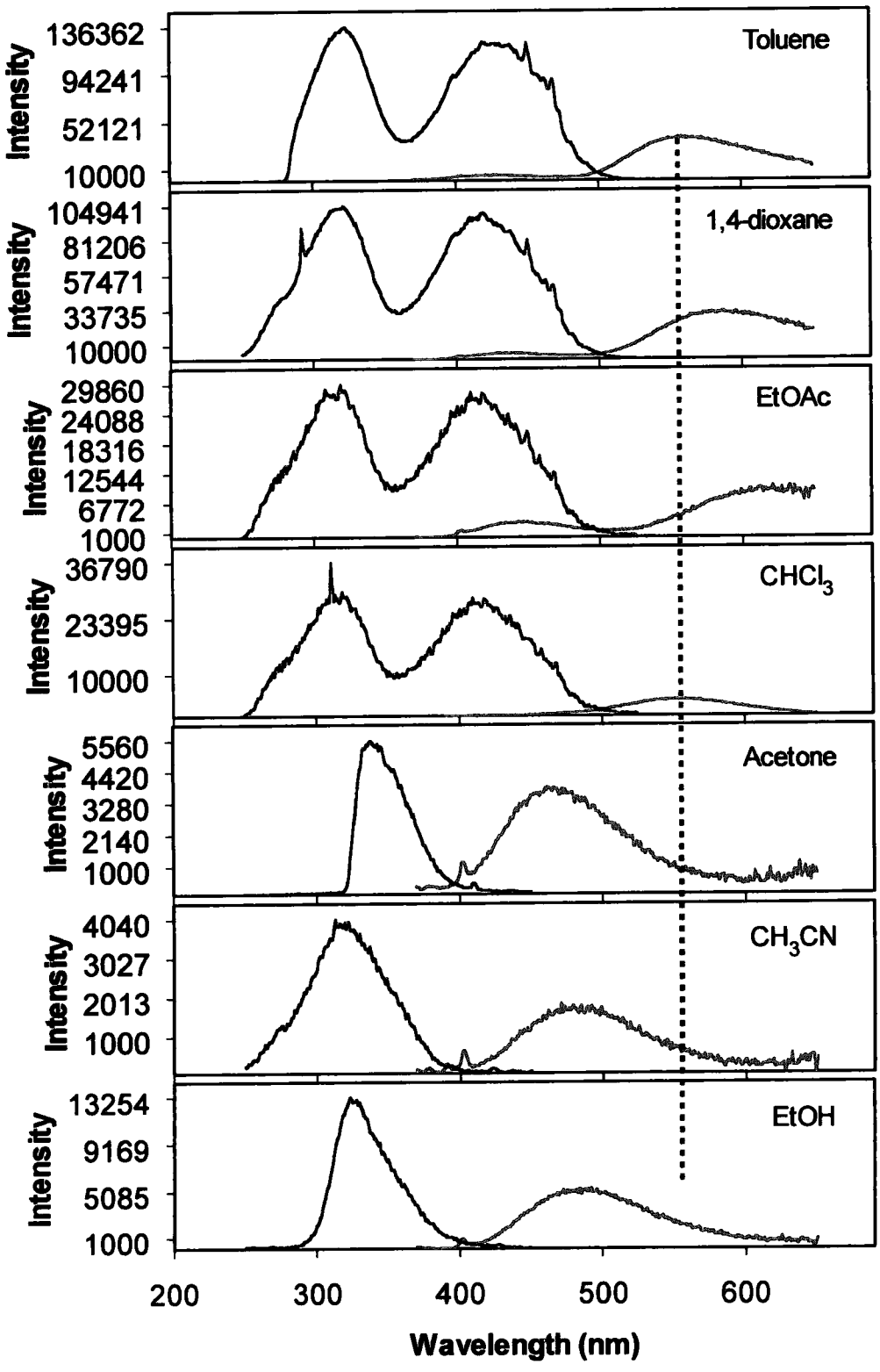

Figure 11. *Excitation (left band) and emission (right band) spectra of* **5d**.

Note that for each fluorophore (**5a-d**) the absorption is relatively insensitive to solvent polarity and the emission band shifts to lower energy with increasing solvent polarity. These facts suggest the existence of two excited states. The latter is common in fluorescent molecules that undergo intramolecular charge transfer.

There are molecules that exhibit dual fluorescence as a result of both a locally excited (LE) state and intramolecular charge transfer (ICT) excited state. In these cases the emission of the LE state band tends to be relatively insensitive to solvent polarity and the ICT state band shifts to lower energy with increasing solvent polarity. Dual fluorescence in molecules possessing intramolecular charge transfer transitions can be described on the basis of the mechanism shown in Figure 12.[25,26] According to this mechanism, the dual fluorescence arises from two states termed as locally excited state (LE) and intramolecular charge transfer (ICT) states in equilibrium. The LE state refers to a state which can be reached directly by absorption from ground state (S_o). In the ICT excited state, which originates from the LE state, considerable charge separation between the donor and the acceptor groups is expected. The kinetics of the dual fluorescence can be treated on the basis of the mechanism shown in Figure 12, where k_a and k_d are the rate constants for the forward and backward ICT reactions, and τ_o and τ'_o are the fluorescence lifetimes for LE and ICT states, respectively. The k_f and k'_f are the radiative rate constants. The forward and backward reactions represented by this mechanism commonly involve orientational relaxation of the solvent molecules following the changes in the charge distribution.

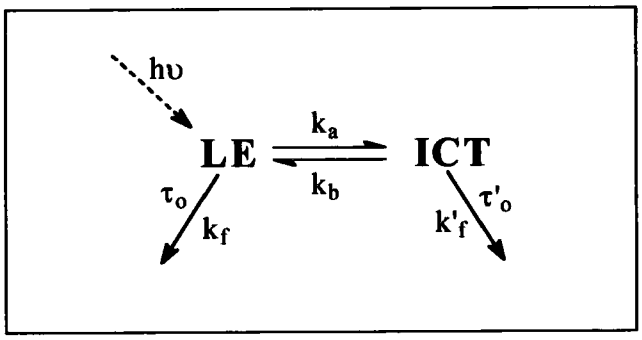

Figure 12. *General mechanism for dual fluorescence in molecules possessing intramolecular charge transfer transitions.*

However, molecules with two excited states that exhibit only one emission band are well known. For these types of molecules the LE and ICT states can be visualized by plotting the frequency of the absorption and emission maxima, respectively, versus the solvent polarity function Δf (Eq. 10), where ε is the dielectric constant and n is the refractive index of the solvent.[26]

$$\Delta f = \frac{\varepsilon - 1}{2\varepsilon + 1} - \frac{n^2 - 1}{2n^2 + 1} \qquad \text{Eq. 10}$$

Table 7 shows that the absorption maxima of substituted **5** remain relatively unchanged with respect to solvent polarity. This indicates that a direct absorption of a photon by **5** produces a non-polar locally excited (LE) state. On the other hand, the emission spectra (Table 8, Figures 8 to 11) are extremely solvent sensitive. For example, the emission maximum of **5c** in ethanol is red shifted by 78 nm from that in ethyl acetate. The observed bathochromic shift in the fluorescence spectra of

substituted **5** is consistent with emission from a polar charge transfer (ICT) excited state. Figures 13 and 14 show solvatochromic plots (from data on Tables 7 and 8) of substituted **5**, frequency (ν) of the absorption and emission maxima, as a function of solvent polarity parameter Δf. Plots for the LE state display a flat line behavior (solvent insensitivity) while those for the polar ICT excited state have a positive slope. Thus, the solvatochromic behavior in the absorption and emission spectra reveals the formation of two excited states.

The existence of both a non-polar excited state and a polar ICT excited state together with the broadness of the emission band, twisted ground state geometry (revealed by X-ray structure analysis), and the potential rotational motions of **5**, suggest that these are TICT molecules.[14]

A close analysis of the emission spectra of **5d** shows two emission bands in toluene, 1,4-dioxane, and ethyl acetate. The band at high energy is significantly small in intensity compared to the other one. This dual fluorescence can be attributed to the rotational motion of the dimethylamino groups, which is very well known.[7d,15] On the other hand, the small intensity of the emission band at high energy indicates that the equilibrium of the dual fluorescence mechanism (Figure 12) is more inclined to form the ICT excited state. However, the fact that only one emission band is observed in chloroform, acetone, acetonitrile, and ethanol, suggests an extremely rapid conversion of the LE state to the ICT excited state. Note that in the latter solvents the emission band shifts to high energy. Its cause needs to be determined.

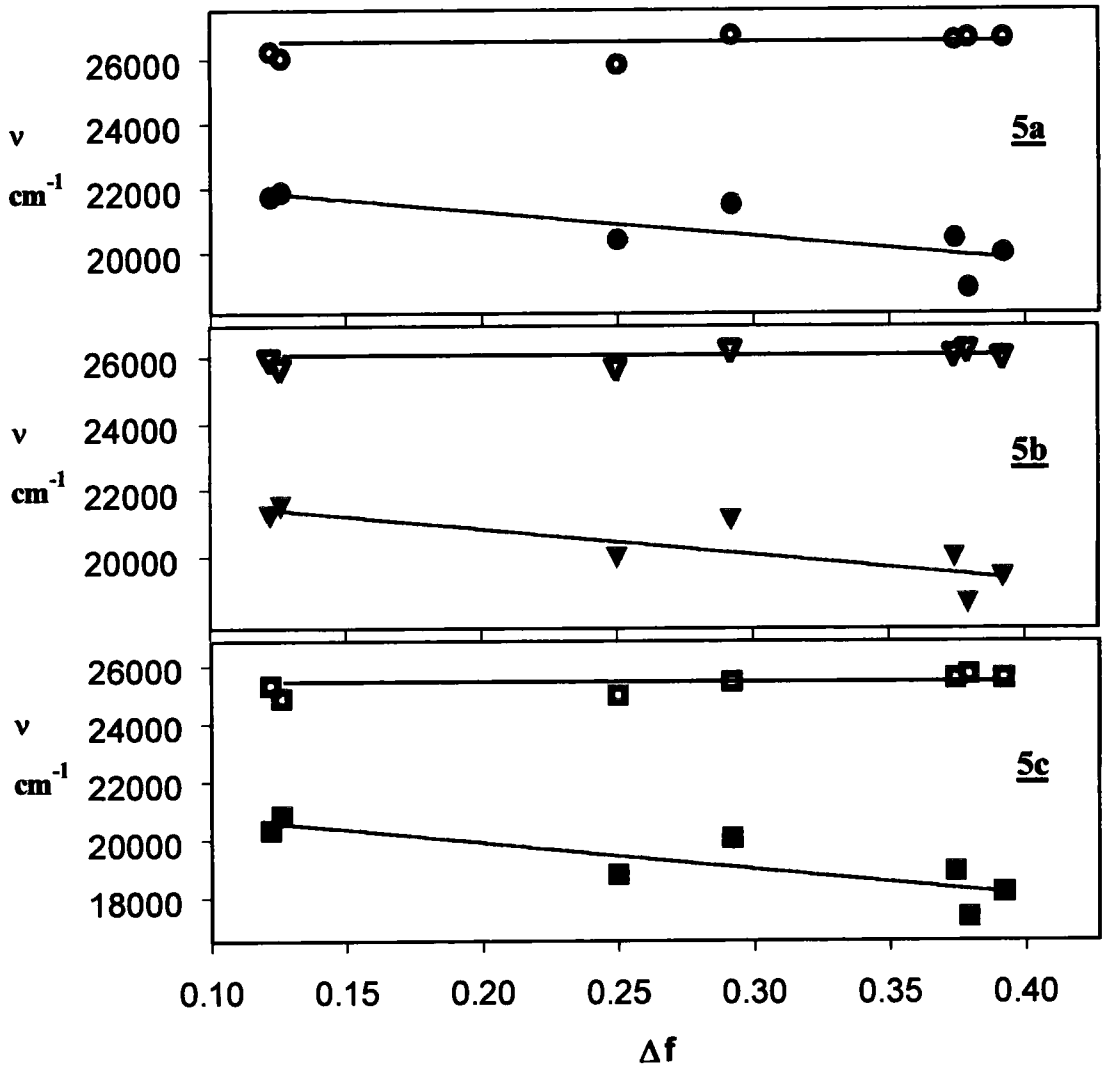

Figure 13. *Frequency of absorption (open symbols) and emission (solid symbols) maxima of* **5a-c** *as a function of solvent polarity parameter,* Δf.

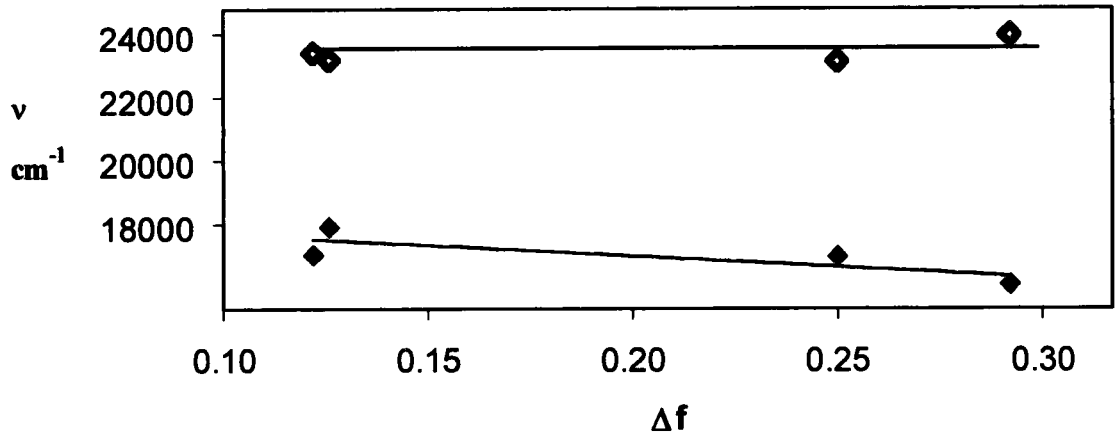

Figure 14. *Frequency of absorption (empty symbols) and emission (solid symbols) maxima of* **5d** *as a function of solvent polarity parameter,* Δf.

A large Stokes shift is a characteristic of molecules possessing donor and acceptor moieties with excited state relaxation where large amplitude motions are involved.[15] Molecules with rotation around the bond linking the donor and acceptor groups are more likely to possess large Stokes shifts than the analogous compounds with less ability of rotation. TICT compounds represent a particular class of molecules that exhibit a large Stokes shift.[15] Those compounds possessing a dimethylamino group are well known to show large Stokes shift values, especially in polar solvents where stabilization of the TICT state occurs.[15,16] However, a few TICT compounds have been reported to exhibit enormous Stokes shifts even in non-polar solvents.[17]

The Stokes shift values (from Eq. 1) of substituted **5** in different solvents are listed in Table 8. This constant was found to be both solvent and substituent group dependent. The Stokes shift of a given substituted **5** increases as solvent

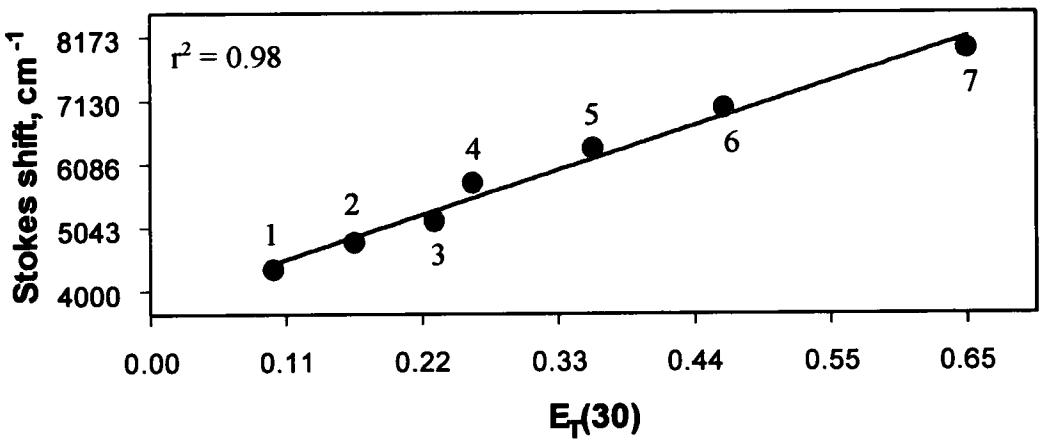

Figure 15. *Plot of Stokes shift versus solvent polarity parameter* $E_T(30)$ *for* **5c**. *(1=toluene, 2=1,4-dioxane, 3=EtOAc, 4=$CHCl_3$, 5=acetone, 6=CH_3CN, 7=EtOH)*

polarity increases. In fact, a linear correlation is observed between the Stokes shift values for **5** and the solvent polarity parameter $E_T(30)$ in all cases. Figure 15 shows a representative plot. This behavior suggests that polar solvents stabilize the polar CT excited state.

Compound **5d** gives the larger Stokes shifts. The extent of the shift is dramatic in different solvents. The shifts in ethanol (10414 cm^{-1}) and acetonitrile (10515 cm^{-1}) are almost twice of that in toluene (5443 cm^{-1}). The same trend is also found to exist for compounds **5a-c**. The larger Stokes shifts for substituted **5** were found in ethanol, the solvent with the highest polarity. For **5a**, **5b**, and **5c**, the Stokes shifts obtained in ethanol were 7763 cm^{-1}, 7937 cm^{-1}, and 7985 cm^{-1}, respectively. However, larger Stokes shifts were obtained for **5d** in less polar solvents such as acetonitrile (10515 cm^{-1}) and acetone (8126 cm^{-1}). Note that the Stokes shifts for **5d** in acetonitrile (10515 cm^{-1}) and ethanol (10414 cm^{-1}) are very close, a difference of only 0.48% (101 cm^{-1}).

Although substituted **5** have the same basic structure, the electron donor capability and the size of the substituent groups are different. The substituent effect on the Stokes shifts is different in the two groups of solvents. In ethanol, acetonitrile, acetone, ethyl acetate, and 1,4-dioxane the Stokes shifts increases in the order **5a** > **5b** > **5c** > **5d**. On the other hand, in chloroform, and toluene, the Stokes shift of **5b** decreases. In general, the tendency of the Stokes shifts is to increase as the electron donor capability of the substituent groups increases. This observation indicates that increasing intramolecular charge transfer and the ability of the substituent groups to create large motions in the excited state favor the dissipation of large amounts of energy during the excited state relaxation (decay to the ground state). The Stokes shifts of substituted **5** show a linear correlation between the energy of the CT excited state and Hammett's constant, σ^+, in all of the solvents investigated. A representative plot is given in Figure 16. Therefore, the intramolecular charge transfer must be responsible in part for these large Stoke shift values.

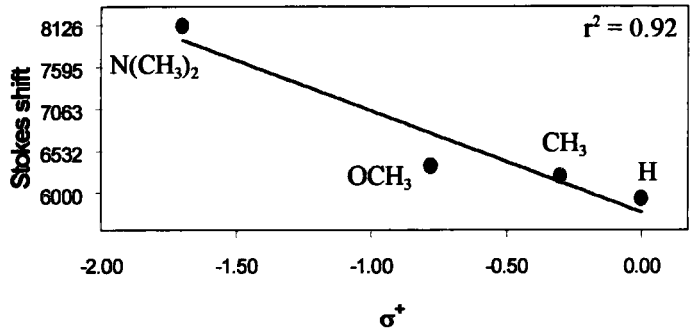

Figure 16. *Stokes shift (cm^{-1}) versus Hammett's constant for* **5** *in acetone.*

The stabilization of the CT state by solvents can be assessed using linear solvation energy relationships, e.g., Taft's π^*[18] or Dimroth's $E_T(30)$.[19] The energy of the fluorescence transition (E_{fl} in kcal/mol) is a linear function of a solvent parameter, π^* or $E_T(30)$ as shown in Eqs. 11 and 12 respectively. The slope s and b are a function of the degree of stabilization of the fluorescent excited state by polar solvents. Plots of E_{fl} versus π^* and E_{fl} versus $E_T(30)$ for **5a-d** are shown in Figures 17 to 21.

$$E_{fl} = E_o + s\pi^* \qquad \text{Eq. 11}$$

$$E_{fl} = E_o + bE_T(30) \qquad \text{Eq. 12}$$

In the plot of E_{fl} versus π^* (Figure 17), solvents that may cause hydrogen bonding (for example EtOH) and polychlorinated solvents (such as $CHCl_3$) were avoided since these are known to complicate the Taft-Kamlet equation (Eq. 13).[20] The energy of the fluorescence transition of **5d** in ethanol, acetonitrile, and acetone has been omitted because of its anomalous behavior (Figure 11) in these solvents. These plots show linear correlations of $\geq$ 0.94, except for **5d,** where it is 0.59. On the other hand, when the E_{fl} in EtOH and $CHCl_3$ are included a poor linear relationship ($\leq$ 0.1) is obtained. For comparison purposes the fluorescence energy of **5a-c** in acetonitrile, and acetone were not considered in Figure 18.

$$E_{Fl} = E_o + s(\pi^* + d\delta) + a\alpha \qquad \text{Eq. 10}$$

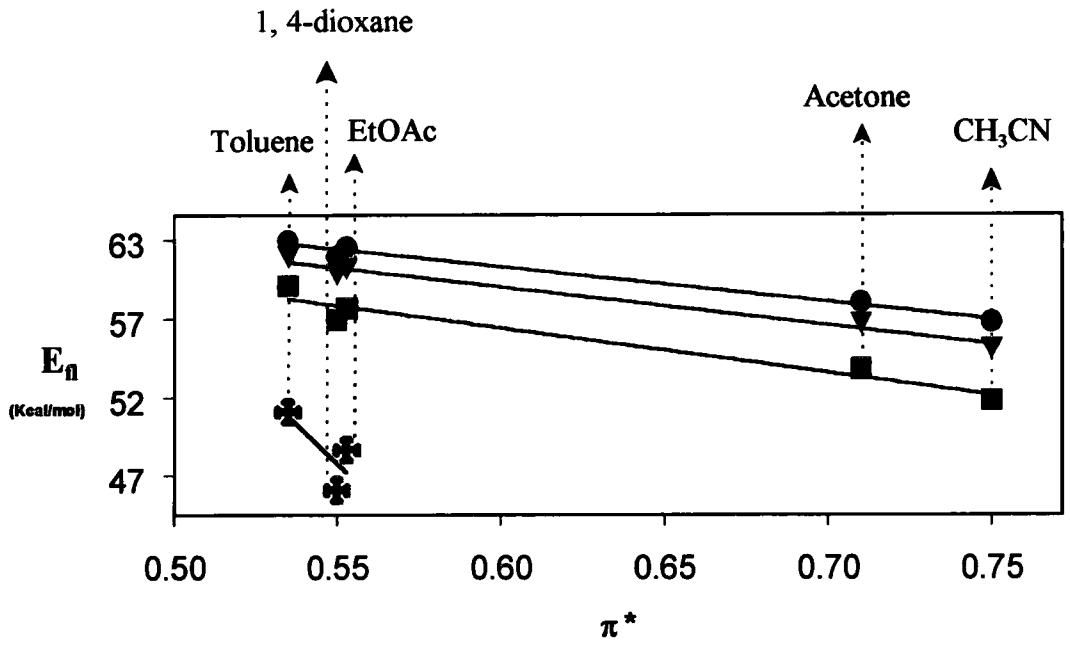

Figure 17. *Fluorescence energy as a function of solvent parameter π* for* **5a-d**.

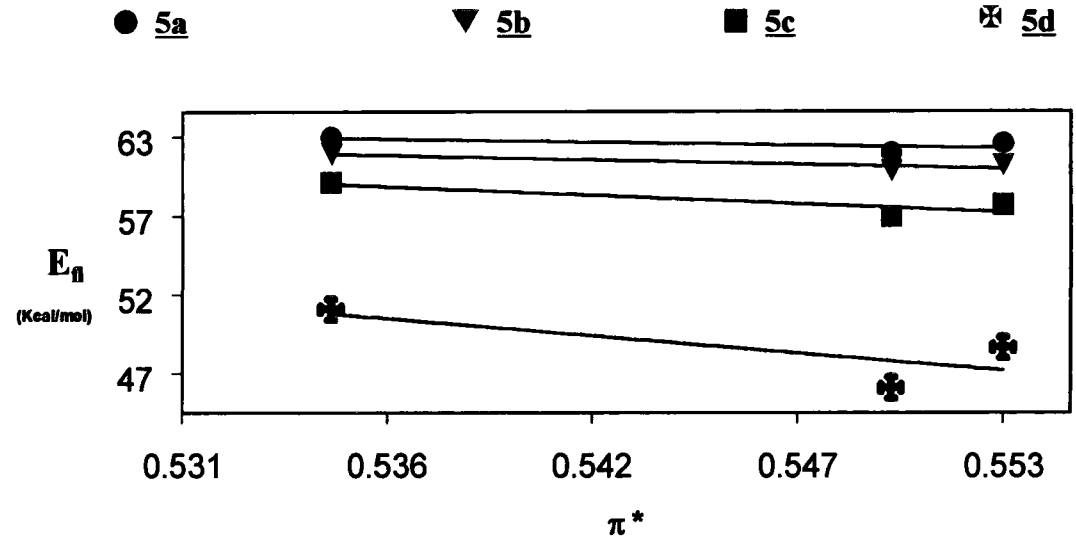

Figure 18. E_f *in toluene, 1,4-dioxane and EtOAc as a function of π* for* **5a-d**.

The slopes of the plots for **5a-c** on Figures 17 and 18 are not equal. When acetone and acetonitrile are not considered (Figure 18) the magnitude of the slopes (s) is larger (Table 9). However, the linear correlations (r^2) are insignificantly perturbed or not perturbed at all. The slopes increase with increasing electron donor strength: $N(CH_3)_2 > OCH_3 > CH_3 > H$, indicating the sensitivity to polar solvents.

Table 9. *Results of π* Plots on Figures* 17 *and* 18 *for Substituted* **5**

	Figure 17		Figure 18	
Fluorophore	**s**	**r^2**	**s**	**r^2**
5a	-23.31	0.982	-38.06	0.980
5b	-25.43	0.981	-54.89	0.980
5c	-29.64	0.946	-103.8	0.946
5d	-207.0	0.590	-207.0	0.590

Plots of E_{fl} versus $E_T(30)$ (Figure 19) reveal good linear correlations which are comparable with those for π* (Figures 17 and 18). E_{fl} in acetone, acetonitrile, and ethanol were excluded, for all substituted **5**, in Figure 20 because of the anomalous behavior of **5d** in these solvents (Figure 11). The latter resulted in a significant decrease of the linear correlations. Chloroform was also excluded (Figure 21) because the $E_T(30)$ scale has been shown to be affected by solvents that cause hydrogen bonding, thus revealing its dependence on solvent acidity.[21] Exclusion of chloroform results in an improvement in the linear correlation (r^2) in all cases

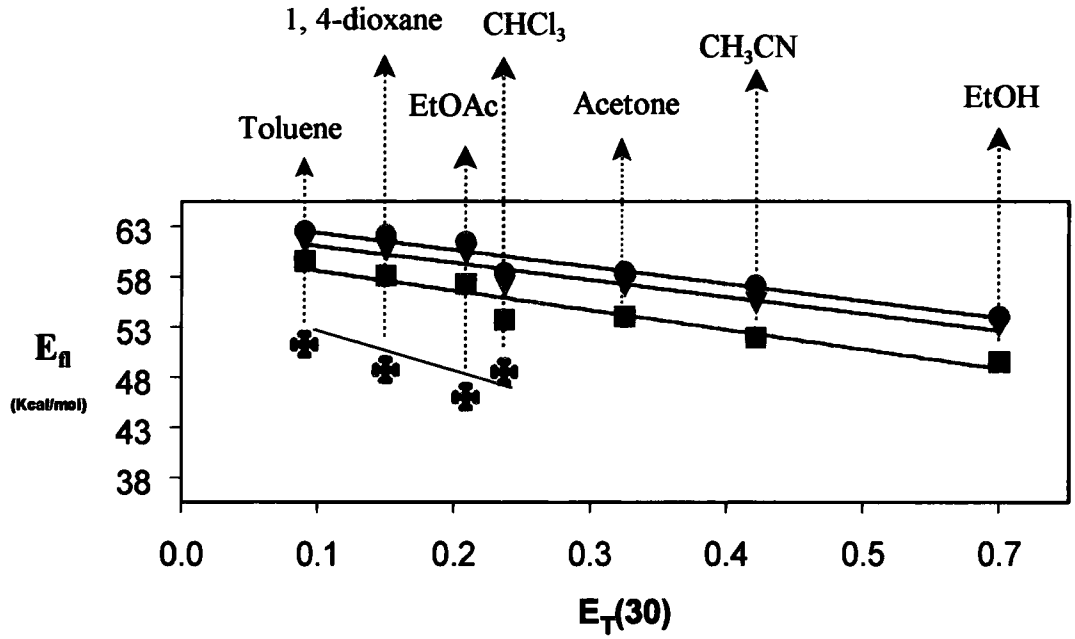

Figure 19. *Fluorescence energy as a function of* $E_T(30)$ *parameter for* **5a-d**.

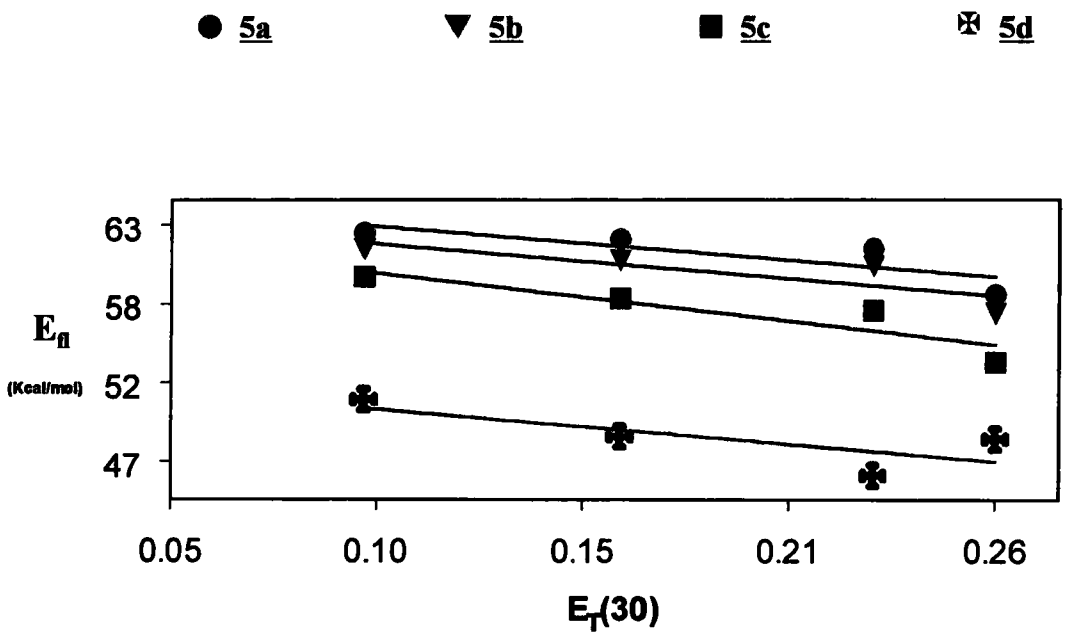

Figure 20. *Fluorescence energy versus* $E_T(30)$ *for* **5a-d** *in selected solvents.*

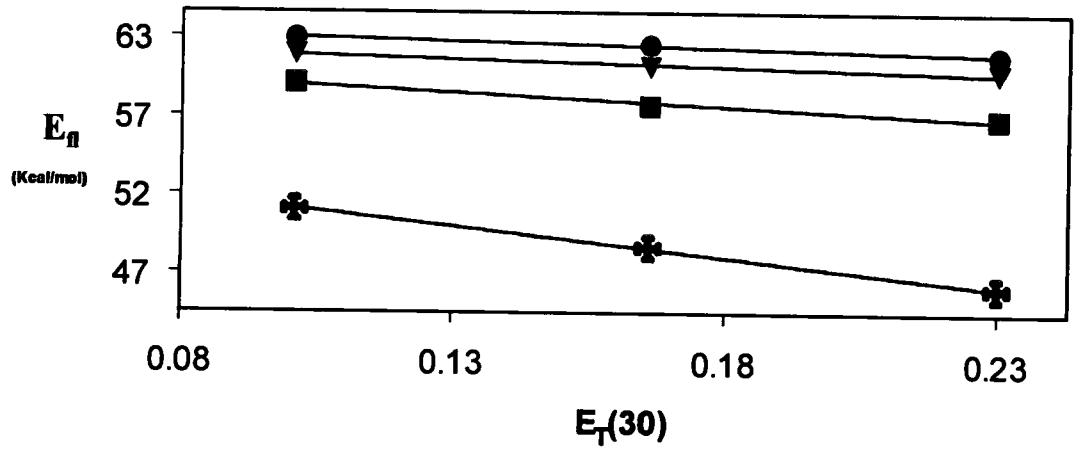

Figure 21. *Fluorescence energy as a function of* $E_T(30)$ *parameter for* **5a-d** *in toluene, 1,4-dioxane, and ethyl acetate.*

Table 10. *Results of* $E_T(30)$ *Plots on Figures* 19, 20, *and* 21 *for Substituted* **5**

	Figure 19		Figure 20		Figure 21	
	b	r^2	b	r^2	b	r^2
5a	-15.58	0.925	-22.13	0.676	-8.28	0.978
5b	-15.48	0.918	-22.78	0.672	-9.08	0.962
5c	-17.95	0.910	-31.35	0.807	-17.61	0.975
5d	-22.74	0.578	-22.74	0.578	-40.31	0.999

(Figure 21). For **5d**, not only is the linear correlation improved but also a significant change in its slope is observed. The solvent acidity effect on **5** may be responsible for the poor linear correlations observed in Figure 20 (Table 10). Fluorophore **5d**, which is expected to possess a large dipole moment in comparison with **5a-c**, shows a greater solvent sensitivity. For **5d**, the slope (b) and linear correlation (r^2) dramatically change when the fluorescence energy in chloroform is excluded from the plot (Table 10, Figure 21). The slope changes from -22.74 (r^2 = 0.587) (including E_{fl} in $CHCl_3$) to -40.31 (r^2 = 0.999) (excluding E_{fl} in $CHCl_3$). The poor linear correlation may be due to hydrogen bonding interactions between chloroform and **5d** molecules. Note that Figures 18 and 21 end up with the same solvents (ethyl acetate, 1,4-dioxane, and toluene).

The magnitude of the slopes, b and s, suggests which dye is more stabilized in the charge transfer excited state. By using either π^* (Table 10, Figure 18) or $E_T(30)$ (Table 10, Figure 21) the same trend was obtained. The magnitude of the slopes increases as the electron donor capability increases: $N(CH_3)_2 > OCH_3 > CH_3 > H$. These results indicate that the stabilization of the charge transfer excited state by polar solvents follow this order: **5d** > **5c** > **5b** > **5a**.

Improvement of the linear correlation by excluding ethanol and chloroform can be also observed for **5a-c**. From the plot in Figure 19, the exclusion of ethanol and chloroform resulted in an improvement in the linear correlation with only a moderate change in the slopes (Figure 22, Table 11). This is consistent with the results in Table 10. This observation suggests that the molecules of ethanol and

chloroform interact in the excited state with the fluorophores **5a-c** perturbating their photophysical properties in a higher degree than the other solvents investigated.

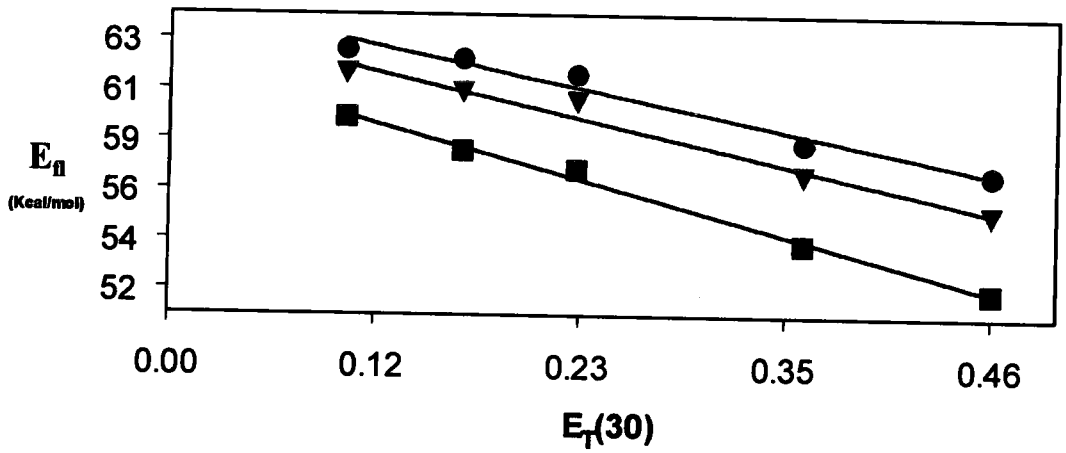

Figure 22. *Fluorescence energy as a function of* $E_T(30)$ *for* **5a-c** *in toluene, 1,4-dioxane, ethyl acetate, acetone and, acetonitrile.*

Table 11. *Results of* $E_T(30)$ *Plots for Fluorophores* **5a-c** *on Selected Solvents*

	Figure 19		Figure 22	
Fluorophore	**b**	**r^2**	**b**	**r^2**
5a	-15.58	0.925	-16.19	0.969
5b	-15.48	0.918	-17.70	0.972
5c	-17.95	0.910	-21.24	0.995

A very good linear correlation between the slopes obtained from both π^* and $E_T(30)$ versus Hammett's constant σ^+ are shown in Figures 23 and 24. This suggests that the stabilization of the charge transfer excited state is strongly linked to the donor strength of the substituents.

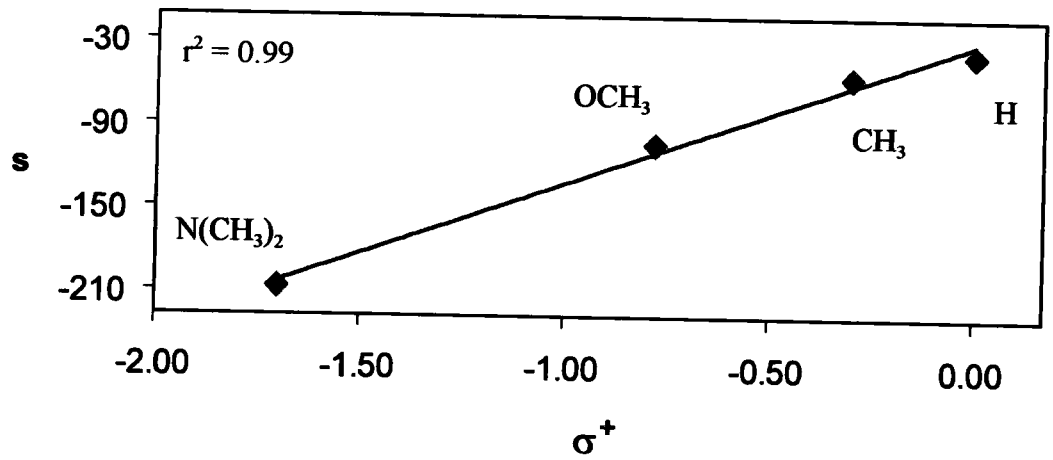

Figure 23. *Degree of CT excited state stabilization* (s) *as a function of* σ^+ *for* **5a-d**.

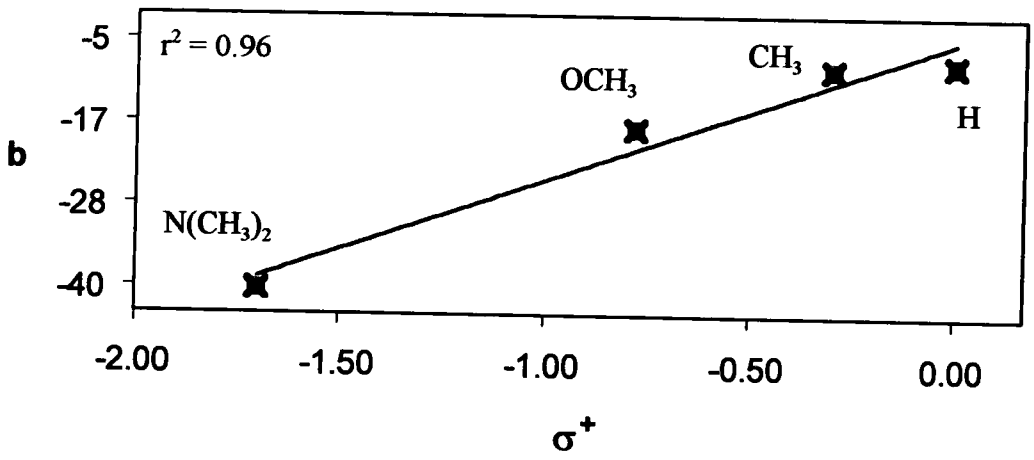

Figure 24. *Degree of CT excited state stabilization* (b) *as a function of* σ^+ *for* **5a-d**.

The fluorescence efficiencies (Φ_{fl}) together with the excited state lifetime (τ) for substituted **5** in toluene are reported in Table 12. The rate constants for radiative (k_r) and non-radiative (k_{nr}) processes were calculated using equations 5 and 6,[22] respectively. The non-radiative constant is the sum of all possible modes of de-excitation including internal conversion, intersystem crossing, and twisting out of the planar geometry in the excited state.[18] Fluorophore **5c** has a k_{nr} of 0.0; thus all electrons excited are returned to the ground state via a radiative process. Since its fluorescence efficiency is 1.0 it can be concluded that all excited molecules decay to the ground state and emit a photon of light. Then, the k_r of **5c** is equivalent to the rate constant for the fluorescence process.

$$\Phi_{fl} = \frac{k_{fl}}{k_{fl} + k_{nr}}$$

$$\tau_{fl} = \frac{1}{k_{fl} + k_{nr}}$$

Table 12. *Excited State Lifetime and Photophysical Rate Constants in Toluene*

Fluorophore	Φ_{fl}	τ (ns)	k_r ($x10^{-8}$ s^{-1})	k_{nr} ($x10^{-8}$ s^{-1})
5a	0.55	2.2	2.4	2.0
5b	0.64	2.9	2.2	1.2
5c	1.0	3.6	2.7	0.0
5d	0.34	5.5	0.6	1.1

The excited state lifetime of substituted **5** shows a linear dependence on the electron donor strength of the substituents (Figure 25). This photophysical property (τ) was found to increase with increasing donor strength (Table 12). The latter finding indicates that the intramolecular charge transfer in **5** must be responsible for the difference in excited state lifetimes.

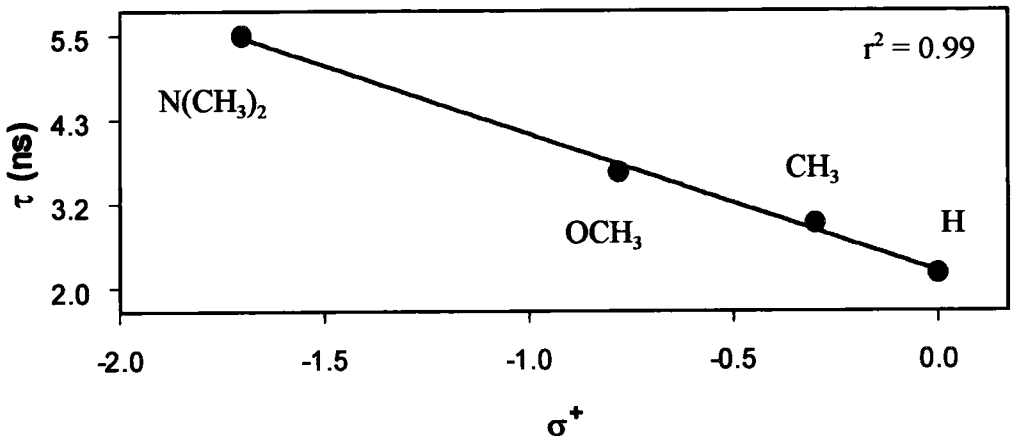

Figure 25. *Excited state lifetime dependence on electron donor strength of* **5a-d** *in toluene.*

The excited state dipole moment (μ_e) of substituted **5** was determined by the solvatochromic shifts method using equation 14,[23] where ν_e^o is the frequency of the emission maxima in vacuum, and 2/(hc) is a constant equal to 1.005 $x10^{-20}$. The excited state dipole moment can be calculated from the slope of a plot of the frequency of the emission maxima (ν_{em}) versus the solvent dependent function Δf (Eq. 14). For reasons discussed earlier (exclusion of solvents), toluene, 1,4-dioxane and ethyl acetate were used in these plots. The volumes of the solvent cavity (V) surrounding the molecule and the ground state dipole moment were calculated using the software *Chem3D Ultra 6.0*.[24] This software calculates the total surface area of the molecule[25] in angstrom (10^{-10} meter). Using this total surface area the volume of the solvent cavity surrounding the molecule (V) was obtained by raising the value of the molecular surface area to the cubic power ([10^{-10} meter]^3).

$$\nu_{em} = \nu_{em}^{o} - \frac{2}{h\,c\,V}\,\mu_e^{2}\,\Delta f \qquad \text{Eq. 14}$$

Plots of frequency of the emission maxima versus the solvent polarity function Δf are shown in Figure 26. The excited state dipole moment resulting from these plots, the calculated ground state, and the volume of the molecular cavities (V) are presented in Table 13. The excited state dipole moment of **5a** (7.56 Debye) and **5b** (7.46 Debye) are very close to each other, suggesting that their intramolecular charge transfer in the excited state are not that different. For **5c** the value is 10.8 D while **5d** shows 18.4 D. A linear relationship was found when the μ_e is plotted against

the Hammett's σ^+ constant (Figure 27).

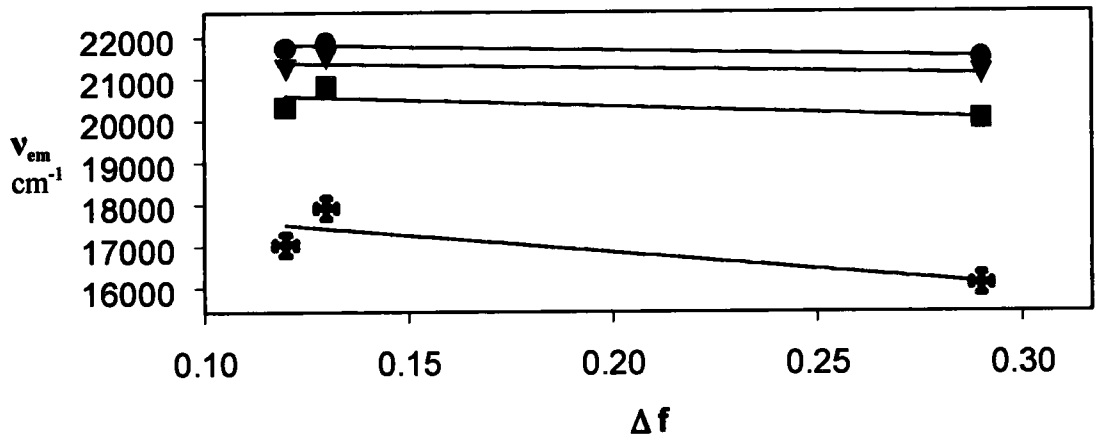

Figure 26. *Frequency of the emission maxima of* **5a-d** *as a function of the solvent parameter* Δf.

Table 13. *Ground State* (μ_g) *and Excited State* (μ_e) *Dipole Moments with their Respective Molecular Cavity* (**V**) *Volumes for Fluorophores* **5** *in Toluene*

Fluorophore	μ_g (Debye)	μ_e (Debye)	V (Å^3)
5a	2.26	7.56 ± 0.05	319
5b	2.80	7.46 ± 0.05	358
5c	2.50	10.8 ± 0.05	376
5d	3.03	18.4 ± 0.05	423

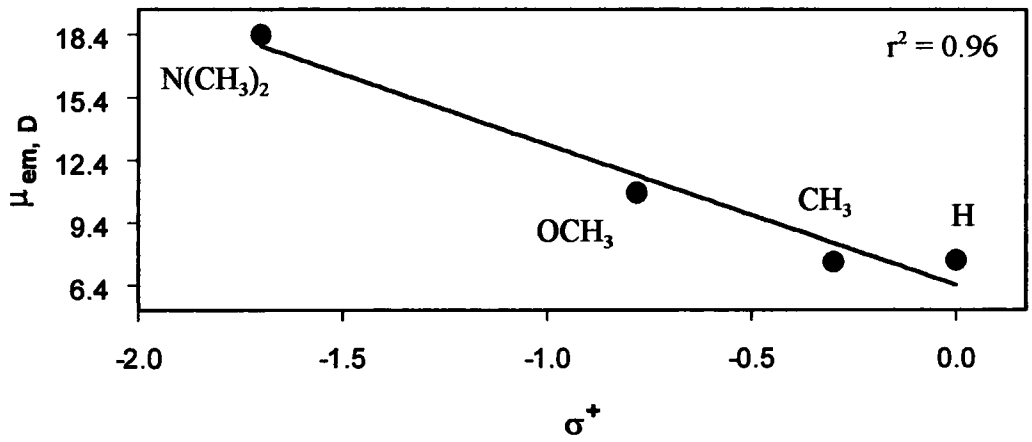

Figure 27. *Excited state dipole moment versus Hammett's constant* σ^+ *in toluene for* **5**.

These results suggest that the emission of **5a-d** is from the polar CT excited state since μ_e is dependent upon the electron donor strength of the substituent. The μ_e is intramolecular charge transfer dependent as expected since the dipole moment of a molecule is directly related to the charge distribution.[26] However, the charge distribution in a molecule may be affected by the torsion angles between the positive (donor group) and negative (acceptor group) charge. In fact, during the calculations of the μ_g it was noted that different dihedral angles generate a variety of μ_g values. For that reason, the dihedral angles of **5b** and **5c** were set as obtained from the x-ray structure determination (Table 6) in order to calculate the μ_g. Since it was not possible to grow crystals for **5a** and **5d** their dihedral angles were assumed to be similar to those of **5b** and **5c**.

For the sake of comparison, the fluorescence efficiency (Figure 28), and the excitation and emission spectra (Figure 29) of **4a** and **5a** in DMSO were analyzed. The introduction of the formyl group, which acts as an electron acceptor and extends the molecular conjugation of **4a**, dramatically improves the fluorescence efficiency. At an excitation wavelength of 334 nm the fluorescence efficiency of **4a** is 0.48, however, when the formyl group is attached to the 5 position on the thiophenyl ring (**5a**) the fluorescence efficiency increases to 0.97. It was found that the fluorescence efficiency is reduced to 0.49 when **5a** is excited at 365 nm. Thus, the fluorescence efficiency of **5a** is not only solvent dependent (Table 8) but also sensitive to the frequency of excitation. Similar behavior has been observed for quinine[27] (see page 7). It is worth mentioning that **5a-c** exhibit a green visual fluorescence in most organic solvents while their respective precursors **4a-c** do not.

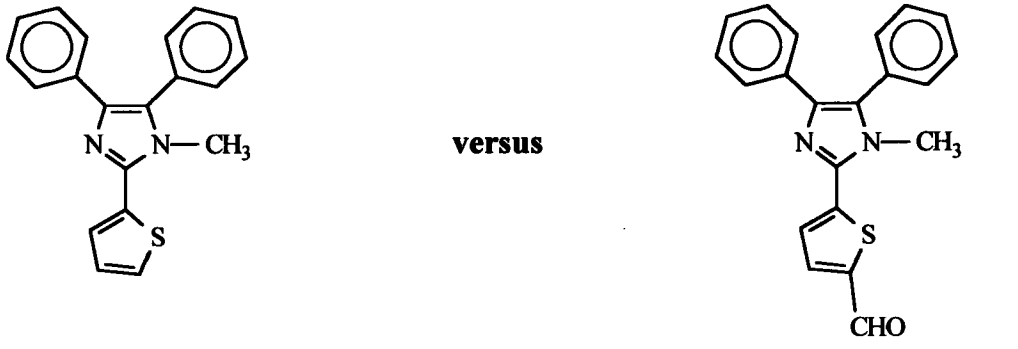

4a
$\Phi_{fl} = 0.48$
$\lambda_{exc} = 320$ nm
$\lambda_{em} = 386$ nm

5a
$\Phi_{fl} = 0.97$
$\lambda_{exc} = 295, 384$ nm
$\lambda_{em} = 506$ nm

Figure 28. *Comparison of fluorescence efficiency, excitation, and emission maxima for fluorophores without formyl group* (**4a**) *and with it* (**5a**) *in DMSO.*

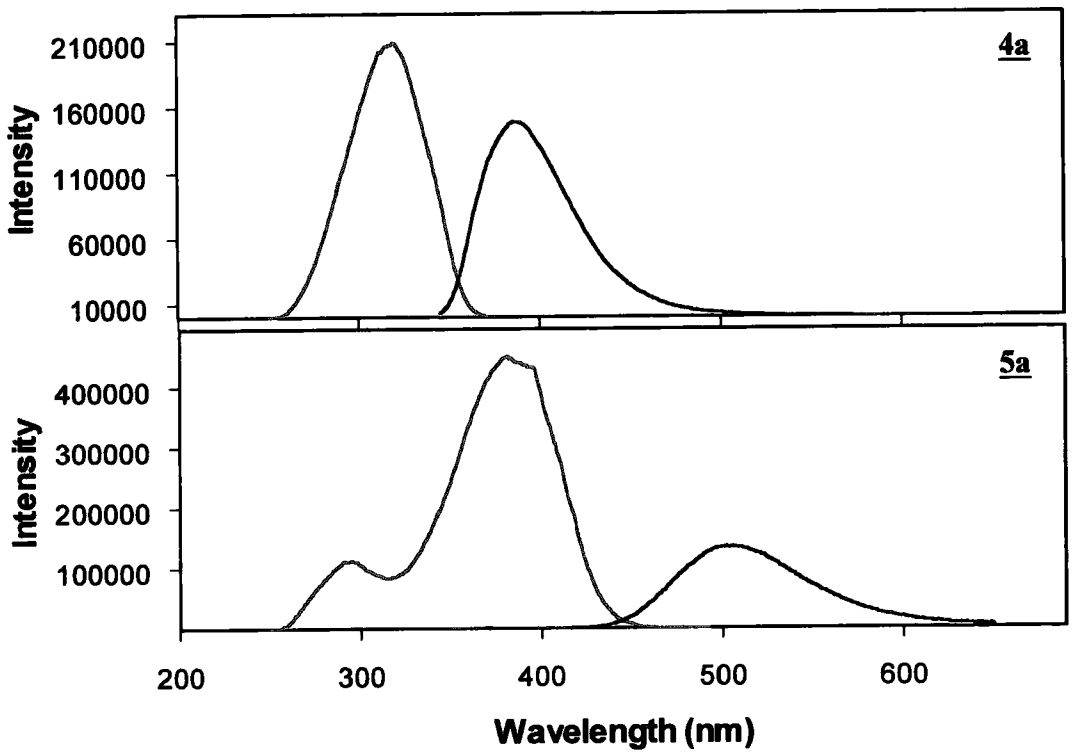

Figure 29. *Comparison of excitation (left band) and emission (right band) spectra of* **4a** *and* **5a** *in DMSO.*

The emission spectra in Figure 29 were recorded using an excitation wavelength of 334 nm and the excitation spectra were measured using the corresponding emission maxima. The excitation and emission spectra of **4a** appear as one band each (Figure 29). For **5a** the excitation spectrum shows two bands, one at 295 nm and another of larger intensity at 384 nm. The emission spectrum of **5a** is a broad band relative to that for **4a**. The excitation and emission maxima of **5a** are considerably red shifted relative to those of **4a** (the parent compound). These spectral properties imply that the observed longer excitation and fluorescence emission bands of **5a** might result from the intramolecular charge transfer.

Oxygen is a well known fluorescence quencher.[28] For that reason further studies were made to investigate the effects of oxygen on the fluorescence efficiency of **5c**. Fluorophore **5c** has a fluorescence efficiency of 1.0 at an excitation wavelength of 365 nm in toluene. A solution sample of **5c** having an absorption intensity no higher than 0.05 ($1.5x10^{-6}$ M) was prepared using anhydrous toluene. This sample was purged with either nitrogen or oxygen gas. First, using the solvent just as taken from the bottle the fluorescence efficiency is 1.0 (Φ_{fl1}). Second, ultra high pure nitrogen was bubbled into the solution for two minutes, then the fluorescence spectra were recorded giving fluorescence efficiency (Φ_{fl2}) of 1.0. Finally, oxygen was bubbled into the same solution for two minutes, resulting in 0.58 of fluorescence efficiency (Φ_{fl3}). Clearly, the presence of oxygen in the solution containing **5c** reduced the fluorescence efficiency. However, 0.58 can still be considered a high value of fluorescence efficiency. Results are given in Table 14.

Table 14. *Fluorescence Efficiency of* **5c** *in Anhydrous Toluene Under Different Treatments; in the Solvent just as Taken from the Bottle* (Φ_{fl1}), *after Bubbling Nitrogen* (Φ_{fl2}) *and Oxygen* (Φ_{fl3})

Φ_{fl1} No Purge	Φ_{fl2} After purge N_2	Φ_{fl3} After purge O_2
1.0	1.0	0.58

4.3 *Synthesis of Macromolecules Containing Fluorescent Dyes*

The synthetic strategy for the preparation of macromolecular systems containing fluorescent dyes **5** required functionalization of the corresponding fluorophore. For this purpose the 1-position of the imidazole ring was functionalized with 2-hydroxyethane as shown in Scheme 8. In order to introduce an aldehyde group at the 5-position of the thienyl ring the hydroxy group needs to be protected. Tert-butylchlorodiphenyl silane (t-BCDPS) was used for this purpose (Scheme 8). The advantage of this protecting group is its great stability under moderate acid conditions and facile removal.[29]

It was found that the stability of the t-BDPS (tert-butyldiphenyl silyl) group in presence of n-BuLi was good enough to obtain the desired products **9** in high yields (Scheme 9). The X-ray structure determination of **9c** clearly shows the protection of the hydroxy group by t-BDPS (Figure 30). The collection parameters for this X-ray structure are listed in Table 15. Comparison of selected dihedral angles of **5b**, **5c** and **9c** are given in Table 16. In the solid state, **9c** shows that the phenyl ring adjacent to 1-position of the imidazole ring is more twisted (69.85°) than the other (9.8°). The thienyl ring was found to have a twist of only 3.48° relative to the imidazole ring. The oxygen of the aldehyde is nearly co-planar to the thienyl ring, twisted by 1.4°. In a manner similar to **5b** and **5c** (Figures 3 and 4) the electron rich atoms (sulfur and oxygen) were found to be syn to each other.

The tert-butyldiphenyl silyl group was easily removed with an excess of tetrabutyl ammonium fluoride in 1.0 M THF solution.[29] Then unprotected dyes **10**

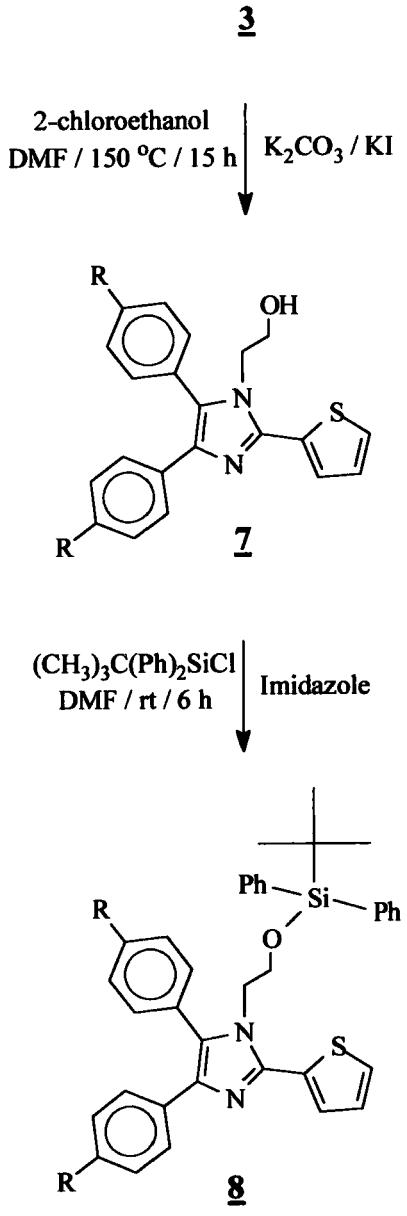

	a	c
R=	H,	OCH_3
Yield=	95%	65%

	a	c
R=	H,	OCH_3
Yield=	70%	89%

Scheme 8. *Functionalization of dyes* 3a *and* 3c.

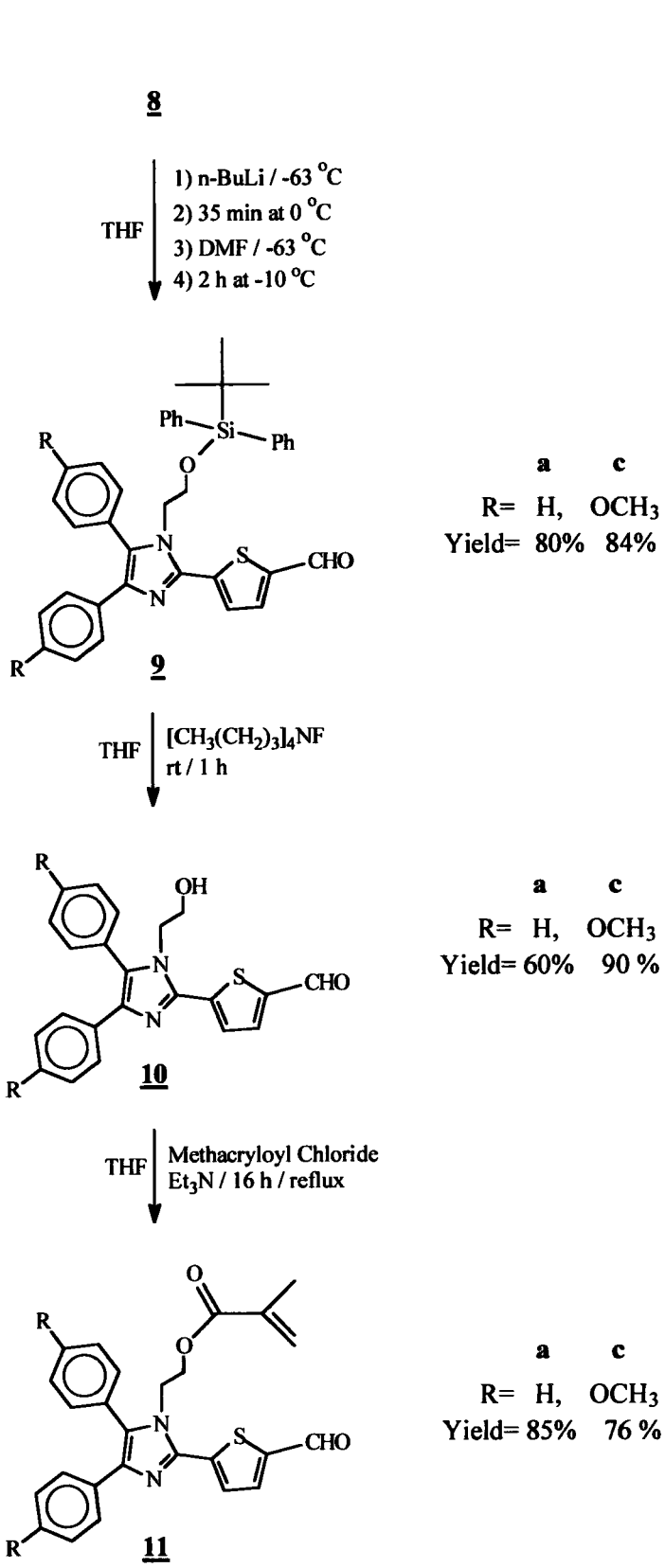

Scheme 9. *Synthesis of the methylacrylate monomers* **11**.

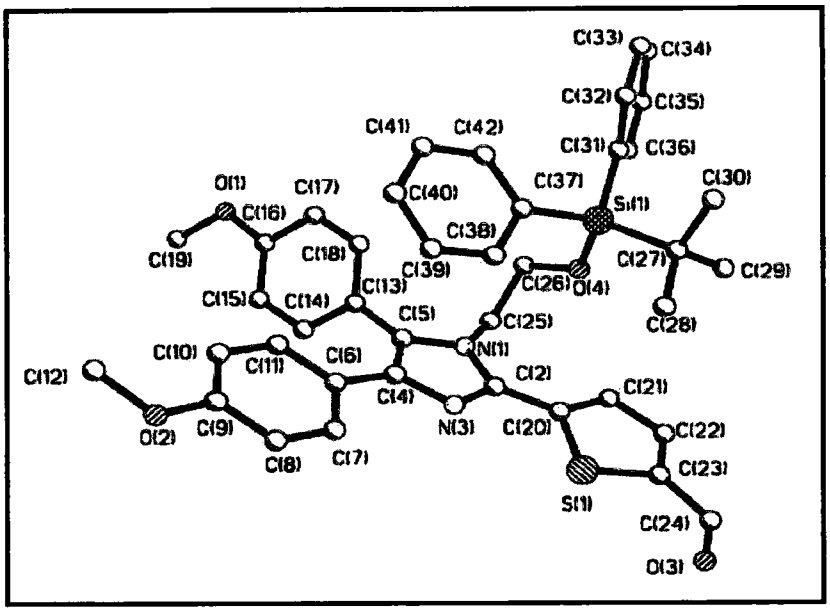

Figure 30. *X-ray structure of protected fluorophore* **9c**.

Table 15. *Data Collection Parameters for the X-ray Structure of* **9c**

Temperature:	173(2) K	Θ range collection:	1.57 - 25.50 deg.
Wavelength:	0.71073 Å	Refl. collected/unique:	18435 / 6423
Crystal system:	monoclinic, P2(1)/n	Refinement method:	Full matrix l-s F^2
Molecule per unit:	4	Data/rest./param.:	6423 / 0 /466
Calculated density:	1.297 mg/m^3	Goodness fit on F^2:	0.924
Crystal size (mm):	0.51x0.34x0.20	Final R indices:	R1 = 0.0298

Table 16. *Selected Dihedral Angles (deg.) of Fluorescent Dyes* **5b**, **5c**, *and* **9c**

Angles*	**5b**	**5c**	**9c***
N(1)-C(5)-C(13)-C(18)	58.9(2)	89.43(18)	69.85(19)
C(5)-C(4)-C(6)-C(11)	21.3(3)	16.8(2)	9.8(2)
S(1)-C(20)-C(2)-N(3)	10.0(2)	22.81(19)	3.48(18)
O(3)-C(24)-C(23)-S(1)	3.4(3)	2.6(2)	1.4(2)

were reacted with methacryloyl chloride in the presence of triethylamine resulting in functionalized monomers. Each of the products in Schemes 8 and 9 was purified by flash column chromatography, using silica gel, prior to use in the synthesis. When no purification was carried out a significant decrease in yields was obtained. Compounds **9**, **10**, and **11** exhibit green visual fluorescence in polar solvents such as acetone. All of these dyes are solids with a characteristic color; compounds **9** are white solids, **10** are yellow solids and **11** are red solids. It is worth mentioning that **9c** is a solid with an intense brilliant yellow color.

After esterification of the hydroxyl group with methacryloyl chloride a polymerization reaction was carried out using free radical conditions as shown in Scheme 10. The reaction was performed in an air free ampul. The air was removed by vacuum in order to improve the molecular weight of the target systems. Once all reactants were dissolved in the ampul, a rubber cap was placed on its open neck to close it. Then, the mixture was treated using a freeze-thaw and vacuum protocol. After that, the ampul was sealed and warmed to 60 °C. The target macromolecule was precipitated with methanol and obtained as a yellow solid.

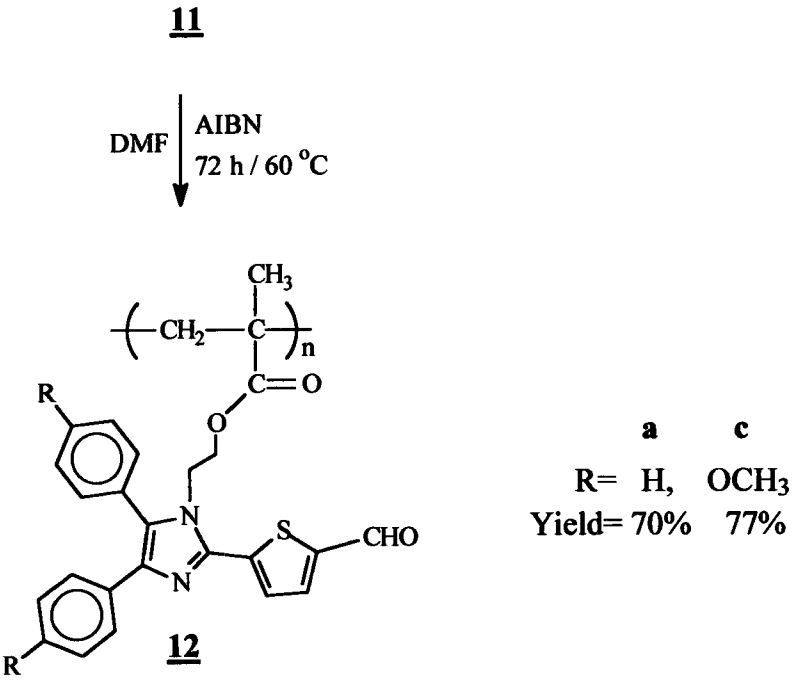

Scheme 10. *Preparation of macromolecules* **12** *containing fluorescent dyes.*

A representative comparison of the ^{1}H NMR spectra between monomer **11** and macromolecule **12** is shown in Figure 31. The peaks of the ^{1}H NMR spectra of **12a** are considerably broader than those of **11a**. As expected, the peaks corresponding to the double bond (between 5 and 6 ppm) of the methacryloyl group on **11a** do not appear in the ^{1}H NMR spectra of **12a**, indicating that this double bond has reacted. For monomer **11a**, the aldehyde proton appears at 9.91 ppm while for the **12a** at 9.54 ppm. This observed shifts could be attributed to the interactions of the neighboring monomeric units in **12a**.

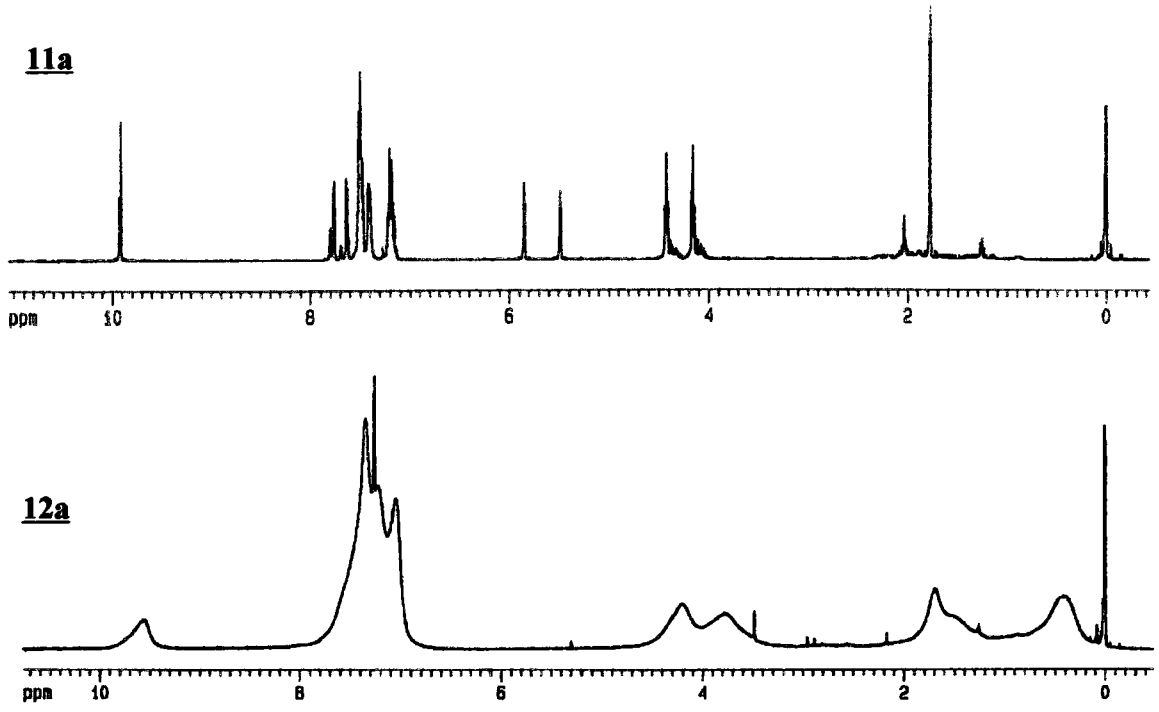

Figure 31. *Comparison of ^1H NMR spectra for monomer* **11a** *and macromolecule* **12a**.

Co-polymerization of **11a** with methyl methacrylate (MMA) using AIBN was carried out to give the corresponding system as shown in Scheme 11. The reaction was performed in a sealed ampul from which the oxygen was removed using the freeze-thaw and vacuum cycle. The target system was precipitated from methanol and obtained as a yellow solid. By ^1H NMR analysis the average ratio of the units in **13a** was determinated to be 1:10, where n = 1 and m = 10 (Scheme 11).

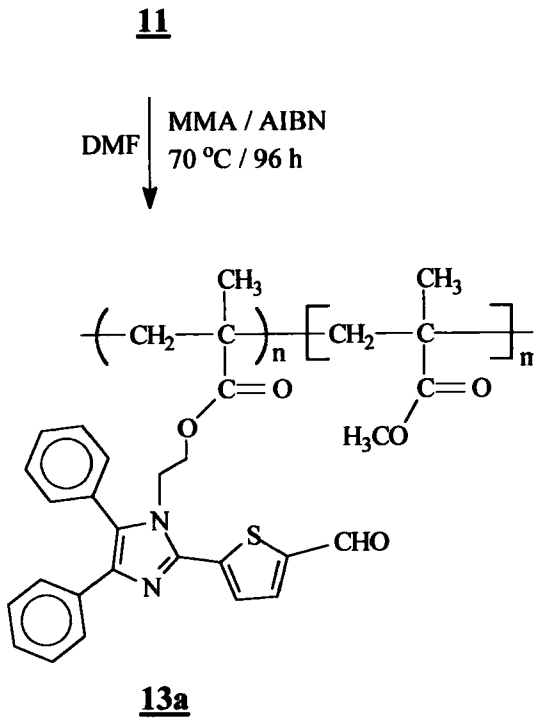

Scheme 11. *Co-polymerization of dye* **11a** *with methyl methacrylate (MMA).*

In the following section the photophysical properties of monomers **11**, and macromolecules **12** and **13** are discussed.

4.4 *Photophysical Properties of Monomeric and Macromolecular Systems*

The photophysical properties of monomers **11a** and **11c** are listed in Table 17. Each absorption spectrum shows two characteristic bands (Figure 32). For **11a**, the band at higher energy was found to be relatively insensitive to increasing the strength of the donor group (λ_{max} at 260 nm for **11a** and 262 nm for **11c** in DMSO). The band at lower energy was red-shifted with the introduction of methoxy groups, being consistent with an intramolecular charge transfer process. The band at higher energy can be assigned to π-π^* transitions while the bands at lower energy to n-π^* transitions. The emission spectrum for **11a** exhibit one band at 496 nm while **11c** at 547 nm (Figure 32). These emission spectra were recorded using an excitation wavelength of 365 nm in DMSO. The excitation spectra were obtained using their respective emission maxima as excitation wavelength giving two bands as shown in Figure 33. Fluorophore **11a** was found to possess higher fluorescence efficiency (0.82) than its analogue **11c** (0.38). Longer excited state lifetimes (τ) were obtained for the monomer having methoxy groups. The rate constants for radiative (k_r) and non-radiative (k_{nr}) processes were calculated using equations 5 and 6.

11a **11c**
R= H, OCH_3

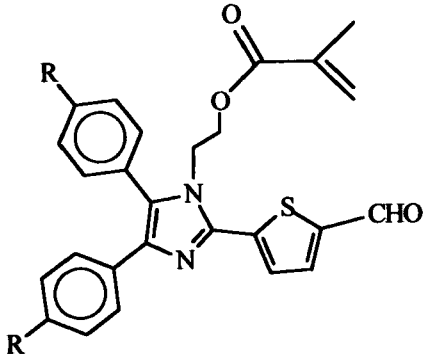

Table 17. *Photophysical Properties of Monomers* **11a** *and* **11c** *in DMSO at rt*

Monomer	λ_{abs}	λ_{exc}	λ_{em}	Φ_{fl}	τ	k_r ($x10^{-8}$)	k_{nr} ($x10^{-8}$)
11a	260, 378	284, 379	496	0.82	4.0	2.1	0.45
11c	262, 394	285, 394	547	0.38	5.9	0.06	0.10

λ in nm τ in ns $\Phi_{fl} \pm 0.04$

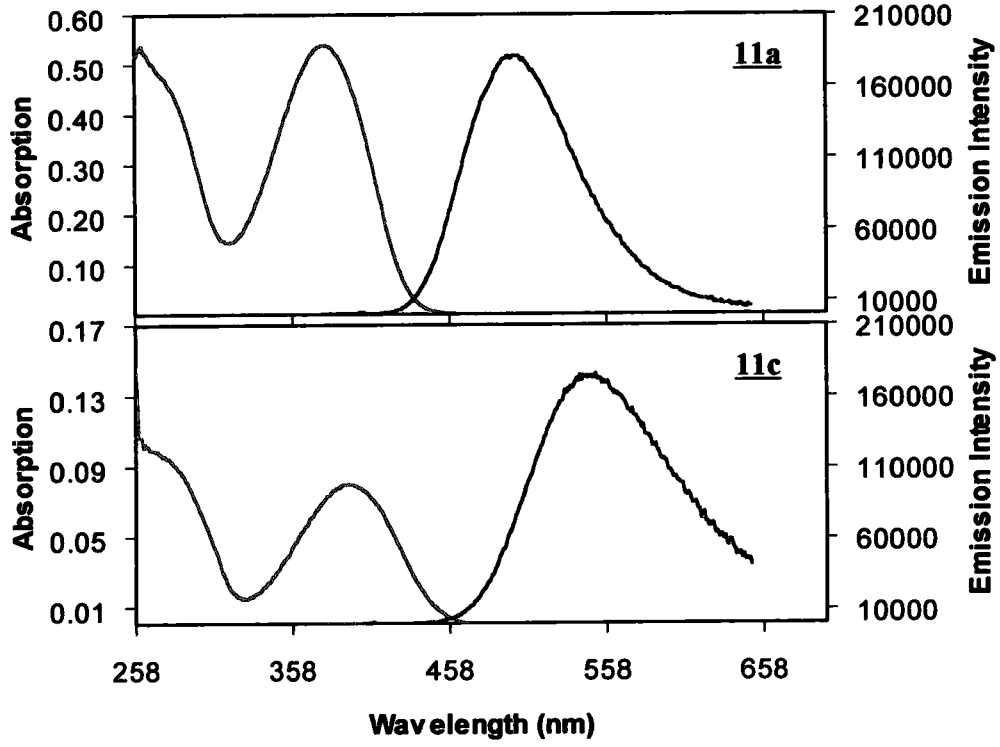

Figure 32. *Absorption and emission spectra of* **11a** *and* **11c** *in DMSO.*

The low fluorescence efficiency of **11c** in comparison with that of **11a** is expected since the same result was obtained for the analogous compounds **5a** and **5c** in polar solvents. Fluorophore **5a** showed higher fluorescence efficiency than **5c** in all polar solvents investigated (Table 8). The methyl methacrylate moiety on **11a** and **11c** was found to have no significant effect on their fluorescence efficiencies.

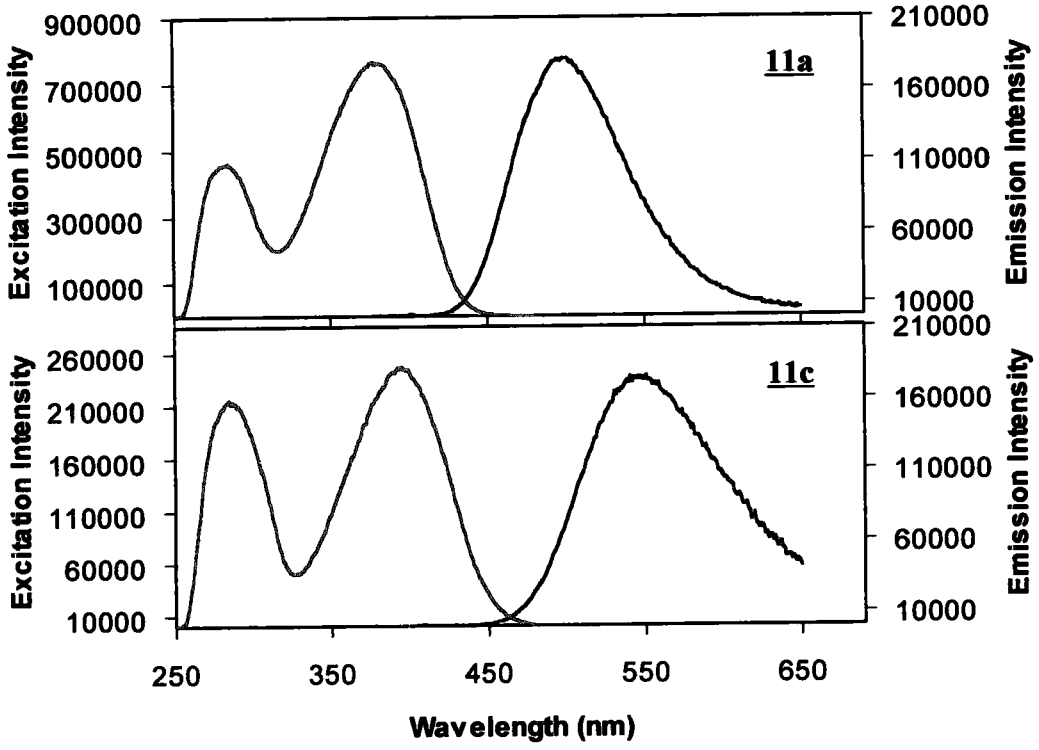

Figure 33. *Excitation and emission spectra of* **11a** *and* **11c** *in DMSO.*

The photophysical properties of **12** and **13a** are given in Table 18. First, it was observed that the absorption, emission, and excitation spectra for these macromolecular systems did not change considerably in solvents such as DMSO and CH_2Cl_2. The fluorescence efficiency remains relatively uniform for **13a**, in these solvents, while small quenching was observed for **12c**. Second, a comparison with their respective monomer shows that the polymer backbones do not affect significantly the absorption, emission or excitation spectra (Table 18, Figure 34). However, the fluorescence efficiency of the monomers was found to be higher than their respective macromolecular systems in all cases. For example, monomer **11a** possesses a fluorescence efficiency of 0.82 (Table 17) while the corresponding macromolecule **12a** has a fluorescence efficiency of 0.22 and **13a** is 0.76.

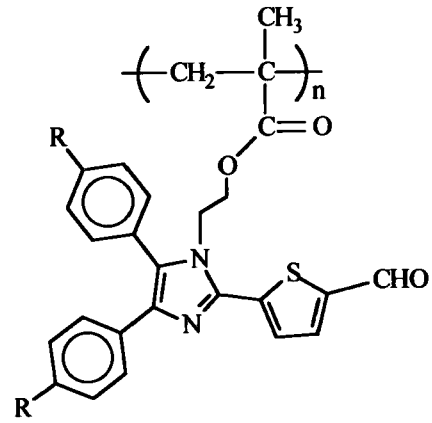

12a **12c**

R= H, OCH_3

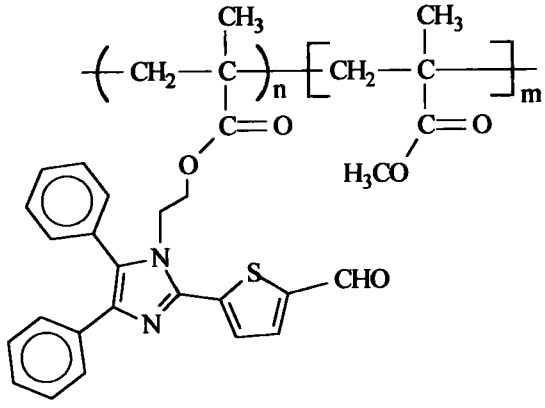

13a

Table 18. *Photophysical Data of Macromolecules* **12** *and* **13**

System	Solvent	λ_{abs}	λ_{exc}	λ_{em}	Φ_{fl}
12a	DMSO	266, 383	294, 381	494	0.22
12a	CH_2Cl_2	266, 376	294, 381	491	0.14
12c	DMSO	272, 390	286, 392	544	0.13
13a	DMSO	260, 379	295, 381	492	0.76
13a	CH_2Cl_2	266, 377	292, 380	479	0.77

λ in nm $\Phi_{fl} \pm 0.04$

The decrease in fluorescence efficiency of **12a** and **13a** in comparison with **11a** may suggest a significant interaction between the fluorophore units. For **12a**, a possible explanation is that the fluorophore units are so close to one another that the interactions between them result in self-quenching. However, **13a** undergoes much less fluorescence quenching in comparison with **12a**. The macromolecule **13a** possesses MMA units that serve as spacers between the fluorophore molecules. Thus, the fluorescent units could be significantly distant from one to another, reducing the fluorescence self-quenching, resulting in Φ_{fl} = 0.76 for **13a** that is close to the 0.82 obtained for the monomer **11a**. Although the latter could explain the quenching in Φ_{fl} of **12a** and **13a** relative to monomer **11a**, additional experiments may confirm the statement. In the future, it would be a good idea to have the molecular weight of the macromolecules available and make a relationship between them and the Φ_{fl} quenching.

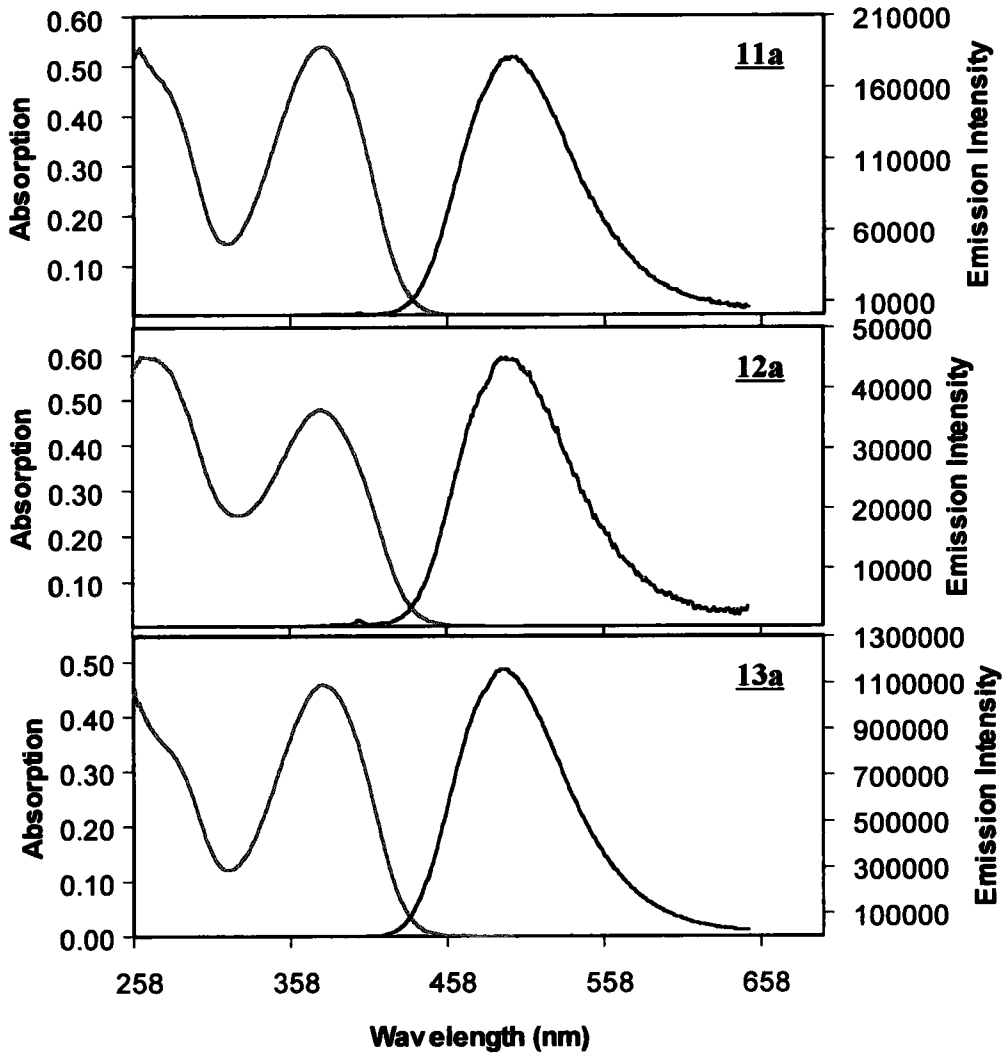

Figure 34. *Absorption and emission spectra of* 11a, 12a, 13a *in DMSO.*

The photophysical properties of the monomers 11 were obtained from a sample of 1.5×10^{-6} M while 3.7×10^{-5} M was used for the macromolecular systems 12 and 13. The higher concentration was used because at 1.5×10^{-6} M the 12 and 13 spectra were too weak to measure accurately.

4.5 *Dilution Effect on the Emission Spectra of Monomer* **11a**

The tolerance of dilution is a valuable information in the investigation of molecular fluorescent sensors, especially when the analyte is in solution. Sensor probe experiments usually consist of the gradual addition of an analyte into a fluorophore solution. When the analyte in solution is added to the fluorophore sample two potential emission quenching effects are introduced, which are the analyte itself and the dilution. Usually, the presence of an analyte results in an increase or decrease in the emission intensity of the fluorophore depending on its inherent response. On the other hand, dilution of the fluorophore solution will produce a decrease in the emission intensity. Therefore, the sensor ability of a fluorophore must be investigated in the dilution range where the emission intensity of the fluorophore is not affected. The latter needs to be done when using the emission spectra as the only tool to demonstrate the sensor ability.

Monomer **11a** was subjected to a dilution effect experiment, as follows. The emission spectra was obtained from a cuvette containing 3 mL of a 1.50×10^{-6} M solution of **11a** in DMSO. To this solution, DMSO was added gradually and the emission spectra recorded for each addition (Figure 35). The emission intensity, volume of solvent added, and concentration of **11a** are listed in Table 19. A constant emission intensity was obtained up to the addition of 80 μL of DMSO, where the concentration of **11a** is 1.461×10^{-6} M. The emission intensity was detected to decrease when a total of 90 μL of DMSO was added.

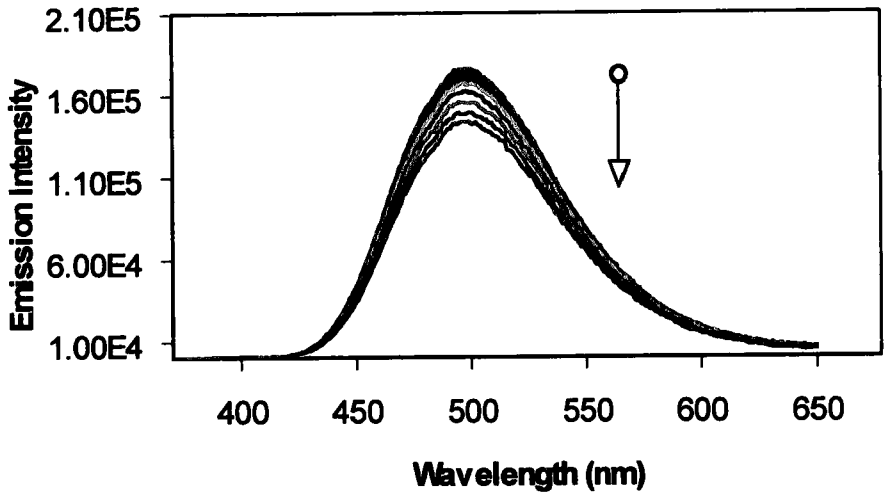

Figure 35. *Quenching of the emission intensity of* **11a** *by addition of DMSO (the arrow indicates that the emission intensity decreases with the addition of DMSO).*

The dilution effect of **11a** using DMSO as a solvent is clearly visualized from the plot of 'Emission Intensity vs. Concentration' as shown in Figure 36.

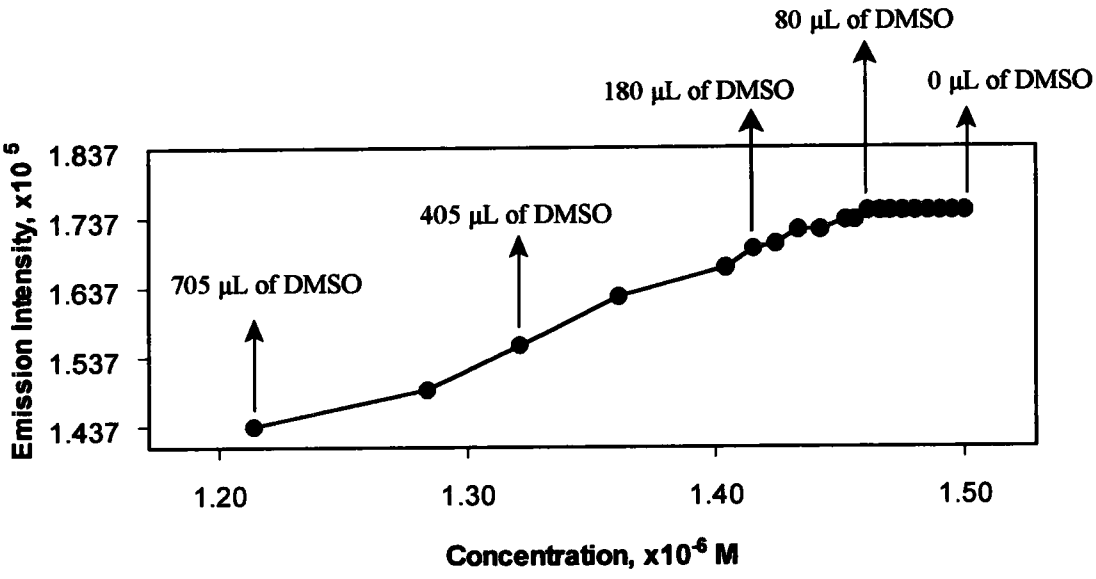

Figure 36. *Sensitivity of* **11a** *to dilution with DMSO.*

Table 19. *Emission Intensity and Concentration of* **11a** *from Dilution in DMSO*

Emission intensity, $x10^5$	Volume of DMSO added, μL	Total Volume of DMSO added, μL	Concentration of **11a**, $x10^{-6}$ mol/L
1.746	0	0	1.500*
1.746	10	10	1.495
1.746	10	20	1.490
1.746	10	30	1.485
1.746	10	40	1.480
1.746	10	50	1.475
1.746	10	60	1.470
1.746	10	70	1.466
1.746	10	80	1.461
1.733	10	90	1.456
1.733	10	100	1.452
1.719	20	120	1.442
1.719	20	140	1.433
1.699	20	160	1.424
1.692	20	180	1.415
1.665	25	205	1.404
1.624	100	305	1.361
1.554	100	405	1.321
1.490	100	505	1.284
1.437	200	705	1.214

*Initial concentration of **11a**. The initial volume of **11a** ($1.50x10^{-6}$ M) in the cuvette was 3 mL. Notes: The error for the emission instrument was determined to be ± $0.05x10^5$ and ± 0.01 μL (manufacture error) for the 20 μL syringe used.

4.6 *Ability of Monomer* 11a, *and Macromolecules* 12a *and* 13a *to Detect Nickel and Lead Ions: Emission and Stern-Volmer Plot*

The sensitivity to environmental perturbations and high fluorescence efficiencies makes the fluorophores 5 and their derivatives (11, 12, and 13) very attractive for the detection of analytes, such as metal ions. Their ability to bond metal ions is expected from the potential coordination sites shown in Figure 37. For example, the nitrogen and sulfur atoms in the imidazole and thiophene rings, respectively, could interact with metal ions to produce a fluorescence response.

An important consideration in order to choose the analyte is the absorption and emission. The analyte should not absorb or emit energy at the same wavelength range that the fluorophore does. The introduction of an analyte that absorbs energy at the excitation wavelength will result in an emission spectra behavior that count both the analyte and fluorophore absorption. Therefore, such emission spectra behavior will not demonstrate the real sensor capability of the fluorophore.

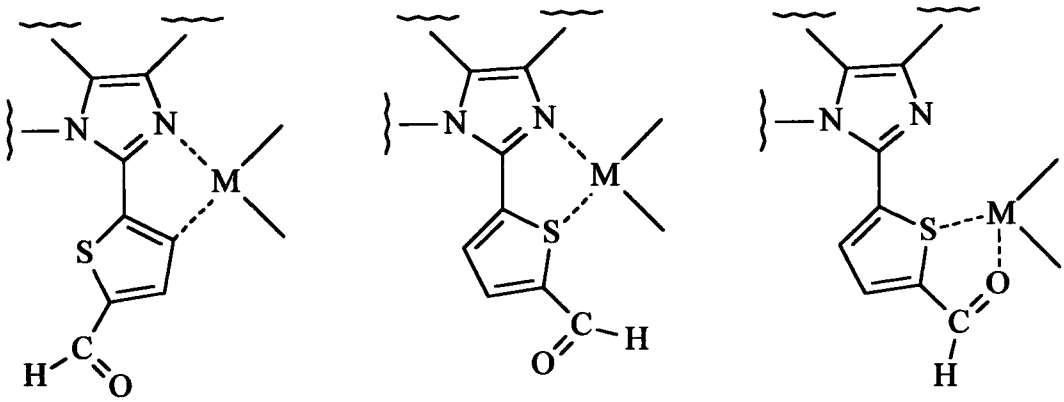

Figure 37. *Potential coordination sites of fluorescent dyes.*

For example, if the analyte absorbs energy at the excitation wavelength used for the emission measurements, the emission intensity could decrease upon addition of the analyte just because of the energy absorbed by the analyte itself and not because of the interaction between the analyte and the fluorophore.

For this investigation the emission measurements were obtained using an excitation wavelength of 365 nm; otherwise it will be indicated. Nickel(II) perchlorate hexahydrate, $[Ni(ClO_4)_2 \cdot 6H_2O]$, and lead(II) perchlorate trihydrate, $[Pd(ClO_4)_2 \cdot 3H_2O]$ were chosen as metal ion sources for the sensor probes. Ni^{+2} and Pb^{+2} are known to form complexes with carbon, nitrogen, oxygen and sulfur atoms.[32] Therefore, at least one of the complexes shown in the Figure 37 may occur. The absorption spectra of **11a**, nickel(II) perchlorate hexahydrate and lead(II) perchlorate trihydrate are shown in Figure 38. Nickel(II) perchlorate hexahydrate absorbs energy in the range of 380 nm to 520 nm with absorption maxima at 417 nm. On the other hand, lead(II) perchlorate trihydrate absorbs energy in the range of 250 nm to 280 nm with an absorption maxima at 253 nm.

The probes showed that the emission intensity of **11a**, **12a**, and **13a** (3.7×10^{-6} M solution in DMSO) decreases upon addition of $Ni(ClO_4)_2 \cdot 6H_2O$ (Figure 39). Such quenching may be attributed to the presence of the analyte.

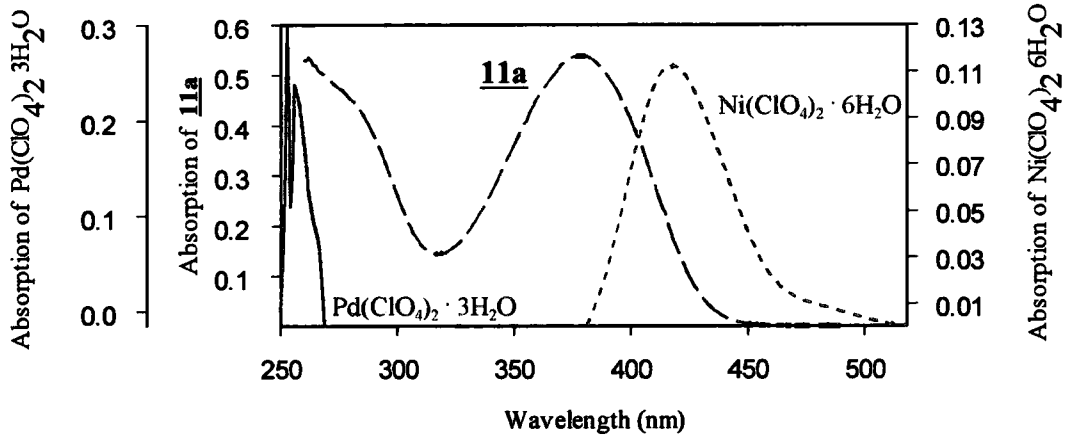

Figure 38. *Absorption of lead(II) perchlorate trihydrate, fluorophore* **11a** *and nickel(II) perchlorate hexahydrate in DMSO.*

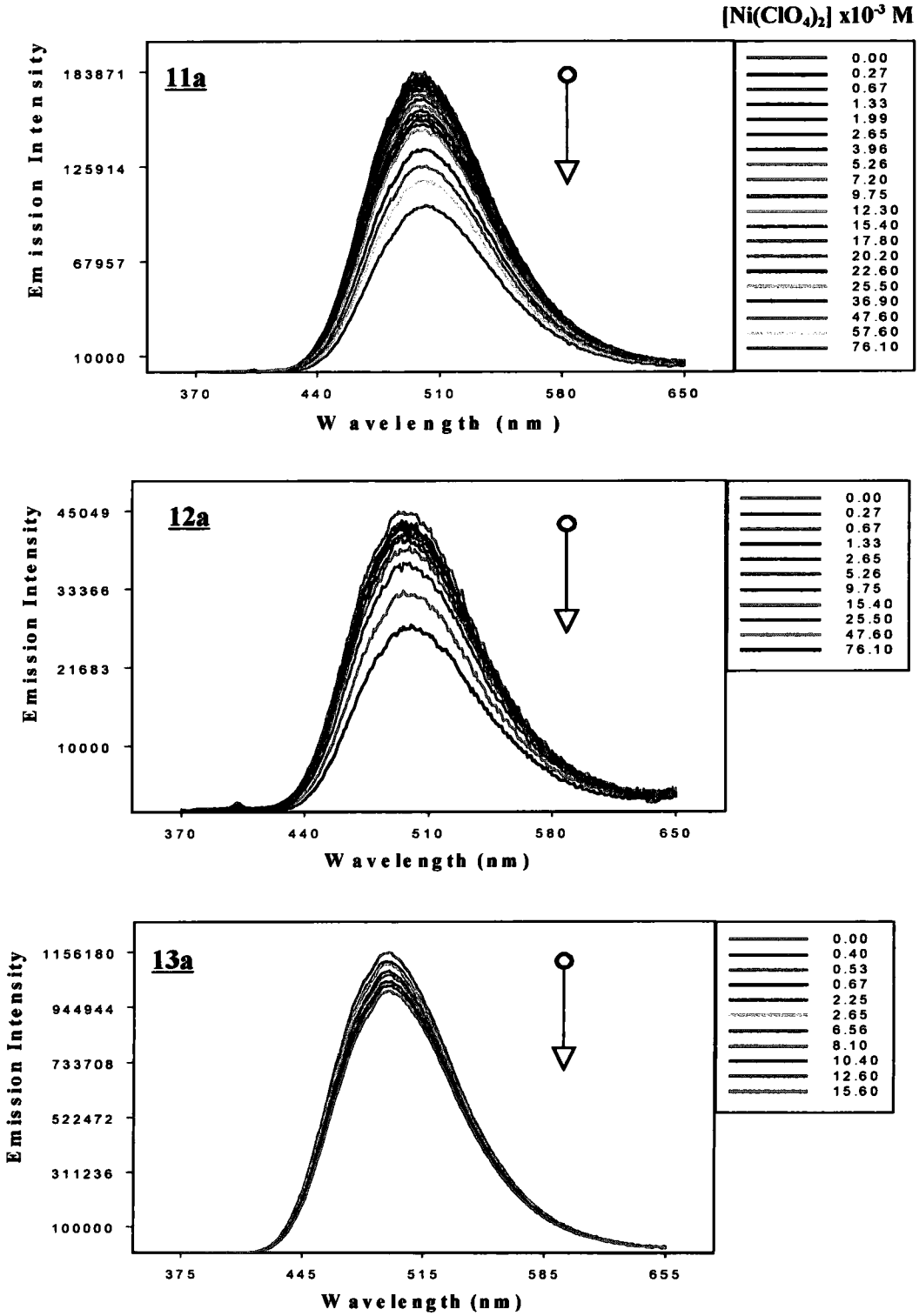

Figure 39. *Effect of* $Ni(ClO_4)_2 \cdot 6H_2O$ *on the emission spectra of* **11a**, **12a**, *and* **13a**.

The Stern-Volmer equation[33] (Eq. 15) was used to analyze the sensitivity of **11a**, **12a**, and **13a** to the gradual addition of $Ni(ClO_4)_2 \cdot 6H_2O$ and $Pd(ClO_4)_2 \cdot 3H_2O$ at room temperature. This equation can be also employed to determine the rate constant of the quenching (k_q) when the following are known: the emission intensity of the fluorophore in absence of quencher (I^o), the emission intensity of the fluorophore in presence of the quencher (I), the concentration of the quencher ([Q]), and the excited state lifetime (τ) of the fluorophore in absence of the quencher. The slope of a Stern-Volmer plot is proportional to the quenching rate constant. Therefore, the slope represents the sensitivity of the fluorophore to the analyte. Although Eq. 15 does not differentiate between static or dynamic quenching, it provides sufficient information to discard the dilution effect as a possible quencher.

$$\frac{I^o}{I} = k_q [Q] \tau + 1 \qquad \text{Eq. 15}$$

The Stern-Volmer plots for **11a**, **12a**, and **13a** as a function of $Ni(ClO_4)_2$ concentration are presented in Figure 40. The slope of these plots revealed about the same sensitivity for monomer **11a** (slope = 0.00845 ± 0.0002) and **13a** (slope = 0.00759 ± 0.0002). However, lower sensitivity was obtained for **12a** (slope = 0.00570 ± 0.0003). Between **12a** and **13a** it is noticed that better sensitivity was obtained for **13a**, where the fluorophore molecules are distant from one to another by MMA units. A similar pattern was observed for the goodness of the fit plot (r^2) and the fluorescence efficiencies.

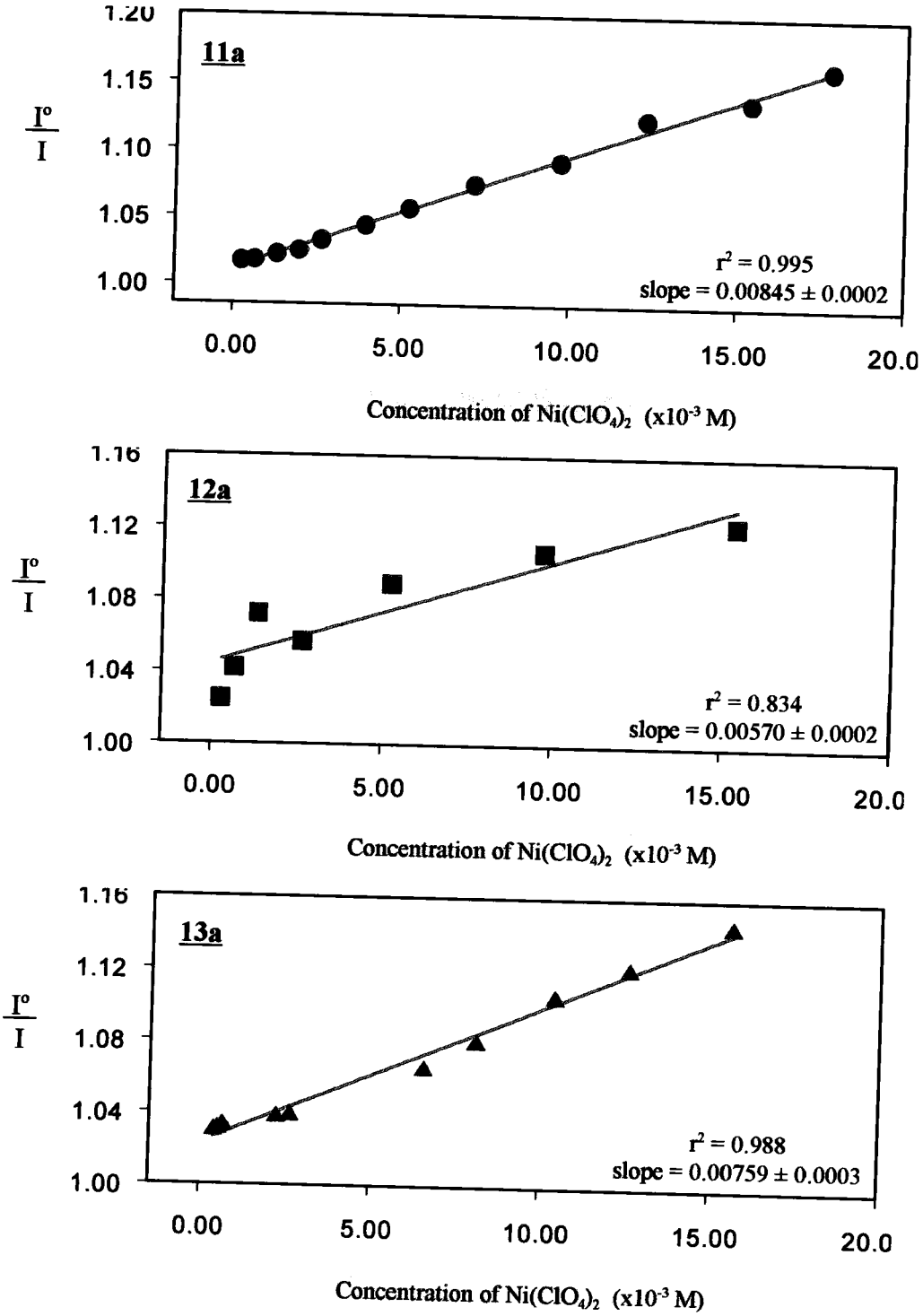

Figure 40. *Sensitivity of fluorophores* **11a**, **12a**, *and* **13a** *to* $Ni(ClO_4)_2 \cdot 6H_2O$.

The low sensitivity of **12a** may be attributed to the crowding of the fluorophore units in the macromolecule. The fluorophore units in **12a** may be too close from one to another hindering the interaction between the analyte and the coordination site.

A decrease in emission intensity of **11a** and **12a** (both at $3.7x10^{-5}$ M in DMSO) was also observed in probes using $Pb(ClO_4)_2 \cdot 3H_2O$. Figure 41 shows the emission intensities of **11a** and **12a** at concentration of 0.0 to $34x10^{-3}$ M of $Pb(ClO_4)_2 \cdot 3H_2O$. This quenching was analyzed using Stern-Volmer plots as shown in Figure 42. It was found that there was no significant sensitivity for **11a** or **12a** to the addition of $Pb(ClO_4)_2 \cdot 3H_2O$ as indicated by the slope of these plots.

A comparison of Stern-Volmer plots (Figure 43) revealed that **11a** is more sensitive to $Ni(ClO_4)_2 \cdot 6H_2O$ than to $Pb(ClO_4)_2 \cdot 3H_2O$. The dilution effect of **11a** (Section 4.5) was taken into account in the plots in Figures 40 and 42. As discussed earlier (Section 4.5) the dilution effect in **11a** takes place after the addition of 80 μL of DMSO. Therefore, the selected concentration, used in the plots, does not contain more that 80 μL of DMSO.

The ion selectivity of **11a** may be attributed to the ionic radii. Ni^{+2} has an ionic radius of 0.69 Å while Pb^{+2} is 1.33 Å.[34] Perhaps the lead ions are too large to fit in the coordination site of the fluorophore (Figure 37). However, further investigation is needed to confirm the complexation of the metal ions with the fluorophores and the effect of the H_2O molecules (from the metal ion sources) in the probes.

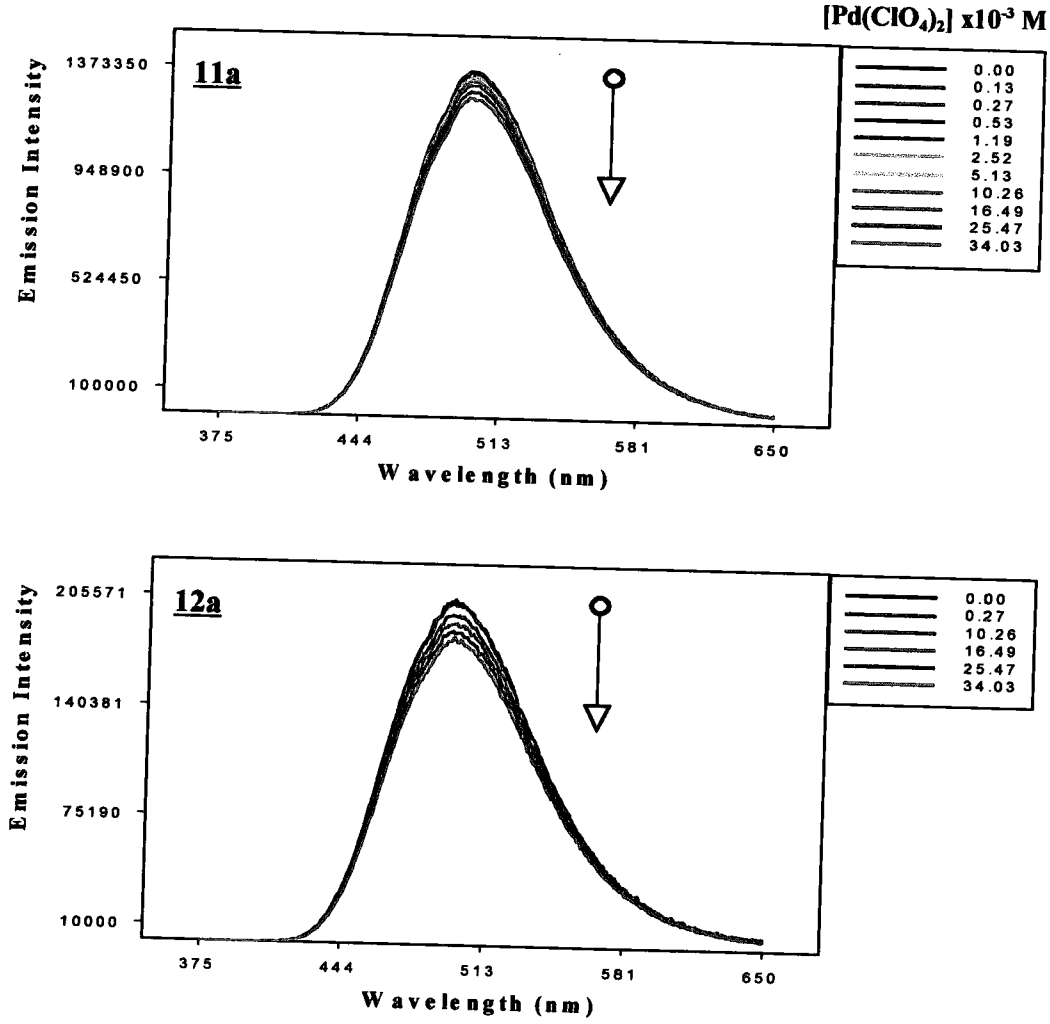

Figure 41. *Effect of $Pb(ClO_4)_2 \cdot 3H_2O$ on the emission spectra of* **11a** *and* **12a**.

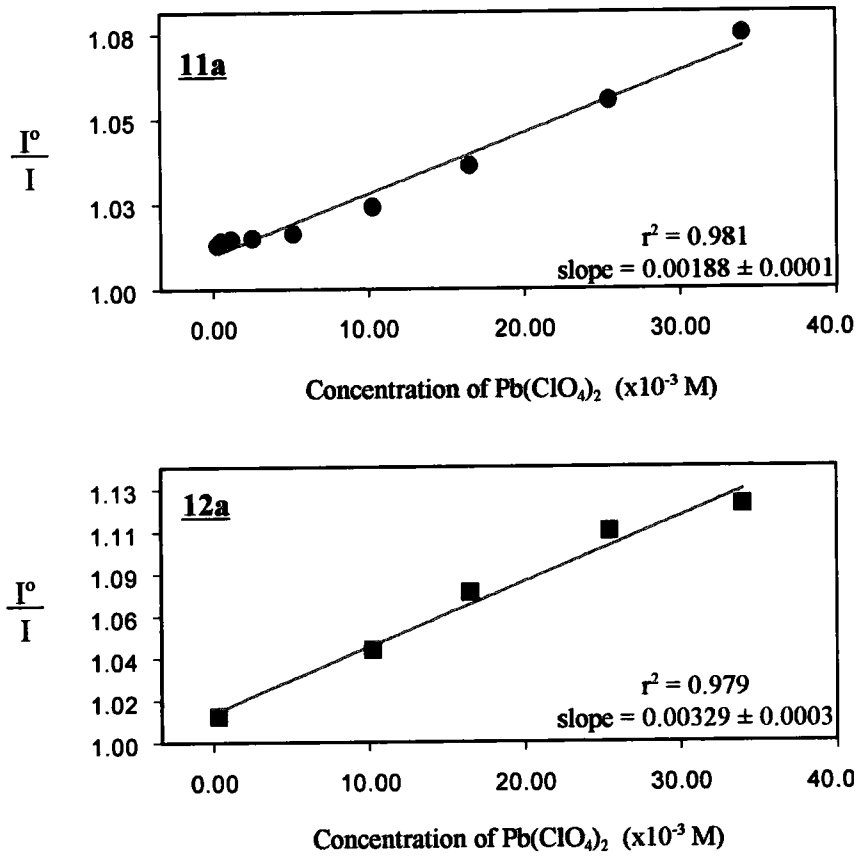

Figure 42. *Sensitivity of fluorophores* **11a** *and* **12a** *to* $Pb(ClO_4)_2 \cdot 3H_2O$.

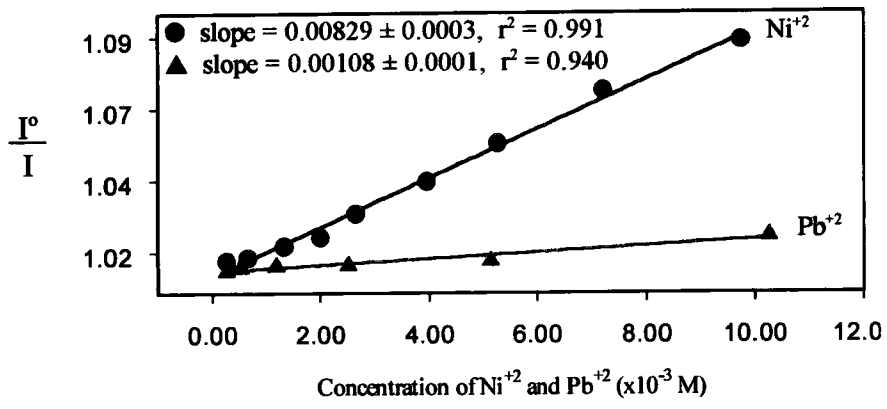

Figure 43. *Sensitivity of dye* **11a** *over* $Ni(ClO_4)_2 \cdot 6H_2O$ *and* $Pb(ClO_4)_2 \cdot 3H_2O$.

References

1. R. Adams, J. R. Johnson, C. F. Wilcox Jr., Laboratory Experiments in Organic Chemistry, 7th edition, Macmillan Publishing Co., Inc., New York, **1979**, p. 379.

2. Paula Yurkanis Bruice, Organic Chemistry, Prentice Hall Inc., New Jersey, USA, **1995**, p. 950, 966.

3. A. E. Ceniceros-Gómez, A. Ramos-Organillo, *Heteroatom Chemistry*, **2000**, *11*, 392.

4. Anne Leprette, Xiu R. Bu, Unpublished results.

5. Jerry March, Advanced Organic Chemistry, 4th Ed., John Wiley & Sons, Inc., New York, **1992**, p. 19.

6. a) C. Cornelissen-Gude, W. Rettig, *J. Phys. Chem. A*, **1998**, *102*, 7754. b) S-L Wang, T-I Ho, *Journal of Photochemisry and Photobiology A: Chemistry*, **2000**, *135*, 119-126.

7. a) H. Li, J. Santos, D. Van Derveer, E. A. Mintz, X. R. Bu, Proceedings of the NASA URC Technical Conference, Technical Advance in Aeronautic Space and Technology, (Huntsville, Alabama, USA), **1998**, vol. 3, 671. b) X. R. Bu, H. Li, D. Van Derveer, E. A. Mintz, *Tetrahedron Letters*, **1996**, *37*, 7331. c) L. Van Meervelt, *Acta Crystallogr., C49*, 593, **1993**. d) A. Onkelinx, et. al., *J. Am. Chem. Soc.*, **1996**, *118*, 2892.

8. A.Onkelinx, F. C. De Schryver, L. Viaene, M. Van der Auweraer, K. Iwai, M. Ymamoto, M Ichikama, H. Masuhara, M. Maus, W. Rettig, *J. Am. Chem. Soc.* **1996**, *118*, 2892-2902.

9. a) L. P. Hammett, *Trans. Faraday Soc.*, **1938**, *34*, 156. b) J. Shorter Correlation Analysis in Organic Chemistry: An Introduction to Linear Free-Energy Relationships; Clarendon Press: Oxford, **1973**. c) H. H. Jaffé, *Chem. Rev.* **1953**, *53*, 191. d) Ref. 5, pag. 280. e) Neil Isaacs, Physical Organic Chemistry, 2nd edition, Longman Group UK Limited, 1995, pag. 152.

10. F. E. Gostev, L. S. Kol'tsova, *Journal of Photochemistry and Photobiology A: Chemistry,* **2003**, *156*, 15-22.

11. R. P. Thummel, C-Y Hung, et al., *J, Chem, Soc., Chem. Commun.*, **1994**, 857.

12. a) Y. Tajima, H. Ishikawa, T. Miyazawa, M. Kira, N. Mikami, *J. Am. Chem. Soc.* **1997**, *119*, 7400-7401. b) W. Rettig, *J. Phys. Chem.* **1982**, *86*, 1970-1976. c) Z. R. Grabowski, J. Dobkowski, *Pure & Appl. Chem.*,**1983**, *55*, 245-252.

13. a) W. Rettig, *Topics in Current Chemistry*, **1994**, *169*, 253. b) C. C-Gude, W. Rettig, R. Lapouyade, *J. Phys. Chem. A*, **1997**, *101*, 9673-9677.

14. a) W. Rettig, *Angew. Chem. Int.* Ed. Engl., **1986**, *25*, 971-988. b) Michael A. Meador, NASA Glenn Research Center, Unpublished work. c) E. M. Kosower, H. Dodiuk, *J. Am Chem Soc.*, **1976**, *98*, 924.

15. C. C-Gude, W. Rettig, *J. Phys. Chem. A*, **1998**, 102, 7754-7760.

16. P. R. Bangal, S. Panja, S. Chakravorti, *Journal of Photochemistry and Photobiology A: Chemistry*, **2001**, *139*, 5-16.

17. D. R. Britelli, D. F. Eaton, *J. Phys. Org. Chem.*, **1989**, *2*, 89.

18. M. J. Kamlet, J. L. Abboud, R. W. Taft, *J. Am. Chem. Soc.*, **1977**, *99*, 6027-6037.

19. Christian Reichardt, Solvents and Solvent Effects in Organic Chemistry, 2nd Ed., New York, N.Y.: VCH **1988**, p. 408.

20. J. L. Abboud, M. J. Kamlet, R. W. Taft, *J. Org. Chem.*, **1977**, *99*, 8325.

21. P. R. Bangal, S. Panja, S. Chakravorti, *Journal of Photochemistry and Photobiology A: Chemistry*, **2001**, *139*, 5-16.

22. S. Fery-Forgues, M-T Le Bris, J-P Guette, B. Valeur, *J. Phys. Chem.* **1988**, *92*, 6233-6237.

23. a) W. Rettig, *Journal of Molecular Structure*, 84 (**1982**), 303, 327. b) D. F. Lewis, J. M. Wagner-Brennan, A. M. Miller, *Can. J. Chem.*, 77, 595, **1999**. c) A. Onkelinx, F. C. De Schryver, L. Viaene, M. Van der Auweraer, K. Iwai, M. Yamamoto, M. Ichikawa. H. Masuhara, M. Maus, W. Rettig, *J.*

Am. Chem. Soc., **1996**, *118*, 2892-2902. d) A. M. Swinnen, M. Van der Auweraer, F. C. De Schryver, K. Nakatani, T. Okada, N. Mataga, *J. Am. Chem. Soc.*, **1987**, *109*, 321-330.

24. Molecular surface areas were calculated by Dr. Gabriel Garcia at the Drugs Discovery Institute, Germany.

25. N. Srividya, P. Ramamurthy, V.T. Ramakrishnan, *Spectrochimica Acta, Part A*, 53, (**1997**), 1743-1753.

26. Steven S. Zumdahl, Chemical Principles, D. C. Heath and Company, USA, **1992**, p. 543.

27. W. R. Dawson, M. W. Winsor, *The Journal of Physical Chemistry*, **1968**, 72, 9.

28. a) D. El, A. Samy, *Spectrochim. Acta Part A*, **1998**, 54: 5 677-684. b) C. Wirp, H. Guester, H-D Brauer, *Ber. Bunsen-Ges. Phys. Chem.*, **1996**, 100: 7 1217-1225. c) Y. Rharbi, A. Yekta, M. A. Winnik, *Anal. Chem.*, **1999**, 71: 22 5045-5053. d) U. Grafs, H. Niikura, S. Hirayama, *J. Phys. Chem. A*, **1997**, 101: 7 1292-1298.

29. a) S. Hanessian, P. Lavallee, *Canadian Journal of Chemistry*, **1975**, *53*, 2975. b) G. Cardillo, M. Orena, S. Sandri, C. Tomasini, *Chemistry and Industry*, **1983**, 643. c) E. J. Corey, A. Venkateswarlu, *J. Am. Chem. Soc.*, **1972**, *94*, 6190. d) M. Lafonde, T. H. Chan, Synthesis, **1985**, 817.

30. A. Demeter, S. Druzhinin, M. George, E. Haselbach, J.L. Roulin, K. A. Zachariasse, *Chem. Phys. Lett.*, **2000**, *323*, 351.

31. R. Davis, S. Das, M. George, K. A. Zachariasse, *The Journal of Physical Chemistry A*: **2001**, *105*, 4790-4798.

32. a) G. A. Foulds, *Coordination Chemistry Review*, **1997**, *162*, 75-154. b) L. M. Engelhardt, *Aust. J. Chem.*, **1989**, *42*, 335-338. c) H. Schmidbaur, *Chem. Ber.*, **1989**, *122*, 265-270. d) P. Jutzi, et al., *Chem. Ber.*, **1989**, *122*, 865-870.

33. a) R. A. Alberty, R. J. Silbey, Physical chemistry, 2nd Ed. **1997**, John Wiley & Sons, Inc., New York. b) J. Kagan, Organic Photochemistry: Principle and Applications, **1993**, Academic Press Inc. c) Suzanne Fery-Forgues, Marie Therese Le Bris, Jean Paul Guette, Bernard Valeur, *The Journal of Physical Chemistry*, **1988**, *92*, 6233. d) Marvin, J. S.; Hellinga, H. W., *J. Am. Chem. Soc.*, **1998**, *120*, 7-11. e) Qin Zhou, Timothy M. Swager, *J. Am. Chem Soc.*,

1995, *117*, 7017-7018. f) Suzanne Fery-Forgues, Marie Therese Le Bris, Jean Paul Guette, Bernard Valeur, *J. Phys. Chem.*, **1998**, *92*, 6233-6237. g) Qin Zhou, Timothy M. Swager, *J. Am. Chem Soc.*, **1995**, *117*, 12593-12602.

34. a) Shannon and Prewitt, *Acta Crystallogr.*, **1976**, *A32*, 751. b) F. A. Cotton, G. Wilkinson, P. L. Gau, Basic Inorganic Chemistry, 3rd Ed., John Wiley & Sons, Inc., New York, **1995**, pp. 815.

35. S. Nigam, S. Rutan, *Applied Spectroscopy*, **2001**, *11*, 362A.

Section 5 Syntheses and Properties of 2nd Order Nonlinear Optical Chromophores

5.1 *Synthesis of Thienyl Imidazole-Based Stilbene Chromophores*

Dyes **5** are highly fluorescent molecules but also precursors to thermally stable compounds with second order nonlinear optical (NLO) properties. A series of NLO chromophores with stilbene type conjugation and nitro as electron acceptor group were synthesized (Scheme 12). These chromophores do not show fluorescence as their aldehydes precursors do. The color of these solid compounds is dark red except for **6d** that is dark brownish-red. Chromophore **6d** tends to decompose when it is exposed to light and with time even when it is kept from light. Its decomposition was observed by thin layer chromatography (TLC) after six months of storage. Chromophores **6** are soluble in most organic solvents, including methyl dichloride, chloroform, THF, acetone, 1,4-dioxane, ethyl acetate, and others. Purity of potassium tert-butoxide (t-BuOK), and dryness of reagents and solvent are essential to optimize the yield of these chromophores. It was observed that the yield decreases significantly if t-BuOK has been exposed to moisture. Interestingly, the yields of chromophores **6** decrease with increasing donor properties of the substituents as shown in Scheme 12. In general, the yield trend suggests that the aldehydes with strong electron donor groups are more stable; therefore they are less reactive, resulting in low yield.

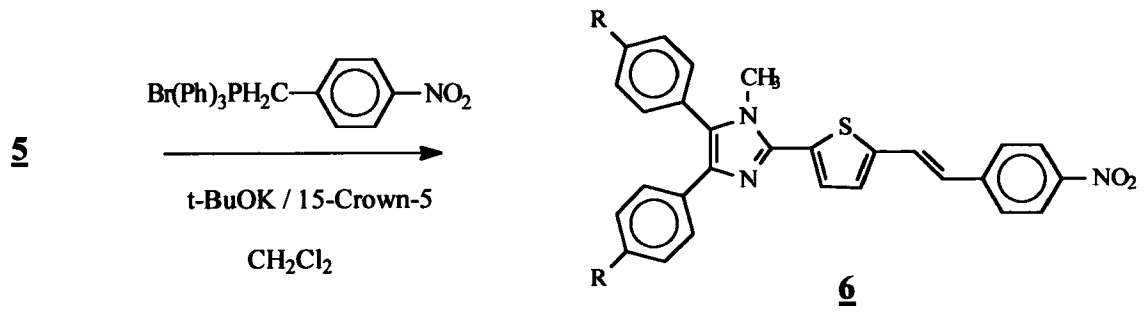

a **b** **c** **d**

R= H, CH_3, OCH_3, $N(CH_3)_2$

Yield= 75%, 65%, 67%, 43%

Scheme 12. *Synthesis of thienyl imidazole-based stilbene chromophores.*

Compounds **6** were designed to possess intramolecular charge transfer. It is well known that in "push-pull" compounds like these, where an electron donating group and an electron withdrawing group interact via a π-conjugated pathway, a partial intramolecular charge transfer occurs from the donor moiety to the acceptor through the conjugated bridge. This induces an asymmetric polarization of the ground state, which can lead to a significant ground state dipole.[1] In solution these compounds are characterized by an intense absorption band in the UV-visible region. The latter will be discussed in the next section.

5.2 *Photophysical, Optical, and Thermal Properties of Chromophores* 6.

Chromophores have unique electronic properties owing to their molecular charge transfer and compounds 6 are not an exception.[2] The low energy absorption band for 6 is observed in the 425-465 nm region. Its absorption maxima depend on the nature of both substituent groups and solvents. Chromophores 6 were designed to have intramolecular charge transfer (ICT), high thermal stability, and relatively large NLO properties (Figure 44). For example, thiophenyl ring was chosen because of its ability to enhance NLO properties while maintaining a high thermal stability.[3] On the other hand, the thiophenyl-stilbene moiety can serve as an extension of the conjugation pathway between the electron-donor and electron-withdrawing groups, which have been demonstrated to increase NLO properties.[4]

For comparison purposes, a series of analogous chromophores 19[5] were prepared as shown in Scheme 13. These chromophores 19 do not possess the thiophenyl-stilbene moiety. Thus, the effect of this conjugated pathway (thiophenyl-stilbene moiety) can be investigated in terms of intramolecular charge transfer, thermal stability, and NLO properties.

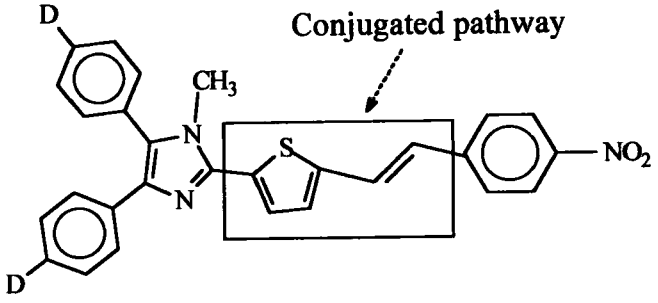

Figure 44. *Stilbene-thiophenyl pathway of chromophores* 6 *(*D = *donor group).*

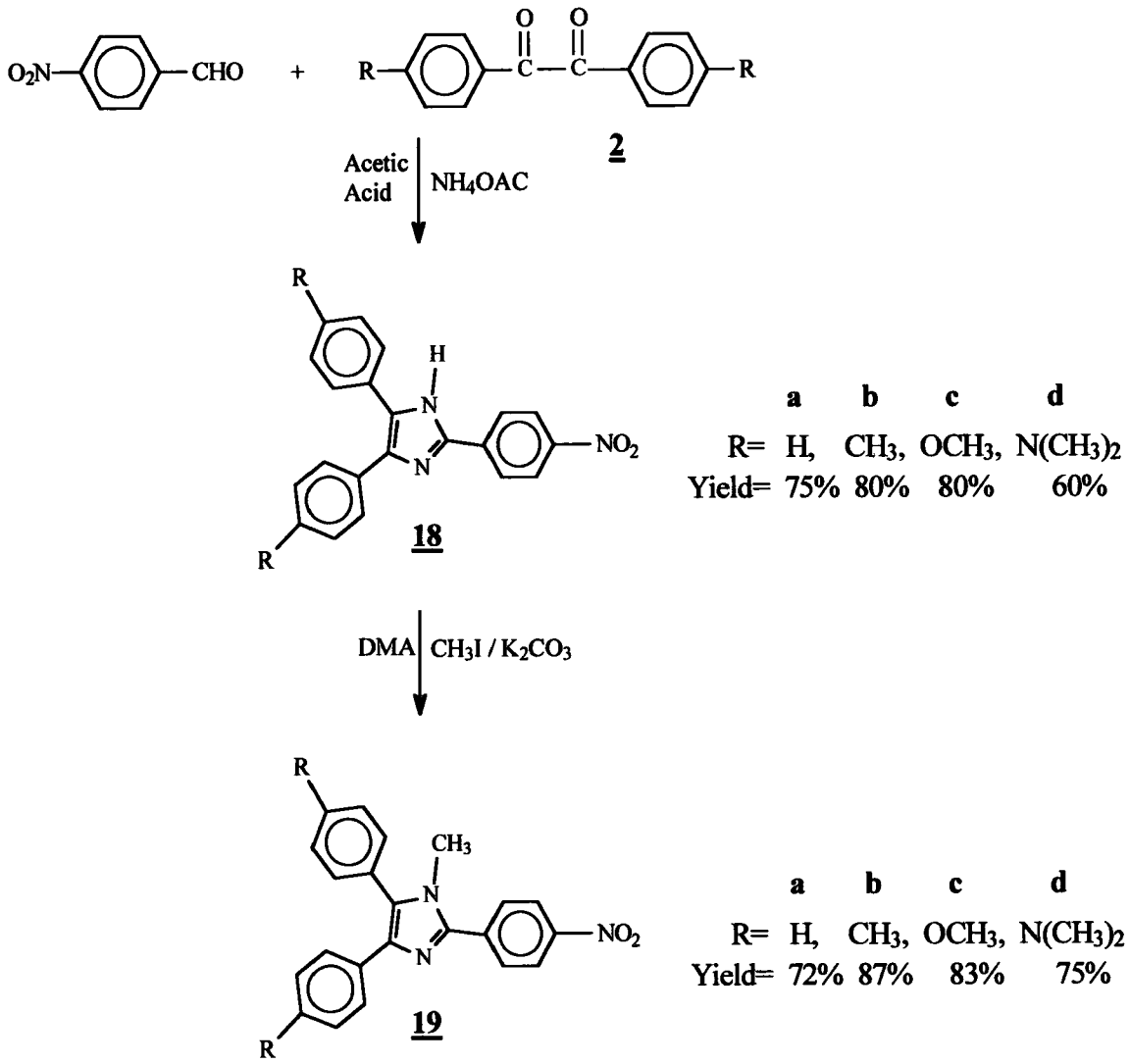

	a	b	c	d
R=	H,	CH_3,	OCH_3,	$N(CH_3)_2$
Yield=	75%	80%	80%	60%

	a	b	c	d
R=	H,	CH_3,	OCH_3,	$N(CH_3)_2$
Yield=	72%	87%	83%	75%

Scheme 13. *Synthesis of chromophores* 19.

The absorption maxima of chromophores **6** and **19** are listed in Table 20 and 21, respectively. For both types of chromophores the absorption maximum is red shifted with increasing donor properties of the substituent groups. A comparison of absorption maxima between **6a** and **19a** shows the expected longer wavelength absorption for **6a** since it possesses the longer conjugation pathway. The same behavior was observed for **6b**, **6c**, and **6d**. Note that the extended conjugation increases the molar absorptivity (ε) of **6**, relative to its corresponding analog **19**. The latter suggests larger dipole moment for **6**, therefore more efficient ICT.[6]

Table 20. *Absorption and Molar Absorptivity for Chromophore* **6** *in 1,4-Dioxane*

Chormophore	λ_{max} (nm)	ε ($M^{-1}cm^{-1}$)	$\lambda_{cut\text{-}off}$ (nm)
6a	426	$7.14x10^4$	550
6b	433	$3.83x10^4$	525
6c	437	$7.43x10^4$	550
6d	454	$1.89x10^4$	600

Table 21. *Absorption and Molar Absorptivity for Chromophores* **19** *in 1,4-Dioxane*

Chormophore	λ_{max} (nm)	ε ($M^{-1}cm^{-1}$)	$\lambda_{cut\text{-}off}$ (nm)
19a	383	$3.47x10^4$	468
19b	388	$1.89x10^4$	470
19c	394	$5.15x10^4$	490
19d	436	$1.61x10^4$	560

The molecular nonlinearity (μβ values) of **6** and **19** was determined by the dc-electric field induced second harmonic generation (EFISH) technique.[7] Chromophores **6** showed a significant improvement in μβ values relative to their respective analogs **19** (Table 22). The latter demonstrates that the thiophenyl-stilbene conjugation pathway affects the NLO properties positively. For example, the μβ value for **6c** is $945x10^{-48}$ esu while for its analog **19c** it is $145x10^{-48}$ esu.

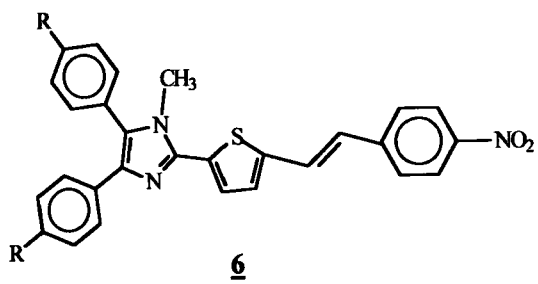

6

a b c d

R= H, CH_3, OCH_3, $N(CH_3)_2$

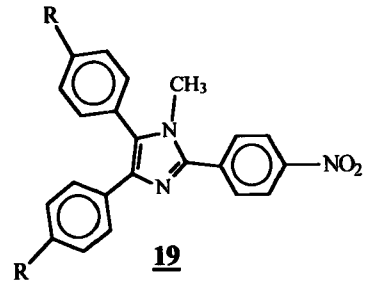

19

a b c d

R= H, CH_3, OCH_3, $N(CH_3)_2$

Table 22. *Second Order Nonlinear Optical Values* (μβ) *for* **6** *and* **19**

Chromophore	λ_{max} (nm)	μβ	Chromophore	λ_{max} (nm)	μβ
6a	426	370	**19a**	390	100
6b	431	945	**19b**	393	145
6c	436	475	**19c**	401	130
6d	463	590	**19d**	444	360

λ_{max} measured in $CHCl_3$. μβ in $x10^{-48}$ esu and measured at 1907 nm in $CHCl_3$ using a quartz reference (d_{11} = 0.277 pm/V).

Thermal stability of chromophores **6** (Table 23) were evaluated by means of differential scanning calorimetry (DSC) and thermogravimetric analysis (TGA). The onset decomposition temperatures (T_d) were found to be in the range of 240-340 °C. Chromophore **6a** showed the highest T_d (339 °C) while the lowest is for **6d** (242 °C). 5% decomposition temperatures (T_5) are in the range of 255-310 °C. The higher value of T_5 was obtained for **6c** at 337 °C while the lowest is for **6d** at 251 °C. An interesting feature for **6d** is that both T_d and T_m are at 242 °C (see DSC spectrum in the appendix). The melting point temperatures (T_m) were found to be in the range of 115-245 °C. Chromophores **6d** and **6b** showed the highest and lowest T_m at 242 and 119 °C, respectively.

Although the thiophenyl-stilbene conjugation pathway improves the nonlinearity properties (Table 22), it compromises the thermal stability of **6**. For example, chromophore **6c** is about 28 °C less stable than **19c**. A comparison of decomposition temperatures is presented in Figure 45.

Table 23. *Comparison of Thermal Stability for Chromophores* **6**

Chromophore	T_d (°C)[a]	T_5 (°C)[a]	T_m (°C)
6a	339	317	213
6b	320	316	236
6c	332	337	119
6d	242	251	242

[a] heating rate of 10 °C min^{-1} in air.

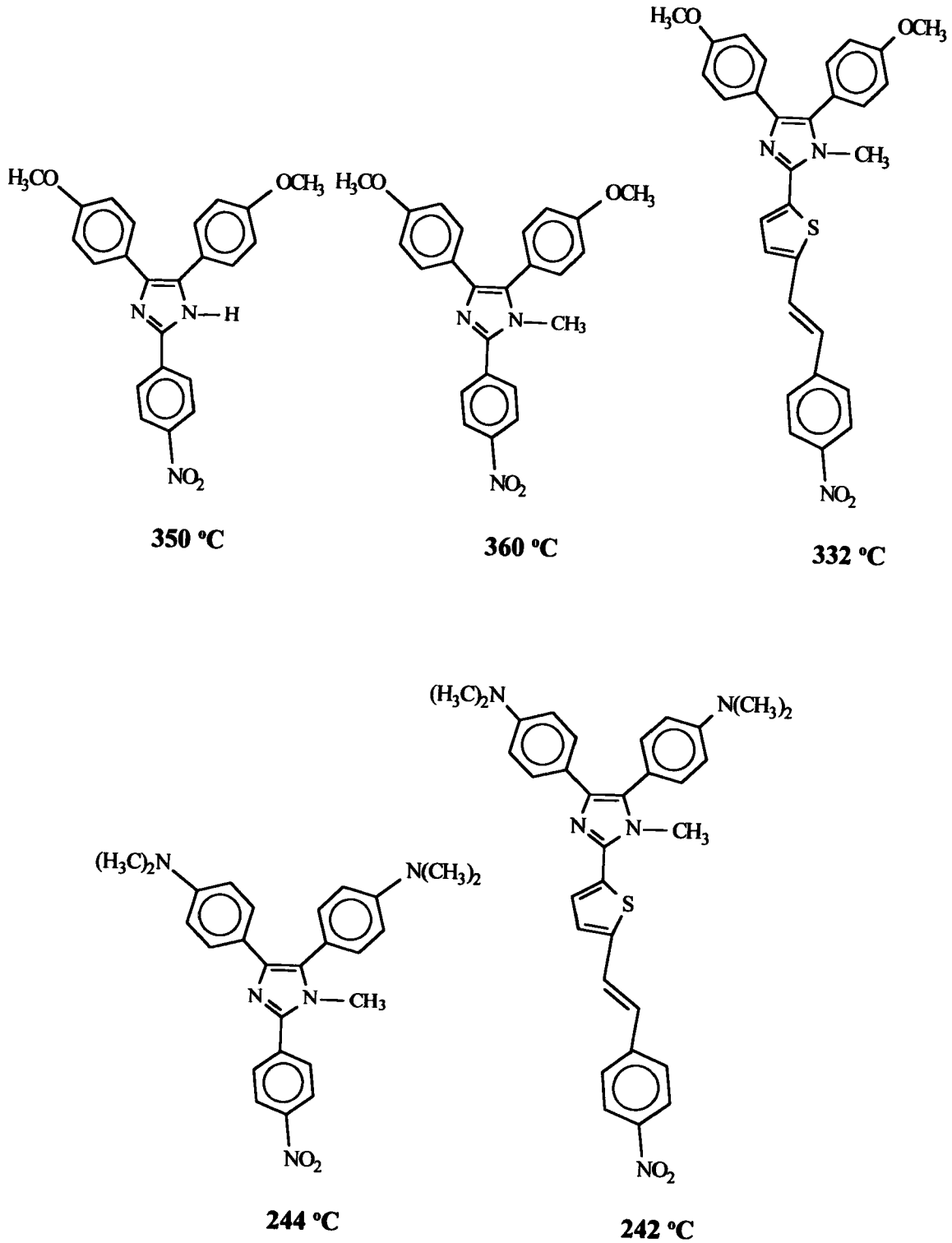

Figure 45. *A comparison of decomposition temperatures* (T_d) *of chromophores.*

5.3 *Macromolecules Containing Chromophores* 6.

Approaches to develop macromolecules containing **6** require functionalization of the corresponding chromophore. The polymethylmathacrylate backbone was chosen to develop macromolecules containing chromophores **6**. These systems are expected to display nonlinear optical properties because of the donor-acceptor nature of the monomer units. Macromolecules containing chromophores **6a** and **6c** were prepared.

Monomers **16** were prepared using the corresponding aldehydes **9** (Scheme 9) as shown in Scheme 14. The crude product **14** was purified by silica gel column chromatography, otherwise, the de-protection of the hydroxy group results in a significant low yield. Chromophores **15** were also purified by silica gel column chromatography and then reacted with methacryloyl chloride in the presence of triethyl amine at reflux for 16 h,[8] giving the desired monomer **16**.

The X-ray structure of chromophore **15c** is shown in Figure 46. The dihedral angles between the phenyl rings at the 4 and 5 positions and the imidazole ring are 37.0(2) and 74.9(2) degrees. Between the imidazole and the thiophenyl rings the dihedral angle is 25.4(2) degrees. Selected collection parameters and structure refinement data for the X-ray structure determination of **15c** are listed in Table 24.

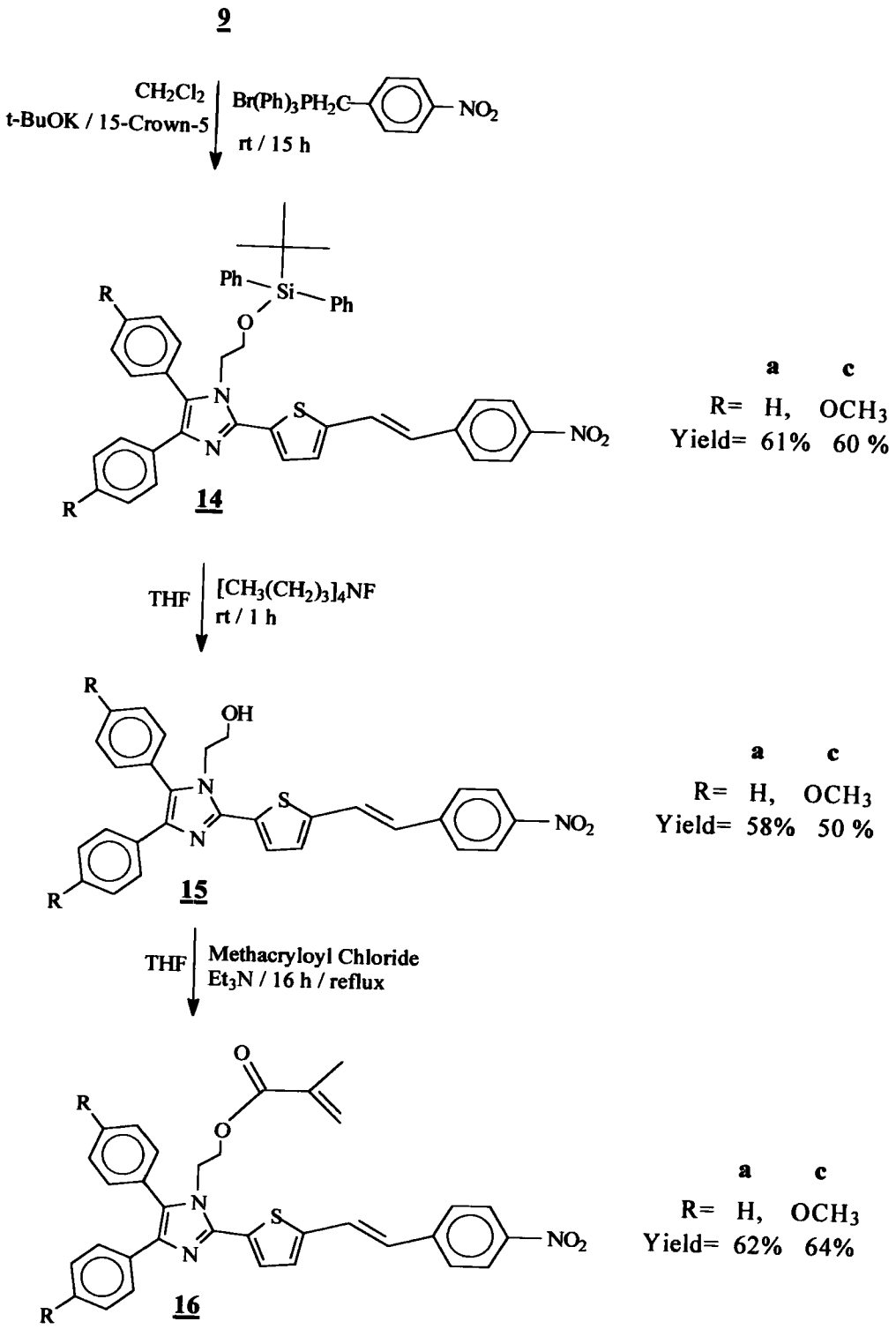

Scheme 14. *Synthesis of second order nonlinear optical chromophores* **16**.

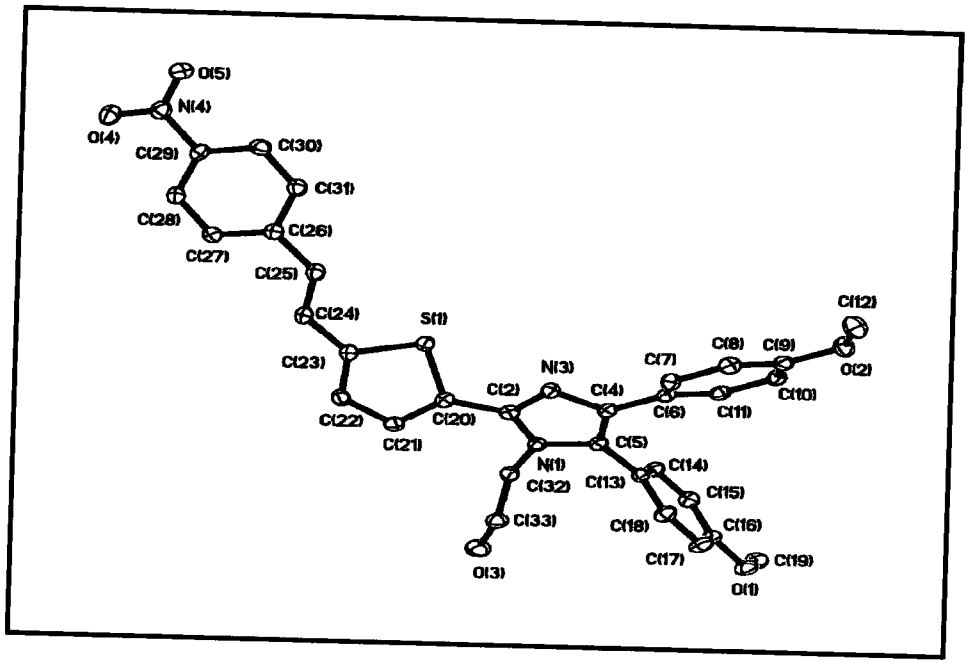

Figure 46. *X-ray structure of chromophore* **15c**.

Table 24. *Selected X-ray Collection and Refinement Parameters for* **15c**

Temperature:	173(2) K	Data collection:	1.67 to 28.28 deg.
Wavelength:	0.71073 Å	R. collected/unique:	17288 / 6539
Crystal system:	monoclinic, P2(1)/c	Refin. method:	Full matrix l-s F^2
Molecule per unit:	4	Data/rest./param.:	6539 / 0 / 394
Calculated density:	1.382 mg/m^3	Goodness fit on F^2:	0.831
Crystal size (mm):	0.37 x 0.22 x 0.17	Final R indices:	R1 = 0.0373

Macromolecules containing methyl methacrylate and chromophores **6a** and **6c** were successfully prepared using free radical conditions according to Scheme 15. The synthesis of **17** was performed in an ampul in which the solvent was de-oxygenated using vacuum and purging nitrogen alternately upon freezing thaw cycles. The ampul was sealed and the red solution was stirred at 80 °C for 96 h.[9] Then the reaction mixture was poured into methanol, giving a cloudy red solution. This mixture was cooled to -10 °C and the macromolecule was precipitated as a red solid. This solid was washed with cold methanol. Upon ^{1}H NMR analysis the average ratio of the units for **17a** was found to be 1:3, where n = 1 and m = 3.

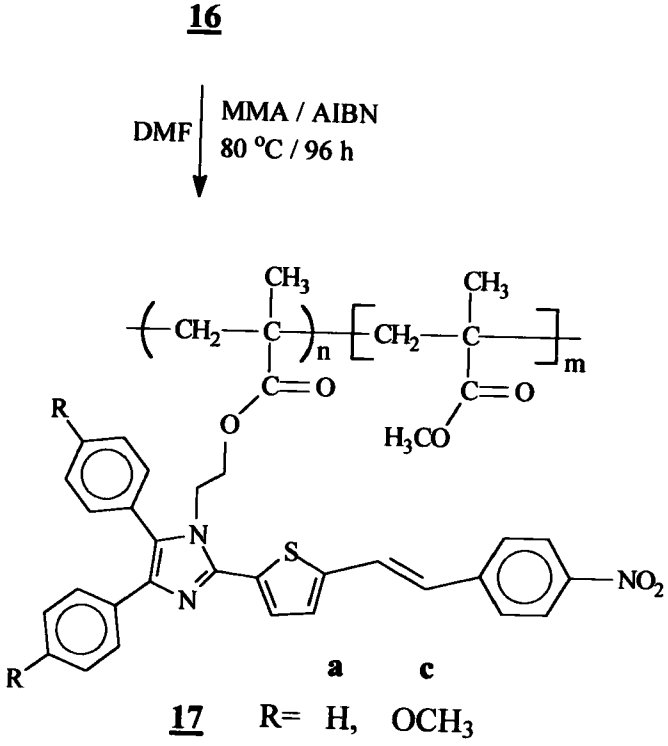

Scheme 15. *Synthesis of macromolecules containing NLO chromophore* **6**.

References

1. a) M. Blanchard-Desce, V. Alain, L. Midrier, R. Wortmann, S. Lebus, C. Glania, P. Kramer, A. Fort, J. Muller, M. Barzoukas, *Journal of Photochemistry and Photobiology A: Chemistry*, **1997**, *105*, 115-121. b) W. Liptay, in C. Lim (ed.) *Excited State*, Vol. I, Academic Press, New York, **1974**, p. 129. c) F. Lahmani, E. Breheret, A. Zehnacker-Rentien, C. Amatore, A. Jutand, *Journal of Photochemistry and Photobiology A: Chemistry*, **1993**, *70*, 39. d) E. Stiegman, E. M. Graham, K. L. Perry, L. R. Khundkar, L-T Cheng, J. W. Perry, *J. Am. Chem. Soc.*, **1991**, *113*, 7658. e) F. Wurthner, F. Effenberger, R. Wortmann, P. Kramer, *Chem. Phys.*, **1993**, *173*, 3051.

2. V. P. Rao, A. K. Jen, K. Y. Wong, K. Drost, R. M. Mininni, *SPIE Vol. 1775 Nonlinear Optical Properties of Organic Materilas V*, **1992**, 32.

3. C-F Shu, W-J Tsai, A. K-Y Jen, *Tetrahedron Letters*, **1996**, *37*, 7055.

4. a) V. P. Rao, A. K-Y Jen, K. Y. Wong, K. J. Drost, *Tetrahedron Letters*, *34*, **1993**, 1747. b) V. P. Rao, A. K-Y Jen, K. Y. Wong, K. J. Drost, *J. Chem. Soc., Chem. Commun.*, **1993**, 1118.

5. For synthesis and properties of similar compounds see: a) C. R. Moylan, R. D. Miller, R. J. Twieg, K. M. Betterton, V. Y. Lee, T. J. Matray, C. Nguyen, *Chem. Mater.*, **1993**, *5*, 1499. b) S. Sarshar, D. Siev, A. M. M. Mjalli, *Tetrahedron Letters*, **1996**, *37*, 835. c) A. C. Testa, *Journal of Luminescence*, **1991**, *50*, 243. d) Y. Inouye, S. Shimokoshi, Y. Sakaino, *Acta Cryst.*, **1999**, C55, 2084.

6. For similar observations see: W. Wu, C. Ye, D. Wang, *ARKIVOC*, **2003**, (ii) 59-69. [ISSN 1424-6376]

7. The $\mu\beta$ values were determinated by Oliver Zehnder, Christian Bosshard, and Peter Gunter at the Swiss Federal Institute of Technology at Switzerland.

8. For similar synthesis see: D. R. Robello, P. T. Dao, J. S. Schildkraut, M. Scozzafava, E. J. Urankar, C. S. Willard, *Chem. Mater.*, **1995**, *7*, 284.

9. For similar reaction conditions see: H. Li, A. Mintz, X. R. Bu, *Polymer Pre-print (ACS)*, **1996**, 290.

For synthesis and properties of nonlinear optical chromophores see:

10. Farrell, T.; Meyer-Friedrichsen, T.; Heck, J.; Manning, A. R.; *Organometallics*; **2000**; 19(17); 3410-3419.

11. Pizzotti, M.; Ugo, R.; Roberto, D.; Bruni, S.; Fantucci, P.; Rovizzi, C.; *Organometallics*; **2002**; 21(26); 5830-5840.

12. Raimundo, J.-M.; Blanchard, P.; Gallego-Planas, N.; Mercier, N.; Ledoux-Rak, I.; Hierle, R.; Roncali, J.; *J. Org. Chem.*; **2002**; 67(1); 205-218.

13. Cho, B. R.; Chajara, K.; Oh, H. J.; Son, K. H.; Jeon, S.-J.; *Org. Lett.*; **2002**; 4(10); 1703-1706.

14. Wang, J.; Lu, M.; Pan, Y.; Peng, Z.; *J. Org. Chem.*; **2002**; 67(22); 7781-7786.

15. Dorrestein, P. C.; Poole, K.; Begley, T. P.; *Org. Lett.*; **2003**; 5(13); 2215-2217.

16. Liu, R. S. H.; Muthyala, R. S.; Wang, X.-s.; Asato, A. E.; Wang, P.; Ye, C.; *Org. Lett.*; **2000**; 2(3); 269-271.

17. He, X.; Bell, A. F.; Tonge, P. J.; *Org. Lett.*; **2002**; 4(9); 1523-1526.

18. Ciulei, S. C.; Tykwinski, R. R.; *Org. Lett.*; **2000**; 2(23); 3607-3610.

19. Steinle, W.; Ruck-Braun, K.; *Org. Lett.*; **2003**; 5(2); 141-144.

20. Pasini, D.; Righetti, P. P.; Rossi, V.; *Org. Lett.*; **2002**; 4(1); 23-26.

21. Aqad, E.; Leriche, P.; Mabon, G.; Gorgues, A.; Khodorkovsky, V.; *Org. Lett.*; **2001**; 3(15); 2329-2332.

22. Yagi, K.; Soong, C. F.; Irie, M.; *J. Org. Chem.*; **2001**; 66(16); 5419-5423.

23. Karpov, A. S.; Rominger, F.; Muller, T. J. J.; *J. Org. Chem.*; **2003**; 68(4); 1503-1511.

24. Richeter, S.; Jeandon, C.; Kyritsakas, N.; Ruppert, R.; Callot, H. J.; *J. Org. Chem.*; **2003**; 68(24); 9200-9208.

25. Takagi, Koichi; Ozaki, Mitsuo; Nakatsu, Kazumi; Matsuoka, Masaru; Kitao, Teijiro, *Chem.Lett.* **1989**, 173-176.

26. Li, DeQuan; Ratner, Mark A.; Marks, Tobin J., *J.Amer.Chem.Soc.* **1988**, 110: *6*:

1707-1715.

27. Staub, Katrin; Levina, Galina A.; Barlow, Stephen; Kowalczyk, Tony C.; Lackritz, Hilary; Barzoukas, Marguerite; Fort, Alain; Marder, Seth R., *J.Mater.Chem.* **2003**, 13: *4*: 825 - 833.

28. Zhang, Wei; Hua, Jianli; Shao, Pin; Ren, Peng; Qin, Jingui; Zhang, Yu; Lu, Zuhong; Hu, Huaimin; Zhang, Deqing, *Chem.Lett.* **2003**, 32: *4*: 386 - 387.

29. Leclerc, N.; Galmiche, L.; Attias, A-J, *Tetrahedron Lett.* **2003**, 44: *31*: 5883 - 5888.

Section 6. Precursors of Photoresponsive and Thermally Stable Molecules

6.1 *Preparation of Substituted Imidazoles Containing Triphenylamine*

A series of chromophores containing different electron donor groups, the imidazole ring, and triphenylamine were synthesized. The synthetic approach for these chromophores required 4-formyltriphenylamine, **21**, as a key starting material.

The treatment of triphenylamine with almost stoichiometric amount of $POCl_3$ in DMF at 95-100 °C for 20 h provided the monoaldehyde **21** in 94% yield (Scheme 16). Excess of $POCl_3$ was avoided since it resulted in the formation of the dialdehyde to some extent.[1]

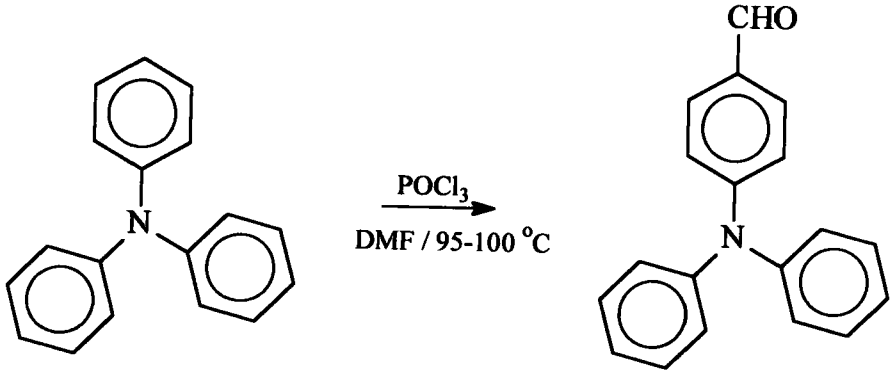

20 **21**

Scheme 16. *Mono-formylation of triphenylamine.*

The aldehyde **21** and the corresponding benzil **2** in the presence of ammonium acetate in acetic acid was heated at 50 °C for 15 h or until the starting materials disappeared from TLC (Scheme 17). Chromophores **22** were purified by re-crystallization from CH_2Cl_2 or methanol. The active proton on the imidazole ring was protected with a methyl group as shown for **23e**. Pure compound **23e** was obtained after recrystallization with CH_2Cl_2 or purification via column chromatography using silica gel.

The X-ray structure determination of **23e** is shown in Figure 47. Selected bond lengths and angles are given in Table 25. Note that the bond length of C(4)-C(7), and C(5)-C(17) is 1.464 and 1.479 Å, respectively, while the bond lengths of C(22)-N(37), N(37)-C(31), and N(37)-C(25) are in the range of 1.41-1.43 Å. The phenyl rings on the 4 and 5 position of the imidazole ring are twisted as well as those phenyl rings on the amine moiety. The dihedral angle for the bromo-substituted phenyl rings is 12.9° for N(3)-C(4)-C(7)-C(8) and 53.5° for C(4)-C(5)-C(17)-C(18). On the other hand, the dihedral angles for the phenyl rings on the triphenylamine moiety are 31.5° for those attached to the imidazole ring, and 56.0°, and 35.5° for the other two. Once again a comparison between dihedral angles and bond lengths for the donor-substituted rings revealed that larger dihedral angles correspond to longer bond lengths. The same was observed for compound **5b** and **5c**. Table 26 shows the comparison between dihedral angles and bond lengths for those bromo-substituted rings at the 4 and 5 position on the imidazole ring.

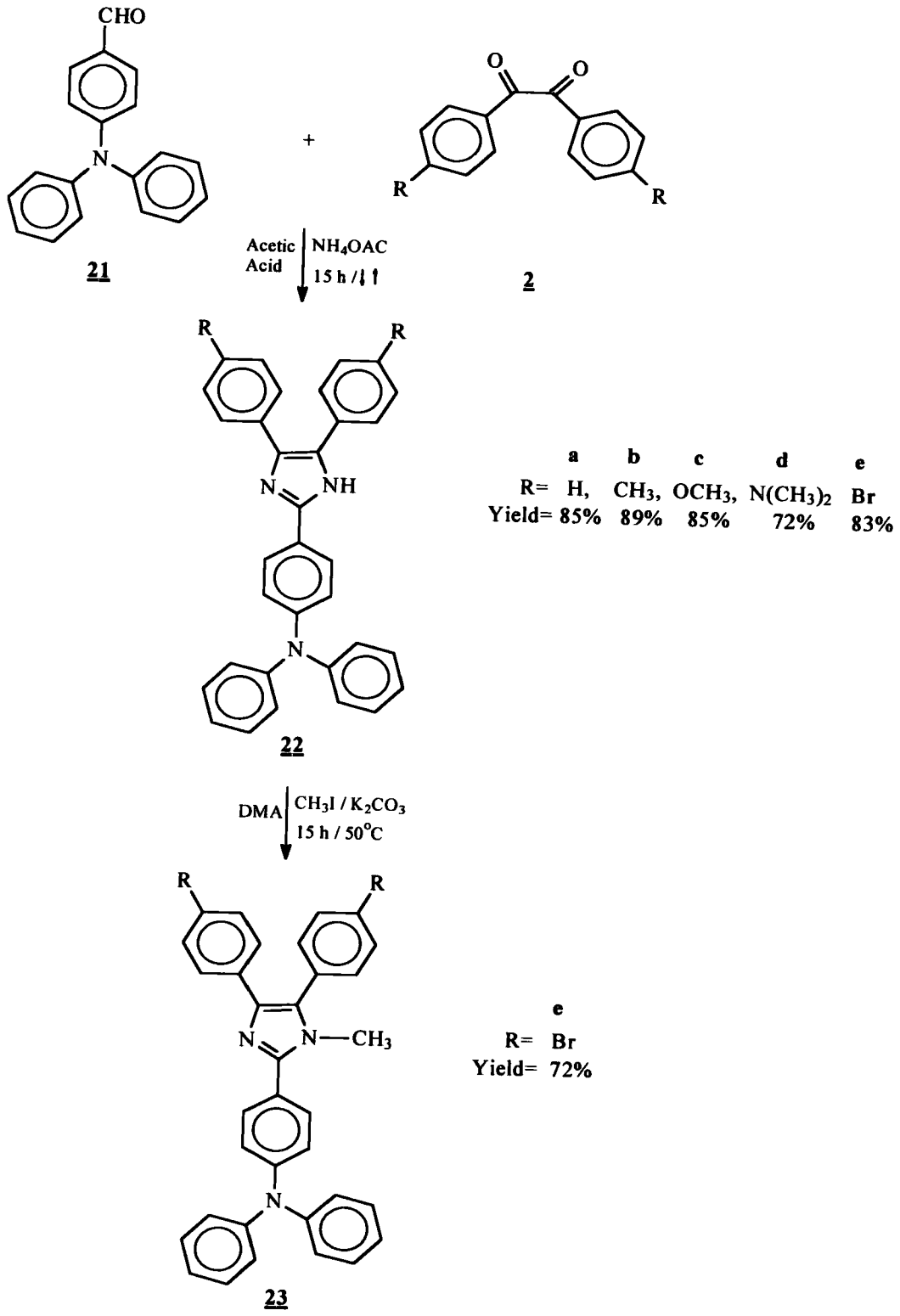

	a	b	c	d	e
R=	H,	CH_3,	OCH_3,	$N(CH_3)_2$	Br
Yield=	85%	89%	85%	72%	83%

	e
R=	Br
Yield=	72%

Scheme 17. *Synthesis of chromophores* **23**.

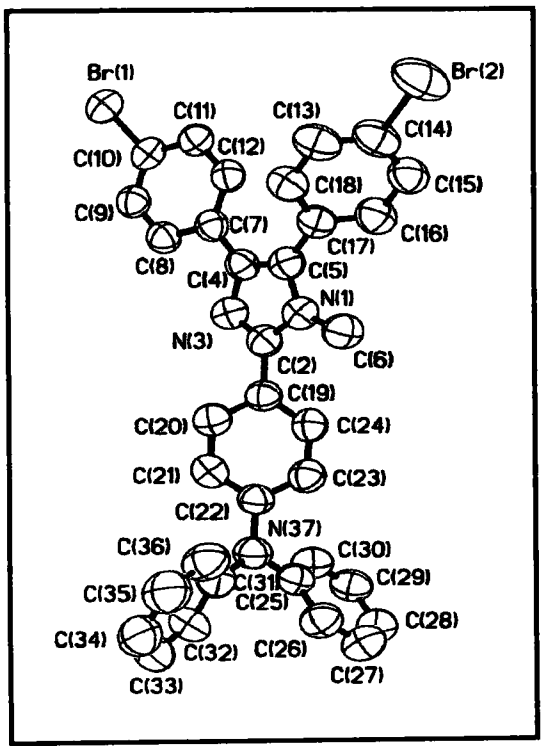

Figure 47. *X-ray structure of chromophore* **23e**.

Table 25. *Selected Bond Lengths and Angles for* **23e**

Bond	Bond length, Å	Angle	Angle, deg.
C(4)-C(7)	1.464(4)	N(3)-C(4)-C(7)	119.5(3)
C(5)-C(17)	1.479(5)	C(4)-C(5)-C(17)	133.2(3)
C(2)-C(19)	1.473(4)	N(3)-C(2)-C(19)	123.5(3)
C(22)-N(37)	1.426(4)	C(21)-C(22)-N(37)	120.4(3)
N(37)-C(31)	1.418(4)	C(22)-N(37)-C(31)	118.5(3)
N(37)-C(25)	1.428(4)	C(22)-N(37)-C(25)	118.1(3)

The largest angle is C(4)-C(5)-C(17)-C(18) with a dihedral angle of 53.5°, which corresponds with the bond C(5)-C(17) that has the longest bond length, 1.479 Å. This observation suggests that C(5)-C(17) has more character carbon-carbon single bond than C(4)-C(5), which appears to be a consequence of the bromo-substituted ring twist. The highly twisted geometry is expected to affect the conjugation between the corresponding ring and the imidazole ring, which at the same time negatively affects the intramolecular charge transfer.

Table 26. *Dihedral Angles and Bond Lengths for those Phenyl Rings at the 4 and 5 Positions on the Imidazole Ring of Compound* **23e**

	Dihedral angle, deg.	**Bond**	**Bond length, Å**
N(3)-C(4)-C(7)-C(8)	12.9(4)	C(4)-C(5)	1.464(4)
C(4)-C(5)-C(17)-C(18)	53.5(4)	C(5)-C(17)	1.479(4)

6.2 *Synthesis of Dendron Containing Disperse Red-1*

Dendrons are a class of macromolecules that contain multiple branch points as one traverses from the focal point to the peripheral point of the molecular structure.[3] These structures are relatively new molecular architectures, especially, in the synthesis of dendrimers in which various dendrons are covalently linked to a core structure.[4] These macromolecules have been found to be photo-responsive[5] and used as a low dielectric materials in the semiconductor industry.[6]

In this research 4,4-bis(4'-hydroxyphenyl)pentanol (**26**) was chosen as the core structure and disperse red-1 (**27**) as chromophore. The repeat unit **26** was synthesized as reported[3a] resulting in ≥ 90% yield (Scheme 18). Diphenolic acid (**24**) is an inexpensive starting material from which the corresponding methyl ester (**25**) was prepared and then reduced using lithium aluminum hydrate to give the desired triol **26**. Chromophore **27** was activated with the mesylate group, which is a good leaving group. Mesylate **28** was prepared from **27** in the presence of triethyl amine using methanesulfonyl chloride and a catalytic amount of 4-(dimethylamino)pyridine in dry dimethylchloride at room temperature as illustrated in Scheme 19.

The first generation dendron was obtained by a coupling reaction between **26** and **28**. A mixture containing **26** and **28** in the presence of K_2CO_3 and 18-crown-6 in dry acetone at reflux condition afforded **29** in 50% yield (Scheme 20).

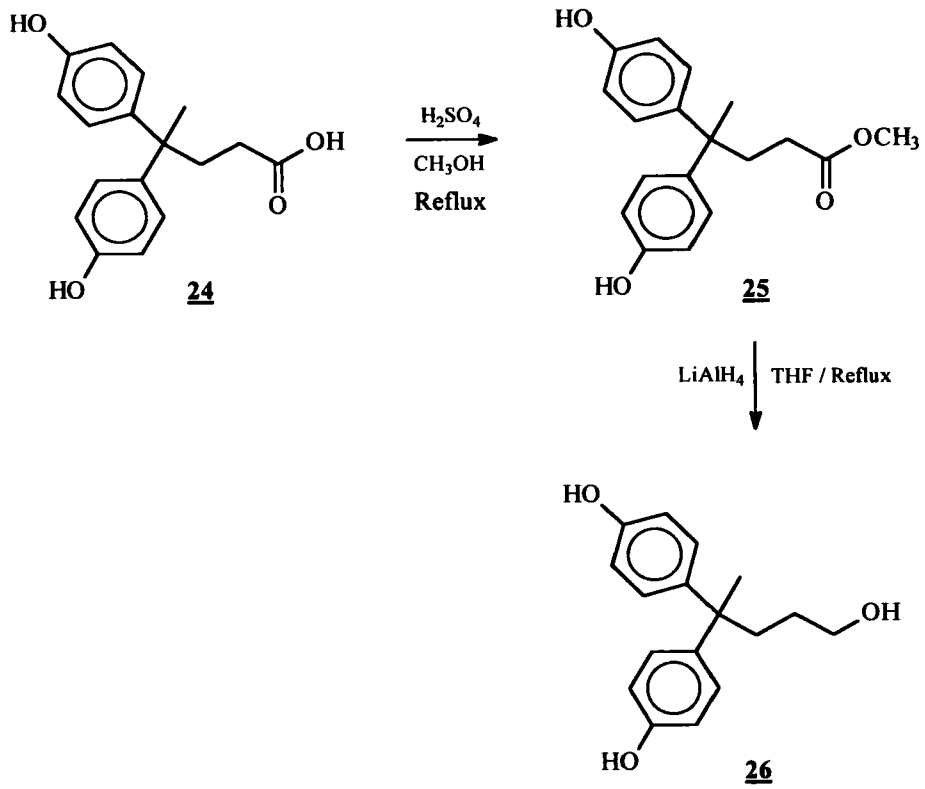

Scheme 18. *Synthesis of the repeat unit 4,4-bis(4'-hydroxyphenyl)pentanol.*

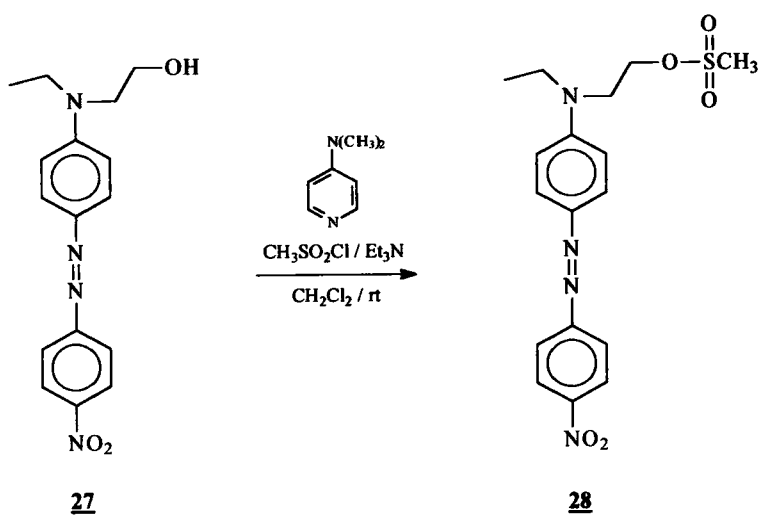

Scheme 19. *Mesylate activation of disperse red-1.*

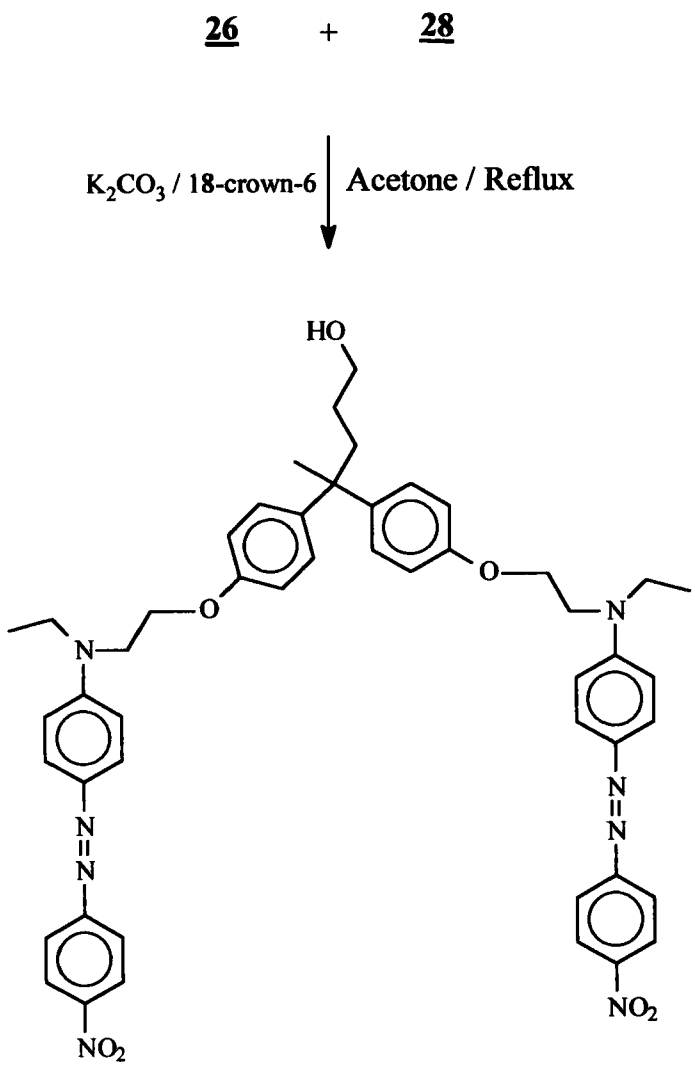

29

Scheme 20. *Preparation of the first generation dendron.*

6.3 *Phase Transfer Catalyst and Ultrasound as a New N-Substitution Method Against Elimination*

Phase transfer catalyst[7] and ultrasound[8] have demonstrated their powerful use in synthetic organic chemistry.[9] For example, a phase transfer catalyst such as tetrabutylammonium hydrogen sulfate is essential for the synthesis of benzyl ethers.[10] In the absence of the catalyst only low yield or no product at all of the desired compound is obtained. On the other hand, ultrasound has been used to promote specific reaction such as N-hydroxymethylation.[11]

N-substitution is a common methodology in synthetic organic chemistry. Despite this fact, N-alkylation is a challenge for specific systems. It has been found that carbazole containing alkyl bromide undergoes elimination leading to the formation of the related olefins (Scheme 21). In other cases carbazole containing alkyl bromides are not obtained at all. In this research phase transfer catalyst and ultrasound were used to investigate whether or not they can selectively accelerate and improve the reaction yield.

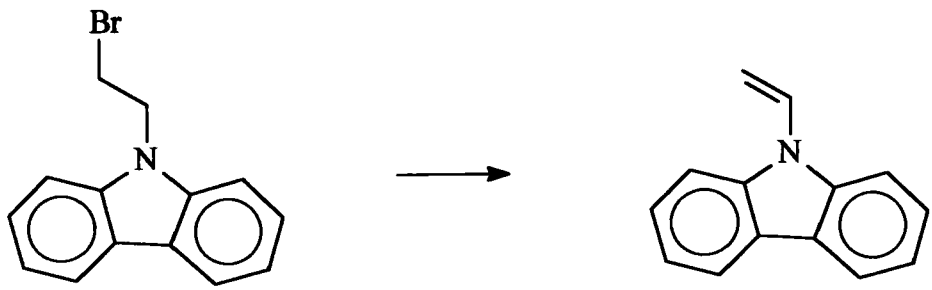

Scheme 21. *Elimination of bromine on carbazole containing alkyl bromide.*

In attempt to prepare a carbazole containing alkyl bromide the carbazole **30** was magnetically stirred in the presence of a base and 1,2-dibromoethane in DMF at 50 °C (Scheme 22). The reaction was monitored by TLC for 24 h. No reaction was observed based on TLC. Only carbazole **30** was recovered from the reaction mixture.

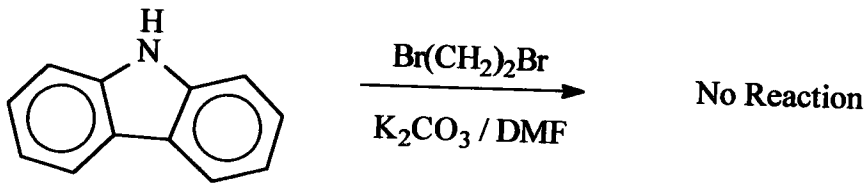

30

Scheme 22. *Attempt of N-alkylation of carbazole in the presence of a base at 50 °C.*

Then carbazole **30** was magnetically stirred in the presence of 50% NaOH, tetrabutyl ammonium bromide (TBAB, phase transfer catalyst) and 1,2-dibromoethane in benzene at room temperature for 24 h. In these conditions no reaction was obtained based on TLC. To this reaction mixture ultrasound was applied and the magnetic stirring was stopped (Scheme 23). After 5 h of reaction under ultrasound condition at 25-30 °C a new spot was observed on the TLC. Then the reaction mixture was kept under these conditions for additional 19 h. The crude product of this reaction was recrystallized with ethanol giving 5% yield of the desired carbazole containing ethyl bromide (**31**). Some carbazole **30** was recovered, however, no related olefins were obtained.

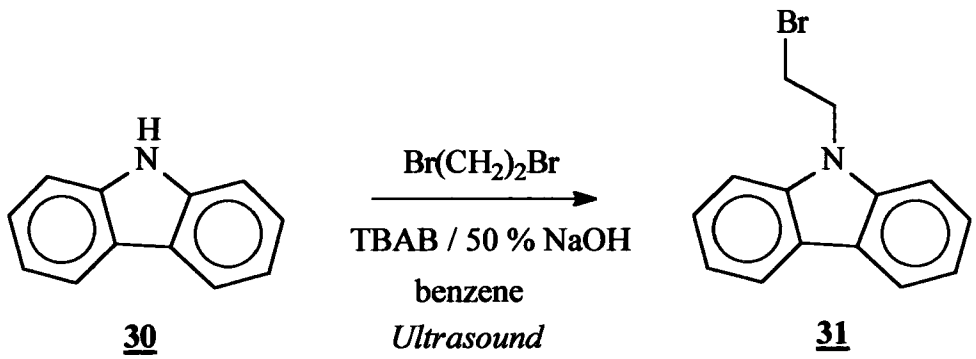

30 31

Scheme 23. *N-alkylation of carbazole under phase transfer catalyst and ultrasound.*

In an attempt to improve the yield of **31**, the N-substitution reaction was performed in CH_2Cl_2 (as solvent) but keeping the reaction condition mentioned above. The crude product was purified by column chromatography using silica gel, resulting in 5% yield of **31**. Carbazole **30** and traces of the related olefin were observed on TLC. Use of CH_2Cl_2 as solvent seems to promote the formation of the corresponding olefin. Therefore, to slow-down the reaction rate the above N-alkylation reaction was set-up but keeping the reaction temperature to 0 °C for 6 h. Purification of the crude product afforded 10% yield of **31**. Some carbazole **30** was recovered and traces of the related olefin was determinated by TLC.

In this investigation the bromo alkylation of carbazole was improved from a 0% to 10% yield by using tetrabutyl ammonium bromide as phase transfer catalyst and ultrasound at 0 °C.

6.4 *Synthesis of Isophorone-Triphenyl Amine Based Chromophores*

The ability of the isophorone unit and dicyanomethylidene [C=C(CN)$_2$] to improve the second order hyperpolarizability as well as thermal stability has been reported. The isophorone unit has been used as an extension of the conjugated pathway between the donor and acceptor groups to increase the molecular hyperpolarizability value ($\beta\mu$).[12] Strong electron acceptor groups such as dicyanomethylidene and tricyanoethylene improve not only the $\beta\mu$ value but also the thermal stability of the analogous chromophores.[12,13] Different methodologies have been successful in order to incorporate the isophorone unit into an aromatic aldehyde. One of the most common procedure involves the presence of piperidine or triethylamine, acetic acid, and solvent such as benzene, toluene, $CHCl_3$ or DMF at reflux condition for at least 13 h. The yield for these reactions is in the range of 40-78%. To avoid tedious separation of reaction mixtures other procedures have been designed; for example, condensation of the aromatic aldehyde and isophorone in the presence of base (KOH, NaOH, or t-BuOK) in a solvent such as ethanol/H_2O or t-BuOH at reflux or room temperature condition depending on the reactivity of the aromatic aldehyde.[12]

Isophorone, malononitrile and donor substituted triphenylamine have been condensed in a one-pot reaction in the presence of piperidine, acetic acid, and acetic anhydride in DMF giving the desired chromophore in 40-60% yield. However, this synthetic procedure results in tedious work-up and purification processes.[14] The complicated work-up and purification process were eliminated by preparing the

desired chromophore in two easy reactions. The first reaction was the condensation between the donor substituted formyltriphenylamine (32) and isophorone (33) in the presence of t-BuOK in t-BuOH at reflux condition under nitrogen for 30 minutes. Tert-butanol was carefully dried over Mg/I_2 and used just after distillation. After 30 minutes the reaction mixture was cooled to room temperature and concentrated under reduced pressure. The crude product was purified by column chromatography using silica gel to give 34 in 40% and 42% yield, as depicted in Scheme 24.

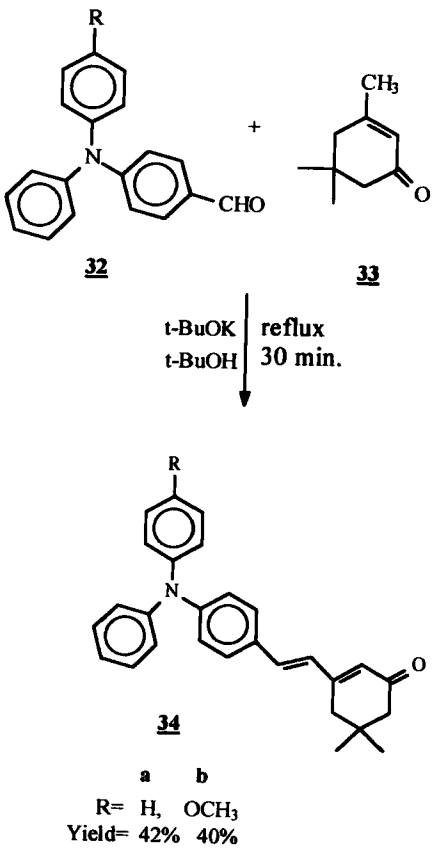

Scheme 24. *Condensation of formyltriphenylamine and isophorone.*

It is worth mentioning that compounds **34** exhibit visual fluorescence in organic solvents such as ethyl acetate, acetone or CH_2Cl_2 when exposed to UV-vis light (fluorescence properties of **34** have not been published to date). The second reaction was the incorporation of the dicyanomethylidene group. The corresponding compound **34** was reacted with malononitrile in presence of triethylamine in $CHCl_3$ under nitrogen at 50 °C for 3 h. After washes the crude product with water and extract the organic phase with CH_2Cl_2 the chromophores **35** were purified by column chromatography using silica gel and it was obtained in about 40% yield as shown in Scheme 25.

This synthetic approach make the work-up and purification process simple but also decreases the reaction time to 3.5 h versus 13 h for that published[14] procedure.

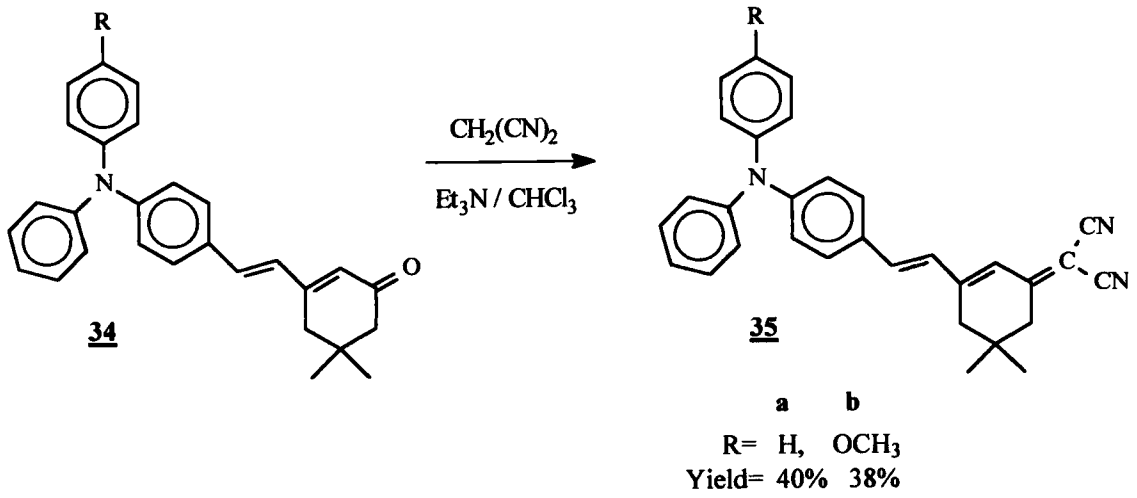

Scheme 25. *Synthesis of chromophores containing dicyanomethylidene group.*

6.5 *Preparation of 2-(2'-Pyridil)-4,5-bis(Thyenyl)Imidazole*

Upon successful synthesis of fluorophores **5** and chromophores **6**, the preparation of dye **36** was pursued.

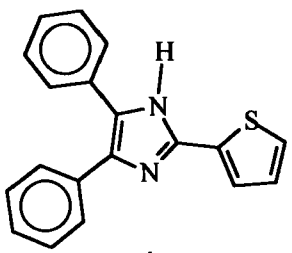

4a

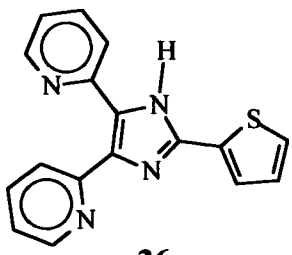

36

In an attempt to prepare the dye **36** the same procedure and reaction conditions to synthesize **4a** was used. Thus, 2-thiophene carboxaldehyde (**1**) was reacted with 2,2'-pyridil (**37**) in presence of ammonium acetate in acetic acid and refluxed for 15 h. The reaction mixture was cooled to room temperature and then poured into a water-ice bath. Since no solid was precipitated, contrary to what happens in the case of **4a**, the organic phase was extracted with CH_2Cl_2 resulting in a black oil after solvent removal. The black oil was passed through a column chromatography using silica gel and a mixture of hexane and ethyl acetate (1:0.3 v/v). The collected samples were concentrated under reduced pressure giving a dark brown solid. The latter was recrystalized twice with methanol resulting in a pure compound that was characterized by ^{1}H and ^{13}C NMR, elemental analysis and X-ray structure determination. The X-ray crystal diffraction revealed the structure of **38** as the product obtained after purification (Figure 48 and Table 27). No other pure product

was obtained from the complex mixture of the crude.

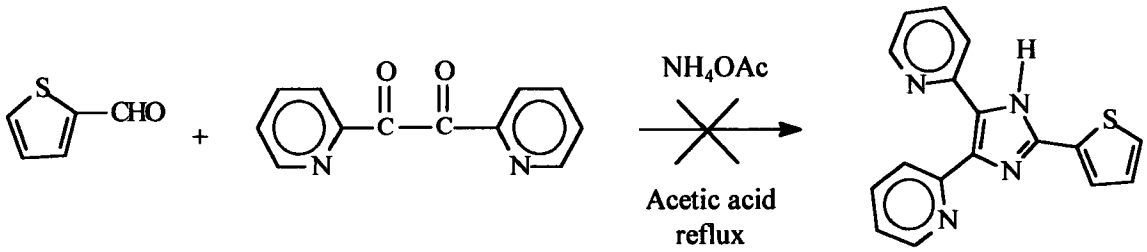

1 **37** **36**

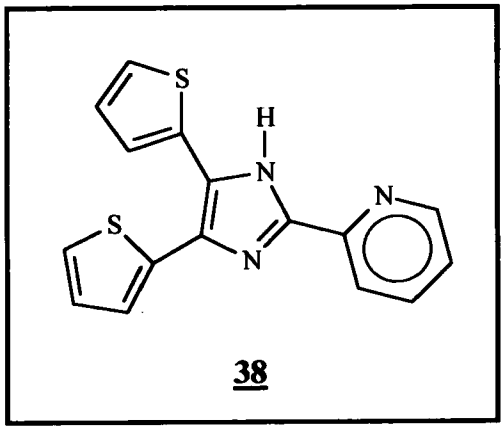

38

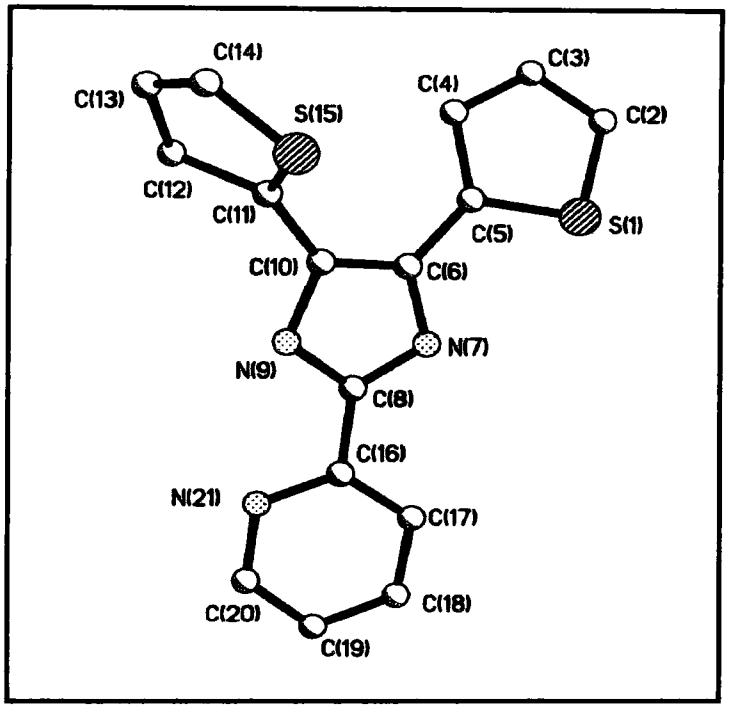

Figure 48. *X-ray structure of 2-(2'-pyridil)-4,5-bis(thyenyl)imidazole* (**38**).

Table 27. *Selected X-ray Collection and Refinement Parameters for* **38**

Temperature:	173(2) K	Data collection:	1.62 to 28.28 deg.
Wavelength:	0.71073 Å	R.collected/unique:	13424 / 6796
Volume:	1457.0(4) $Å^3$	Refin. method:	Full matrix l-s F^2
Molecule per unit:	4	Data/rest./param.:	6796 / 0 / 405
Calculated density:	1.297 mg/m^3	Goodness fit on F^2:	1.143
Completeness to theta:	98.2%	Final R indices:	R1 = 0.0538

The dihedral angles for the thiophenyl ring are 69.5° and 18.6° while the pyridyl ring showed 10.5°, relative to the imidazole ring.

A mechanism was proposed (Scheme 26) in order to explain such unexpected results. The proposed mechanism is via free radical process. It assumes that 2,2'-pyridil (**37**) is unstable in the reaction conditions generating free radicals, which produce the respective aldehyde **39**. Also, 2,2'-thienyl (**40**) is produced in the process. In theory, **39** and **40** in the presence of ammonium acetate should give compound **38**. In order to verify this mechanism, a series of reactions were performed. First, 2-thiophene carboxaldehyde (**1**) and 2,2'-pyridil (**37**) were dissolved in acetic acid and refluxed for 15 h. This reaction was an attempt to generate intermediates **39** and **40**. However, after refluxing for 15 h only starting materials were present based on TLC. Second, 2,2'-thienyl (**40**) and pyridinecarboxaldehyde (**39**) were reacted with ammonium acetate in acetic acid. This mixture was stirred for 5 minutes at room temperature from where TLC indicated that **39** is almost gone while **40** is present in a significant amount. After 30 minutes at room temperature **39** was totally gone based on TLC but **40** was still observed. The absence of **39** was expected since ammonium acetate may react with it to generate an intermediate. Therefore, the reaction mixture was refluxed for 15 h. A significant amount of **40** was present in the reaction mixture based on TLC. The same work-up as for **38** was done. The crude product was a black oil from which no **38** was obtained.

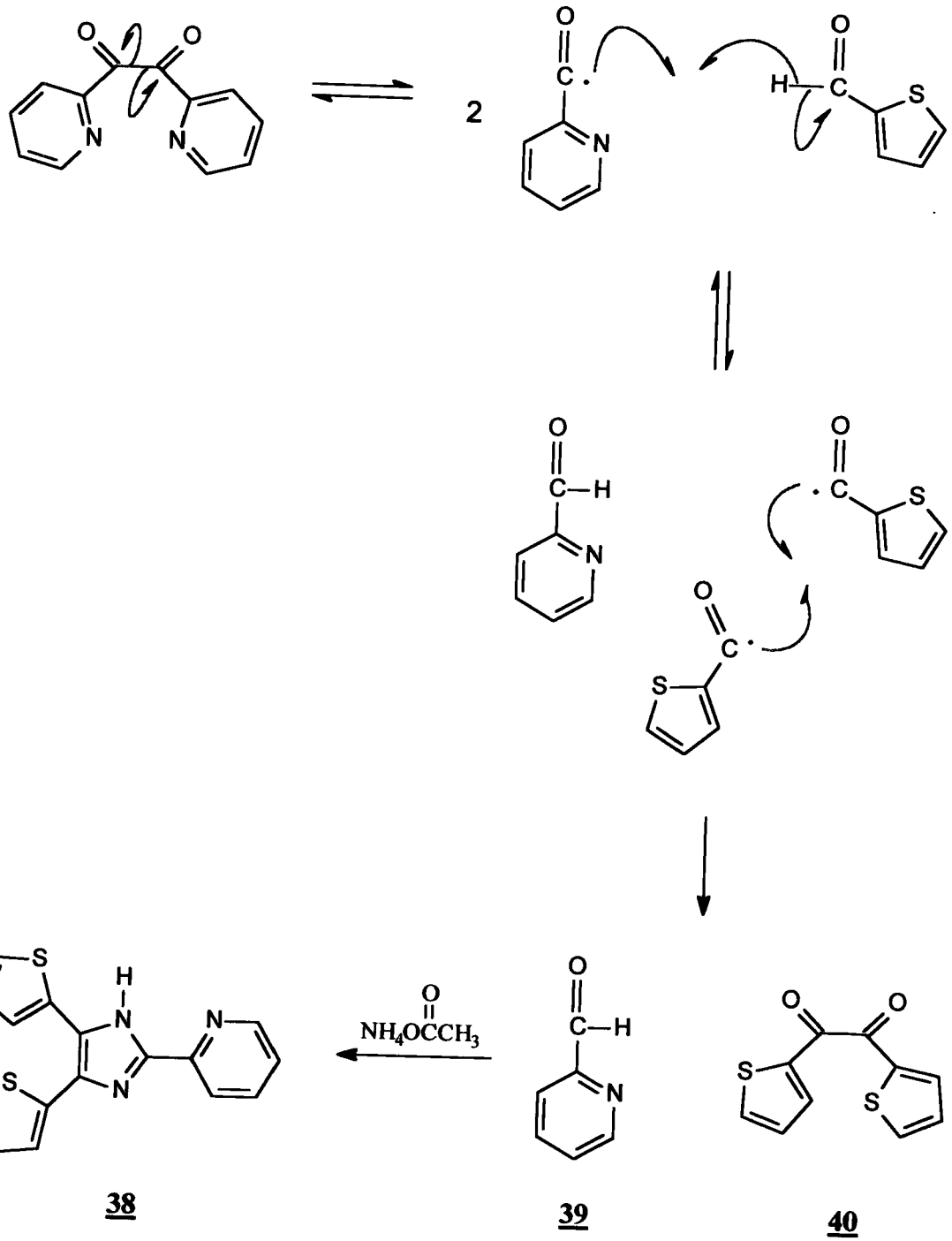

38 **39** **40**

Scheme 26. *Proposed mechanism for the formation of compound* **38**.

Other attempts to prepare compound **38** using **1** and **37** in the presence of ammonium acetate are summarized in Table 28. Based on this data it is clear that the reaction temperature and solvent play essential roles to generate **38**. Heating at 100 °C for 15 h generated the unexpected compound **38** in 10% yield.

Table 28. *Conditions and Observations in Attempts to Prepare* **38** *from* **1** *and* **37**

Procedure	Solvent	Conditions	38, % yield	Observations
1	acetic acid	100 °C, 15 h	10	Crude product: *black oil* Pure product: *brown crystals*
2	acetic acid	rt*, 1 h	0	No reaction at rt
3	acetic acid	50 °C, 15 h	0	Crude product: *black sticky oil* No solid obtained after purification by column chromatography
4	ethanol	116, °C, 17 h	0	Reaction mixture was a brownish red mixture. TLC showed a lot of by-products

* room temperature

The novel compound **38** was unexpectedly prepared and its structure was elucidated by the X-ray structure determination (Figure 48). No evidence was found to support the proposed mechanism (Scheme 26) for the synthesis of **38**.

References

1. G. Lai, X. R. Bu, J. Santos, E. A. Mintz, *SYNLETT*, 1275, November **1997**.

2. R. Adams, J. R. Johnson, C. F. Wilcox Jr., Laboratory Experiments in Organic Chemistry, 7th edition, Macmillan Publishing Co., Inc., New York, **1979**, p. 379.

3. a) K-Y Cheng, C. B. Gorman, *J. Org. Chem.*, **1996**, *61*, 9229-9235. b) D. A. Tomalia, H. D. Durst, *Top. Curr. Chem.*, **1993**, *165*, 192-313. c) C. J. Hawker, J. M. Fréchet, *J. Am. Chem. Soc.*, **1990**, *112*, 7638-7647.

4. a) P. Bharathi, U. Patel, T. Kawaguchi, D. J. Pesak, J. S. Moore, *Macromolecules*, **1994**, *28*, 5955-5963. b) C. J. Hawker, R. Lee, J. M. Fréchet, *J. Am. Chem. Soc.*, **1991**, *11*, 4583-4588. c) Z. Xu, M. Kahr, K. L. Walker, C. L. Wilkins, J. S. Moore, *J. Am. Chem. Soc.*, **1994**, *116*, 4537-4550.

5. a) D. M. Junge, D. V. McGrath, *Chem. Commun.*, **1997**, 857. b) H-F Chow, C. C. Mak, *Tetrahedron Letters*, *37*, **1996**, 5935-5938.

6. J. L. Hedrick, R. D. Miller, C. J. Hawer, K. R. Carter, W. Volksen, D. Y. Yoon, M. Trollsas, *Advanced Materials*, **1998**, *10*, 1049.

7. a) M. A. Gol'tsberg, A. Grabalek, O. Farsa, A. Krebs, P. Dolezhal, G. I. Koldobsky, *Russ. L. Org. Chem.*, **1996**, *32*, 9, 1367-1369. b) Y. Sasson, H. A. Zahalka, *J. Chem. Soc. Chem. Commun.* **1983**, *22*, 1347-1349. c) R. Annunziata, M. Benaglia, M. Cinquini, F. Cozzi, G. Tocco, *Org.Lett.* **2000**, *2*, 12, 1737 - 1740. d) J. Sanetra, D. Bogdal, M. Warzala, A. Boron, *Chem. Mater.* **2002**, *14*, 89-95.

8. a) P. D. Lickiss, R. Lucas, *J.Organomet.Chem.* **1993**, *444*, 1.2, 25-28. b) A. H. D. Groot, R. A. Dommisse, G. L. Lemiere, *Tetrahedron* **2000**, *56*, 11, 1541 - 1550. c) A. Gaplovsky, M. Gaplovsky, S.Toma, J. L. Luche, *J. Org. Chem.*, **2000**, *65*, 25, 8444 - 8447.

9. X. Li, J. Santos, X. R. Bu, Tetrahedron Letters, *41* (**2000**), 4057.

10. M. Abdul-Aziz, J. V. Auping, M. A. Meador, *J. Org. Chem.*, **1995**, *60*, 1303-1308.

11. W. Zhong, G. Song, Y. Peng, X. Qian, *Synth.Commu,.*, **2000**, *30*, 20, 3801 - 3808.

12. C-F Shu, W. J. Tsai, J-Y Chen, A. K-Y Jen, Y. Zhang, T-A Chen, *Chem. Commun.*, **1996**, 2279.

13. a) C-F Shu, W. J. Tsai, A. K-Y Jen, *Tetrahedron Letters*, *37*, 7055-7058, **1996**. b) B. R. Cho, K. N. Son, S. J. Lee, T. I. Kang, M. S. Han, S. J. Jeon, N. W. Song, D. Kim, *Tetrahedron Letters*, 39, 3167-3170, **1998**.

14. S. Ermer, S. M. Lovejoy, D. S. Leung, H. Warren, *Chem. Mater.*, **1997**, *9*, 1437-1442.

CHAPTER III

EXPERIMENTAL

All glassware used were dried in an oven or under open flame and vacuum. Reactions were conducted under purified nitrogen atmosphere and stirred using magnetic bars. Chemicals purchased from Aldrich Chemical Co. and their treatment before use are as follow: 2-thiophenecarboxaldehyde (used without further purification); benzoin, 4,4'-dimethylbenzoin, Anisoin, and 4,4'-dibromobenzil (used as received); n-butillitium in 1.6 M in hexane, 15-crown-5, 2-chloroethanol, anhydrous potassium carbonate, potassium iodide, anhydrous magnesium sulfate, anhydrous sodium sulfate, and methyl iodide (used as received); potassium tert-butoxide, anhydrous N,N'-dimethylformamide (DMF), anhydrous N,N'-dimethylacetamide (DMA), tetrabutyl ammonium fluoride (1.0 M in THF), methacryloyl chloride and triethyl amine, 2,2'-azobis(2-methylpropionitrile) (AIBN) (it was kept refrigerated), 4,4-bis(4'-hydroxyphenyl)valeric acid (used as received), isophorone (used a received), tetrabutyl ammonium bromide (used a received), methanesulfonyl chloride (used a received), tetrabutyl ammonium fluoride (used a received), 2,2'-pyridil (used a received), and preparative thin layer chromatography (PTLC) plates. Chemicals purchased from Fisher Scientific and their treatments before use are given below: CH_2Cl_2 (dried over CaH_2), tetrahydrofuran (dried over sodium with bezophenone as indicator), hexane, ethyl acetate, diethyl ether, acetone (dried from 4 Δ

molecular sieves), methanol (dried from magnesium), and tert-butanol (dried from magnesium/I_2).

NMR spectra were obtained using a Bruker ARX 400 MHz. Infrared spectra were acquired on a 400 FT-IR spectrometer. The electronic absorption (UV-vis) spectra were obtained from a Beckman DU-70 spectrophotometer. Elemental analyses were performed by Atlantic Microlab, Inc. Atlanta. Thermal analyses were carried out on a Seiko DSC 220C and TG/DTA 320 instruments. The fluorescence data were recorded by a PTI QuantaMaster™ Model C-61. The melting points were determined using a Mel-Temp II apparatus (reported values are uncorrected) or extracted from the DSC spectra.

Benzoins **2** were prepared as reported by Adams, Johnson, and Wilcox in Laboratory Experiments in Organic Chemistry, 7th Ed., New York, Macmillan: 1979, page 379. The Wittig reagent (1-triphenylphosphoniomethylbromide-4-nitrobenzene) was synthesized by modifying a published procedure (M. Zheng, L. Ding, E, E. Gurel, P. M. Lahti, F. E. Karasz, *Macromolecules* 2001, *34*, 4124-4129). 4,4-Bis(4'-hydroxyphenyl)pentanol (**26**) was prepared as reported by K-Y Chen and co-workers (K-Y Chen and C. B. Gorman, *J. Org. Chem.*, 1996, *61*, 9229-9235).

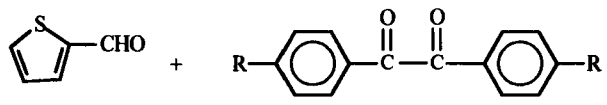

1 + 2

Acetic Acid / NH_4OAC

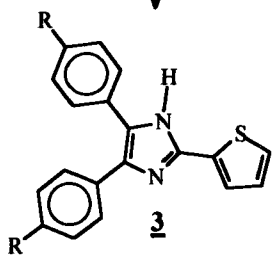

3

	a	b	c	d
R=	H,	CH_3,	OCH_3,	$N(CH_3)_2$
Yield=	87%,	75%,	82%,	70%

DMA / CH_3I / K_2CO_3

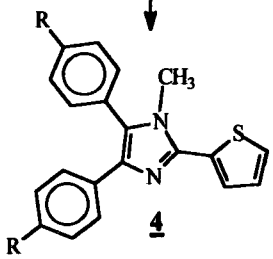

4

	a	b	c	d
R=	H,	CH_3,	OCH_3,	$N(CH_3)_2$
Yield=	65%,	90%,	86%,	78%

THF / 1) n-BuLi 2)DMF

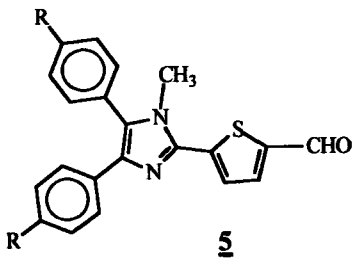

5

	a	b	c	d
R=	H,	CH_3,	OCH_3,	$N(CH_3)_2$
Yield=	68%,	54%,	75%,	53%

CH_2Cl_2 / t-BuOK / 15-Crown-5 / $Br(Ph)_3P$–CH–Ar–NO_2

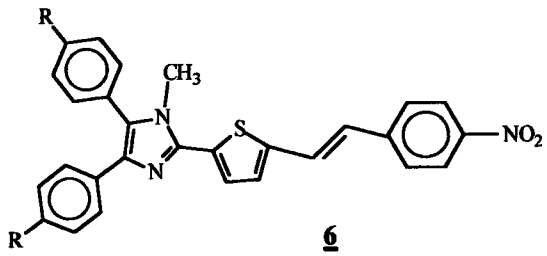

6

	a	b	c	d
R=	H,	CH_3,	OCH_3,	$N(CH_3)_2$
Yield=	75%,	65%,	67%,	43%

2-(2'-thienyl)-4,5-bis (phenyl)imidazole (3a) (X. R. Bu, H. Li, D. V. Derveer, E. A. Mintz, *Tetrahedron Letters* **1996**, *37*, 7331-7334)

Benzil (1.20 g, 5.69 mmol) was dissolved in glacial acetic acid (50 mL). 2-Thiophene carboxaldehyde (0.53 mL, 5.69 mmol) and ammonium acetate (4.38 g, 56.9 mmol) were added. This reaction mixture was refluxed for 6 h under nitrogen atmosphere, then it was cooled to ambient temperature and poured into a water-ice bath. The resulting precipitate was filtered, washed with water and dried overnight under ambient air. The crude product was purified by recrystallization from methanol to give 1.50 g (87% yield, *m.p.* 268-270 °C) of **3a**.

Elemental Analysis: Calculated for $C_{19}H_{14}N_2S$ + 1/9 CH_3OH: **C** 75.02, **H** 4.76, **N** 9.15 Found: **C** 74.99, **H** 4.84, **N** 9.16

^1H NMR (DMSO-d_6/TMS): δ 7.70 (d, J = 3.6 Hz, 1H, thienyl), 7.56 (d, J = 4.8 Hz, 1H, thienyl), 7.51 (d, J = 7.2 Hz, 4H, aromatic), 7.34 (s, 6H, aromatic), 7.15 (m, 1H, thienyl) ppm.

^{13}C NMR (DMSO-d_6/TMS): δ 142.3, 142.1, 137.4, 135.3, 134.7, 134.5, 131.3, 130.0, 138.8, 128.6, 128.4, 127.7, 137.3, 126.9, 126.7, 125.0, 124.8 ppm.

2-(2'-thienyl)-4,5-bis(4'-methylphenyl)imidazole (3b), 2-(2'-thienyl)-4,5-bis(4'-metoxyphenyl)imidazole (3c), and **2-(2'-thienyl)-4,5-bis(4'-methylaminophenyl)imidazole (3d)** were prepared in a similar manner as **3a**.

3b: (75% yield, *m.p.* 260-262 °C) *Elemental Analysis*: Calculated for $C_{21}H_{18}N_2S$: **C** 76.30, **H** 5.49, **N** 8.48 Found: **C** 76.16, **H** 5.52, **N** 8.32. *^1H NMR* ($CDCl_3$/TMS):

δ 7.41(m, 4H aromatic, 1H thienyl), 7.31(m, 1H, thienyl), 7.15 (d, *J*=8 Hz, 4H, aromatic), 7.08(m, 1H, thienyl), 2.36 (s, 6H, CH_3) ppm. *^{13}C NMR* ($CDCl_3$/TMS): δ 141.286, 133.509, 129.310, 127.917, 127.717, 125.864, 123.883, 21.273 ppm.

3c: (82% yield, *m.p.* 186-190 °C) *Elemental Analysis*: Calculated for $C_{21}H_{18}N_2O_2S$: **C** 69.59, **H** 5.01, **N** 7.73 Found: **C** 69.57, **H** 5.03, **N** 7.77. *^{1}H NMR* ($CDCl_3$/TMS): δ 7.39 (m, 4H aromatic, 1H thienyl), 7.27 (t, *J*=2.8 Hz, 1H, thienyl), 7.03 (d, *J*=4.2 Hz, 1H,thienyl), 6.82 (d, *J*=8.4 Hz,4H, aromatic), 3.79 (s, 6H, OCH_3) ppm. *^{13}C NMR* ($CDCl_3$/TMS): δ 158.949, 141.184, 133.531, 129.304, 129.106, 127.668, 125.714, 123.888, 114.000, 55.470, 55.274 ppm.

3d: (70% yield) *Elemental Analysis*: Calculated for $C_{23}H_{24}N_4S$: **C** 71.10, **H** 6.22, **N** 14.42 Found: **C** 69.15, **H** 6.37, **N** 13.90. *^{1}H NMR* (DMSO-d_6/TMS): δ 7.64 (d, *J* = 3.6 Hz, 1H, thienyl), 7.49 (d, *J* = 4.8 Hz, 1H, thienyl), 7.39 (d, *J* = 8.4 Hz, 2H, aromatic) 7.32 (d, *J* = 8.4 Hz, 2H, aromatic), 7.11 (m, 1H, thienyl), 6.76 (d, *J* = 8.0 Hz, 2H, aromatic), 6.66 (d, *J* = 8.0 Hz, 2H, aromatic), 2.93 (s, 6H, $N(CH_3)_2$), 2.88 (s, 6H, $N(CH_3)_2$) ppm. *^{13}C NMR* (DMSO-d_6/TMS): δ 150.3, 150.1, 149.6, 149.4, 141.0, 140.8, 136.5, 135.3, 135.1, 129.6, 129.4, 128.3, 128.2, 127.2, 125.9, 123.9, 119.2, 112.6, 112.5, 40.47, 40.39 ppm.

1-methyl-2-(2'-thienyl)-4,5-bis(phenyl)imidazole (4a)

A three necked round bottom flask (previously dried in an oven) equipped with a

magnetic stirrer and a condenser was charged with potassium carbonate (1.37 g, 9.92 mmol) and then dried with an open flame under vacuum. Once at room temperature the reaction flask was flushed with nitrogen. 2-(2'-Thienyl)-4,5-bis(phenyl)imidazole (**3a**) (1.5 g, 4.96 mmol) and 50 mL of anhydrous N,N'-dimethylacetamide (DMA) were added and followed by the addition of iodomethane (0.46 g, 7.44 mmol). The mixture was stirred for 15 h at 40-50 °C under a nitrogen atmosphere. The reaction mixture was allowed to cool at room temperature and then it was poured into a water-ice bath. The resulting precipitate was filtered and dried overnight under ambient air. The crude product was purified by recrystallization from methanol or methanol:ethanol (1:1 v/v). to give 1.02 g (65% yield) of **4a**. *Elemental Analysis*: Calculated for $C_{20}H_{16}N_2S$: **C** 75.92, **H** 5.09, **N** 8.85 Found: **C** 75.86, **H** 5.13, **N** 8.95. *^1H NMR* (DMSO-d_6/TMS): δ 7.67 (d, J = 5.2 Hz, 1H, thienyl), 7.53 (m, 4H, aromatic), 7.43 (d, J = 6 Hz, 2H, aromatic), 7.39 (d, J = 8 Hz, 2H, aromatic), 7.20 (m, 2H aromatic, 1H thienyl), 7.13 (m, 1H, thienyl), 3.56 (s, 3H, CH_3) ppm. *^{13}C NMR* (DMSO-d_6/TMS): δ 141.9, 137.0, 134.8, 133.5, 131.5, 131.3, 131.1, 130.8, 129.7, 129.6, 129.4, 128.7, 128.6, 128.5, 127.7, 126.9, 126.8, 126.7, 126.5, 33.3 ppm.

1-methyl-2-(2'-thienyl) -4,5-bis(4'-methylphenyl)imidazole (4b), 1-methyl-2-(2'-thienyl)-4,5-bis(4'-methoxyphenyl)imidazole (4c), and **1-methyl-2-(2'-thienyl)-4,5-bis(4'-dimethylaminophenyl)imidazole (4d)** were prepared in a similar manner as **4a**. **4b**: (90% yield, recrystallization from methanol, pale yellow solid) *^1H NMR* ($CDCl_3$/TMS): δ 7.43 (d, J=1.6 Hz, 1H, thienyl), 7.40 (m, 2H aromatic, 1H thienyl),

7.26 (d, *J*=2.8 Hz, 4H, aromatic), 7.12 (m, 1H, thienyl), 7.02 (d, *J*=8, 2H, aromatic), 3.56 (s, 3H, NCH_3), 2.42 (s, 3H, CH_3), 2.27 (s, 3H, CH_3) ppm. *^{13}C NMR* ($CDCl_3$/TMS): δ 142.16, 138.87, 138.30, 136.242, 134.00, 132.05, 131.20, 131.17, 130.62, 130.30, 130.11, 129.35, 129.11, 128.38, 127.72, 127.40, 127.20, 126.89, 126.64, 33.16, 21.74, 21.50 ppm.

4c: (86% yield, recrystallized twice from methanol, yellow solid, *m.p.* 134-138 °C) *Elemental Analysis*: Calculated for $C_{22}H_{20}N_2O_2S$: **C** 70.19, **H** 5.35, **N** 7.44 Found: **C** 70.18, **H** 5.36, **N** 7.43 *^1H NMR* ($CDCl_3$/TMS): δ 7.47 (d, *J* = 8.7Hz, 2H, aromatic), 7.40 (d, *J* = 4.0Hz, 1H, thienyl), 7.31 (m, 2H aromatic, 1H thienyl), 7.13 (t, *J* = 4.4 Hz, 1H, thienyl), 7.00 (d, *J* = 8.5Hz, 2H, aromatic), 6.77 (d, *J* = 8.7Hz, 2H, aromatic), 3.88 (s, 3H, OCH_3), 3.77 (s, 3H, OCH_3), 3.57 (s, 3H, NCH_3) ppm. *^{13}C NMR* ($CDCl_3$/TMS): δ 159.75, 158.17, 141.59, 137.61, 133.31, 132.21, 129.45, 128.02, 127.40, 127.27, 126.49, 126.11, 123.03, 114.48, 113.47, 55.31, 55.15, 32.77 ppm. *IR* (KBr): 3441, 3072, 3002, 2953, 2906, 2837, 1612, 1572, 1517, 1495, 1452, 1410, 1389, 1289, 1248, 1175, 1107, 1027, 952, 850, 838, 744, 713, 589, cm^{-1}.

4d: (78 % yield, recrystallized from CH_2Cl_2) *^1H NMR* ($CDCl_3$/TMS): δ 7.48 (d, *J*=8.8 Hz, 2H, aromatic), 7.36 (m, 2H, thienyl), 7.22 (d, *J*=8.8 Hz, 2H, aromatic), 7.10 (m, 1H thienyl), 6.78 (d, *J*=8.8 Hz, 2H, aromatic), 6.62 (d, *J*=8.8 Hz, 2H, aromatic), 3.54 (s, 3H, NCH_3), 3.01 (s, 6H, $N(CH_3)_2$), 2.88 (s, 6H, $N(CH_3)_2$) ppm. *^{13}C NMR* ($CDCl_3$/TMS): δ 150.2, 149.1, 141.1, 137.8, 133.7, 132.0, 131.9, 129.7,

127.5, 127.6, 127.4, 126.1, 126.2, 126.0, 123.5, 118.4, 112.3, 112.4, 110.9, 40.69, 40.66, 40.39, 40.37, 32.75 ppm.

1-methyl-2[2'-(5'-formyl)thienyl]-4,5-bis(phenyl)imidazole (5a)

(J. Santos, E. A. Mintz, O. Zehnder, C. Bosshard, X. R. Bu, P. Gunter, Tetrahedron Letters 2001, 42, 805-808)

The reaction was performed in a 100 mL three neck round bottom flask (equipped with a dropping funnel, nitrogen line and a magnetic stirrer) which was dried with an open flame. The reaction flask was charged with freshly distilled tetrahydrofuran (THF) (15 mL). Meanwhile **4a** (1g, 3.16 mmol) was dissolved (in a vial with rubber cap) with THF (15 mL) and transferred into the dropping funnel by syringe. The flask containing THF was cooled to -63 °C (using a $CHCl_3$ and liquid N_2 bath) followed by the addition of n-butyllithium (2.37 mL, 4.11 mmol of a 1.6 M solution in hexane). Then, compound **4a** was added dropwise. Once the addition was completed, the reaction mixture was warmed to 0 °C and stirred at that temperature for 30 minutes. The solution was, once again, cooled to -63 °C, and anhydrous N,N'-dimethylformamide (DMF) (0.36 mL, 4.59 mmol) was added dropwise via syringe. The reaction mixture was then stirred at -10 °C (using an ice and NaCl bath) for 2 h, and then poured into 100 mL of water and carefully neutralized with concentrated hydrochloric acid. The organic phase was extracted with methylene chloride, dried over magnesium sulfate, and concentrated under reduced pressure. The crude product was purified by recrystallization from methanol to give 0.741 g (68%

yield) of **5a**. *Elemental Analysis*: Calculated for $C_{21}H_{16}N_2SO$ + ½ CH_3OH: **C** 71.64, **H** 5.03, **N** 7.77 Found: **C** 71.70, **H** 4.72, **N** 7.89. *^1H NMR* ($CDCl_3$/TMS): δ 9.95 (s, 1H, CHO), 7.79 (d, *J* = 4 Hz, 1H, thienyl), 7.62 (d, *J* = 4 Hz, 1H, thienyl), 7.49 (m, 5H, aromatic), 7.38 (m, 2H, aromatic), 7.19 (m, 3H, aromatic), 3.67 (s, 3H, NCH_3) ppm. *^{13}C NMR* ($CDCl_3$/TMS): δ 182.9, 143.2, 142.2, 140.9, 139.1, 136.5, 133.9, 132.2, 130.9, 130.2, 129.3, 129.1, 128.2, 127.0, 126.9, 126.7, 33.23 ppm.

1-methyl-2[2'-(5'-formyl)thienyl]-4,5-bis(4'-methylphenyl)imidazole (5b), 1-methyl-2[2'-(5'-formyl)thienyl]-4,5-bis(4'-methoxyphenyl) imidazole (5c), and **1-methyl-2[2'-(5'-formyl) thienyl]-4,5-bis(4'-dimethylaminophenyl) imidazole (5d)** were prepared in a similar manner as **5a**.

5b: The crude product was purified by recrystallization from methanol or ethyl acetate. Also it was purified by column chromatography using silica gel and 30% ethyl acetate in hexane resulting in 54% yield. *Elemental Analysis*: Calculated for $C_{23}H_{20}N_2SO$: **C** 74.16, **H** 5.41, **N** 7.52 Found: **C** 74.17, **H** 5.42, **N** 7.55. *^1H NMR* ($CDCl_3$/TMS): δ 9.93 (s, 1H, CHO), 7.77(d, *J* = 4.0 Hz, 1H, thienyl), 7.60 (d, *J* = 4.0 Hz, 1H, thienyl), 7.42 (d, *J* = 8.4 Hz, 2H, aromatic), 7.27 (m, 4H, aromatic), 7.04 (d, *J* = 8.0 Hz, 2H, aromatic), 3.64 (s, 3H, NCH_3), 2.44 (s, 3H, CH_3), 2.28 (s, 3H, CH_3) ppm. *^{13}C NMR* ($CDCl_3$/TMS): δ 183.107, 143.462, 142.856, 140.997, 139.499, 139.398, 136.799, 136.71, 132.29, 131.55, 131.23, 131.136, 130.490, 130.27, 129.70 129.25, 127.70, 129.40, 127.235, 126.921, 33.467, 21.78, 21.53 ppm.

5c: The crude product was purified by column chromatography on silica gel using 30% ethyl acetate in hexane as eluent to give 75% yield (*m.p.* 192-196 °C). The crude product was also purified by recrystallization from methanol or ethyl acetate. *Elemental Analysis*:Calculated for $C_{23}H_{20}N_2O_3S$: **C** 68.30, **H** 4.98, **N** 6.93 Found: **C** 68.31, **H** 5.03, **N** 6.86. *^1H NMR* ($CDCl_3$/TMS): δ 9.93 (s, 1H, CHO), 7.77(d, *J* = 3.96 Hz, 1H, thienyl), 7.59 (d, *J* = 4.0 Hz, 1H, thienyl), 7.46 (d, *J* = 8.75 Hz, 2H, aromatic), 7.28 (d, *J* = 8.56 Hz, 2H ,aromatic), 7.01 (d, *J* = 8.59 Hz, 2H, aromatic), 6.78 (d, *J* = 8.73 Hz, 2H, aromatic), 3.88 (s, 3H, OCH_3), 3.77 (s, 3H, OCH_3), 3.65 (S, 3H, NCH_3) ppm. *^{13}C NMR* ($CDCl_3$/TMS): δ 182.77, 160.14, 158.60, 142.98, 142.57, 140.45, 138.92, 138.44, 132.23, 131.20, 128.11, 126.80, 126.38, 122.38, 114.68, 113.67, 55.37, 55.20, 33.05 ppm. *UV-Vis*: (acetronitrile): $\lambda_{max.}$ (ε) 205 (29,420), 231 (22,030), 277 (19,962), 389 (19,590) nm.

5d: The crude product was purified by column chromatography using silica gel and 50% ethyl acetate in hexane as eluent to give 53% yield. *Elemental Analysis*: Calculated for $C_{25}H_{26}N_4SO$: **C** 69.97, **H** 6.08, **N** 13.01 Found: **C** 69.90, **H** 6.16, **N** 12.89. *^1H NMR* ($CDCl_3$/TMS): δ 9.95 (s, 1H, CHO), 7.75(d, *J* = 5.2 Hz, 1H, thienyl), 7.57 (d, J = 4.0 Hz, 1H, thienyl), 7.48 (d, *J* = 7.6 Hz, 2H, aromatic), 7.22 (d, *J* = 7.6 Hz, 2H, aromatic), 6.80 (d, *J* = 7.6 Hz, 2H, aromatic), 6.63 (d, *J* = 7.6 Hz, 2H, aromatic), 3.64 (s, 3H, NCH_3), 3.04 (s, 6H, $N(CH_3)_2$), 2.91 (S, 6H, $N(CH_3)_2$) ppm. *^{13}C NMR* ($CDCl_3$/TMS): δ 182.9, 150.4, 149.3, 143.1, 142.5, 139.9, 139.2, 136.7, 131.9, 131.8, 131.6, 127.8, 127.7, 126.0, 122.9, 117.5, 112.4, 112.3, 40.58, 40.32, 33.05 ppm.

1-methyl-2-[2'-(stilbene-4'-nitrophenyl)thienyl]-4,5-bis(phenyl)imidazole (6a)

A mixture of potassium *tert*-butoxide (1.0 g, 9.03 mmol), 1-triphenylphosphonio methylbromide-4-nitrobenzene (wittig reagent) (1.13 g, 2.36 mmol), **5a** (0.740 g, 2.15 mmol) and 15-crown-5 (0.118 g, 0.537 mmol) in dry dichloromethane (50 mL) was stirred at room temperature under nitrogen for 15 h. Then the solution was poured into a water bath, the organic phase was extracted with CH_2Cl_2, dried over $MgSO_4$ and concentrated under reduced pressure. The crude product was purified by column chromatography on silica gel using 33% ethyl acetate in hexane as eluent to give 0.750 g (75% yield) of **6a**. *Elemental Analysis*: Calculated for $C_{28}H_{21}N_3O_2S$ + ½ $CH_3CH_2OCOCH_3$: **C** 71.26, **H** 4.59, **N** 8.31 Found: **C** 71.45, **H** 4.65, **N** 8.72. *^1H NMR* ($CDCl_3$/TMS): δ 8.24 (d, J = 8.4 Hz, 2H, aromatic), 7.62(d, J = 8.8 Hz, 2H, aromatic), 7.54-7.45 (m, 2H thienyl, 3H aromatic), 7.39-7.30 (m, 4H, aromatic), 7.25-7.15 (m, 3H aromatic, 1H CH=C), 7.05 (d, J = 16Hz, 1H, C=CH), 3.66 (s, 3H, NCH_3) ppm. *^{13}C NMR* ($CDCl_3$/TMS): δ 146.7, 143.4, 142.3, 141.7, 138.5, 134.2, 133.8, 131.3, 130.9, 130.5, 129.2, 128.9, 128.8, 128.2, 127.0, 126.7, 126.7, 126.4, 126.3, 125.9, 124.3, 33.1 ppm.

1-methyl-2-[2'-(stilbene-4'-nitrophenyl)thienyl]-4,5-bis(methylphenyl)imidazole (6b), 1-methyl-2-[2'-(stilbene-4'-nitrophenyl)thienyl]-4,5-bis(methoxyphenyl)imidazole (6c), and **1-methyl-2-[2'-(stilbene-4'-nitrophenyl)thienyl]-,5-bis(dimethylaminophenyl)imidazole (6d)** were prepared in a similar manner as **6a**. **6b**: The crude product was purified by column chromatography using silica gel and

23% ethyl acetate in hexane as eluent to give 65% yield. *Elemental Analysis*: Calculated for $C_{30}H_{25}N_3O_2S$: **C** 73.30, **H** 5.13, **N** 8.55 Found: **C** 73.28, **H** 5.21, **N** 8.41. *^1H NMR* ($CDCl_3$/TMS): δ 8.24 (d, *J* = 8.4Hz, 2H, aromatic), 7.62(d, *J* = 8.8Hz, 2H, aromatic), 7.42 (m, 2H, aromatic), 7.35 (m, 2H, aromatic), 7.27 (m, 4H, aromatic), 7.19 (d, J = 4.0Hz, 1H, CH=C), 7.04 (m, 1H C=CH, 2H thienyl), 3.64 (s, 3H, NCH_3), 2.45 (s, 3H, CH_3), 2.30 (s, 3H, CH_3) ppm. *^{13}C NMR* ($CDCl_3$/TMS): δ 146.7, 143.5, 142.1, 141.4, 138.8, 138.4, 136.2, 134.1, 131.4, 131.0, 130.8, 130.0, 129.9, 129.1, 128.9, 127.6, 127.2, 126.9, 126.7, 126.2, 126.1, 126.0, 124.5, 124.3, 33.05, 21.47, 21.23 ppm.

6c: The crude product was purified by column chromatography using silica gel and 30% ethyl acetate in hexane as eluent to give 67% yield. *Elemental Analysis*: Calculated for $C_{30}H_{25}N_3O_4S$: **C** 68.82, **H** 4.81, **N** 8.03 Found: **C** 68.74, **H** 4.80, **N** 8.03. *^1H NMR* ($CDCl_3$/TMS): δ 8.22 (d, *J*=8.0 Hz, 2H, aromatic), 7.60 (d, *J*=8.0 Hz, 2H, aromatic), 7.49 (d, *J*=8.0 Hz, 2H, aromatic), 7.32 (m, 4H, aromatic), 7.18 (d, *J*=4.0 Hz, 1H, CH=C), 7.03 (m, 1H C=CH, 2H thienyl), 6.08 (d, *J*=8.0 Hz, 2H, aromatic), 3.89 (s, 3H, OCH_3), 3.81 (s, 3H, OCH_3), 3.64 (s, 3H, CH_3) ppm. *^{13}C NMR* ($CDCl_3$/TMS): δ 160.346, 158.801, 147.089, 143.834, 142.441, 141.553, 138.583, 134.532, 132.823, 132.623, 130.597, 129.127, 128.669, 128.467, 127.509, 127.234, 126.860, 126.326, 124.790, 124.594, 123.127, 114.997, 114.921, 113.979, 113.919, 55.566, 33.124, 21.406 ppm.

6d: The crude product was purified by column chromatography on silica gel using 50% ethyl acetate in hexane as eluent to give 43% yield. *Elemental Analysis*: Calculated for $C_{32}H_{31}N_5O_2S$: **C** 69.92, **H** 5.68, **N** 12.74 Found: **C** 70.01, **H** 5.42, **N** 12.59. *^1H NMR* ($CDCl_3$/TMS): δ 8.21 (d, *J* = 9.2 Hz, 2H ,aromatic), 7.59 (d, *J* = 8.8Hz, 2H, aromatic), 7.47 (d, *J* = 7.2, 2H, aromatic), 7.38 (d, *J* = 16 Hz, 1H, C=CH), 7.31 (d, *J* = 3.6 Hz, 1H, thienyl), 7.23 (d, *J* = 8.8 Hz, 2H, aromatic), 7.15 (d, *J* = 4 Hz, 1H, thienyl), 7.00 (d, *J* = 12.8 Hz, 1H, CH=C), 6.79 (d, *J* = 8.8 Hz, 2H, aromatic), 6.81 (d, *J* = 9.2 Hz, 2H, aromatic), 3.61 (s, 3H, NCH_3), 3.03 (s, 6H, $N(CH_3)_2$), 2.90 (s, 6H, $N(CH_3)_2$) ppm. *^{13}C NMR* ($CDCl_3$/TMS): δ 150.3, 149.2, 146.6, 143.6, 141.7, 140.7, 138.4, 134.6, 131.9, 131.8, 130.5, 128.9, 127.7, 127.6, 126.6, 126.1, 125.9, 125.7, 124.5, 124.3, 123.3, 118.0, 112.4, 112.4, 40.64, 40.35, 32.9 ppm.

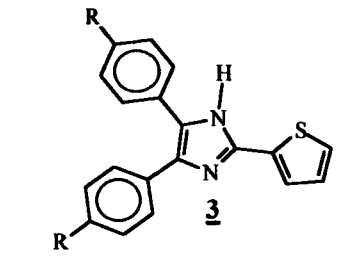

3

2-chloroethanol
DMF / 150 °C / 15 h | K_2CO_3 / KI

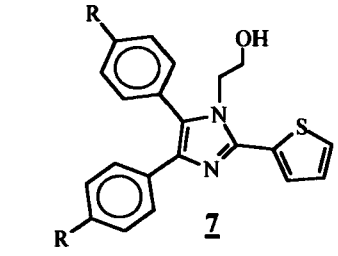

7

	a	c
R=	H,	OCH_3
Yield=	95%	65%

$(CH_3)CPh_2SiCl$
DMF / rt / 6 h | Imidazole

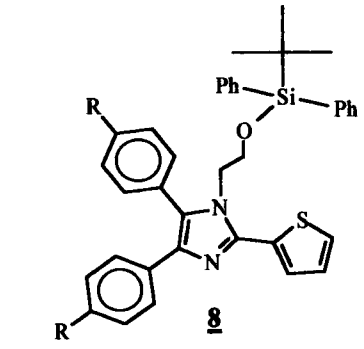

8

	a	c
R=	H,	OCH_3
Yield=	70%	89%

THF | 1) n-BuLi / -63 °C
2) 35 min at 0 °C
3) DMF / -63 °C
4) 2 h at -10 °C

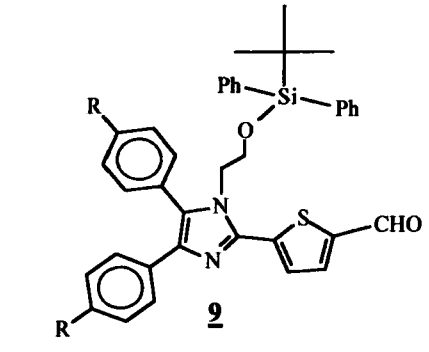

9

	a	c
R=	H,	OCH_3
Yield=	80%	84%

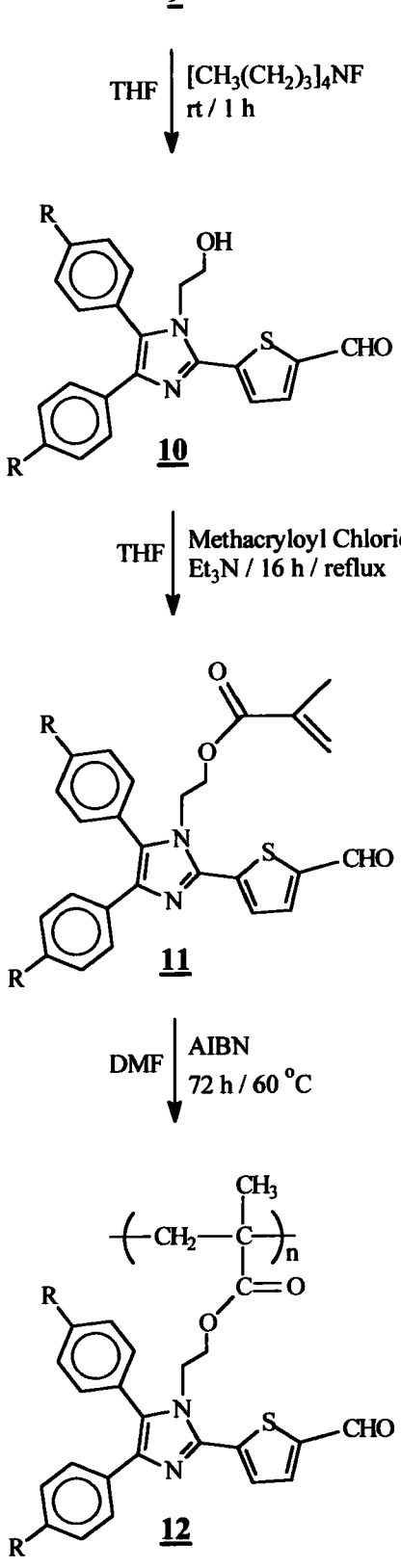

a **c**

R= H, OCH_3

Yield= 60% 90 %

a **c**

R= H, OCH_3

Yield= 85% 76 %

a **c**

R= H, OCH_3

Yield= 70% 65%

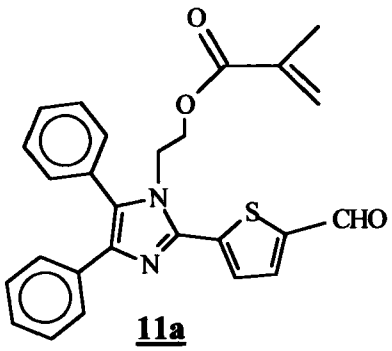

11a

DMF | MMA / AIBN, 70 °C / 96 h

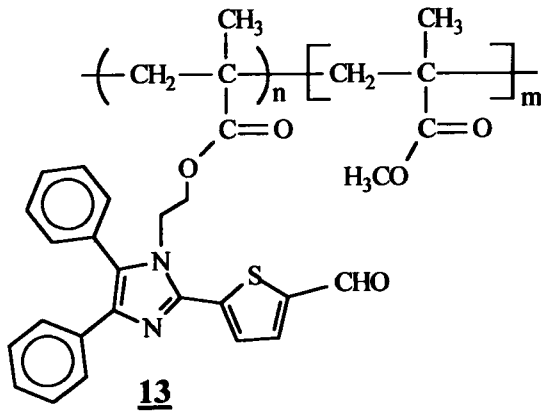

13

1-(2'-hydroxyethyl)-2-(2'-thienyl)-4,5-bis(phenyl)imidazole (7a)

In a 250 mL three neck round bottom flask, equipped with a stirring bar, a nitrogen inlet adapter, a nitrogen bubbler, and a condenser, 1.0 g (3.31 mmol) of **3a** was dissolved in 30 mL of anhydrous DMF. Then 0.399 g (0.33 mL, 4.96 mmol) of 2-chloroethanol, 0.914 g (6.61 mmol) of potassium carbonate and 0.549 g (3.31 mmol) of potassium iodide were placed into the reaction flask. The mixture was heated to 140-150 °C for 15 h. Upon cooling to room temperature, the reaction mixture was poured into 300 mL of an ice-water bath with vigorous stirring. The resulting white precipitate was filtered, washed with 300 mL of water and dried under ambient air for 15 h. Compound **7a** was obtained as a pale yellow solid in 95% yield (1.09 g). *^{1}H NMR* ($CDCl_3$/TMS): δ 7.50 (d, J = 3.6 Hz, 1H, thienyl), 7.48 (d, J = 6.8 Hz, 2H, aromatic), 7.38 (m, 4H, aromatic), 7.19 (m, 4H, aromatic, 1H, thienyl), 7.02 (m, 1H, thienyl), 4.07 (t, J = 6.0 Hz, 2H, CH_2O), 3.64 (t, J = 6.0 Hz, 2H, CH_2N) ppm. *^{13}C NMR* ($CDCl_3$/TMS): δ 142.04, 137.94, 134.06, 132.45, 131.35, 130.83, 130.14, 129.06, 128.92, 128.19, 127.65, 127.32, 126.90, 126.78, 126.50, 61.57, 46.50 ppm.

The same procedure was applied to prepare **1-(2'-hydroxyethyl)-2-(2'-thienyl)-4,5-bis(4'-methoxyphenyl)imidazole (7c)**

The crude product was purified by column chromatography on silica gel and 30% ethyl acetate in hexane. Pure **7c** was isolated in 65% yield as a yellow solid. *Elemental Analysis:* Calculated for $C_{23}H_{22}N_2O_3S$: **C** 67.96, **H** 5.45, **N** 6.89 Found:

C 67.73, **H** 5.46, **N** 6.85. *^1H NMR* ($CDCl_3$/TMS): δ 7.45 (d, *J* = 3.2 Hz, 1H, thienyl), 7.41 (d, *J* = 8.8 Hz, 2H, aromatic), 7.30 (d, *J* = 4.8 Hz, 1H, thienyl), 6.90 (m, 2H aromatic, 1H thienyl), 6.80 (m, 4H, aromatic), 3.93 (t, *J* = 5.6 Hz, 2H, CH_2OH), 3.82 (s, 3H, OCH_3), 3.80 (s, 3H, OCH_3), 3.64 (t, *J* = 5.6 Hz, 2H, NCH_2) ppm. *^{13}C NMR* ($CDCl_3$/TMS): δ 159.74, 158.33, 141.70, 137.46, 132.82, 132.49, 128.92, 127.85, 128.38, 127.85, 127.68, 127.13, 127.04, 126.49, 122.81, 114.21, 113.82, 113.63, 61.65, 55.20, 55.17, 46.52 ppm.

1-(2'-t-butyl diphenyl sylilethyl)-2-(2'-thienyl)-4,5-bis(phenyl)imidazole (8a)

A 50 mL one neck round bottom flask containing 0.500 g (1.14 mmol) of **7a** was charged with 10 mL of anhydrous DMF. Then t-butyldiphenylsylil chloride (0.436 g, 0.41 mL, 1.59 mol) and imidazole (0.216 g, 3.17 mmol) were added. The reaction mixture was stirred at room temperature under a nitrogen atmosphere for 6 h. Then the mixture was poured into an ice-water bath and stirred for 20 minutes. The precipitate was filtered and dried under ambient air for 15 h. Compound **8a** was obtained pure in 70% yield (0.591 g). *^1H NMR* ($CDCl_3$/TMS): δ 7.67 (d, *J* = 7.6 Hz, 1H, thienyl), 7.50 (m, 3H, aromatic), 7.44 (d, *J* = 8.0 Hz, 4H, aromatic), 7.31 (m, 9H, aromatic), 7.16 (m, 4H, aromatic), 7.14 (d, *J* = 7.0 Hz, 1H, thienyl), 7.04 (m, 1H, thienyl), 4.22 (t, *J* = 6.0 Hz, 2H, OCH_2), 3.59 (t, *J* = 6.0 Hz, 2H, NCH_2), 0.92 (s, 9H, t-butyl) ppm. *^{13}C NMR* ($CDCl_3$ / TMS): δ 142.29, 138.33, 135.54, 134.98, 134.42, 133.06, 132.88, 131.20, 130.90, 130.19, 129.90, 129.52, 129.09, 128.85, 128.17, 128.10, 127.91, 127.69, 127.46, 127.15, 127.06, 126.94,

126.50, 62.71, 46.32, 26.81, 19.13 ppm.

The same procedure was applied to prepare **1-(2'-t-butyldiphenylsylilethyl)-2-(2'-thienyl)-4,5-bis(4'-methoxyphenyl)imidazole (8c)**

The crude product was purified by column chromatography on silica gel using 23% ethyl acetate in hexane as eluent. Pure compound **8c** was isolated in 89% yield. *^{1}H NMR* ($CDCl_3$/TMS): δ 7.52 (d, J = 3.6 Hz, 1H, thienyl), 7.43 (m, 6H, aromatic), 7.36 (m, 2H aromatic, 1H thienyl), 7.29 (m, 3H aromatic, 1H thienyl), 7.06 (m, 3H, aromatic), 6.85 (d, J = 8.8 Hz, 2H, aromatic), 6.76 (d, J = 8.8 Hz, 2H, aromatic), 4.20 (t, J = 6.0 Hz, 2H, OCH_2), 3.82 (s, 3H, OCH_3), 3.74 (s, 3H, OCH_3), 3.62 (t, J = 6.4 Hz, 2H, NCH_2), 0.92 (s, 9H, t-butyl) ppm. *^{13}C NMR* ($CDCl_3$/TMS): δ 159.8, 158.2, 141.7, 138.0, 135.7, 135.5, 133..49, 133.27, 133.10, 132.88, 132.70, 132.46, 130.01, 129.80, 129.11, 128.92, 128.20, 128.02, 127.80, 127.36, 127.32, 126.80, 126.65, 123.0, 114.4, 113.5, 62.73, 55.29, 55.17, 46.14, 26.72, 19.07 ppm.

1-(2'-t-butyl diphenyl sylil ethyl)-2[2'-(5'-formyl)thienyl]-4,5-bis (phenyl)imidazole (9a)

Compound **8a** (2.5 g, 4.27 mmol) was dissolved with 15 mL of dry THF in a 25 mL vial (previously dried) and then transferred to the dropping funnel via syringe. The reaction flask containing dry THF (10 mL) was cooled to -63 °C (using a $CHCl_3$ and liquid nitrogen bath) followed by the addition of n-butillithium (3.23 mL, 6.46 mmol, 1.5 equiv from 1.6 M solution in hexane). Compound **8a** was added

dropwise over 2 minutes while the reaction flask is kept at -63 °C. After addition, the reaction mixture was warmed to 0 °C and kept at that temperature for 35 minutes. The reaction was cooled to -63 °C, followed by the dropwise addition of anhydrous N,N'-dimethylformamide (0.67 mL, 0.629 g, 8.61 mmol). The reaction mixture was then warmed to -10 °C and kept at that temperature for 2 h. The reaction mixture was poured into 100 mL of water and carefully neutralized with hydrochloric acid (12 N). The organic phase was extracted with methylene chloride, dried under magnesium sulfate and concentrated under reduced pressure. The crude product was purified by column chromatography using silica gel and 16% ethyl acetate in hexane as eluent. After removal of solvent 80% yield (2.07 g) of **9a** was obtained. *^{1}H NMR* ($CDCl_3$/TMS): δ 9.92 (s, 1H, CHO), 7.72 (m, 2H, thienyl), 7.48 (d, J = 7.6 Hz, 2H, aromatic), 7.43 (d, J = 7.6 Hz, 4H, aromatic), 7.36 (m, 6H, aromatic), 7.29 (m, 2H, aromatic), 7.23 (m, 4H, aromatic), 7.13 (d, J = 6.8 Hz, 2H, aromatic), 4.30 (t, J = 5.6 Hz, 2H, OCH_2), 3.62 (t, J = 5.6 Hz, 2H, NCH_2), 0.90 (s, 9H, t-butyl) ppm. *^{13}C NMR* ($CDCl_3$/TMS): δ 180.21, 143.2, 142.6, 141.1, 139.3, 136.3, 135.4, 135.3, 133.8, 132.5, 131.6, 131.0, 130.2, 129.9, 129.1, 128.3, 138.2, 127.9, 127.3, 126.9, 126.8, 62.70, 46.62, 26.65, 19.00 ppm.

The same procedure was applied to prepare **1-(2'-t-butyldiphenylsylilethyl)-2[2'-(5'-formyl)thienyl]-4,5-bis(4'-methoxyphenyl)imidazole (9c)**

The crude product was purified by column chromatography on silica gel using 16% ethyl acetate in hexane as eluent. After solvent removal 84% yield of **9c** was

obtained. *^1H NMR* ($CDCl_3$/TMS): δ 9.91 (s, 1H, CHO), 7.70 (s, 2H, thienyl), 7.44 (d, J = 8 Hz, 6H, aromatic), 7.37 (m, 2H, aromatic), 7.29 (m, 4H, aromatic), 7.01 (d, J = 8.4 Hz, 2H, aromatic), 6.86 (d, J = 8.8 Hz, 2H, aromatic), 6.78 (8.8 Hz, 2H, aromatic), 4.26 (t, J = 5.6 Hz, 2H, OCH_2), 3.83 (s, 3H, OCH_3), 3.76 (s, 3H, OCH_3), 3.64 (t, J = 5.6 Hz, 2H, NCH_2), 0.90 (s, 9H, t-butyl) ppm. *^{13}C NMR* ($CDCl_3$/TMS): δ 182.88, 159.98, 158.49, 142.95, 140.70, 139.23, 136.36, 135.47, 132.59, 132.36, 130.53, 129.89, 128.01, 127.84, 126.96, 126.79, 122.33, 114.56, 113.62, 62.791, 55.27, 55.18, 46.51, 26.65, 19.00 ppm.

1-(2'-hydroxyethyl)-2[2'-(5'-formyl)thienyl]-4,5-bis(phenyl)imidazole (10a)

A 100 mL one neck round bottom flask equipped with a magnetic stirring bar, and a nitrogen inlet adapter was charged with **9a** (0.154 g, 0.259 mmol), 5 mL of dry THF and 0.50 mL (0.51 mmol from 1.0 M in THF) of tetrabutyl ammonium fluoride. The reaction mixture was stirred at room temperature for 1 h. Then 20 mL of water was poured into the reaction mixture. The organic phase was extracted with methylene chloride, dried over magnesium sulfate and concentrated under reduced pressure. The crude product was recrystallized with 10% methylene chloride in ethyl acetate to give red crystals of **10a** in 60% yield (0.57 g). *Elemental Analysis*: Calculated for $C_{22}H_{18}N_2O_2S$ + 1/4 $CH_3CH_2OCOCH_3$:

C 69.67, **H** 5.08, **N** 7.06 Found: **C** 69.81, **H** 4.96, **N** 7.36. *^1H NMR* ($CDCl_3$/TMS): δ 9.94 (s, 1H, CHO), 7.75 (d, J = 4.0 Hz, 1H, thienyl), 7.72 (d, J = 4.0 Hz, 1H, thienyl), 7.49-7.46 (m, 5H, aromatic), 7.36-7.33 (m, 2H, aromatic),

7.21-7.19 (m, 3H, aromatic), 4.22 (t, J = 6.0 Hz, 2H, CH_2O), 3.70 (t, J = 6.0 Hz, 2H, NCH_2) ppm. *^{13}C NMR* ($CDCl_3$/TMS): δ 182.87, 143.40, 141.78, 140.96, 138.84, 136.38, 135.23, 134.83, 133.54, 131.69, 131.32, 130.15, 129.67, 129.25, 129.13, 128.43, 127.92, 127.74, 126.99, 126.76, 61.62, 46.92 ppm.

The same procedure was applied to prepare **1-(2'-hydroxyethyl)-2[2'-(5'-formyl)thienyl]-4,5-bis(4'-methoxyphenyl) imidazole (10c)**

The crude product was purified by column chromatography using silica gel and 23% ethyl acetate in hexane. After removal of solvent compound **10c** was obtained in 90% yield. *^{1}H NMR* (DMSO-d_6/$CDCl_3$/TMS): δ 9.97 (s, 1H, CHO), 8.07 (d, J = 4.4 Hz, 1H, thienyl), 7.77 (d, J = 4.0 Hz, 1H, thienyl), 7.39 (d, J = 8.4 Hz, 2H, aromatic), 7.32 (d, J = 8.4 Hz, 2H, aromatic), 7.11 (d, J = 8.4 Hz, 2H, aromatic), 6.82 (d, J = 8.8 Hz, 2H, aromatic), 5.09 (t, J = 5.2 Hz, 1H, OH), 4.09 (t, J = 6.4 Hz, 2H, CH_2O), 3.84 (s, 3H, OCH_3), 3.70 (s, 3H, OCH_3), 3.47 (t, J = 6.0 Hz, 2H, NCH_2). *^{13}C NMR* (DMSO-d_6/$CDCl_3$/TMS): δ 184.79, 160.18, 158.50, 142.81, 142.72, 140.00, 139.13, 138.13, 132.99, 131.39, 127.75, 127.00, 126.71, 122.51, 115.07, 114.13, 59.93, 55.66, 55.46, 47.08 ppm.

1-(1'-oxo-2'-methylethenyl)-2[2'-(5'-formyl)thienyl]-4,5-bis(phenyl) imidazole (11a)

A 50 mL two neck round bottom flask was charged with 0.100 g (0.267 mmol) of **10a** and 10 mL of dry THF. Then methacryloyl chloride (0.0418 g, 0.04 mL, 0.40 mmol) and triethyl amine (0.0811 g, 0.11 mL, 0.80 mmol) were added. The reaction

mixture was refluxed for 16 h under a nitrogen atmosphere. The reaction was cooled to room temperature and poured into 100 mL of water. The organic phase was extracted with 3 portions of 100 mL of methylene chloride, dried over sodium sulfate and concentrated under reduced pressure. The crude product was purified by column chromatography using silica gel and 30% ethyl acetate in hexane. The solvent was removed under reduced pressure to give 85% yield (0.100 g) of **11a**. *Elemental Analysis*: Calculated for $C_{26}H_{22}N_2O_3S$ + 1/1.5 $CH_3COCH_2CH_3$: **C** 68.69, **H** 5.49, **N** 5.58 Found: **C** 68.50, **H** 5.15, **N** 5.83. *^1H NMR* ($CDCl_3$/TMS): δ 9.91 (s, 1H, CHO), 7.76 (d, *J* = 4.0 Hz, 1H, thienyl), 7.63 (d, *J* = 4.0 Hz, 1H, thienyl), 7.51-7.46 (m, 5H, aromatic), 7.41-7.38 (m, 2H, aromatic), 7.22-7.15 (m, 3H, aromatic), 5.84 (s, 1H, C=CH), 5.48 (s, 1H, C=CH), 4.42 (t, *J* = 5.6 Hz, 2H, CH_2O), 4.15 (t, *J* = 5.6 Hz, 2H, NCH_2), 1.77 (s, 3H, CH_3) ppm. *^{13}C NMR* ($CDCl_3$/TMS): δ 182.81, 166.69, 143.51, 143.36, 142.05, 141.58, 140.72, 139.53, 139.37, 136.65, 135.26, 133.52, 131.51, 130.99, 130.77, 129.95, 129+.53, 129.45, 128.21, 128.16, 126.99, 126.91, 126.85, 126.83, 126.63, 62.55, 43.58, 18.14 ppm.

The same procedure was applied to prepare **1-(1'-oxo-2'-methylethenyl)-2[2'-(5'-formyl)thienyl]-4,5-bis(4'-methoxyphenyl)imidazole (11c)**

The crude product was purified by column chromatography using silica gel and hexane and ethyl acetate (1:1). The solvent was removed under reduced pressure to give 76% yield. *Elemental Analysis*: Calculated for $C_{28}H_{26}N_2O_5S$ + ½ $CH_3COOCH_2CH_3$: **C** 65.92, **H** 5.53, **N** 5.12 Found: **C** 65.64, **H** 5.26, **N** 5.14. *^1H NMR*

($CDCl_3$/TMS): δ 9.98 (s, 1H, CHO), 7.77 (d, *J* = 4.0 Hz, 1H, thienyl), 6.64 (d, *J* = 4.0 Hz, 1H, thienyl), 7.44 (d, *J* = 8.8 Hz, 2H, aromatic), 7.32 (d, J=8.4 Hz, 2H, aromatic), 7.03 (d, *J* = 8.8 Hz, 2H, aromatic), 6.78 (d, *J* = 8.8 Hz, 2H, aromatic), 5.91 (s, 1H, C=CH), 5.54 (s, 1H, C=CH), 4.41 (t, *J* = 6.0 Hz, 2H, CH_2O), 4.17 (t, *J* = 5.6 Hz, 2H, NCH_2), 3.89 (s, 3H, OCH_3), 3.76 (s, 3H, OCH_3), 1.79 (s, 3H, CH_3) ppm. *^{13}C NMR* ($CDCl_3$/TMS): δ 182.82, 166.80, 160.29, 158.63, 143.26, 142.29, 140.36, 139.32, 136.54, 135.36, 132.39, 130.44, 127.99, 126.77, 126.64, 126.39, 122.02, 115.02, 114.93, 113.65, 62.67, 55.35, 55.21, 43.53, 18.20 ppm.

Polymerization of 11a into a polymer 12a

A dry ampul equipped with a magnetic stirring bar was charged with 290 mg (0.655 mmol) of **11a**, 10 mg (0.0609 mmol) of 2,2' azobisisobutyronitrile (AIBN), and 6 mL of anhydrous N,N'-dimethylformamide. After all solids were dissolved, the reaction mixture was de-oxygenated using nitrogen and freeze thaw cycles. The ampul was sealed and the reaction mixture was stirred at 60 °C for 72 h. The reaction was poured into 150 mL of methanol with vigorous stirring, the resulting precipitate was filtered and re-dissolved in THF, and re-precipitated in methanol. The resulting yellow solid was filtered, washed with 500 mL of methanol and dried under vacuum to give 70% yield (0.202 g) of polymer **12a**. *^{1}H NMR* ($CDCl_3$/TMS): δ 9.54 (s-broad, 1H, CHO), 7.51-7.04 (m-broad, 12H, aromatic), 4.19 (s-broad, 2H, CH_2O), 3.77 (s-broad, 2H, NCH_2), 1.60 (s-broad, 3H, CH_3), 0.39 (s-broad, 2H, CH2) ppm. *^{13}C NMR* ($CDCl_3$/TMS): δ 182.86, 175.77, 142.95, 142.03, 140.55, 139.40, 133.46,

131.38, 130.83, 129.72, 129.54, 129.45, 129.35, 128.20, 127.00, 126.82, 62.76, 44.60, 43.03, 19.02 ppm. *FT-IR* (KBr): 3430, 3064, 2947, 2821, 2733, 1958, 1895, 1734, 1676, 1471, 1223, 1145 cm^{-1}.

The same procedure was applied to prepare **Polymerization of 11c into polymer 12c** 65% yield. *^1H NMR* ($CDCl_3$/TMS): δ 9.67 (s-broad, 1H, CHO), 7.81-6.71 (m-broad, 10 H, aromatic), 4.23 (s-broad, 2H, CH_2O), 3.80 (s-broad, 8H, $2OCH_3$, NCH_2), 1.27 (s, 3H, CH_3), 0.41 (s-broad, 2H, CH_2) ppm. *^{13}C NMR* ($CDCl_3$/TMS): δ 182.9, 175.52, 160.3, 158.6, 142.7, 140.2, 139.3, 137.39, 132.3, 130.5, 128.0, 126.4, 121.7, 115.0, 113.6, 62.77, 55.17, 44.49, 42.79, 29.73, 18.54, 14.15 ppm. *FT-IR* (KBr): 3433, 3002, 2958, 2905, 2836, 2738, 2543, 2054, 1998, 1731, 1668, 1575 cm^{-1}.

Copolymerization of 11a and methyl methacrylate (MMA) (13a)

A dry ampul equipped with a magnetic stirring bar was charged with 355 mg (0.802 mmol) of **11a**, 361 mg (0.39 mL, 3.61 mmol) of MMA, 18 mg (0.11 mmol) of 2,2' azobisisobutyronitrile (AIBN), and 15 mL of N,N'-dimethylformamide. After all solids were dissolved, the reaction mixture was de-oxygenated using nitrogen and freeze thaw cycles. The ampul was sealed and the reaction mixture was heated at 85 °C for 96 h. The reaction mixture was transferred (dropwise) into 100 mL of methanol with vigorous stirring. The resulting precipitate was filtered and re-dissolved in THF, re-precipitated in methanol, filtered and washed with 250 mL of methanol. The yellow solid was dried under vacuum to give 150 mg of copolymer **13a**.

^1H NMR ($CDCl_3$/TMS): δ 9.96 (s, 1H, CHO), 7.84 (1H, thienyl), 7.65 (1H, thienyl), 7.51-7.46 (8H, aromatic), 7.20 (2H, aromatic), 4.43 (2H, CH_2O), 3.91 (2H, NCH_2), 3.59 (30H, OCH_3), 1.81 (3H, CH_3), 1.55 (30H, CH_3), 0.84 (20H, CH_2), 0.65 (2H, CH_2) ppm.

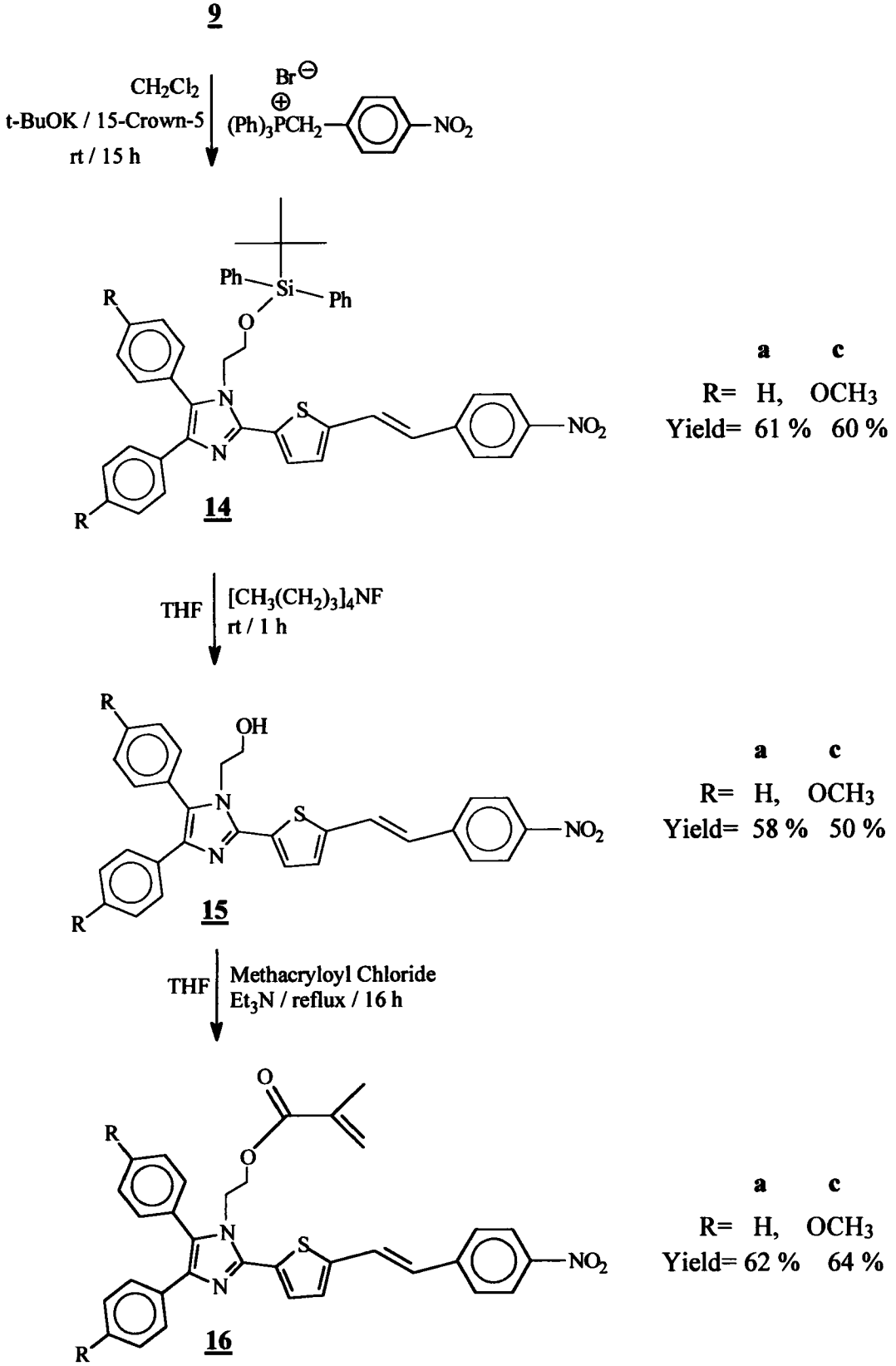

	a	c
R=	H,	OCH_3
Yield=	61 %	60 %

	a	c
R=	H,	OCH_3
Yield=	58 %	50 %

	a	c
R=	H,	OCH_3
Yield=	62 %	64 %

16

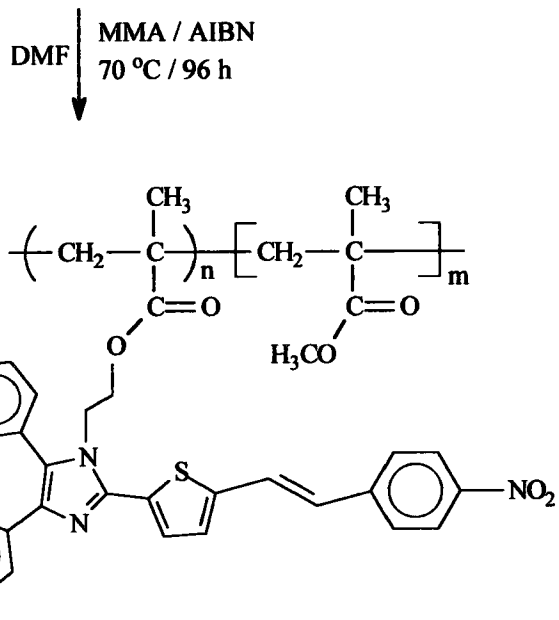

17

a **b**

R = H, OCH_3

1-(2'-t-butyl diphenyl sylilethyl)-2-[2'-(stilbene-4'-nitrophenyl)thienyl]-4,5-bis(phenyl) imidazole (14a)

A 250 mL three neck round bottom flask, previously dried, was charged with 4.33 g of **9a** and 50 mL of dry CH_2Cl_2. Then t-BuOK (3.17 g, 28.26 mmol, 4 equiv), 1-triphenylphosphonio methylbromide-4-nitrobenzene (wittig reagent) (3.72 g, 7.77 mmol, 1.1 equiv) and 15-crown-5 (0.35 g, 1.77 mmol, 0.25 equiv) were added. The reaction mixture was stirred at room temperature for 15 h under a nitrogen atmosphere. The solution was poured into a water bath, the organic phase was extracted with CH_2Cl_2, dried over $MgSO_4$ and concentrated under reduced pressure. The crude product was purified by column chromatography on silica gel and 16% ethyl acetate in hexane. Compound **14a** was obtained as a viscous red oil in 61% yield (3.15 g). *^1H NMR* ($CDCl_3$/TMS): δ 8.22 (d, J = 8.8 Hz, 2H, aromatic), 7.60 (d, J = 8.8 Hz, 2H, aromatic), 7.51-7.44 (m, 5H aromatic, 1H thienyl), 7.39-7.30 (m, 9H, aromatic, 1H CH=C), 7.21-7.13 (m, 6H aromatic, 1H thienyl), 7.00 (d, J = 13.6 Hz, 1H, C=CH), 4.28 (t, J = 6.0 Hz, 2H, CH_2O), 3.66 (t, J = 6.0 Hz, 2H, NCH_2), 0.92 (s, 9H, $3CH_3$) ppm. *^{13}C NMR* ($CDCl_3$/TMS): δ 146.68, 143.51, 142.37, 141.80, 138.63, 135.47, 134.16, 133.92, 132.71, 131.10, 130.69, 130.57, 129.87, 129.09, 128.94, 128.79, 128.14, 127.84, 127.74, 126.92, 126.69, 126.59, 126.21, 126.03, 124.28, 62.73, 46.40, 26.80, 19.06 ppm.

1-(2'-t-butyl diphenyl sylilethyl)-2-[2'-(stilbene-4'-nitrophenyl)thienyl]-4,5-bis(4'-methoxyphenyl)imidazole (14c)

A 100 mL three neck round bottom flask, previously dried, was charged with 0.649 g (28.2 mmol, 4 equiv) of t-BuOK followed by 0.761 g (7.77 mmol, 1.1 equiv) of 1-triphenylphosphoniomethylbromide-4-nitrobenzene (wittig reagent), 0.950 g (7.06 mmol, 1 equiv) of **9a** and 50 mL of dry methyl dichloride. Then 15-crown-5 (0.07 mL, 79.5 mg, 0.361 mmol. 0.25 equiv.) was added. The reaction mixture was stirred at room temperature for 24 h under a nitrogen atmosphere. Then the solution was poured into a water bath, the organic phase was extracted with CH_2Cl_2, dried over $MgSO_4$ and concentrated under reduced pressure. The crude product was purified by column chromatography on silica gel and 16% ethyl acetate in hexane. **14c** was obtained as a viscous orange-red oil in 60% yield (0.685 g). *^1H NMR* ($CDCl_3$/TMS): δ 8.21 (d, J = 8.8 Hz, 2H, aromatic), 7.58 (d, J = 8.8 Hz, 2H, aromatic), 7.45-7.28 (m, 12H, aromatic, 2H thienyl), 7.12 (d, J = 3.6 Hz, 1H, CH=C), 7.03 (d, J = 8.4 Hz, 2H, aromatic), 6.99 (d, J = 16 Hz, 1H, C=CH), 6.86 (d, J = 8.4 Hz, 2H, aromatic), 6.78 (d, J = 8.8 Hz, 2H, aromatic), 4.24 (t, J = 6.0 Hz, 2H, OCH_2), 3.38 (s, 3H, OCH_3), 3.76 (s, 3H, OCH_3), 3.67 (t, J = 6.0 Hz, 2H, CH_2N), 0.93 (s, 9H, t-butyl) ppm. *^{13}C NMR* ($CDCl_3$/TMS): δ 159.81, 158.28, 146.58, 143.51, 142.09, 141.29, 138.51, 135.44, 134.15, 132.70, 132.37, 129.81, 129.52, 128.79, 127.96, 127.78, 127.04, 126.62, 126.05, 126.02, 124.22, 122.60, 62.76, 55.24, 55.15, 46.24, 26.65, 19.01 ppm.

1-(2'-hydroxyethyl)-2-[2'-(stilbene-4'-nitrophenyl)thienyl]-4,5-bis(phenyl)imidazole (15a)

Chromophore **14a** (3.96 g, 5.41 mmol) was weighed into a one neck round bottom flask and dissolved with 40 mL of dry tetrahydrofuran. To the latter mixture tetrabutylammonium fluoride (8.11 mL, 8.11 mmol, 1.5 equiv of 1.0 M in THF) was added dropwise. The reaction mixture was magnetically stirred for 1.5 h. Then 100 mL of water was poured into the reaction flask. The organic phase was extracted with methyl dichloride (three portion of 100 mL). The crude product was purified by column chromatography using silica gel and 33% ethyl acetate in hexane. After removal of the solvent 1.54 g (58% yield) of **15a** was obtained. *^{1}H NMR* ($CDCl_3$/TMS): δ 8.17 (d, *J*=8.8 Hz, 2H, aromatic), 7.58-7.45 (m, 4H aromatic, 1H, CH=C), 7.38-7.25 (m, 8H aromatic, 1H C=CH), 7.05 (d, *J*=7.2 Hz, 1H, thienyl), 6.98 (d, *J*=7.2 Hz, 1H,thienyl), 3.96 (t, *J*=5.2 Hz, 2H, OCH2), 3.72 (t, *J*=5.2 Hz, 2H, NCH2) ppm. *^{13}C NMR* ($CDCl_3$/TMS): δ 146.6, 143.3, 142.6, 141.9, 138.0, 133.8, 132.9, 131.5, 130.7, 130.4, 129.0, 128.4, 128.1, 126.8, 126.67, 126.66, 126.1, 125.8, 124.2, 61.82, 46.88 ppm.

The same procedure was applied to prepare **1-(2'-hydroxyethyl)-2-[2'-(stilbene-4'-nitrophenyl)thienyl]-4,5-bis(4'-methoxyphenyl)imidazole (15c)**

(50% yield) *^{1}H NMR* ($CDCl_3$/TMS): δ 8.17 (d, *J*=8.7 Hz, 2H, aromatic), 7.53-7.50 (m, 2H aromatic, 1H, C=CH), 7.43 (d, *J*=8.7 Hz, 2H aromatic), 7.33 (d, *J*=16.2 Hz, 1H, thienyl), 6.98 (d, *J*=15.9 Hz, 1H, thienyl), 6.95 (s, 1H, CH=C), 6.84-6.79 (m,

6H, aromatic), 3.94 (t, *J*=4.8 Hz, 2H, OCH2), 3.84 (s, 3H, OCH_3), 3.82 (s, 3H, OCH_3), 3.72 (t, *J*=4.8 Hz, 2H, NCH2) ppm. *^{13}C NMR* ($CDCl_3$/TMS): δ 160.06, 158.65, 146.77, 143.43, 142.42, 141.32, 138.17, 133.41, 132.82, 129.62, 128.83, 127.94, 127.54, 126.89, 126.59, 126.14, 125.93, 124.20, 122.66, 114.46, 113.79, 61.77, 55.25, 46.73 ppm.

1-(1'-oxo-2'-methylethenyl)-2[2'-(stilbene-4'-nitrophenyl)thienyl]-4,5-bis(phenyl) imidazole (16a)

A 50 mL two neck round bottom flask was charged with 0.511 g (1.03 mmol) of **15a** and 15 mL of dry THF. Then methacryloyl chloride (162 mg, 0.15 mL, 1.55 mmol) and triethylamine (314 mg, 0.43 mL, 3.11 mmol) were added. The reaction mixture was refluxed for 16 h under a nitrogen atmosphere, then poured into 100 mL of water. The organic phase was extracted with 3 portions of 100 mL of CH_2Cl_2, dried over $NaSO_4$ and concentrated under reduced pressure. The crude product was purified by column chromatography on silica gel and 33% ethyl acetate in hexane. Compound **16a** was obtained in 62% yield (0.360 g). *Elemental Analysis*: Calculated for $C_{33}H_{27}N_3O_4S$: **C** 70.57, **H** 4.84, **N** 7.48 Found: **C** 70.71, **H** 4.54, **N** 7.38. *^{1}H NMR* ($CDCl_3$/TMS): δ 8.21 (d, *J*=8.8 Hz, 2H, aromatic), 7.59 (d, *J*=8.4 Hz, 2H, aromatic), 7.48 (m, 4H aromatic, 1H thienyl), 7.39 (m, 2H, aromatic), 7.37 (d, *J*=12.4 Hz, 1H, CH=C), 7.20 (m, 4H aromatic, 1H thienyl), 7.01 (d, *J*=11.2 Hz, 1H, C=CH), 5.90 (s, 1H, $C=CH_2$), 5.50 (s, 1H, $C=CH_2$), 4.40 (t, *J*=6.0 Hz, 2H, OCH_2), 4.18 (t, *J*=6.0 Hz, 2H, NCH_2), 1.80 (s, 3H, CH_3) ppm.

^{13}C NMR ($CDCl_3$/TMS): δ 172.49, 167.47, 146.7, 143.4, 142.6, 141.5, 138.8, 135.4, 133.9, 133.4, 131.1, 130.7, 130.3, 129.5, 129.4, 129.3, 129.0, 128.9, 128.2, 127.1, 126.9, 126.8, 126.7, 126.6, 126.5, 125.8, 124.3, 102.45, 82.48, 62.70, 43.44, 18.26 ppm.

1-(1'-oxo-2'-methylethenyl)-2[2'-(stilbene-4'-nitrophenyl)thienyl]-4,5-bis(4'-methoxyphenyl)imidazole (16c)

A 50 mL two neck round bottom flask was charged with 0.100 g (0.181 mmol) of **15c** and 15 mL of dry THF. Then methacryloyl chloride (162 mg, 0.026 mL, 0.271 mmol and triethylamine (54.8 mg, 0.075 mL, 0.542 mmol) were added. The reaction mixture was refluxed for 15 h under a nitrogen atmosphere. The reaction was poured into 100 mL of water. The organic phase was extracted with 3 portion of 100 mL of CH_2Cl_2, dried over $NaSO_4$ and concentrated under reduced pressure. The crude product was purified by column chromatography on silica gel, and 33% ethyl acetate in hexane. Compound **16c** was obtained in 64% yield (0.072 g). *Elemental Analysis*: Calculated for $C_{35}H_{31}N_3O_6S$ + ½$CH_3COOCH_2CH_3$: **C** 66.75, **H** 5.30, **N** 6.31 Found: **C** 66.42, **H** 5.26, **N** 6.12. *^1H NMR* ($CDCl_3$/TMS): δ 8.22 (d, *J*=8.8 Hz, 2H, aromatic), 7.60 (d, *J*=8.8 Hz, 2H, aromatic), 7.44 (d, *J*=6.8 Hz, 2H, aromatic), 7.40 (d, *J*=4 Hz, 1H, thienyl), 7.33 (s, 1H, CH=C), 7.32 (d, *J*=8.4 Hz, 2H, aromatic), 7.16 (d, *J*=4 Hz, 1H, thienyl), 7.02-7.00 (m, 2H, aromatic; 1H, C=CH), 6.77 (d, *J*=8.8 Hz, 2H, aromatic), 5.91 (s, 1H, $=CH_2$), 5.51 (s, 1H, $=CH_2$), 4.38 (t, *J*=6.0 Hz, 2H, OCH_2), 4.19 (t, *J*=6.0 Hz, 2H, CH_2N), 3.88 (s, 3H, OCH_3), 3.75 (s, 3H, OCH_3), 1.82 (s, 3H, CH_3) ppm.

^{13}C NMR ($CDCl_3$/TMS): δ 166.90, 160.15, 158.46, 146.72, 143.40, 142.40, 141.07, 138.71, 135.48, 133.76, 132.47, 129.50, 128.84, 127.96, 126.79, 126.71, 126.58, 126.47, 126.35, 126.27, 125.86, 124.25, 124.25, 122.42, 114.85, 113.59, 62.75, 55.36, 55.19, 43.31, 18.25 ppm.

Copolymerization of 16a and methyl methylacrylate (MMA) (17a)

A dry ampul equipped with a magnetic stirring bar was charged with 359 mg (0.639 mmol) of **16a**, 95.97 mg (0.10 mL, 0.958 mmol, 1.5 equiv) of MMA, 6.3 mg (0.0383 mmol, 0.06 equiv) of 2,2' azobisisobutyronitrile (AIBN), and 8 mL of anhydrous N,N'-dimethylformamide. After all solids were dissolved, the reaction mixture was de-oxygenated using nitrogen and freeze thaw cycles. The ampul was sealed and the red solution was heated to 85 °C for 96 h. The reaction mixture was transferred dropwise into 150 mL of methanol with vigorous stirring. The resulting orange precipitate was filtered. The solid was re-dissolved in THF, re-precipitated in methanol, filtered and washed with 250 mL of methanol. The orange solid was dried under vacuum at 56 °C for 24 h to give 145 mg of **17a**. *^{1}H NMR* ($CDCl_3$/TMS): δ 8.13 (2H, aromatic), 7.47-7.01 (aromatic), 4.35 (2H, CH_2O), 3.94 (2H, NCH_2), 3.54-2.97 (9H, $3OCH_3$), 1.82 (12H, $4CH_3$), 1.29 (2H, CH_2), 1.03-0.71 (6H, $3CH_2$) ppm. *^{13}C NMR* ($CDCl_3$/TMS): δ 177.84, 146.68, 143.23, 142.49, 141.43, 139.08, 133.83, 131.15, 130.18, 129.45, 128.20, 126.91, 124.19, 54.09, 51.97, 44.60, 18.79, 16.44 ppm. *FT-IR* (KBr): 3058, 2994, 2946, 2838, 2450, 5357, 2333, 2240, 1956, 1731, 1590, 1516, 1340, 1145 cm^{-1}.

Copolymerization of 16c and methyl methylacrylate (MMA) (17c)

A dry ampul equipped with a magnetic stirring bar was charged with 608 mg (0.978 mmol) of **16c**, 146 mg (0.16 mL, 1.47 mmol, 1.5 equiv) of MMA, 9.63 mg (0.0587 mmol, 0.06 equiv) of 2,2' azobisisobutyronitrile (AIBN), and 10 mL of anhydrous N,N'-dimethylformamide. After all solids were dissolved, the reaction mixture was de-oxygenated using nitrogen and freeze thaw cycles. The ampul was sealed and the red solution was heated to 75 °C for 72 h. The reaction was transferred dropwise into 300 mL of methanol with vigorous stirring. The orange precipitated was filtered. The solid was re-dissolved in THF, re-precipitated in methanol, filtered and washed with 250 mL of methanol. The orange solid was dried under vacuum at 56 °C for 24 h to give 385 mg of **17c**.

^1H NMR ($CDCl_3$/TMS): δ 8.24 (d, *J*=10.0 Hz, 2H, aromatic), 7.62 (d, *J*=10.0 Hz, 2H, aromatic), 7.47-6.82 (m, 10H, aromatic), 6.79 (d, *J*=8.0 Hz, 2H, aromatic), 4.39 (t, *J*=6.0 Hz, 2H, OCH_2), 4.19 (t, 6.0 Hz, 2H, CH_2N), 3.89 (s, 3H, OCH_3), 3.77 (s, 3H, OCH_3), 3.59-3.53 (OCH_3 from MMA unit), 1.82 (CH_3), 1.63-1.25 (CH_2), 1.00-0.68 (CH_2 from MMA unit) ppm.

FT-IR (KBr): 3058.2, 2994.8, 2838.6, 2448.2, 2228.6, 1965.0, 1735.7, 1589.3, 1516.1, 1345.2, 1150.0 cm^{-1}.

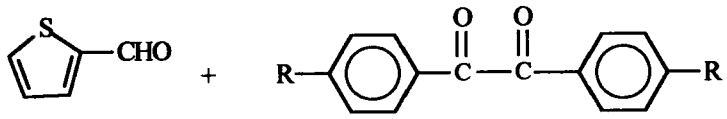

1 2

Acetic Acid | NH_4OAC

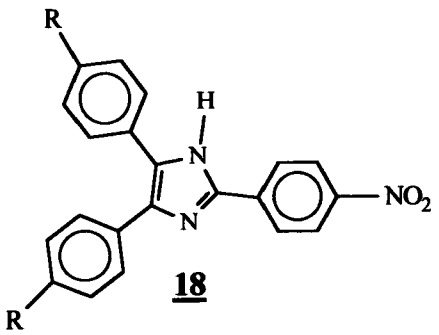

18

	a	b	c	d
R=	H,	CH_3,	OCH_3,	$N(CH_3)_2$
Yield=	75%	80%	80%	60%

DMA | CH_3I / K_2CO_3

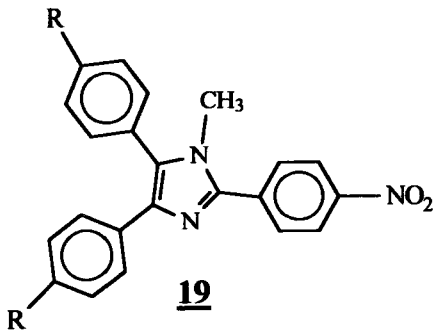

19

	a	b	c	d
R=	H,	CH_3,	OCH_3,	$N(CH_3)_2$
Yield=	72%	87%	83%	75%

2-(4'-nitrophenyl)-4,5-bis(phenyl)imidazole (18a)

Benzil (**2a**) (0.500 g, 2.38 mmol) was dissolved in glacial acetic acid (30 mL). Then 4-nitrobenzaldehyde (359 mg, 2.37 mmol) and ammonium acetate (1.83 g, 23.7 mmol) were added. This reaction mixture was refluxed for 15 h under a nitrogen atmosphere. The reaction mixture was then cooled to ambient temperature and poured into a water-ice bath. The resulting precipitate was filtered, washed with water and dried overnight under ambient air, giving 0.608 g (75% yield) of pure product **18a**. *^1H NMR* ($CDCl_3$/DMSO/TMS): δ 8.25 (s, 4H, aromatic), 7.57 (d, *J* = 6.8 Hz, 4H, aromatic), 7.30 (m, 6H, aromatic) ppm. *^{13}C NMR* ($CDCl_3$/DMSO/TMS): δ 173.8, 146.9, 144.0, 136.4, 128.7, 128.5, 128.4, 128.2, 127.6, 125.9, 124.1 ppm.

2-(4'-nitrophenyl)-4,5-bis(4'-methoxyphenyl)imidazole (18c)

4,4'-Dimethoxy benzil (**2c**) (1g, 3.69 mmol) was dissolved in glacial acetic acid (50 mL). Then 4-nitrobenzaldehyde (0.557 g, 3.69 mmol) and ammonium acetate (2.84 g, 36.9 mmol) were added. This reaction mixture was refluxed for 15 h under a nitrogen atmosphere. The reaction mixture was then cooled to ambient temperature and poured into a water-ice bath. The resulting precipitate was filtered, washed with water and dried overnight under ambient air, giving 1.17 g (80% yield) of pure product **18c**. (*m.p.* 220.5 °C from DSC) (decomposition temperature: 350.4 °C) (Note: this compound was reported in Nonlinear Optical Properties of Organic Molecules and Crystals; Academic Press: New York, **1987**; 1, 227)

^1H NMR ($CDCl_3$/DMSO/TMS): δ 8.17 (d, *J*=2.8 Hz, 4H, aromatic), 7.46 (d, *J*=8.4 Hz, 4H, aromatic), 6.86 (d, *J* = 8.4 Hz, 4H, aromatic), 3.80 (s, 6H, OCH_3) ppm. *^{13}C NMR* ($CDCl_3$/DMSO/TMS): δ 159.06, 146.75, 143.43, 136.24, 129.59, 129.40, 125.66, 124.05, 114.12, 113.92, 55.30, 55.27 ppm.

2-(4'-nitrophenyl)-4,5-bis(4'-dimethylaminophenyl)imidazole (18d)

4,4'-Dimethylamino benzil (**2d**) (1g, 3.37 mmol) was dissolved in glacial acetic acid (50 mL). Then 4-nitrobenzaldehyde (0.510 g, 3.37 mmol) and ammonium acetate (2.60 g, 33.7 mmol) were added. This reaction mixture was refluxed for 15 h under a nitrogen atmosphere. The reaction mixture was then cooled to ambient temperature and poured into a water-ice bath. The resulting precipitate was filtered, washed with water and dried overnight under ambient air giving 0.864 g (60% yield) of **18d**. (*m.p.* 111.6 °C) (decomposition temperature: 252.8 °C). *^1H NMR* ($CDCl_3$/TMS): δ 8.09 (d, *J* = 8.8 Hz, 2H, aromatic), 7.88 (d, *J* = 8.8 Hz, 2H, aromatic), 7.40 (d, *J* = 8.0 Hz, 4H, aromatic), 6.64 (d, *J* = 8.8 Hz, 4H, aromatic), 2.93 (s, 12H, $N(CH_3)_2$) ppm. *^{13}C NMR* ($CDCl_3$/TMS): δ 149.8, 146.6, 142.7, 135.9, 128.7, 125.2, 124.1, 112.3, 40.42, 40.40 ppm.

1-methyl-2-(4'-nitrophenyl)-4,5-bis(methylphenyl)imidazole (19b)

A 100 mL three neck round-bottom flask equipped with a magnetic stirrer and a condenser was charged with potassium carbonate (280 mg, 2.01 mmol) then dried with an open flame and vacuum. Once at room temperature the reaction flask

containing the potassium carbonate was flushed with nitrogen. Compound **18b** (373 mg, 1.00 mmol) and DMA (30 mL) were added followed by iodomethane (0.062 mL, 143 mg, 1.00 mmol). The reaction mixture was stirred for 15 h at 40-50 °C under a nitrogen atmosphere. Once at room temperature the mixture was poured into a water-ice bath. The resulting precipitate was filtered and dried overnight in ambient air. The crude product was purified by column chromatography using silica gel and 20% ethyl acetate in hexane. After solvent removal 0.335 g (87% yield) of **19b** was obtained. *^1H NMR* ($CDCl_3$/TMS): δ 8.34 (d, J = 8.8 Hz, 2H, aromatic), 7.97 (d, J = 8.4 Hz, 2H, aromatic), 7.44 (d, J = 8.4 Hz, 2H, aromatic), 7.28 (s, 4H, aromatic), 7.05 (d, J = 8.0 Hz, 2H, aromatic), 3.56 (s, 3H, NCH_3), 2.44 (s, 3H, CH_3), 2.29 (s, 3H, CH_3) ppm. *^{13}C NMR* ($CDCl_3$/TMS): δ 147.38, 145.14, 138.94, 138.92, 137.14, 136.39, 131.90, 131.34, 130.67, 129.92, 129.28, 128.96, 127.51, 126.84, 123.92, 33.58, 21.46, 21.22 ppm.

1-methyl-2-(4'-nitrophenyl)-4,5-bis(methoxyphenyl)imidazole (19c)

A 50 mL three neck round-bottom flask equipped with a magnetic stirrer and a condenser was charged with potassium carbonate (69 mg, 0.499 mmol) then dried with an open flame and vacuum. Once at room temperature the reaction flask containing the potassium carbonate was flushed with nitrogen. Compound **18c** (100 mg, 0.249 mmol) and DMA (20 mL) were added followed by iodomethane (0.015 mL, 35.4 mg, 0.249 mmol). The reaction mixture was stirred for 15 h at 40-50 °C under a nitrogen atmosphere. Once at room temperature the mixture was poured

into a water-ice bath. The resulting precipitate was filtered and dried overnight under ambient air. The crude product was purified by column chromatography using silica gel and 37% ethyl acetate in hexane. After solvent removal 0.085 g (83% yield) of **19c** was obtained. (*m.p.* 122.8 °C) (decomposition temperature: 360.3 °C) *^{1}H NMR* ($CDCl_3$/TMS): δ 8.34 (d, *J* = 7.2Hz, 2H, aromatic), 7.97 (d, *J* = 7.2 Hz, 2H, aromatic), 7.48 (d, *J* = 5.2 Hz, 2H, aromatic), 7.32 (d, *J* = 7.2 Hz, 2H, aromatic), 7.02 (d, *J* = 7.2Hz, 2H, aromatic), 6.79 (d, *J* = 7.2Hz, 2H, aromatic), 3.88 (s, 3H, OCH_3), 3.77 (s, 3H, OCH_3), 3.56 (s, 3H, NCH_3) ppm. *^{13}C NMR* ($CDCl_3$/TMS): δ 160.44, 158.92, 147.76, 145.31, 139.14, 137.56, 132.50, 131.51, 129.54, 128.46, 127.36, 124.26, 123.03, 115.04, 114.06, 55.37, 55.18, 34.18 ppm.

1-methyl-2-(4'-nitrophenyl)-4,5-bis(dimethylaminophenyl)imidazole (19d)

A 50 mL three neck round-bottom flask equipped with a magnetic stirrer and a condenser was charged with potassium carbonate (130 mg, 2 equiv) then dried with an open flame and vacuum. Once at room temperature the reaction flask containing the potassium carbonate was flushed with nitrogen. Compound **18d** (200 mg, 0.468 mmol) and DMA (30 mL) were added followed by iodomethane (0.029 mL, 66.5 mg, 0.468 mmol). The reaction mixture was stirred for 15 h at 40-50 °C under a nitrogen atmosphere. Once at room temperature the mixture was poured into a water-ice bath. The resulting precipitate was filtered and dried overnight in ambient air. The crude product was purified by column chromatography using silica gel and 37% ethyl acetate in hexane. After solvent removal 0.155 g (75% yield) of **19d**

was obtained. (*m.p.* 202.2 °C) (decomposition temperature: 241.9 °C)

^1H NMR ($CDCl_3$/TMS): δ 8.34 (d, *J* = 7.2 Hz, 2H aromatic), 7.99 (d, *J* = 7.2 Hz, 2H aromatic), 7.50 (d, *J* = 7.2 Hz, 2H aromatic), 7.26 (d, *J* = 5.2 Hz, 2H aromatic), 6.81 (d, *J* = 7.2 Hz, 2H aromatic), 6.65 (d, *J* = 7.2 Hz, 2H aromatic), 3.57 (s, 3H, NCH_3), 3.05 (s, 6H, $N(CH_3)_2$), 2.93 (s, 6H, $N(CH_3)_2$) ppm. *^{13}C NMR* ($CDCl_3$ / TMS): δ 150.41, 149.31, 147.13, 144.46, 139.05, 137.56, 131.73, 131.52, 129.01, 127.64, 123.85, 123.18, 117.97, 112.43, 112.38, 40.57, 40.31, 33.48 ppm.

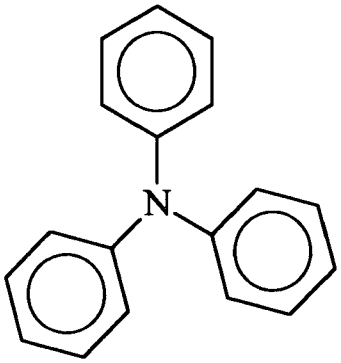

20

$POCl_3$ | DMF / 95-100 °C

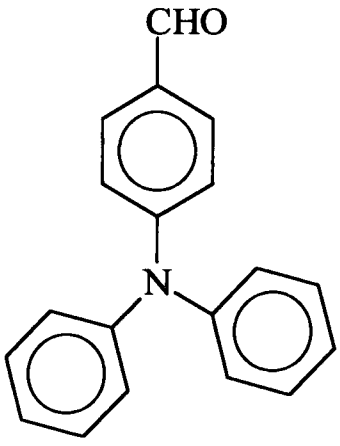

21

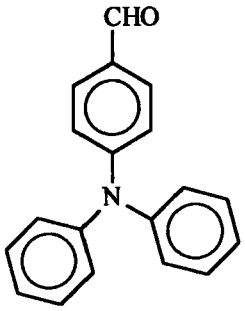

21

+

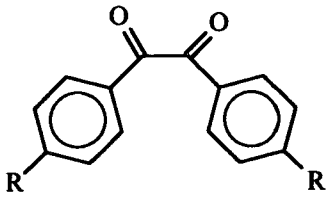

2

Acetic Acid | NH_4OAC | 15 h / reflux

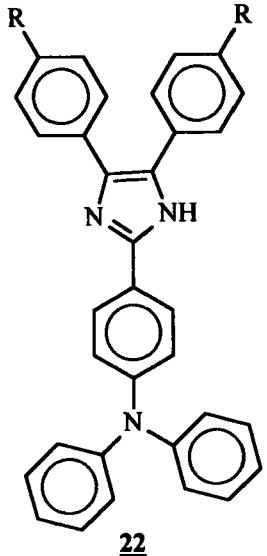

22

	a	b	c	d	e
R=	H,	CH_3,	OCH_3,	$N(CH_3)_2$	Br
Yield=	85%	89%	85%	72%	83%

DMA | CH_3I / K_2CO_3 | 15 h / 50°C

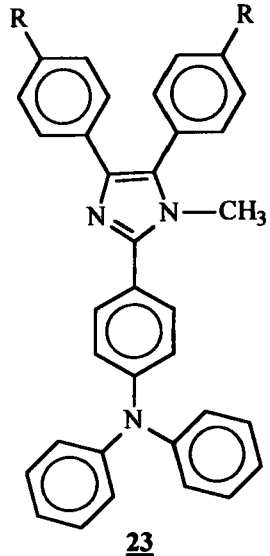

23

	e
R=	Br
Yield=	72%

4-formyltriphenylamine (21)

(G. Li, X. R. Bu, J. Santos, E. A. Mintz, *SYNLETT* **1997**, 1275-1276)

To a mixture of triphenyl amine **20** (3 g, 12.23 mmol) and DMF (40 mL) at 0°C, phosphorus oxychloride ($POCl_3$) (1.2 mL, 12.87 mmol, 1.05 equiv.) was added dropwise. The resulting mixture was heated at 95-100 °C for 20 h under a nitrogen atmosphere. The mixture was cooled to room temperature, poured into an ice-water bath (150 mL), and neutralized with 4 M NaOH solution. The resulting precipitate was filtered, washed with water, and dried under ambient air. Purification by column chromatography on silica gel and 33% ethyl acetate in hexane as eluent afforded 3.14 g (94% yield) of monoaldehyde **21**. (*m.p.* 129-131 °C) Elemental Analysis: Calculated for $C_{19}H_{15}NO$: **C** 83.49, **H** 5.53, **N** 5.13

Found: **C** 83.49, **H** 5.57, **N** 5.15. *^1H NMR* ($CDCl_3$/TMS): δ 9.82 (s, 1H, CHO), 7.70 (d, J = 8.7 Hz, 2H, aromatic), 7.36 (t, J = 8.2 Hz, 4H, aromatic), 7.21-7.17 (m, 6H, aromatic), 7.04 (d, J = 8.7 Hz, 2H, aromatic) ppm. *^{13}C NMR* ($CDCl_3$/TMS): δ 189.94, 153.32, 146.58, 132.45, 130.89, 129.37, 127.51, 126.25, 120.54 ppm. FT-IR: (KBr) 1690, 1591, 1492, 1335, 1308, 1229, 1157 cm^{-1}.

2-(4'-triphenylamine)-4,5-bis(phenyl)imidazole (22a)

A 250 mL three neck round bottom flask was charged with benzil (1.54 g, 7.29 mmol) which was dissolved in glacial acetic acid (75 mL). 4-Formyltriphenylamine (**21**) (2 g, 7.29 mmol) and ammonium acetate (5.62 g, 72.9 mmol) were added. The reaction mixture was refluxed for 15 h. The reaction mixture was cooled to ambient

temperature. The mixture was poured into a water-ice bath. The resulting precipitate was filtered, washed with water and dried overnight under ambient air. The crude product was purified by re-crystallization from CH_2Cl_2 resulting in 2.87 g (85% yield) of **22a**. *Elemental Analysis*: Calculated for $C_{33}H_{25}N_3$ + 1/10 CH_2Cl_2: **C** 84.21, **H** 5.38, **N** 8.90 Found: **C** 84.65, **H** 5.53, **N** 8.82.

2-(4'-triphenylamine)-4,5-bis(4'-methylphenyl)imidazole (22b), 2-(4'-triphenylamine)-4, 5-bis(4'-methoxyphenyl) imidazole (22c), 2-(4'-triphenylamine)-4,5-bis(4'-dimethylaminophenyl) amidazole (22d), and **2-(4'-triphenylamine)-4,5-bis(4'-bromophenyl) amidazole (22e)** were prepared in a similar manner as **22a**.

22b: The crude product was purified by crystallization from CH_2Cl_2 resulting in 89% yield. (m.p. 246-247 °C) *Elemental Analysis*: Calculated for $C_{35}H_{29}N_3$: **C** 85.51, **H** 5.95, **N** 8.55 Found: **C** 85.38, **H** 6.05, **N** 8.29. *^{1}H NMR* (DMSO-d_6/TMS): δ 7.96 (d, J = 8.4 Hz, 2H, aromatic), 7.43 (d, J = 8.0 Hz, 2H, aromatic), 7.37-7.31 (m, 6H, aromatic), 7.23 (d, J = 8.0 Hz, 2H, aromatic), 7.10-7.00 (m, 10H, aromatic), 2.34 (s, 3H, CH_3), 2.28 (s, 3H, CH_3) ppm. *^{13}C NMR* (DMSO-d_6/TMS): δ 147.99, 147.82, 145.99, 137.71, 137.60, 136.27, 133.39, 130.68, 130.48, 130.20, 130.01, 129.57, 129.19, 128.99, 128.32, 127.83, 127.23, 125.48, 125.29, 125.10, 124.21, 123.61, 21.69, 21.62 ppm.

22c: The crude product was purified by re-crystallization from methanol resulting in 85% yield. *Elemental Analysis:* Calculated for $C_{35}H_{29}N_3O_2$ + CH_3OH: **C** 77.82, **H**

5.99, **N** 7.56 Found: **C** 77.59, **H** 6.02, **N** 7.65.

22d: The crude product was purified by re-crystallization from CH_2Cl_2 then washed with methanol to give 72% yield. *Elemental Analysis*: Calculated for $C_{37}H_{35}N_5$: **C** 80.84, **H** 6.42, **N** 12.74 Found: **C** 80.93, **H** 6.40, **N** 12.71. *^1H NMR* (DMSO-d_6/TMS): δ 7.95 (d, *J* = 8.0 Hz, 2H, aromatic), 7.36 (m, 10H, aromatic), 7.05 (m, 6H, aromatic), 6.79 (d, *J* = 8.0 Hz, 2H, aromatic), 6.63 (d, *J* = 8.0 Hz, 2H, aromatic), 2.95 (s, 6H, $N(CH_3)_2$), 2.89 (s, 6H, $N(CH_3)_2$) ppm.

22e: The crude product was purified by re-crystallization from 9% benzene in $CHCl_3$ then washed with methanol to result in 83% yield. *Elemental Analysis*: Calculated for $C_{33}H_{23}N_3Br_2$: **C** 63.79, **H** 3.73, **N** 6.76 Found: **C** 63.93, **H** 3.83, **N** 6.73. *^1H NMR* (DMSO-d_6/TMS): δ 12.46 (s, 1H, NH), 7.95 (d, *J* = 12.0 Hz, 2H, aromatic), 7.64 (d, *J* = 8.0 Hz, 2H, aromatic), 7.46 (m, 6H, aromatic), 7.34 (m, 4H, aromatic), 7.50 (m, 8H, aromatic) ppm. *^{13}C NMR* (DMSO-d_6/TMS): δ 148.20, 147.51, 146.32, 135.37, 135.01, 133.07, 132.15, 131.97, 131.51, 131.08, 131.00, 128.11, 127.51, 126.07, 125.00, 124.87, 123.91, 122.67, 121.96 ppm.

1-methyl-2-(4'-triphenylamine)-4,5-bis(4'-bromophenyl)imidazole (23e)

Potassium carbonate (650 mg, 4.70 mmol, 2 equiv) was added to a three neck round bottom flask (previously dried in an oven) equipped with a magnetic stirrer and condenser. The flask and the K_2CO_3 were dried with an open flame under vacuum,

then flushed with nitrogen upon cooling. Compound **22e** (1.46 g, 2.35 mmol) and 50 mL of N,N'-dimethylacetamide (DMA) were added followed by the dropwise addition of iodomethane (500 mg, 0.22 mL, 3.52 mmol, 1.5 equiv). The mixture was stirred for 15 h at 40-50 °C under nitrogen atmosphere and then poured into a water-ice bath. The resulting precipitate was filtered and dried overnight under ambient air. The crude product was purified by column chromatography on silica gel and 23% of ethyl acetate in hexane resulting in 1.07 g (≥76% yield) of **23e**. (Alternatively **23e** can be purified by re-crystallization from CH_2Cl_2) *Elemental Analysis*: Calculated for $C_{34}H_{25}N_3Br_2$: **C** 61.13, **H** 3.87, **N** 6.20 Found: **C** 61.27, **H** 3.89, **N** 6.19. *^1H NMR* ($CDCl_3$/TMS): δ 7.65 (d, J = 8.0 Hz, 2H, aromatic), 7.58 (d, J = 8.4 Hz, 2H, aromatic), 7.43 (d, J = 8.4 Hz, 2H, aromatic), 7.37 (d, J = 8.8 Hz, 2H, aromatic), 7.32-7.27 (m, 6H, aromatic), 7.17 (d, J = 7.6 Hz, 6H, aromatic), 7.10-7.07 (m, 2H, aromatic), 3.52 (s, 3H, CH_3) ppm. *^{13}C NMR* ($CDCl_3$/TMS): δ 149.04, 148.87, 147.71, 137.32, 133.79, 132.87, 132.71, 131.66, 130.34, 130.22, 129.98, 129.78129.50, 128.89, 125.53, 125.33, 124.15, 123.90, 123.48, 123.07, 120.76, 33.61 ppm.

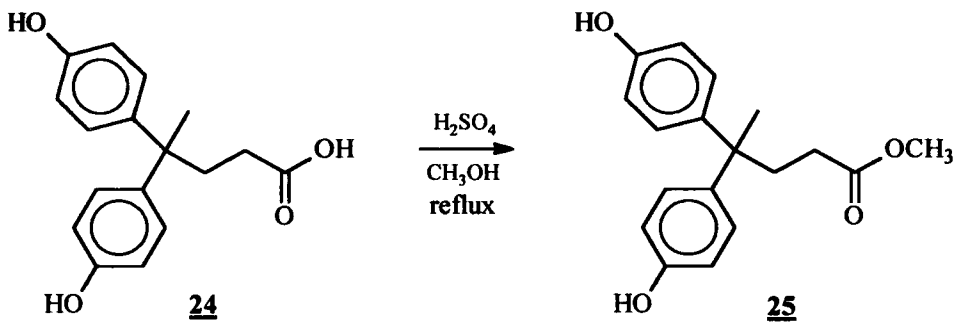
HO
OH
O
HO
H_2SO_4
CH_3OH
reflux
HO
OCH_3
O
HO

24 25


$LiAlH_4$
THF / reflux

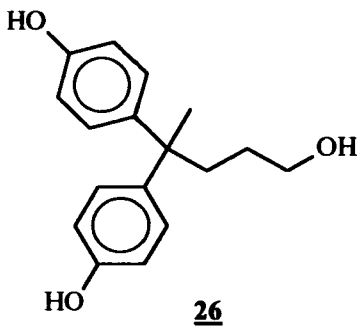
HO
OH
HO

26

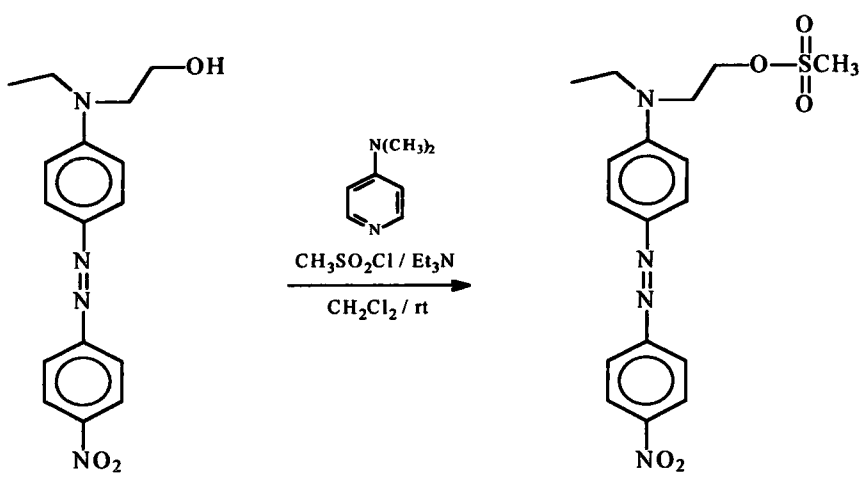
OH
N
N
N
NO_2
$N(CH_3)_2$
N
CH_3SO_2Cl / Et_3N
CH_2Cl_2 / rt
O
O—SCH_3
O
N
N
N
NO_2

27 28

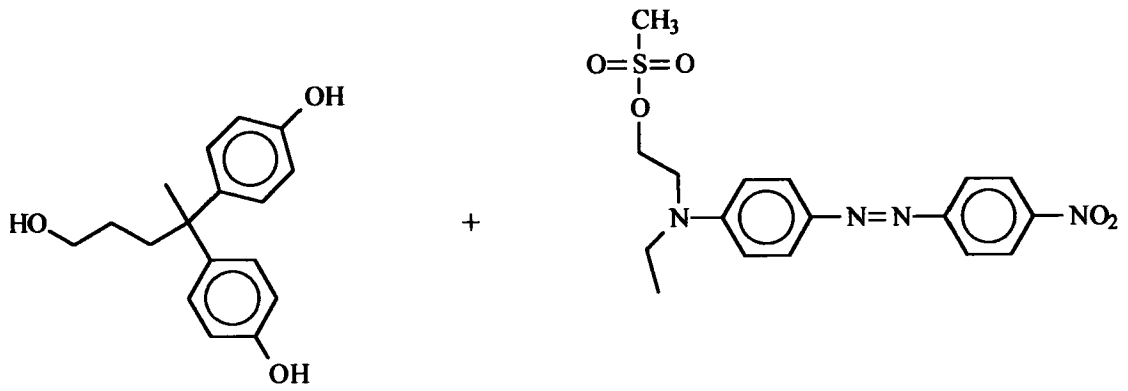

26 **28**

K_2CO_3 / 18-crown-6 | Acetone / reflux

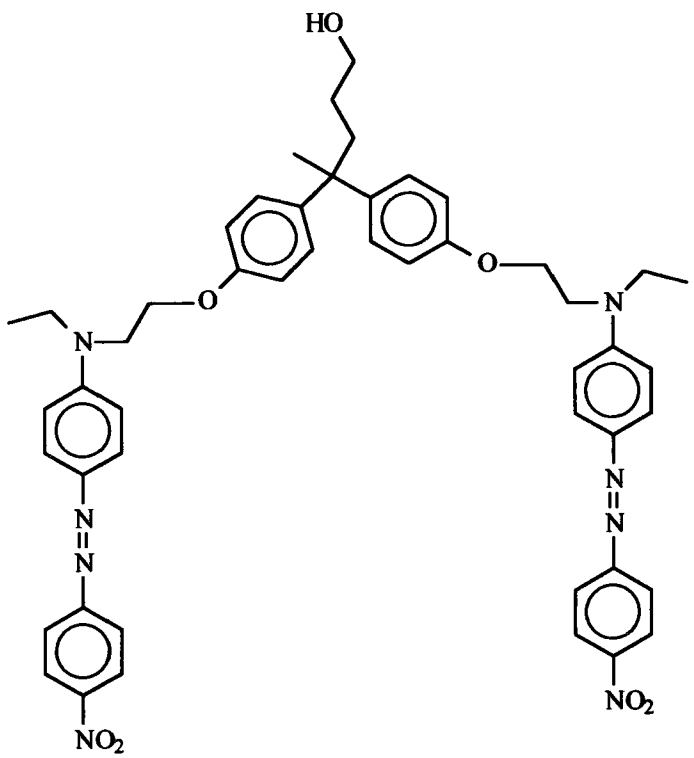

29

methyl-4, 4-bis(4'-hydroxyphenyl)valerate (25)

(K-Y Chen, C. B. Gorman, *J. Org. Chem.* **1996**, *61*, 9229-9235)

A 250 mL three neck round bottom flask equipped with a magnetic stirring bar and a condenser was charged with 4,4-bis(4'-hydroxyphenyl)valeric acid (**24**) (5 g, 17.46 mmol) and 50 mL of methanol (previously dried under Mg). Then H_2SO_4 (0.25 mL, 4.85 mmol) was added dropwise and the reaction mixture was refluxed for 12 h under a nitrogen atmosphere. The reaction mixture was cooled at room temperature, quenched with water and extracted with ethyl ether. The organic phase was dried over magnesium sulfate, filtered and concentrated under reduced pressure to give 4.82 g (92% yield) of **25** as a yellow oil.

4,4-bis(4'-hydroxyphenyl)pentanol (26)

(K-Y Chen, C. B. Gorman, *J. Org. Chem.* **1996**, *61*, 9229-9235)

A 250 mL three neck round bottom flask equipped with a magnetic stirring bar and a condenser was charged with lithium aluminum hydride ($LiAlH_4$) and 40 mL of dry THF. This heterogeneous mixture was cooled to 0 °C followed by the dropwise addition of **25** (4.81 g, 16.03 mmol). Once the addition was completed, the mixture was warmed to room temperature and then refluxed for 2 h. The reaction mixture was cooled to 0 °C and then a saturated ammonium chloride solution (NH_4Cl, 10 mL) was added dropwise. This mixture was filtered and the filtered cake was washed with ethyl ether (500 mL). The collected organic phase was extracted with brine (H_2O + NaCl), dried over $MgSO_4$, filtered and concentrated under reduced

pressure. The crude product was purified by flash column chromatography using silica gel and ethyl acetate as eluent. After removal of the solvent 3.91 g (90% yield) of **26** was obtained.

Mesylation of disperse red-1 (28)

A 50 mL three neck round bottom flask equipped with a magnetic stirring bar was charged with disperse red-1 (**27**) (2 g, 6.36 mmol, 1 equiv) and 18 mL of dry CH_2Cl_2. This mixture was cooled to 0 °C follow by the addition of methanesulfonyl chloride (MsCl, 0.98 mL, 12.72 mmol, 2 equiv), triethylamine (Et_3N, 2.66 mL, 19.08 mmol, 3equiv) and 4-(dimethylamino)pyridine (15.5 mg, 0.127 mmol, 0.02 equiv). The ice bath was removed and the reaction mixture was stirred at room temperature for 21 h under a nitrogen atmosphere. The reaction mixture was quenched with water, the organic phase was extracted with CH_2Cl_2, dried over $MgSO_4$, filtered and concentrated under reduced pressure. The crude product was purified by column chromatography on silica gel and hexane and ethyl acetate (1:1) as eluent. After removal of the solvent 1.5 g (60% yield) of **28** (cis and trans isomer) was obtained. *^1H NMR* ($CDCl_3$/TMS): δ 8.33 (d, *J*=4.0 Hz, 2H, aromatic), 7.94 (d, *J*=5.2 Hz, 2H, aromatic), 6.80 (d, *J*=4 Hz, 2H, aromatic), 4.42 (t, *J*=6.0 Hz, 2H, OCH_2), 3.83 (t, *J*=6.0 Hz, 2H, NCH_2-CO), 3.57 (q, *J*=7.2 Hz, 2H, NCH_2-C), 3.49 (q, isomer, NCH_2-C), 3.14 (s, isomer, SCH_3), 3.01 (s, 3H, SCH_3), 1.27 (t, *J*=7.2 Hz, 3H, CH_3), 1.22 (t, isomer, CH_3) ppm. *^{13}C NMR* ($CDCl_3$ / TMS): δ 156.41, 151.10, 148.49, 144.57, 126.63, 125.07, 123.12, 111.96, 66.29, 49.76, 46.39, 38.04, 32.40, 15.14, 12.69 ppm.

Dendritic alcohol 29

A 50 mL three neck round bottom flask equipped with a magnetic stirring bar and a condenser was charged with K_2CO_3 (1.02 g, 7.41 mmol, 4 equiv) and dried with an open flame. Then mesylated disperse red-1 (**28**) (1.52 g, 3.89 mmol, 2.1 equiv), 18 mL of dry acetone, **26** (0.5 g, 1.85 mmol, 1 equiv), and 18-crown-6 (97.9 mg, 0.37 mmol, 0.2 equiv) were added. The reaction mixture was refluxed for 48 h under a nitrogen atmosphere. After cooling to room temperature the solution was evaporated to dryness under reduced pressure and then partitionated with CH_2Cl_2 and 15% water. The aqueous layer was extracted with CH_2Cl_2 (3x). The combined organic layers were dried with $MgSO_4$ and evaporated to dryness under reduced pressure. The crude product was purified by column chromatography using silica gel, and the following eluent: first with hexane:ethyl acetate (1:1), then with ethyl acetate and finally with CH_2Cl_2. Compound **29** was obtained in 50% yield (0.827 g). *Elemental Analysis*: Calculated for $C_{49}H_{51}N_8O_7$ + ½$CH_3COOCH_2CH_3$: **C** 67.45, **H** 6.10, **N** 12.34 Found: **C** 67.94, **H** 6.45, **N** 11.51. *^1H NMR* ($CDCl_3$/TMS): δ 8.32 (d, *J*=8.8 Hz, 4H, aromatic), 7.91-7.87 (m, 8H, aromatic), 7.09 (d, *J*=8.8 Hz, 4H, aromatic), 6.80-6.76 (m, 8H, aromatic), 4.15 (t, *J*= 5.6 Hz, 4H, $2CH_2O$-Ar), 3.82 (t, *J*=5.6 Hz, 4H, 2N-CH_2-C-OAr), 3.59 (m, 6H, OCH_2, $2NCH_2$-C), 2.08 (m, 2H, CH_2), 1.56 (s, 3H, CH_3), 1.32 (m, 2H, CH_2), 1.27 (s, 6H, $2CH_3$) ppm. UV-Vis ($CHCl_3$), λ (ε, $M^{-1}cm^{-1}$): 284 (43667), 479 (108798) nm.

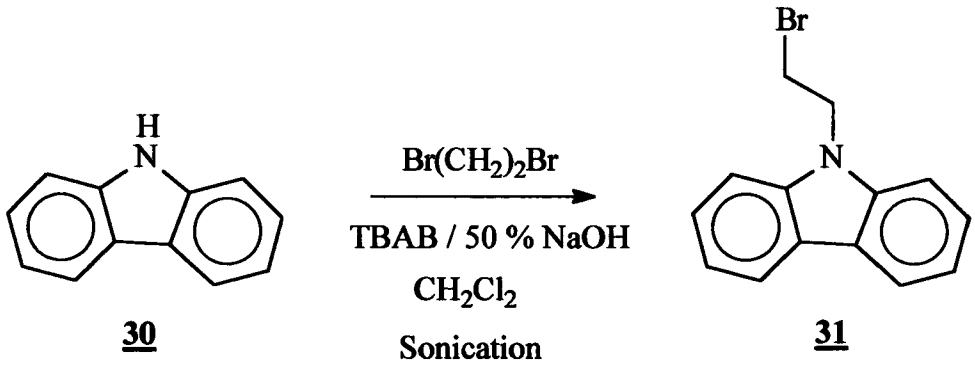

30 31

N-bromo ethyl carbazole (31)

A 50 mL two neck round bottom flask was charged with carbazole (**30**) (1.0 g, 5.98 mmol) and 30 mL of CH_2Cl_2. After most carbazole solids was dissolved 15 mL of 50% NaOH was added to the reaction flask. Then this mixture was cooled to 0 °C followed by the addition of tetrabutyl ammonium bromide (TBAB) (17.94 mmol, 1.54 mL, 3 equiv) and 1,2-bromoethane. Sonication was applied while the temperature was kept between 0-10 °C (using ice) for 5 h. The reaction mixture was then poured into a water bath and stirred. The organic phase was extracted with CH_2Cl_2 and concentrated under reduced pressure resulting in a pale yellow solid. The crude product was purified by column chromatography on silica gel and hexane. Compound **31** was obtained in 10% yield (0.164 g) as a white solid. *^1H NMR* ($CDCl_3$/TMS): δ 8.10 (d, J = 8.0 Hz, 2H, aromatic), 7.50 -7.42 (m, 4H, aromatic), 7.28-7.24 (m, 2H, aromatic), 4.71 (t, J = 7.6 Hz, 2H, CH_2Br), 3.67 (t, J = 7.6 Hz, 2H, NCH_2) ppm.

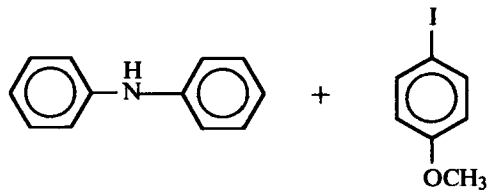

A **B**

15-crown-5 | 1,2-dichlorobenzene
K_2CO_3 / Cu

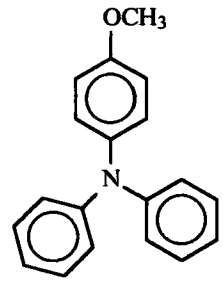

C

$POCl_3$ | DMF / 95-100 °C

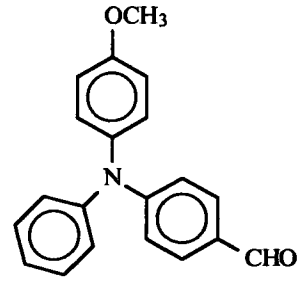

32

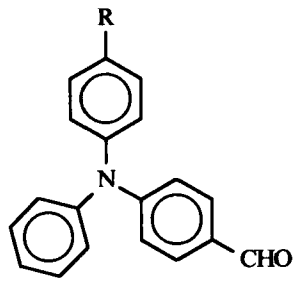

	21	32
R =	H,	OCH_3

Isophorone | t-BuOK / t-BuOH, reflux

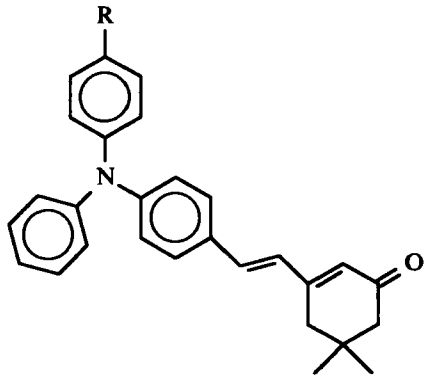

	a	b
R =	H,	OCH_3
	45 %,	43 %

34

Et_3N, $CH_2(CN)_2$ | $CHCl_3$

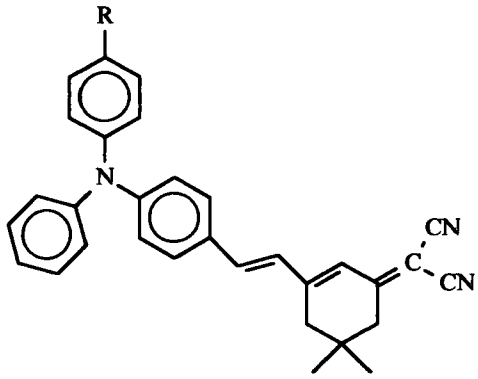

	a	b
R =	H,	OCH_3
	40 %,	41 %

35

4-methoxy triphenylamine (C)

A 1000 mL three neck round bottom flask was charged with K_2CO_3 (65.33 g, 472.72 mmol, 4 equiv) and dried with an open flame. Once at room temperature o-dichlorobenzene (250 mL), Cu (15.77 g, 248.17 mmol, 2.1 equiv), 15-crown-5 (1.5 mL), diphenylamine (20 g, 118.18 mmol, 1 equiv), and 4-iodoanisole (41.49 g, 177.3 mmol, 1.5 equiv) were added. This mixture was refluxed for 30 h. Once at room temperature the reaction mixture was poured into a 500 mL one neck round bottom flask. The reaction flask was washed with ethyl acetate. The latter was removed by simple distillation while o-dichlorobenzene was removed by vacuum distillation. A brown solid was obtained as crude product, which was crystallized from $CHCl_3$ and hexane to give 60% yield (19.5 g) of C. *^1H NMR* ($CDCl_3$/TMS): δ 7.25-7.20 (m, 4H, aromatic), 7.10-7.03 (m, 6H, aromatic), 6.97-6.94 (m, 2H, aromatic), 6.87 (d, J = 8.8 Hz, 2H, aromatic), 3.82 (s, 3H, OCH_3) ppm. *^{13}C NMR* ($CDCl_3$/TMS): δ 155.66, 148.60, 141.98, 129.43, 127.67, 123.29, 122.22, 115.17, 55.86 ppm.

4-methoxy-4-formyl triphenylamine (32)

A 250 mL three neck round bottom flask (previously dried) was charged with 4-methoxy triphenylamine (C) (10 g, 36.32 mmol, 1 equiv) and 100 mL of anhydrous DMF. This solution was cooled to 0 °C. Then $POCl_3$ (3.59 mL, 5.90 g, 38.49 mmol, 1.06 equiv) was added dropwise during 10 minutes. Once the addition is completed, the reaction mixture was stirred for 10 minutes at 0 °C. The mixture

was allowed to warm to room temperature and then heated to 100 °C for 21 h under a nitrogen atmosphere. Upon cooling the reaction mixture was poured into a water-ice bath. This solution was carefully neutralized with 4 M NaOH solution. The resulting precipitate was filtered, washed with water and dried under ambient air. The crude product was purified by column chromatography on silica gel and 16% ethyl acetate in hexane affording 9.91 g (90% yield) of **37** after removal of the solvent.

Condensation of 21 with isophorone to give 34a

A previously dried 25 mL one neck round bottom flask equipped with a magnetic stirrer and a condenser was charged with aldehyde **21** (300 mg, 1.1 mmol, 1 equiv) and 5 mL of fresh distilled t-BuOH. Then t-BuOK (271 mg, 2.41 mmol, 2.2 equiv) and isophorone (0.16 mL, 152 mg, 1 equiv) were added. This mixture was refluxed for 30 minutes under a nitrogen atmosphere. The reaction was quenched with 25 mL of water. The resulting precipitate was filtered, washed with 200 mL of water and dried under ambient air. The crude product was purified by column chromatography using silica gel and 16% ethyl acetate in hexane to give 45% yield (0.195 g) of **34a**. *^{1}H NMR* ($CDCl_3$/TMS): δ 7.40 (d, J = 8.8 Hz, 2H, aromatic), 7.29-7.25 (m, 4H, aromatic), 7.12-7.04 (m, 6H, aromatic), 7.02 (d, J = 8.8 Hz, 2H, aromatic), 6.96 (d, J = 16.0 Hz, 1H, stilbene), 6.80 (d, J = 16.0 Hz, 1H, stilbene), 6.03 (s, 1H, CH), 2.46 (s, 2H, CH_2), 2.30 (s, 2H, CH_2), 1.10 (s, 6H, $2CH_3$) ppm. *^{13}C NMR* ($CDCl_3$/TMS): δ 200.20, 160.10, 155.2, 148.8, 147.1, 134.7, 129.6, 129.5,

129.4, 128.3, 127.5, 126.3, 125.6, 125.3, 125.1, 123.7, 122.5, 51.47, 50.81, 45.33, 39.14, 33.56, 33.36, 28.55, 24.54 ppm.

Condensation of 32 with isophorone to give 34b

The same methodology for the preparation of **34a** was used. 200 mg (0.659 mmol) of **32** was dissolved with 5 mL of freshly dried t-BuOH. Then t-BuOK (163 mg, 1.45 mmol, 2.2 equiv) and isophorone (0.11 mL, 100 mg, 0.725 mmol, 1.1 equiv) were added into the reaction flask. Additional 5 mL of t-BuOH was added, then the red solution was refluxed (~80 °C) for 30 minutes. After cooling, 25 mL of water was added to the reaction mixture. The yellow precipitated was filtered and re-dissolved in CH_2Cl_2 followed by the addition of water. The organic phase was extracted with CH_2Cl_2 and concentrated under reduced pressure. The crude product was purified by column chromatography using silica gel and 16% ethyl acetate in hexane to give 43% yield (0.120 g) of **34b** after removal of the solvent.

Elemental Analysis: Calculated for $C_{29}H_{29}NO_2$: **C** 82.23, **H** 6.90, **N** 3.31 Found: **C** 81.81, **H** 6.94, **N** 3.36. *^1H NMR* ($CDCl_3$/TMS): δ 7.33 (d, J = 8.4 Hz, 2H, aromatic), 7.25 (t, J = 8.0 Hz, 2H, aromatic), 7.09 (d (d), J = 8.0 Hz (J = 8.8 Hz), 4H, aromatic), 7.02 (t, J = 7.2 Hz, 1H, aromatic), 6.96 (d, J = 8.4 Hz, 2H, aromatic), 6.90 (d, J = 13.2 Hz, 1H, stilbene), 6.87 (d, J = 12.4 Hz, 2H, aromatic), 6.78 (d, J = 16.0 Hz, 1H, stilbene), 6.03 (s, 1H, CH), 3.80 (s, 3H, OCH_3), 2.45 (s, 2H, CH_2), 2.29 (s, 2H, CH_2), 1.10 (s, 6H, $2CH_3$) ppm. *^{13}C NMR* ($CDCl_3$/TMS): δ 200.1, 156.7, 155.3, 149.2, 147.3, 139.95, 134.8, 129.3, 128.7, 128.2, 127.8,

127.0, 126.1, 124.2, 123.1, 121.1, 114.9, 55.50, 51.46, 39.14, 33.34, 31.59, 28.54, 21.53, 14.26 ppm.

Condensation of 34b with malononitrile to prepare 35b

A dry one neck round bottom flask was charged with ketone **34b** (0.080 g, 0.189 mmol, 1 equiv) which was dissolved in 5 mL of $CHCl_3$. Then malononitrile (0.012 mL, 0.193 mmol, 1.02 equiv) and triethylamine (0.04 mL, 0.283 mmol, 1.5 equiv) were added dropwise. The reaction mixture was stirred at room temperature for 2 h, then the reaction mixture was warmed to 50 °C and stirred at that temperature for 2 additional hours under a nitrogen atmosphere. Once at room temperature, 50 mL of water was poured into the reaction flask. The organic phase was extracted with CH_2Cl_2, dried over Na_2SO_4, and concentrated under reduced pressure. The crude product was purified by column chromatography using silica gel and 23% ethyl acetate in hexane affording **35b** as a red solid in 41% yield (0.033 g). *^1H NMR* ($CDCl_3$/TMS): δ 7.33 (d, J = 8.8 Hz, 2H, aromatic), 7.30-7.28 (m, 2H, aromatic), 7.12-7.08 (m, 4H, aromatic), 6.97-6.93 (m, 3H aromatic), 6.91 (d, J = 11.6 Hz, 1H, stilbene), 6.89 (d, J = 8.8 Hz, 2H, aromatic), 6.85 (d, J = 16 Hz, 1H, stilbene), 6.77 (s, 1H, CH), 3.82 (s, 3H, OCH_3), 2.58 (s, 2H, CH_2), 2.50 (s, 2H, CH_2), 1.07 (s, 6H, $2CH_3$) ppm.

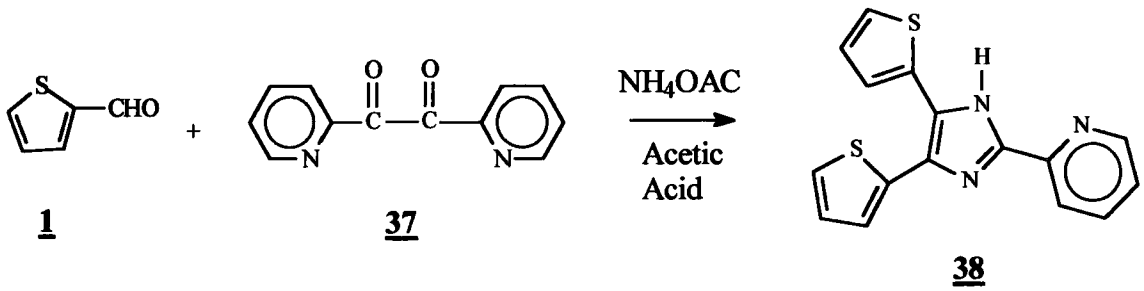

1 37 38

2-(2'-pyridil)-4,5-bis(thienyl)imidazole (38)

2,2'-pyridil (37) (1.0 g, 4.71 mmol) was dissolved in glacial acetic acid (40 mL). Then 2-thiophene carboxaldehyde (0.44 mL, 4.71 mmol) and ammonium acetate (3.63 g, 47.12 mmol, 10 equiv) were added. This solution was heated to 100 °C for 15 h under a nitrogen atmosphere. The reaction mixture was cooled to ambient temperature and poured into a water-ice bath. The organic phase was extracted with CH_2Cl_2 and concentrated under reduced pressure resulting in a black oil. The crude product was purified by column chromatography using silica gel and 30% ethyl acetate in hexane. After mixing the collected fractions and removal of the solvent by reduced pressure a black solid was obtained. This solid was crystallized with methanol resulting in 0.145 g (10% yield, brown crystals) of 38. *Elemental Analysis*: Calculated for $C_{16}H_{11}N_3S_2$ + 1/6 $CH_3COOCH_2CH_3$: **C** 61.77, **H** 3.83, **N** 12.96 Found: **C** 61.45, **H** 3.90, **N** 13.15. *^1H NMR* (DMSO-d_6/TMS): δ 13.30 (s, 1H, NH), 8.65 (d, *J* = 4.4 Hz, 1H, thienyl), 8.11 (d, *J* = 8.0 Hz, 1H, thienyl), 7.93 (t (d, *J* = 1.6 Hz)(d, *J*= 1.6 Hz)(d, *J* = 2.0 Hz), 1H, thienyl), 7.64 (d, *J* = 5.04 Hz, 1H, thienyl), 7.50 (d, *J*=3.2 Hz, 1H, aromatic), 7.47 (d, *J*=5.05 Hz, 1H, thienyl), 7.43-7.40 (m, 1H, thienyl), 7.19-7.15 (m, 2H, aromatic), 7.03 (t, *J*=4.0 Hz, 1H, aromatic) ppm.